

Characterisation of aphid-derived components involved in plant innate immune responses

James Canham

University of East Anglia

A thesis submitted for the degree of Doctor of Philosophy

March 2022

This copy of the thesis has been supplied on condition that anyone who consults it is understood to recognise that its copyright rests with the author and that use of any information derived there from must be in accordance with current UK Copyright law. In addition, any quotation or extract must include full attribution.

This page is intentionally left blank.

Abstract

As obligate herbivores and important vectors of many plant viruses, aphids represent a considerable and increasing threat to agriculture and food security. An increasing body of evidence suggests that plants may perceive aphid-derived cues during feeding events, resulting in plant innate immune responses. The aim of this thesis is to uncover the underlying aphid and plant components that contribute to the induction of plant innate immunity to aphids.

To reveal the breadth of plant innate immune responses that may be induced upon perception of *Myzus persicae*, partially purified elicitor fractions were generated from these aphids and used to investigate microbe-associated molecular pattern-triggered immunity (MTI) responses of *Arabidopsis thaliana*. Fractions strongly induce MTI via activating MAPK cascades and inducing the expression of genes previously shown to impact *M. persicae* resistance of *A. thaliana*, such as camalexin biosynthesis pathway genes and *WRKY33*, a regulator of camalexin production. Furthermore, the co-receptor, SUPPRESSOR OF BIR1-1 (SOBIR1) was found to be required for aphid-derived elicitor-triggered MTI in *A. thaliana*. As SOBIR1 is required for receptor-like protein (RLP) mediated immunity, a collection of single *Atrlp* mutant *A. thaliana* lines were screened for altered MAPK activation to the aphid fractions. In addition, EMS-mutagenised *pWRKY33::fLUC* seedlings were screened for altered responses to the aphid elicitors. Neither of these screens elucidated obvious receptor candidates suggesting that more than one receptor may be involved in aphid elicitor perception.

Further analysis of aphid-derived fractions suggest that elicitor function is conferred by a peptide and requires proteolytic liberation, most likely by an aphid protease, before inducing MTI in plants. Natural variation for aphid-derived elicitor-induced seedling growth inhibition within *A. thaliana* accessions validated this approach for future investigations. By revealing novel components of MTI to aphids, this study offers insights into the mechanisms that mediate plant perception of aphid cues.

Access Condition and Agreement

Each deposit in UEA Digital Repository is protected by copyright and other intellectual property rights, and duplication or sale of all or part of any of the Data Collections is not permitted, except that material may be duplicated by you for your research use or for educational purposes in electronic or print form. You must obtain permission from the copyright holder, usually the author, for any other use. Exceptions only apply where a deposit may be explicitly provided under a stated licence, such as a Creative Commons licence or Open Government licence.

Electronic or print copies may not be offered, whether for sale or otherwise to anyone, unless explicitly stated under a Creative Commons or Open Government license. Unauthorised reproduction, editing or reformatting for resale purposes is explicitly prohibited (except where approved by the copyright holder themselves) and UEA reserves the right to take immediate 'take down' action on behalf of the copyright and/or rights holder if this Access condition of the UEA Digital Repository is breached. Any material in this database has been supplied on the understanding that it is copyright material and that no quotation from the material may be published without proper acknowledgement.

Table of contents

Abstract	3
Table of contents.....	4
Acknowledgements	6
List of Figures.....	7
List of Tables	8
List of common abbreviations	8
Chapter 1.....	10
Introduction	10
1 Introduction.....	11
1.1 Aphids as important pests in agriculture	11
1.2 Plant innate immunity	14
1.3 NLR-mediated immunity	33
1.4 Interdependency of PRRs and NLRs	34
1.5 Herbivores as inducers and suppressors of plant immunity	35
1.6 This project	44
Chapter 2.....	46
Materials and Methods.....	46
2.1 Insect rearing conditions	47
2.2 Plant growth conditions	47
2.3 Plant lines	48
2.4 Biochemical isolation and characterisation of aphid-derived elicitors	49
2.5 DNA / RNA extractions	58
2.6 Plant immune assays	59
2.7 Insect experimentation	65
Chapter 3.....	69
Aphid-derived extracts contain an immunogenic epitope, likely to be a peptide motif.....	69
3.1 Introduction.....	70
3.2 Results	76
3.3 Discussion	98
Chapter 4.....	108
The receptor-like protein <i>AtSOBIR1</i> and SERK-family kinases <i>AtBAK1</i> and <i>AtBKK1</i> regulate immune signalling to aphid-derived elicitors.....	108
4.1 Introduction.....	109

4.2	Results.....	115
4.3	Discussion.....	133
Chapter 5.....		142
Forward- and reverse-genetic approaches to uncover receptors mediating aphid perception		142
5.1	Introduction	143
5.2	Results.....	151
5.3	Discussion.....	159
Chapter 6.....		164
Discussion		164
Appendices		178
References		191

Acknowledgements

I'd like to acknowledge the considerable contribution of my primary supervisor, Prof. Saskia Hogenhout. I thank Saskia for her guidance and encouragement. I'd also like to acknowledge the Hogenhout lab team members for their support and friendship. Thanks to my supervisory team, Dr Myriam Charpentier, Dr Sam Mugford, Dr Matteo Gravino and Dr Yazhou Chen for the stimulating discussions and advice. Similarly, the Menke group who were always forthcoming with advice and particularly, thanks to Dr Jan Sklenar whose positive influence on me and my project was invaluable. Additionally, I'd like to recognise the considerable contribution of Josh Joyce to this project and my time at JIC.

I wish to acknowledge the hardworking support staff of the JIC who make the research conducted in the institute possible and for their dedication and support for this project. This project is supported by the BBSRC and the Doctoral Training Program.

I want to thank my family for all they do for me.

To my wife Amy, you're an inspiration to me and your unwavering support has been amazing. I love you.

List of Figures

- Figure 1.1 Homeostasis of pattern recognition complexes involved in innate immunity in plants
- Figure 1.2 MAMP-triggered immune signalling in plants
- Figure 2.1 Standard curve of bovine serum albumin (BSA) within a BCA assay to determine aphid extract protein concentrations
- Figure 3.1 Illustrated protocol of aphid extract filtrate elicitor (AEFE)-containing fraction production
- Figure 3.2 Aphid-derived elicitors induce MAMP-triggered immune responses in *A. thaliana*
- Figure 3.3 Elicitor activity of aphid-derived extract (AEFE) is sensitive to pronase treatment
- Figure 3.4 Elicitor activity of aphid-derived extract (AEFE) requires cysteine proteases
- Figure 3.5 Illustrated protocol of purification steps towards the identification of candidate elicitor peptides
- Figure 3.6 Elicitor activity of aphid-derived extract (AEFE) elutes as discrete fractions in ³D-UHPLC
- Figure 3.7 Luminescence of ³D-UHPLC separated fractions of aphid-derived extracts reveals consistent peaks of immune-activity across biological repetitions
- Figure 3.8 Candidate elicitor peptides (CEPs) do not induce *WRKY33* promoter activity in *A. thaliana*
- Figure 4.1 Aphid-derived extracts (aphid extract elicitor filtrate, AEFE) induces innate immune responses in *A. thaliana*
- Figure 4.2 Cytoplasmic calcium elevations are required for full AEFE-induced immune responses in *A. thaliana*
- Figure 4.3 Aphid-derived extracts (aphid extract elicitor filtrate, AEFE) does not confer induced resistance to future aphid fecundity
- Figure 4.4 SERK family kinases *BAK1* and *BKK1* act as positive regulators of AEFE-induced immune signalling
- Figure 4.5 SUPPRESSOR OF BRASSINOSTEROID-ASSOCIATED KINASE 1-ASSOCIATED RECEPTOR 1 (*SOBIR1*) is a positive regulator of AEFE-induced defence signalling
- Figure 4.6 Aphid performance is unaltered on the *A. thaliana sobir1* mutants
- Figure 4.7 Cytosolic calcium influxes ($[Ca^{2+}]_{cyt}$) are altered on *Atsobir1* mutant plants
- Figure 5.1 *A. thaliana* receptor-like proteins (*AtRLPs*)

- Figure 5.2 MAPK activation screen of *A. thaliana* receptor-like protein mutants (*Atrlp*) during AEFE-induced MTI
- Figure 5.3 EMS-mutagenised *pWRKY33::fLUC* *A. thaliana* seedlings exposed to aphid-derived extract, AEFE
- Figure 5.4 Natural variation for AEFE-induced seedling growth inhibition (SGI) within *A. thaliana* ecotypes

List of Tables

- Table 1.1 Pattern recognition receptors, their cognate ligands and co-receptors
- Table 1.2 Immuno-suppressive effectors from piercing-sucking insect herbivores
- Table 2.1 Aphid-derived extract sample absorption as determined in a BCA assay
- Table 2.2 Protein concentrations of aphid-derived extracts
- Table 2.3 Primers used for qRT-PCR
- Table 3.1 Specific activity of partially purified, aphid-derived extracts
- Table 3.2 Candidate elicitor peptides (CEPs), identified in LC-MS/MS of fractions 25 and 26 and satisfying selection characteristics
- Table 3.3 Candidate elicitor peptides (CEPs), identified in LC-MS/MS of fractions 25 and 26 and satisfying selection characteristics
- Table 4.1 Proteins detected in LC-MS/MS samples as putative interactors of BAK1

List of common abbreviations

- AEBSF 4-benzenesulfonyl fluoride hydrochloride
- BAK1 BRI1 associated kinase 1
- BKK1 BAK1-like1
- CDPK Calcium dependent protein kinases
- CERK1 Chitin elicitor receptor kinase 1
- CEP Candidate elicitor peptide
- DAMP Damage-associated pattern

DAB	3, 3'-diaminobenzidine
EDS1	Enhanced disease susceptibility 1
EDTA	Ethylenediaminetetraacetic acid
EFR	EF-TU receptor
EF-Tu	Elongation factor-Tu
EGTA	Ethylene glycol-bis(β -aminoethyl ether)- <i>N,N,N',N'</i> -tetraacetic acid
ETI	Effector-Triggered Immunity
ETS	Effector-triggered susceptibility
FLS2	Flagellin sensing 2
IGS	Indole glucosinolates
JA	Jasmonic acid
LC	Liquid chromatography
Leu	Leucine
LRR	Leucine-rich repeat
Lys	Lysine
MAMP	Microbe-associated molecular pattern
MS	Mass spectroscopy
MTI	Microbe-Triggered Immunity
PAMP	Pathogen-associated molecular pattern
PIC	Protease inhibitor cocktail
PAD3	Phytoalexin deficient 3
Pro	Proline
PRR	Pattern recognition receptor
PTI	PAMP-Triggered Immunity
RLK	Receptor-like kinases
RLP	Receptor-like protein
SA	Salicylic acid
SOBIR1	Suppressor of bir1-1
UHPLC	Ultra-high performance liquid chromatography

Chapter 1

Introduction

1 Introduction

1.1 Aphids as important pests in agriculture

Aphids (order: Hemiptera, family: Aphididae) are exclusively piercing-sucking, phloem-feeding insects that are fully dependent on plants as a source of nutrition, hydration and protection (Holman, 2008, Blackman and Eastop, 2007). The majority of the ~5000 species of aphid are monophagous or oligophagous, and like most parasites, are highly adapted to a limited host range (Blackman and Eastop, 2007). However, whilst host plant specialisation is the rule rather than the exception, several polyphagous or generalist aphid species including the destructive aphid *M. persicae*, are of primary importance as pests in agronomic systems (Dedryver et al., 2010). *M. persicae*, for example, is capable of colonising over 100 species from 40 different families (Blackman and Eastop, 2007). Aphids, and especially *M. persicae*, are considered model organisms, displaying a remarkable ability to locate and exploit plant hosts in diverse environments (Dixon, 1998, Powell et al., 2006). Some species, often thought of as polyphagous generalists, are cryptic specialists consisting of host-adapted biotypes (Bickford et al., 2007, van Emden and Harrington, 2007). One example, the pea aphid (*Acyrtosiphon pisum*), can colonise most plants of the Fabaceae, but consists of different biotypes that colonise specific species of this plant family (Peccoud et al., 2009).

1.1.1 Polyphenic traits of aphids

Part of the success of aphids is attributable to the evolution of parthenogenesis - asexual reproduction involving the birth of live young, enabling reproduction without males for part or all of the life cycle (Simon et al., 2002). Parthenogenesis confers a reproductive advantage by increasing the rate of population increase relative to sexually reproducing individuals (Williams, 1975, Dixon, 1998). For *M. persicae*, sexual reproduction may also occur on *Prunus* spp. during autumn/winter producing eggs from which parthenogenetically reproducing nymphs emerge in the spring (Blackman

and Eastop, 2007). Where *Prunus* spp. are absent *M. persicae* may become facultatively asexual and forgo a sexual stage and such conditions are often maintained in controlled environments used for aphid rearing (Leather, 1989). Another set of biologically important characteristics are polyphenisms such as the ability for aphids to produce winged (alate) and wingless (apterous) adults and exhibit body-colour and caste polymorphisms (Fukatsu, 2010, Tsuchida et al., 2010, Smith and MacKay, 1989). These characteristics allow aphids to migrate and adjust to an extraordinarily diverse range of secondary host species. During their asexual phase, aphids are viviparous, birthing live young to quickly establish several generations of genetically identical individuals on their secondary host (Davis, 2012). The result of these reproductive novelties is remarkable plasticity in respect to adaptation and colonisation of new hosts and to changing environmental conditions.

Aphids, like all Hemiptera, host a number of facultative and obligate symbiotic bacteria. Symbionts can influence a host's biology by improving the host's ecological fitness, immunity to parasites, or by enhancing tolerance to environmental stress (Oliver et al., 2005, Dion et al., 2011). Aphids exhibit a mutualistic association, obligate for both partners, with the intracellular γ proteobacterium *Buchnera* spp. (Munson et al., 1991). Considered the aphids' primary endosymbiont, *Buchnera* has undergone dramatic genome reduction, retaining only essential genes for its lifestyle (Gil et al., 2002). Despite this, *Buchnera* remains capable of the biosynthesis of all essential amino acids, several of which are in short supply in the phloem diet, to supply nutrition to the host (Sandström and Moran, 1999).

1.1.2 Aphid feeding behaviour

Aphids are termed *stealthy* phloem-feeders and use their stylets to penetrate the plant cuticle, navigate through the intercellular space to locate and actively feed from the phloem sieve elements (Tjallingii, 2006, Tjallingii and Hogenesch, 1993). In the apoplastic space, continuously secreted drops of gel saliva form a tubular corridor that protects and guides the stylet (Will et al., 2012). During stylet navigation, cells along the pathway are regularly penetrated by the stylet (Tjallingii, 2006, Hewer et al.,

2010). During these probing events of epidermal or mesophyll cells, watery saliva is secreted into the intracellular space, followed by ingestion of cell sap (Tjallingii, 2006). It is unclear how aphids navigate plant tissue in order to locate phloem sap. An active process of cell rejection is thought to be the primary means by which aphids may decipher cell and/or tissue type during probing and feeding (Hewer et al., 2010). In support of this theory, chemical cues such as sucrose concentrations and pH changes are likely monitored by aphids. Low pH in the vacuole is likely a major cue for aphids to differentiate mesophyll cell penetration and phloem sieve elements which are typically maintained at a neutral pH7.5 (Hewer et al., 2010).

1.1.3 Aphid threat to agriculture

Aphids represent a considerable and increasing threat to agriculture and subsequently, food security (Dedryver et al., 2010). As piercing-sucking insects, aphids are ideally suited as vectors for plant viruses and are reported to transmit around 50% of insect-borne plant viruses (approximately 275 virus species) (Hogenhout et al., 2008, Ng and Perry, 2004, van Emden and Harrington, 2007). Virus transmission by aphids leads to global losses estimated to be in the billions of US dollars per annum (Blackman (Blackman and Eastop, 2007, Dedryver et al., 2010). In the UK, the damage to cereals caused by aphids was estimated to be around £60-120 million annually during the 1980's (Tatchell, 1989), however, this is likely to be far greater today. In addition to virus transmission, aphids directly contribute to crop losses. During photoassimilate acquisition, aphids deplete water and nutrients from the plant leading to deficiencies and leaf curling symptoms. Excretion of waste products of phloem digestion including excess sucrose, also known as honeydew, can promote fungal growth and cause disease (Schwartzberg et al., 2014, Fokkema et al., 1983). However, in most crops, these effects are minor compared to the effect of aphid-transmitted viruses.

Crop losses to aphids are limited by the use of highly effective insecticides. However, persistent exposure to insecticide treatments has led to the emergence of resistance to several classes of chemicals including pyrethroids (Anstead et al., 2007), and neonicotinoids (Puinean et al., 2010, Matsuura and Nakamura, 2014).

M. persicae alone has evolved at least seven mechanisms that allow it to avoid or overcome the toxic effect of insecticides (Bass et al., 2014). The *M. persicae* FRC clone, collected from peach in Southern France, exhibits extremely potent resistance to neonicotinoids (Bass et al., 2011). At least two resistance mechanisms exist in FRC, one based on enhanced detoxification by cytochrome P450s, and another that may be associated with a point mutation (R81T) in the nicotinic acetylcholine receptor (nAChR), the target site for some neonicotinoids (Bass et al., 2011, Puinean et al., 2010), although field studies have cast doubt on this mechanism (Beckingham et al., 2013).

Increased use restrictions within EU member states of active ingredients such as clothianidin, imidacloprid, thiamethoxam, acetamiprid and thiacloprid to protect insect ecology (see Regulation (EU) No 485/2013) have led to reduced effective treatment availability, increasing aphid populations and increased aphid-vectoring virus-associated diseases. Indeed, growing pressure on crops by herbivorous insects has resulted in continuous emergency authorisations for their use (<https://ec.europa.eu/food/plant/pesticides/eu-pesticides-database>). Novel and environmentally sympathetic solutions for the control of insect herbivores within agricultural settings are greatly needed.

1.2 Plant innate immunity

1.2.1 Pattern recognition receptor-mediated immunity

Plant pathogens including bacteria, fungi and oomycete, as well as pests including chewing, rasping and piercing-sucking insects can both induce and suppress plant innate immunity. To overcome these threats, plants have evolved a sophisticated, two-tiered innate immune system, termed pattern-/microbe-associated molecular pattern (PAMP/MAMP)-triggered immunity (PTI/MTI) and effector-triggered immunity (ETI). Surveillance of the extracellular and intracellular environment allows plants to respond to pathogens with a series of inducible defences. Pattern recognition

receptors (PRRs) mediate the perception of extracellular or endogenous cues and transduce stimuli into cellular responses and plant resistance (Couto and Zipfel, 2016). Conversely, ETI is activated by pathogen effector proteins, predominantly via intracellular receptors termed nucleotide-binding, leucine-rich repeat receptors (NLRs) (Cui et al., 2015). These defence tiers are cooperative as PRR and PRR co-receptors are required for full ETI and in reciprocation, NLR signalling acts to potentiate MTI through positive regulation of key MTI components (Ngou et al., 2021, Yuan et al., 2021).

In addition to non-self pathogen- or pest-associated patterns, endogenous cues derived from the host plant, can compensate, complement and potentiate MTI responses (Hou et al., 2019). Such patterns may be released during alterations in cell wall integrity, through mechanical or enzymatic damage (De Lorenzo et al., 2019). These damage-associated molecular patterns (DAMPs) are integral to plant innate immunity and play a greater or lesser role depending on the threat. Where ligands and cognate receptors have been identified, all pest- and pathogen-associated patterns, as well as DAMPs, are listed in (Table 1.1).

Other sources of bioactive ligands have been identified from a range of pests and microbes. The best characterised of these are herbivore-associated molecular patterns (HAMPs) (Mithofer and Boland, 2008), derived primarily from chewing insects such as Lepidoptera including butterflies and moths and Coleoptera such as beetles. The larval stages of Lepidopteran insects present a particular challenge to plants as their specialised mouthparts and dietary needs results in considerable plant tissue damage. Additional patterns such as nematode-associated molecular pattern (NAMP) (Manosalva et al., 2015, Mendy et al., 2017) or parasite-associated molecular pattern (parAMP) (Kaiser et al., 2015, Hegenauer et al., 2016) also contribute to a growing understanding of analogous MTI responses in plants.

1.2.2 Receptor complex formation

PRRs comprise cell-surface localised receptor-like kinases (RLKs) and receptor-like proteins (RLPs) (Boller and Felix, 2009). The highly variable leucine-rich repeat (LRR)

ectodomain (ECD) of RLKs and RLPs provide the means to recognize a wide range of ligands resulting in the first line of inducible defence termed MTI (Breiden and Simon, 2016). Several outstanding reviews summarise current understanding of the topic (Couto and Zipfel, 2016, Corwin and Kliebenstein, 2017, Tang et al., 2017, Jamieson et al., 2018, DeFalco and Zipfel, 2021, Lee et al., 2021, Yu et al., 2021, Ngou et al., 2022).

The *A. thaliana* LRR-RLKs FLAGELLIN SENSING 2 (FLS2) and ELONGATION FACTOR-Tu RECEPTOR (EFR) recognize a conserved 22-amino acid epitope (flg22) of the bacterial flagellin and a conserved epitope (elf18) of the bacterial elongation factor Tu (EF-Tu), respectively (Gómez-Gómez et al., 1999, Kunze et al., 2004). Ligand binding can induce the formation of multimeric complexes involving activated receptors, co-receptors and intracellular kinases (Couto and Zipfel, 2016). PRRs of the LRR-RLK class, including FLS2 and EFR, recruit BRI1-ASSOCIATED RECEPTOR KINASE (BAK1), a member of the SOMATIC EMBRYOGENESIS RECEPTOR KINASE (SERK) family receptors to form heterodimers, resulting in rapid cellular signalling (Chinchilla et al., 2006, Chinchilla et al., 2007, Schulze et al., 2010, Roux et al., 2011). Members of the SERK family kinases can act redundantly to mediate immune signalling and act cooperatively to regulate MTI specificity and amplitude (Roux et al., 2011, Schwessinger et al., 2011). Aberrant immune signalling by BAK1 is prevented by LRR-RLKs BAK1-INTERACTING RECEPTOR-LIKE KINASE 1/2/3 (BIR1/2/3) that sequester BAK1 in the absence of PRR-ligand interaction (Gao et al., 2009, Halter et al., 2014, Ma et al., 2017).

In contrast to FLS2 or EFR-mediated signalling that requires only ligand-dependent BAK1 recruitment and transphosphorylation, LRR-RLP-mediated signalling likely requires an adaptor RLK to regulate downstream responses (Huffaker et al., 2013). The *A. thaliana* LRR-RLK SUPPRESSOR OF BIR1-1/EVERSHED (SOBIR1/EVR) was identified as a suppressor of *bir1-1* autoimmunity (Gao et al., 2009), and is a good candidate as an adaptor RLK during RLP-mediated MTI. Of the 57 RLPs in *A. thaliana* (Fritz-Laylin et al., 2005, Wang et al., 2008a), five (RLP1, RLP23, RLP30, RLP32 and RLP42) require BAK1 and SOBIR1 for full function during the defence response to a variety of pathogens (Jehle et al., 2013, Zhang et al., 2013, Zhang et al., 2014, Albert et al., 2015, Bi et al., 2016, Fan et al., 2022). AtRLPs mediate signalling in a tripartite complex via a two-stage process. Firstly, pattern recognition occurs via RLP-SOBIR1

bimolecular complexes and secondly, activated RLP-SOBIR1 complexes recruit BAK1 (Liebrand et al., 2013). Receptor complex activation is likely conferred by SOBIR1 trans-autophosphorylation as well as SOBIR1 and BAK1 transphosphorylation (van der Burgh et al., 2019)

Evidence that receptor complex components require molecular chaperones has emerged in recent years. The *A. thaliana* malectin-like receptor kinase, FERONIA (FER) and the GPI-anchored protein, LORELEILIKE-GPI-ANCHORED PROTEIN 1 (LLG1) associate with components of the PRR complex where they can promote FLS2-BAK1 complex formation (Shen et al., 2017, Stegmann et al., 2017). FER also recognizes various rapid alkalization factor peptides (RALFs), such as RALF23, to allow fine-tuning of immune responses via perturbation of FLS2-BAK1 heterocomplex formation (Li et al., 2015a, Stegmann et al., 2017, Gronnier et al., 2022). Additional kinases such as INDUCED OOMYCETE SUSCEPTIBILITY 1 (IOS1) and FLS2-INTERACTING RECEPTOR (FIR) may promote the formation of ligand-activated PRR complexes (Yeh et al., 2016, Smakowska-Luzan et al., 2018). The malectin-like domain-containing RLK ANXUR1 (ANX1), together with its homolog ANX2 negatively regulate MAMP-induced immune responses via disruption of FLS2-BAK1 complex formation (Mang et al., 2017). ANX1 constitutively associates with FLS2 and perception of flg22 promotes ANX1 association with BAK1, disrupting complex formation (Mang et al., 2017). Similarly, NSP-INTERACTING KINASE 1 (NIK1) acts as a negative regulator of MTI by associating with FLS2 and BAK1, thereby disrupting complex formation (Li et al., 2019).

Not limited to proteinaceous, bacterial MAMP perception, analogous PRR complexes perceive a multitude of chemical cues derived from a variety of organisms. In rice, the fungal MAMP, chitin, is perceived by the lysin-motif (LysM)-containing CHITIN-ELICITOR BINDING PROTEIN (CEBiP) receptor (Kaku et al., 2006). OsCEBiP forms a complex with the rice CHITIN-ELICITOR RECEPTOR KINASE 1 (OsCERK1) providing an active, intracellular kinase domain to mediate MTI responses (Hayafune et al., 2014, Shimizu et al., 2010). In *A. thaliana*, the perception chitin depends on the LysM RLK, CHITIN ELICITOR RECEPTOR KINASE 1 (CERK1) which associates with LYSIN-MOTIF RECEPTOR LIKE KINASE 5 (LYK5) (Cao et al., 2014, Miya et al., 2007, Wan et al., 2012)

PRRs for herbivory-associated cues (HAMPs) have also been identified and shown to confer resistance to insects (Steinbrenner et al., 2020). HAMPs may originate from several sources including oral secretions (OS), saliva or eggs and are thought to play a key role in plant defence during insect herbivory (Reymond, 2021). However, to date, very few PRRs have been identified that mediate responses to insects. In legumes, the LRR-RLP PRR, inceptin receptor (INR) mediates the perception of proteolytic fragments of chloroplastic ATP synthase, termed inceptins (Schmelz et al., 2006, Schmelz et al., 2007). The most abundant inceptin within caterpillar OS, whilst feeding on cowpea (*Vigna unguiculata*), is the 11-amino acid (AA) peptide, termed *Vu*-In (+¹ICDINGVCVDA⁻) (Steinbrenner et al., 2020). INR constitutively associates with both *At*SOBIR1 and *Vu*SOBIR1 (*Vigun09g096400*), while INR associated more strongly with *At*SERKs (*At*SERK1-4) after *Vu*-In treatment (Steinbrenner et al., 2020).

The clade I L (legume)-type lectin receptor kinases, LecRK-I.8 and LecRK-I.1 modulate *Pieris brassicae* egg-associated elicitor-triggered defence signalling (Gouhier-Darimont et al., 2019, Groux et al., 2021). It is not clear whether LecRKs require co-receptors or adaptor kinases to mediate elicitor perception and signalling. In *A. thaliana*, oviposition by *P. brassicae* triggers salicylic acid (SA) accumulation, defence gene expression and a hypersensitive-like (HR) response (Bruessow et al., 2010, Hilfiker et al., 2014). Evidence that egg deposition may prime a plant to defend against ensuing larval herbivory by SA accumulation and anti-herbivory metabolite biosynthesis has also been reported (Schott et al., 2021). This is, however, contradicted by observations that SA accumulation can antagonise the more effective JA pathways to promote herbivory (Bruessow et al., 2010).

Table 1.1: Pattern recognition receptors, their cognate ligands and co-receptors.

Receptor	Receptor-type / family	Co-receptors / adaptors	Molecular pattern	Host plant	Reference
Recognition of bacterial-associated molecular patterns					
FLS2	LRR-RLK (XII)	BAK1	Flagellin (flg22)	<i>A. thaliana</i>	(Gómez-Gómez et al., 1999); (Schwessinger et al., 2011)
FLS3	LRR-RLK (XII)		Flagellin (flgII-28)	<i>S. pimpinellifolium</i>	(Cai et al., 2011); (Hind et al., 2016)
EFR	LRR-RLK (XII)	BAK1	EF-Tu (elf18)	<i>A. thaliana</i>	(Kunze et al., 2004); (Zipfel et al., 2006); (Chinchilla et al., 2006)
CORE	LRR-RLK		Cold shock protein (cps15/csp22)	Solanaceae	(Felix and Boller, 2003); (Wang et al., 2016)
XA21	LRR-RLK (XII)	OsSERK2	RaxX	<i>O. sativa</i>	(Song et al., 1995); (Pruitt et al., 2015)
XPS1	LRR-RLK (XII)		Permease (xup25)	<i>A. thaliana</i>	(Mott et al., 2016)
LORE	LEC-RLK		Lipopolysaccharide (LPS)	Brassicaceae	(Ranf et al., 2015)
EPR3	LysM-RLK		Extracellular polysaccharides	<i>L. japonicus</i>	(Kawaharada et al., 2015)
RLP1	LRR-RLP	SOBIR1 / BAK1	eMAX	<i>A. thaliana</i>	(Jehle et al., 2013)
RLP23	LRR-RLP	SOBIR1 / BAK1	Nep1-like protein (nlp20)	<i>A. thaliana</i>	(Albert et al., 2015)
RLP32	LRR-RLP	SOBIR1 / BAK1	IF1	<i>A. thaliana</i>	(Fan et al., 2022)
CSPR	LRR-RLP	SOBIR1 / BAK1	Cold shock protein (csp22)	<i>N. benthamiana</i>	(Saur et al., 2016)
LYM1/LYM3	LysM-RLP		Peptidoglycan	<i>A. thaliana</i>	(Willmann et al., 2011)
Recognition of fungal-associated molecular patterns					
CERK1	LysM-RLK	LYK5	Chitin	<i>A. thaliana</i>	(Cao et al., 2014); (Miya et al., 2007)
I-3	LEC-RLK		Avr3/Six1	<i>S. pennellii</i>	(Catanzariti et al., 2015)
RLP30	LRR-RLP	SOBIR1 / BAK1	SCFE1	<i>A. thaliana</i>	(Zhang et al., 2013)
Eix1	LRR-RLP	SOBIR1 / BAK2	xylanase	<i>S. pennellii</i>	(Ron and Avni, 2004), (2004); (Bar et al., 2010)
Eix2	LRR-RLP		xylanase	<i>S. pennellii</i>	(Ron and Avni, 2004)
RLP42	LRR-RLP	SOBIR1 / BAK1	Endopolygalacturonases	<i>A. thaliana</i>	(Zhang et al., 2014)
Cf-2	LRR-RLP	SOBIR1 / BAK1	Avr2	<i>S. pimpinellifolium</i>	(Dixon et al., 1996)
Cf-4	LRR-RLP	SOBIR1 / BAK1	Avr4	<i>S. hirsutum</i>	(Thomas et al., 1997); (Liebrand et al., 2013)
Cf-5	LRR-RLP	SOBIR1 / BAK1	Avr5	<i>S. lycopersicum</i>	(Dixon, 1998)
Cf-9	LRR-RLP	SOBIR1 / BAK1	Avr9	<i>S. pimpinellifolium</i>	(Jones et al., 1994)
Hcr9-4E	LRR-RLP		Avr4E	<i>S. hirsutum</i>	(Thomas et al., 1997); (Westerink et al., 2004)
LepR3/RLM	LRR-RLP	SOBIR1	AvrLm1, AvrLm2	<i>B. napus</i>	(Larkan et al., 2013, Larkan et al., 2015)
I (Immunity)	LRR-RLP	SOBIR1 / BAK1	Avr1/Six4	<i>S. pimpinellifolium</i>	(Catanzariti et al., 2015)
CEBiP	LysM-RLP		Chitin	<i>O. sativa</i>	(Kaku et al., 2006); (Shimizu et al., 2010); (Hayafune et al., 2014)
LYP4, LYP6	LysM-RLP		Chitin, Peptidoglycan	<i>O. sativa</i>	(Liu et al., 2012)
LYM1, LYM3	LysM-RLP		Peptidoglycan	<i>A. thaliana</i>	(Willmann et al., 2011)
LYM2	LysM-RLP		Chitin	<i>A. thaliana</i>	(Faulkner et al., 2013)

Recognition of oomycete-associated molecular patterns					
RLP23	LRR-RLP	SOBIR1 / BAK1	nlp20	<i>A. thaliana</i>	(Albert et al., 2015)
RLP85/ELR	LRR-RLP		Elicitin	<i>S. microdontum</i>	(Du et al., 2015)
Recognition of herbivore-associated molecular patterns (HAMPs)					
INR	LRR-RLP	SOBIR1	Inceptin	legumes	(Schmelz et al., 2006); (Steinbrenner et al., 2020);
LecRK1.8	LEC-RK		Phosphatidylcholine / NAD+	<i>A. thaliana</i>	(Gouhier-Darimont et al., 2019); (Stahl et al., 2020); (Wang et al., 2017)
Recognition of damage-associated molecular patterns (DAMPs) / Endogenous peptides					
PEPR1	LRR-RLK (XI)	BAK1	Pep1-Pep6	<i>A. thaliana</i>	(Yamaguchi et al., 2010)
PEPR2	LRR-RLK (XI)	BAK1	Pep1, Pep2	<i>A. thaliana</i>	(Yamaguchi et al., 2010)
RLK7	LRR-RLK (XI)		PIP1	<i>A. thaliana</i>	(Hou et al., 2014)
SR160	LRR-RLK		Systemin	<i>S. peruvianum</i>	(Scheer and Ryan, 2002)
DORN1	LEC-RLK		Extracellular ATP	<i>A. thaliana</i>	(Choi et al., 2014)
WAK1	EGF-like-RLK		Oligogalacturonides	<i>A. thaliana</i>	(Brutus et al., 2010)
FER	Malectin-RLK		RALF peptides	<i>A. thaliana</i>	(Haruta et al., 2014); (Stegmann et al., 2017)

1.2.3 Receptor complex homeostasis

During flg22-induced MTI, the U-box E3 ubiquitin ligases, PUB12 and PUB13, together with BAK1, are recruited to the FLS2 complex (Lu et al., 2011). Attenuation of FLS2-activation is conferred by PUB12/PUB13, which are phosphorylated by BAK1 leading to FLS2 ubiquitination (Lu et al., 2011). Activated PRRs including FLS2, EFR and PEPR1 internalise via clathrin-dependent endocytosis (Chinchilla et al., 2007, Robatzek et al., 2006). Endocytosis of receptors may lead to temporary desensitization of ligand-induced signalling but is closely followed by replenishment via *de novo* receptor synthesis after 2-h post elicitation (Smith et al., 2014). In a process distinct from endosomal trafficking of activated FLS2, non-activated FLS2 is constitutively recycled at the cell surface to maintain stable levels of the receptor (Beck et al., 2012). Furthermore, *A. thaliana* Orosomucoid (ORM) proteins, ORM1 and ORM2 act as selective autophagy receptors to mediate the degradation of FLS2 independent of ubiquitination (Yang et al., 2019).

1.2.4 Connecting PRR complexes with downstream signalling

Several *A. thaliana* receptor-like cytoplasmic kinases (RLCKs) associate with PRRs and are major components of PRR complexes. The subfamily RLCK-VII/PBL, BOTRYTIS-INDUCED KINASE1 (BIK1) may be the first immune component upon which several immune pathways converge and as such, is subject to multi-layered regulation. BIK1 constitutively associates with FLS2 or EFR and upon ligand perception, is phosphorylated by BAK1 (Veronese et al., 2006, Lu et al., 2010, Zhang et al., 2010). Similarly, the close homolog of BIK1, PBS1-LIKE1 (PBL1) interacts with FLS2 and is phosphorylated upon flg22 treatment (Zhang et al., 2010). Phosphorylated BIK1 dissociates from the PRR complex to activate downstream signalling (Lu et al., 2010). The *A. thaliana* E3 ubiquitin ligases RING-H2 FINGER A3A (RHA3A) and RHA3B mediate the monoubiquitination of BIK1, which is essential for BIK1 release from the FLS2-BAK1 complex (Ma et al., 2021). Additionally, the CALCIUM-DEPENDENT PROTEIN KINASE 28 (CPK28) phosphorylates the E3-ligases PUB25 and PUB26 that target BIK1 for degradation (Monaghan et al., 2014, Liang et al., 2016, Wang et al., 2018). Meanwhile, heterotrimeric G proteins, XLG2/XLG3, AGB1 and AGG1/AGG2 directly inhibit PUB25/26 E3 ligase activity to stabilize BIK1 levels (Wang et al., 2018) (Fig. 1.1).

Protein phosphorylation is an important and ubiquitous means of activation, and accordingly, several phosphatases including PROTEIN PHOSPHATASE 2A (PP2A), interact with, and negatively regulate, receptor complex components (Segonzac (Segonzac et al., 2014, Couto and Zipfel, 2016). BIK1 phosphorylation is subject to negative regulation by the protein phosphatase PP2C38 that associates with BIK1, FLS2 and EFR (Couto et al., 2016). Upon MAMP perception, PP2C38 is phosphorylated and dissociates from the FLS2/EFR-BIK1 complex, enabling full BIK1 activation (Couto et al., 2016). Other PP2Cs have been identified that regulate CERK1 (Liu et al., 2018), while a PP2A complex was found to negatively regulate the activation of BAK1 (Segonzac et al., 2014). In rice, the LRR-RLK, XA21 is negatively regulated by the PP2C XA21-BINDING PROTEIN 15 (XB15), which has been shown to dephosphorylate XA21 *in vitro* (Park et al., 2008). Additional regulation of XA21 is carried out by XB24, an ATPase that is

thought to promote auto-phosphorylation of XA21 and inhibit XA21-mediated immunity (Chen et al., 2010).

During chitin-induced responses, BIK1 associates with CERK1 indicating that BIK1 is a convergent component for different PRR-mediated pathways (Zhang et al., 2010). Interestingly, the role of BIK1 as a positive regulator of RLK-mediated immunity is in contrast with its putative role as a negative regulator of RLP-mediated immunity (Wan et al., 2019).

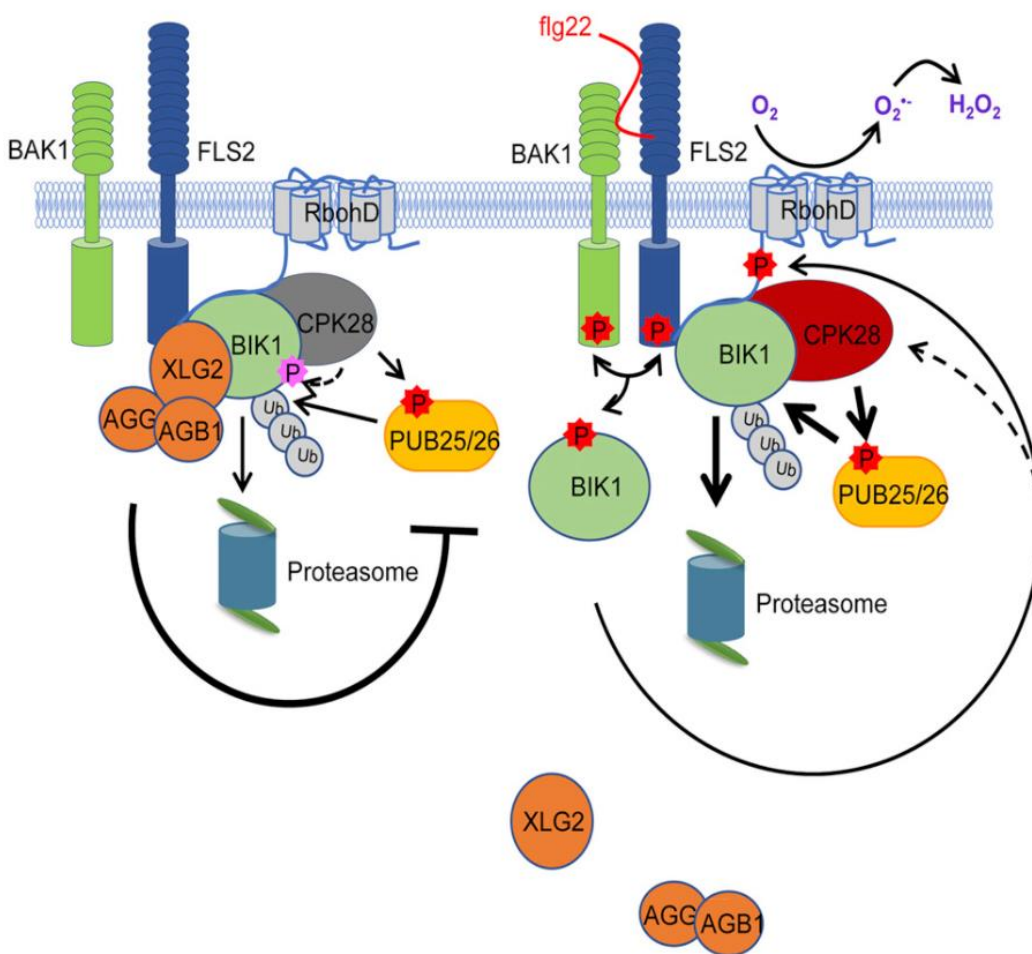


Figure 1.1: Homeostasis of pattern recognition complexes involved in innate immunity in plants. BIK1 phosphorylation is prerequisite for its activation (Couto and Zipfel, 2016), and BIK1 stability is positively regulated by heterotrimeric G proteins composed of XLG2/XLG3 (Ga), AGB1 (Gb), and AGG1/AGG2 (Gg) and negatively regulated by CPK28 through the ubiquitin proteasome system (Monaghan et al., 2014, Liang et al., 2016). Heterotrimeric G proteins inhibit PUB25/26 activity to stabilize BIK1, whereas CPK28 phosphorylates PUB25/26 to enhance their activity and promote BIK1 degradation (Wang et al., 2018). Activated BIK1 can dissociate from immune complexes to phosphorylate RBOHD (Kadota et al., 2014). Taken from (Wang et al., 2018).

1.2.5 MTI signalling

MAMP perception leads to a series of signalling outputs that can be temporally and spatially distinct or overlapping. These responses include ion fluxes, ROS production, MAP kinase and Ca²⁺-dependent protein kinase (CPKs or CDPKs) activation, transcriptional reprogramming and callose deposition (Boller and Felix, 2009).

Calcium signalling

Calcium (Ca²⁺) is a ubiquitous and versatile second messenger in plants and cytosolic elevations ([Ca²⁺]_{cyt}) are amongst the earliest physiological responses to MAMPs (Blume et al., 2000, Lecourieux et al., 2002). Release of Ca²⁺ from stores such as the vacuole and apoplast is achieved through the active movement of ions via calcium-permeable channels (Poovaiah and Reddy, 1993, Kwaaitaal et al., 2011, Thor and Peiter, 2014, Tian et al., 2019). Several calcium-permeable channels have been implicated in the active movement of ions across the vacuolar or plasma membrane during plant immunity.

The glutamate receptor-like (GLR) cation channels mediate systemic Ca²⁺ signal propagation to a variety of stimuli (Mousavi et al., 2013, Choi et al., 2016, Toyota et al., 2018, Nguyen et al., 2018). For example, wounding initiates GLR-dependent propagation of membrane depolarizations and [Ca²⁺]_{cyt} elevations that lead to downstream defence activation (Mousavi et al., 2013, Kiep et al., 2015, Nguyen et al., 2018). GLRs may also mediate a Ca²⁺-ROS wave, involving RBOHD, to modulate systemic signalling (Evans et al., 2016).

There are reported to be 20 cyclic nucleotide gated channels (CNGCs) in *A. thaliana* (Talke et al., 2003). CNGCs are gated by direct binding of cyclic nucleotides (CNs), such as cAMP (cyclic adenosine monophosphate) and cGMP (cyclic guanosine monophosphate), as well as by diverse molecules and ions including Ca²⁺ (Mantulef and Zagotta, 2003, Cukkemane et al., 2011). CNGCs can be inactivated by binding Ca²⁺-activated calmodulin (CaM) which provides a site for Ca²⁺ regulation (Leng et al., 1999,

Cukkemane et al., 2011). CNGC-mediated Ca^{2+} fluxes have been implicated in response to biotic and abiotic stress (Spalding and Harper, 2011). The family of *A. thaliana* signalling peptides (*AtPeps*) are perceived by the leucine-rich repeat receptor kinase, *AtPep RECEPTOR 1* (*AtPEPR1*) during cell wall disintegration (Yamaguchi et al., 2006, Huffaker et al., 2006). *PEPR1* has guanylyl cyclase activity, generating cGMP from GTP which activates *CNGC2* (*DEFENSE NO DEATH 1; DND1*) resulting in Ca^{2+} influx (Clough et al., 2000, Qi et al., 2010, Ma et al., 2012). The closest paralog to *CNGC2*, *CNGC4* is also implicated in defence to pathogens (Jurkowski et al., 2004, Chin et al., 2013). Loss of both *CNGC2* and *CNGC4* disrupts downstream Ca^{2+} -dependent signalling, leading to a hypersensitive response (HR) (Tian et al., 2019). Moreover, *BIK1* activates *CNGC2/4* by phosphorylation, leading to an increase in cytosolic Ca^{2+} downstream of MAMP responses (Tian et al., 2019). *AtPep*-triggered expression of MTI marker genes, *PDF1.2*, *MPK3* and *WRKY33* is downstream of Ca^{2+} signalling mediated by the *AtPep* receptor, *PEPR1* as well as *CNGC2*. Jasmonic acid (JA) can induce cAMP elevations to regulate *CNGC2*-mediated $[\text{Ca}^{2+}]_{\text{cyt}}$ elevations (Lu et al., 2016).

CNGCs may make important contributions to *BAK1-BIK1* signalling pathways as two other *CNGCs*, namely, *CNGC19* and *CNGC20* were recently shown to regulate *bak1* cell death (Yu et al., 2019). Recently, mutations in *CNCG6* were shown to result in compromised eATP-induced $[\text{Ca}^{2+}]_{\text{cyt}}$ elevation, MAPK activation and gene expression (Duong et al., 2021).

The slow vacuolar cation channel, *TWO-PORE CHANNEL 1* (*TPC1*), encodes a class of Ca^{2+} -dependent, Ca^{2+} -release ion channels that catalyse a flux of Ca^{2+} into the cytosol from vacuolar stores (Dadacz-Narloch et al., 2011, Peiter, 2011). Although its role in Ca^{2+} flux during plant responses to stress is not clear (Ranf et al., 2008), such a channel is feasible, if not necessary, to satisfy Ca^{2+} signature models (Gilroy et al., 2014).

The REDUCED HYPEROSMOLALITY-INDUCED $[\text{Ca}^{2+}]_{\text{i}}$ INCREASE (*OSCs*) are hyperosmolality-gated calcium-permeable channels that influx Ca^{2+} into the cytosol (Yuan et al., 2014). Recently, the *OSCA1.3* channel in *A. thaliana* was shown to mediate Ca^{2+} influx in guard cells, regulating their closure upon MAMP perception (Thor et al.,

2020). During treatments with flg22, BIK1 is activated and phosphorylates OSCA1.3, increasing its activity (Thor et al., 2020).

ROS production

In response to pathogens, ROS are propagated from NADPH oxidases, respiratory burst oxidase homologs (RBOHs) that react with superoxide dismutase (SOD) to form H₂O₂ (Bose et al., 2014). In *A. thaliana*, the principal RBOHs responsible for ROS production to pathogens are RBOHD and RBOHF (Torres et al., 2002). RBOHD/F are synergistically regulated by BIK1- and PBL1-mediated phosphorylation as well as Ca²⁺ (Miller et al., 2009, Kimura et al., 2013, Kadota et al., 2014, Torres et al., 2002, Li et al., 2014b). Evidence that PRRs may directly regulate RBOHD/F and subsequent ROS production has also been reported. Cellular damage releases ATP into the apoplast where it can act as a damage-associated signalling molecule via the LecRK-I.9 PRR, DORN1 (Song et al., 2006, Tanaka et al., 2014, Tanaka et al., 2010, Demidchik et al., 2003). Activation of the DORN1 kinase function leads to direct phosphorylation of RBOHD, resulting in an elevation of ROS production and stomatal closure (Chen et al., 2017).

*At*RBOHD function is mainly regulated through ([Ca²⁺]_{cyt}) via direct binding to the EF-hand motifs (Torres et al., 2002). Subsequent activation of CPKs and/or CDPKs results in activation of *At*RBOHD by direct phosphorylation (Boudsocq et al., 2010, Dubiella et al., 2013). For example, CPK5-dependent phosphorylation of *At*RBOHD occurs on both MAMP- and ROS stimulation (Dubiella et al., 2013). These studies, and others, highlight the importance of Ca²⁺ and ROS signalling, which may act in coordination to propagate signalling between cells (Gilroy et al., 2016).

MAP kinase and calcium-dependent protein kinase activation

Of the 34 genes encoding calcium dependent protein kinases (CPKs) in *A. thaliana*, a subset including CPK4, CPK5, CPK6 and CPK11 are rapidly and transiently activated after MAMP treatments (Boudsocq et al., 2010). *A. thaliana* *cpk5/6/11* mutants are defective in *Botrytis cinerea* (*B. cinerea*) induced ethylene production leading to increased susceptibility (Gravino et al., 2015). Amongst these

CPKs, CPK5 plays a central role during MTI and, as mentioned, phosphorylates several serine residues within AtRBOHD to regulate pattern-mediated ROS production (Dubiella et al., 2013). CPK5 and BIK1 phosphorylate AtRBOHD at unique sites, consistent with their role in independently regulating AtRBOHD activity (Kadota et al., 2014). Furthermore, AtCPK5 directly interacts with PRRs to regulate their function (Huang et al., 2020). For example, AtCPK5 interacts with AtCERK1 and AtLYK5 and phosphorylates the latter to mediate chitin-induced defence responses (Huang et al., 2020). Interestingly, CPK5 and its homologs are involved in ETI-induced HR via the phosphorylation of several WRKY transcription factors, which are also targets for NB-LRRs (Gao et al., 2013).

Mitogen-activated protein kinase (MAPK) cascades involve four types of kinase, MAP kinase kinase kinase kinases (MAP4Ks), MAP kinase kinase kinases (MAPKKKs), MAP kinase kinases (MKKs) and MAP kinases (MAPKs) (Colcombet and Hirt, 2008, Zhang et al., 2018b). Over 100 genes encoding MAPK cascade kinases have been identified in *A. thaliana*, including 20 MAPKs, 10 MKKs and 80 MAPKKKs (Zhang et al., 2006, Colcombet and Hirt, 2008). MAP kinase pathway members are typically highly conserved in plants and are rapidly activated up on MAMP perception (Asai et al., 2002, Liu and Zhan, 2004). Their activation is likely mediated by PRR complexes and their activity serves to transduce extracellular stimuli into robust defence signalling and defence gene expression (Yamada et al., 2016). MAPK cascades, MAPKKK3/5-MKK4/5-MPK3/6 and MEKK1-MKK1/2-MPK4 are rapidly but transiently activated upon PAMP perception (Asai et al., 2002), but their sustained activation has also been demonstrated during ETI (Tsuda et al., 2013). The MAP4Ks SERINE/THREONINE KINASE 1 (SIK1)/MAP4K3 and MAP4K4 have been found to also positively regulate BIK1 abundance and PTI signalling via direct interaction and phosphorylation (Zhang et al., 2018a, Jiang et al., 2019).

Several MTI-related signalling pathways converge on the two important, functionally redundant MAPKs, MPK3 and MPK6 (Rodriguez et al., 2010, Sozen et al., 2020, Yang et al., 2020a). The MAPKKKs, MAPKKK3 and MAPKKK5 are rapidly phosphorylated during flg22-, elf18- and chitin-induced MTI and are required for full MTI responses (Bi et al., 2018). Moreover, MAPKKK3 and MAPKKK5 are required for

MPK3/6 activation to these patterns and activated MPK6 phosphorylates MAPKKK5 in a feedback loop, enhancing MAPK activation and concomitant disease resistance (Bi et al., 2018).

Wounding also induces rapid activation of MPK3/6, which is dependent on MKK3, MKK4 and MKK5 as well as the clade C MAPKs, MPK1, MPK2 and MPK7 (Hettenhausen et al., 2015, Sozen et al., 2020). However, wound-induced MPK3/MPK6 activation is not triggered by JA treatment, indicating JA independence of the MKK4/5-MPK3/MPK6 module in wound responses (Hettenhausen et al., 2015). The MKK4/5-MPK1/2 cascade is required for SA/NPR1-mediated leaf senescence where MPK1 directly phosphorylates NPR1 and mediates NPR1 monomerisation (Zhang et al., 2020a).

MAPK activities are also under negative regulation. Similar to BIK1, MAPKs are targeted by phosphatases including the type 2Cs (PP2C) family members, AP2C1, AP2C2, AP2C3 and AP2C4 to regulate MAPK activity during MTI (Schweighofer et al., 2004, Umbrasaite et al., 2010, Galletti et al., 2011, Segonzac et al., 2014). Overexpression of AP2C phosphatases impairs ET production and resistance against *B. cinerea* (Schweighofer et al., 2004, Galletti et al., 2011).

The interdependency of CPKs and MPKs to mediate effective defence responses is becoming clearer. The induction of the tryptophan-derived indolic metabolites, camalexin and 4-methoxyindol-3-ylmethylglucosinolate (4MI3G), are critical to immunity in *A. thaliana* (Bednarek et al., 2009). The CPK5/6 and MPK3/6 signalling pathways promote the biosynthesis of camalexin and 4MI3G in response to *B. cinerea* (Yang et al., 2020a). MPK3/6 regulates camalexin biosynthesis by targeting WRKY33, which binds several promoter sequences of genes integral to the biosynthesis of indolic metabolites (Mao et al., 2011, Birkenbihl et al., 2017) (Fig. 2.1).

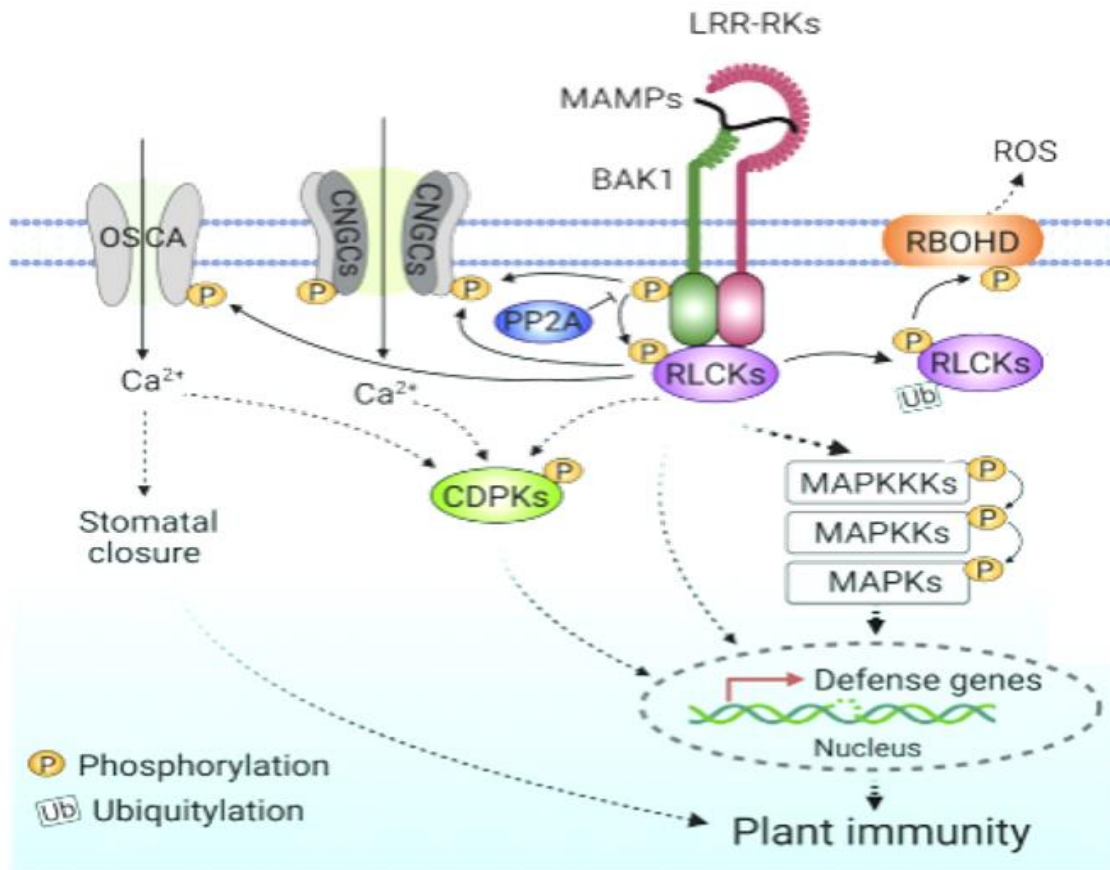


Figure 1.2: MAMP-triggered immune signalling in plants. The LRR-RK PRRs recognise bioactive ligands to mediate MTI in plants. Several activated PRR complexes recruit coreceptor, BAK1 and phosphorylate RLCKs to relay signalling downstream. The phosphatase, PP2A can remove phosphorylation to negatively regulate activated PRR complexes (Segonzac et al., 2014). RLCKs phosphorylate RBOHD to activate ROS production, and Ca^{2+} channels such as CNGCs and OSCAs to promote influx of Ca^{2+} into the cytosol, and promote stomatal closure. MAPK cascades (MAPKKKs–MAPKKs–MAPKs) are activated via phosphorylation to modulate immune gene expression in the nucleus. RLCKs such as BIK1 may migrate to the nucleus to directly regulate gene expression via transcription factors. PRRs regulate gene expression by activating CDPKs via phosphorylation. BAK1, BRI1-ASSOCIATED RECEPTOR KINASE1; CNGC, cyclic nucleotide-gated channel; LRR-RK, leucine-rich repeat receptor kinase; MAMP, microbe-associated molecular pattern; RBOHD, NADPH/respiratory burst oxidase protein D; MAPK, mitogen-activated protein kinase; PROTEIN PHOSPHATASE 2A (PP2A); PRR, pattern recognition receptor; RK, receptor kinase; RLCK, receptor-like cytoplasmic kinase; ROS, reactive oxygen species; CDPKs, calcium-dependent protein kinases. Adapted from (Kong et al., 2021).

Phytohormone signalling

Salicylic acid (SA, 2-hydroxybenzoic acid) is a phenolic plant hormone that serves as an essential signal molecule to confer disease resistance (Vlot et al., 2009, Alhoraibi et al., 2019). Both PTI and ETI rely on the production of SA, which also protects

distal tissues from subsequent infections via systemic acquired resistance (SAR) (Gao et al., 2015, Liu et al., 2020). SA initiates early defence-related gene expression in infected plants, including the expression of *PATHOGENESIS RELATED PROTEIN 1 (PR1)*, encoding an anti-microbe protein (Niderman et al., 1995). The accumulation of PR proteins is closely associated with the induction of HR and SAR to confer broad-spectrum resistance to pathogens (Vlot et al., 2009).

In *A. thaliana*, SA synthesis occurs via two pathways, namely, the phenylalanine ammonia-lyase (PAL) pathway and the isochorismate (IC) pathway (Dempsey et al., 2011). The IC pathway contributes approximately 95% of the SA production and occurs in the chloroplast where two enzymes, ISOCHORISMATE SYNTHASE 1/SALICYLIC ACID INDUCTION DEFICIENT 2 (ICS1/SID2) and ICS2 catalyse the conversion of chorismate to isochorismate (Wildermuth et al., 2001, Garcion et al., 2008). SA is subsequently transported to the cytosol by the multidrug and toxic compound extrusion transporter ENHANCED DISEASE SUSCEPTIBILITY 5 (EDS5) (Nawrath et al., 2002, Serrano et al., 2013). SA is perceived by two classes of receptors, namely, NONEXPRESSER OF PR GENES 1 (NPR1) and NPR1 paralogs, NPR2, NPR3 and NPR4 (Fu et al., 2012, Wu et al., 2012, Castello et al., 2018). NPR1 can directly bind SA and SA can also promote NPR1 via redox changes in the cell (Mou et al., 2003, Wu et al., 2012). Monomeric NPR1 shuttles to the nucleus to regulate transcription of SA-dependent genes, including PR genes, via TGACG SEQUENCE-SPECIFIC BINDING PROTEIN (TGA) transcription factors (Blanco et al., 2005, Kesarwani et al., 2007, Fu and Dong, 2013). The mechanisms of SA perception are not fully understood and biochemical screens have predicted almost 100 candidate SA-binding proteins occur in *A. thaliana* (Manohar et al., 2014).

MPK3 and to a lesser extent MPK6 have been proposed to play an important role in SA-mediated priming and enhancing defence gene activation and resistance (Beckers et al., 2009). Conversely, the MPK4 cascade negatively regulates SA signalling and mutants of this cascade exhibit SA accumulation, constitutive pathogenesis-related gene expression and SAR (Petersen et al., 2000).

Broadly speaking, the SA pathway is primarily induced by and effective in mediating resistance against biotrophic pathogens, whereas the jasmonic acid (JA)

pathway is primarily induced by, and effective in mediating, resistance against herbivores and necrotrophic pathogens (Glazebrook, 2005, Spoel and Dong, 2008). During biotic stress responses, SA and JA have been shown to be mutually antagonistic to the betterment of the plant (Leon-Reyes et al., 2010), and this antagonism may be hijacked by pathogens for the betterment of the pathogen (Cui et al., 2019).

In *A. thaliana*, biosynthesis of JA occurs across chloroplasts, peroxisomes and the cytosol via three pathways. The two pathways that have received most attention are the octadecane pathway starting with α -linolenic acid (18:3), and the hexadecane pathway starting with hexadecatrienoic acid (16:3) (Chini et al., 2018). The synthesis of 12-oxo-phytodienoic acid (12-OPDA) takes place in the chloroplast, which is then converted to JA in the peroxisome. In the cytoplasm, JA is metabolized into different structures by various chemical reactions, such as methyl jasmonate (MeJA), JA-iso-leucine (JA-Ile), *cis*-jasmonone (CJ), and 12-hydroxyjasmonic acid (12-OH-JA). Among these JAs, JA-Ile is the biologically active form of JA in plants (Wasternack and Song, 2017).

JA controls the expression of genes by promoting the ubiquitination and degradation of jasmonate ZIM domain (JAZ) proteins, of which there are 12 members in *A. thaliana* (Chini et al., 2007, Thines et al., 2007). JA signalling is perceived by JA receptor, CORONITINE RECEPTOR 1 (COI1), which binds to JAZs and transcription factors such as MYCs (Katsir et al., 2008). The competitive binding and degradation of JAZ repressors can release MYCs, resulting in the activation of JA responses by MYCs (Gimenez-Ibanez et al., 2017, Dubois et al., 2018).

Herbivores trigger transcriptional changes that are mainly controlled by the JA pathway (Reymond et al., 2004, De Vos et al., 2005b). Accordingly, *A. thaliana* mutants impaired in JA responses are more susceptible to insect feeding (McConn et al., 1997; Reymond et al., 2004). Mechanical damage can promote the hydrolysis of the precursor protein PROPEP1 to AtPep1, which binds to the plasma membrane-localised LRR-RLKs, PEPR1 and PEPR2, activating immune signalling and JA responses (Yamaguchi et al., 2010).

The gaseous hormone, ethylene (C₂H₄) has roles in growth and development as well as in plant immunity. Ethylene biosynthesis is strongly induced during MTI and ETI and is most closely associated with plant responses to necrotrophic infection including infection by *B. cinerea* (Cristescu et al., 2002). MPK3/MPK6 positively regulate ethylene production via phosphorylation of two 1-aminocyclopropane-1-carboxylic acid synthase (ACS) isoforms, ACS2 and ACS6 (Yoo and Sheen, 2008, Xu and Zhang, 2014).

Antagonistic and synergistic interactions between SA, JA and ethylene have been reported (van Loon et al., 2006, Pieterse et al., 2012). For example, ethylene production is strongly induced by SA treatments, and SA potentiates ethylene in *A. thaliana* in response to *Pseudomonas syringae* (*P. syringae*) infection, which is dependent on the MPK3/6-ACS2/6 module (Guan et al., 2015). JA and ethylene are known to co-ordinately regulate plant stress responses (Zhu, 2014). JA treatment regulates the expression of the transcription factor, *ETHYLENE RESPONSE FACTOR 1* (*ERF1*) via JAZ-MYC2 as well as *VEGETATIVE STORAGE PROTEIN 2* (*VSP2*), an acid phosphatase with anti-insect activity (Lorenzo et al., 2003). Subsequently, ERF1 targets the promoter of *PLANT DEFENSIN 1.2* (*PDF1.2*) to drive its expression, thereby conferring protection against necrotrophic pathogens (Pieterse et al., 2012).

Secondary metabolite biosynthesis in defence

Plant secondary metabolites, including phenolics, terpenes, and nitrogen-containing compounds are specialized compounds that mediate plant-environment interactions (Erb and Kliebenstein, 2020). Of the nitrogen-containing metabolites important in defence, the Brassicaceae-specific glucosinolates are precursors of several classes of anti-parasitic compounds including aliphatic glucosinolates (AGSs), aromatic glucosinolates (ARGSs), and indole glucosinolates (IGSs) (Halkier and Gershenzon, 2006). Of the glucosinolates in plants, IGSs have come under particular attention due to their importance in plant immunity (Piaseck et al., 2015). Specifically, the tryptophan-derived IGSs such as 4-methoxyindol-3-ylmethylglucosinolate (4MI3G) and the phytoalexin, camalexin are critical to plant immunity (Tsuji et al., 1992, Thomma et

al., 1999, Bednarek et al., 2009, Schlaeppi et al., 2010, Stotz et al., 2011, Hiruma et al., 2013).

In *A. thaliana* Tryptophan is converted to the key intermediate, indole-3-acetaldoxime (IAOx) in a reaction catalysed by two P450 enzymes, CYP79B2 and CYP79B3 (Zhao et al., 2002). IAOx is required for the biosynthesis of camalexin, IGSs and LMW indoles including auxin indole-3-acetic acid (IAA) (Zhao et al., 2002). In one branch, IAOx is converted to I3G via several intermediates (Sonderby et al., 2010). The conversion of I3G into the two main IGS derivatives, 4MI3G and 1MI3G is regulated by CYP81Fs and IGMT1/IGMT2 (Pfalz et al., 2009).

In another branch, the cytochrome P450 enzymes CYP71A13, CYP71A12, and CYP71B15 (PAD3) catalyse camalexin synthesis from IAOx (Zhou et al., 1999, Schuhegger et al., 2006, Nafisi et al., 2007, Muller et al., 2015, Mucha et al., 2019). IAOx is dehydrated to indole-3-acetonitrile (IAN) by two cytochrome P450s, CYP71A12 and CYP71A13 (Nafisi et al., 2007, Muller et al., 2015). Subsequently, IAN undergoes oxidation and conjugation to glutathione (Nafisi et al., 2007, Bottcher et al., 2009), followed by Cys [Cys(IAN)], requiring γ -GLUTAMYL PEPTIDASE1 (GGP1) and GGP3 (Geu-Flores et al., 2011). Cys(IAN) is then converted to camalexin by PAD3 (Zhou et al., 1999, Schuhegger et al., 2006). Camalexin plays an important role in the response to several necrotrophic and biotrophic fungi including *B. cinerea*, *Alternaria brassicicola* and *Golovinomyces orontii* (Thomma et al., 1999, Consonni et al., 2010), and the oomycete *Phytophthora brassicae* (Schlaeppi et al., 2010).

Biosynthesis of IGSs and camalexin is tightly regulated by several transcription factors including, MYB34, MYB51, and MYB122 (Frerigmann et al., 2016). Furthermore, the *A. thaliana* transcription factors *WRKY18*, *WRKY33*, and *WRKY40* may regulate camalexin production in response to a number of biotic stresses (Mao et al., 2011). Upstream of *WRKY33*-mediated *PAD3* expression, co-regulation of indole glucosinolates and camalexin pathways occurs via the protein kinases, CPK5/CPK6 and MPK3/MPK6 (Yang et al., 2020a). Plants defective in IGSs biosynthesis are compromised for flg22-induced callose deposition, implicating IGS directly in MTI and IGS biosynthesis in callose deposition (Clay et al., 2009). The *A. thaliana* myrosinase, PENETRATION 2 (PEN2) is involved in hydrolysing precursor glucosinolates into active

forms, which are possibly secreted into the apoplast via the plasma membrane-localised ABC transporter (PEN3) (Stein et al., 2006, Bednarek et al., 2009). PEN2 and PEN3, along with PEN1, a protein linked to secretory membrane trafficking (Johansson et al., 2014), act as central components in cell wall-based defence (Bednarek et al., 2009).

1.3 NLR-mediated immunity

Pathogens deliver effector proteins into host cells to neutralize immune responses and promote infection. Plant intracellular nucleotide binding, leucine-rich repeat (NLR) receptors detect effectors to initiate immune responses termed ETI. Plant NLR receptors are classified on the basis of their *N*-terminal signalling domain architectures as either Toll/interleukin-1 (TIR) NLRs (TNLs) or coiled-coil (CC) NLRs (CNLs). Activated TNLs and CNLs form multimeric protein complexes termed “resistosomes” to mediate immune responses and HR (Bi et al., 2021). For example, the canonical CNL, HOPZ-ACTIVATED RESISTANCE 1 (ZAR1), forms a calcium-permeable channel at the plasma membrane through its CC domains, enabling Ca²⁺ influx and subsequent HR in *A. thaliana* and *N. benthamiana* (Bi et al., 2021). ZAR1 indirectly detects multiple plant pathogens using decoy substrates of the RLCK VII subfamily, which are targeted by pathogen effectors including the *P. syringae* type III secretion effector families (HopZ1, HopBA1, HopF1/F2, HopO1 and HopX) (van der Hoorn and Kamoun, 2008, Wang et al., 2015a, Laflamme et al., 2020). In the formation of the resistosome, members of the RLCK VII subfamily become uridylylated and are recruited to the pre-formed ZAR1-RKS1 complex (Seto et al., 2017). Recruitment to ZAR1-RKS1 facilitates the release of ADP from ZAR1, leading to a primed state of the ZAR1-RKS1-RLCK^{UMP} complex that may be readily activated by incorporating dATP or ATP into ZAR1 (Wang et al., 2019a).

In TNL-triggered ETI, the lipase-like protein, ENHANCED SUSCEPTIBILITY 1 (EDS1) forms a complex with PHYTOALEXIN DEFICIENT 4 (PAD4) and SENESCENCE-ASSOCIATED GENE 101 (SAG101) to modulate defence signalling downstream of TNL receptors and promote resistance (Aarts et al., 1998, Feys et al., 2001, Feys et al., 2005).

The EDS1 heterodimeric complex formations, EDS1/PAD4 or EDS1/SAG101 determines subcellular localisation of EDS1, depending on the interacting partner (Zhu et al., 2011). Enzymatic catalysis of NAD⁺ activates EDS1 through an unknown mechanism (Horsefield et al., 2019). TNLs also require so-called ‘helper’ NLRs of the CC-type to mediate immunity such as the two RPW8-NLR R protein subclasses, ADR1 and NRG1 NLRs (Castel et al., 2019). EDS1 complexes promote *ICS1* expression and SA accumulation, leading to HR (Zhou et al., 1999, Feys et al., 2005).

1.4 Interdependency of PRRs and NLRs

Some components of PRR- and NLR-mediated immunity do not fall strictly into MTI or ETI responses (Thomma et al., 2011). For example, the tomato Cf R proteins, Cf-2, Cf-4, Cf-4E, and Cf-9 are cognate receptors for a suite of *C. fulvum* effectors, Avr2, Avr4, Avr4E, and Avr9, respectively (Jones et al., 1994, Dixon et al., 1996, Thomas et al., 1997). Tomato Cf proteins are plasma-membrane localised RLPs and mediate resistance to *C. fulvum* by triggering HR. Hence, RLPs can mediate ETI-like responses at the PM. *At*RLP23-mediated MTI is impaired in *pad4* and *eds1* mutants suggesting that PAD4-EDS1 complexes may associate with PM PRR complexes (Pruitt et al., 2021). Surprisingly, interactions between the RLP adaptor, SOBIR1 and helper NLR, ACTIVATED DISEASE RESISTANCE 1 (ADR1) have been reported (Pruitt et al., 2021). ADR1 is an essential component of PAD4-EDS1-ADR1 complexes and required for PAD4-EDS1-ADR1-mediated ETI (Bonardi et al., 2011). NLR-mediated signalling involves the prototypical MTI components, MAP kinases and NADPH oxidases (Kadota et al., 2019), and activation of PRRs leads to increased transcript accumulation of multiple NLRs (Bjornson et al., 2021). Several studies have reported an interdependency of components typically considered canonical MTI and canonical ETI components (Ngou et al., 2021, Pruitt et al., 2021, Yuan et al., 2021). For example, activation of PRRs enhances NLR-mediated HR, suggesting both pathways cooperate in plant defence against pathogens (Ngou et al., 2021, Yuan et al., 2021).

1.5 Herbivores as inducers and suppressors of plant immunity

1.5.1 The interface of plant-aphid interactions

When addressing the interactions between plants and their herbivorous pests, it is important to consider the diversity of feeding styles adopted these insects. Feeding styles of herbivorous insects are broadly categorised into three groups; chewing insects such as caterpillars and beetles, piercing-sucking insects such as aphids, whiteflies and planthoppers, and rasping insects such as mites and thrips. The distinct feeding styles and behaviours have profound effects on the nature and success of deployable plant defence responses to insect pests (Wu and Baldwin, 2010). See recent reviews for detailed descriptions of plant responses to chewing herbivores (Wu and Baldwin, 2010, Acevedo et al., 2015, Basu et al., 2018, Reymond, 2021).

Herbivorous insects both trigger and suppress plant immunity in parallel; a paradigm not uncommon during plant-pathogen interactions. Herbivore modulation of plant defence responses occurs during insect feeding and direct interactions between insect mouthparts or secretions and plant cells. During feeding, the aphid stylets navigate intercellularly and periodically probe adjacent plant cells (Tjallingii, 2006). This navigational phase is termed the pathway or probing phase. Two distinct types of saliva are secreted into the plant host during the pathway and feeding phases, presumably to modulate plant defence and aid feeding (Will et al., 2013). Watery saliva is secreted into probed cells during the pathway phase, but also for up to 120s after stylets have reached the phloem sieve elements to establish prolonged feeding (Tjallingii and Hogenesch, 1993).

The salivary secretome of aphids and other piercing-sucking insects is a complex milieu of proteins with diverse functions (van Bel and Will, 2016). Numerous enzymes with presumed and proven function in promoting the establishment and maintenance of feeding sites, suppressing plant defences, and acquisition of nutrient uptake have been identified. Watery saliva alone contains hundreds or thousands of proteins. Carolan et al. (2009, 2011) identified hundreds of proteins within pea aphid saliva, and

studies in *M. persicae* have also revealed several hundred secreted proteins (Harmel et al., 2008). A comparison of the cereal aphids, *Sitobion avenae* and *Metopolophium dirhodum* salivary proteomes with that of pea aphid revealed similarities in cereal aphid secretomes indicating conservation in adaptations for the monocot feeding habit (Rao et al., 2013). Meanwhile, other studies deployed proteomic analyses of aphid salivary gland extracts to identify putative secretome components (Atamian et al., 2013, Yang et al., 2018). For example, Atamian et al. (2013) identified over 400 proteins in *Macrosiphum euphorbiae* salivary glands, many containing secretory signal peptides.

During stylet movement through the apoplast, aphids deposit gelling saliva to form a continuous sheath around the stylet that can harden to maintain an open channel. Gelling saliva may offer mechanical protection as well as lubrication to the stylet (Tjallingii and Hogenesch, 1993, Will et al., 2012). It may also modulate host defence by directly interfering with plant defence compounds. Interestingly, gelling saliva contains several enzymes that may detoxify phenolic compounds, presumably to counter plant defence responses (Sharma et al., 2014). The most abundant proteins within gelling saliva are sheath proteins that may help to harden and maintain the rigidity of salivary matrix (Carolan et al., 2011). Not limited to aphids, other piercing-sucking insects, such as whiteflies and planthoppers utilise analogous secretions to modulate plant immunity and promote feeding (Huang et al., 2018, Walling, 2000).

As a consequence of herbivore feeding styles and mouthpart anatomy, saliva or oral secretions are likely to act at the interface between insects and plants. As such, saliva has largely been the focus of studies identifying components that modulate the suppression and induction of host immunity (Mutti et al., 2006, Ramsey et al., 2007, Harmel et al., 2008, Mutti et al., 2008, Carolan et al., 2009, De Vos and Jander, 2009, Bos et al., 2010, Carolan et al., 2011, Bricchi et al., 2012, Atamian et al., 2013, Rao et al., 2013, Chaudhary et al., 2014, Elzinga et al., 2014, van Bel and Will, 2016, Shangguan et al., 2018, Iida et al., 2019, Rao et al., 2019). Approximately two dozen elicitors or herbivore-associated molecular patterns (HAMPs) have been isolated from chewing insects (Reymond, 2021). However, to date, only VuINR (Steinbrenner et al., 2020) and LecRK-1.8 (Stahl et al., 2020) have been characterised as PRRs that perceive elicitors inceptin (*Vu-In*) (Schmelz et al., 2006), and phosphatidylcholines (PCs),

respectively. In contrast with the array of elicitors isolated from chewing insects, very few elicitors have been characterised from piercing-sucking herbivores. The chaperonin, GroEL is derived from the aphid endosymbiont, *Buchnera aphidicola* and is demonstrated to induce an array of plant immune responses, and its expression *in planta* reduces aphid fecundity (Chaudhary et al., 2014, Elzinga et al., 2014). Furthermore, several *M. persicae*-derived secreted proteins named Mp56, Mp57 and Mp58, also display putative elicitor function *in planta* (Elzinga et al., 2014). No PRR recognising aphid-derived elicitors has been characterised to date. However, piercing-sucking insects, such as aphids, are thought to deliver an array of immuno-suppressive virulence factors into their plant host during feeding (Harmel et al., 2008, Carolan et al., 2009, Bos et al., 2010, Carolan et al., 2011, Atamian et al., 2013, Rao et al., 2013, Vandermoten et al., 2014, Mugford et al., 2016, van Bel and Will, 2016). For several of these effectors, direct perturbations in plant defence responses and subsequent insect performance have been characterised.

In addition to saliva, aphid organs, tissues and excretions are in contact with plant cells during infection. Mouthparts, feet/legs and honeydew may shed or contain elicitors/effectors to antagonise or promote feeding and induce or suppress immune responses (Schwartzberg et al., 2014, Will and Vilcinskas, 2015).

1.5.2 The role of MTI to piercing-sucking herbivores

Characteristic MTI responses including ROS production, defence gene expression, phytoalexin production and callose deposition are observed during aphid feeding and exposure of plants to crude extracts (Prince et al., 2014, Jaouannet et al., 2015, Pant and Huang, 2021). However, no aphid PRR has been identified and plant innate immune responses to aphids are not well understood. The most abundant endosymbiont protein, the *B. aphidicola* chaperonin, GroEL, has been identified in aphid saliva and honeydew, and is secreted into plant cells during feeding (Sabri et al., 2013, Vandermoten et al., 2014). GroEL induces plant immune responses in *A. thaliana*

and tomato including ROS production, callose deposition and defence gene expression (Chaudhary et al., 2014, Elzinga et al., 2014). Consistent with its role as a HAMP, heat treatment does not affect its activity, and GroEL-induced MTI is dependent on the LRR-RK co-receptor, BAK1 (Chaudhary et al., 2014). However, no immunogenic epitope has been isolated from the GroEL protein and no PRR identified that recognises GroEL has been characterised (Chaudhary et al., 2014).

Low molecular weight elicitors from aphid extracts (Prince et al., 2014), and aphid saliva (De Vos and Jander, 2009), have been implicated in MTI responses in plants. Prince et al. (2014) used a whole-body aphid homogenate (extract) to induce a slow kinetic ROS burst, defence gene expression and callose deposition. These responses were dependent on BAK1 although the *A. thaliana bak1-5* mutant, defective in immune responses, but not brassinosteroid signalling, did not display altered resistance to *M. persicae*. de Vos and Jander (2009), isolated a proteinaceous, low molecular weight salivary component that induced the conversion of I3M to 4MI3M, an anti-feeding glucosinolate (Kim and Jander, 2007). However, attempts to isolate the immunogenic peptide were unsuccessful (de Vos and Jander, 2009).

ROS accumulation is believed to play a role in plant resistance to invading aphids by providing direct phytotoxicity and regulating downstream immune responses in a variety of plant hosts (Lei et al., 2014, Shoala et al., 2018, Sun et al., 2018, Shao et al., 2019, Pant and Huang, 2021). Evidence of a role for NADPH oxidases in generating ROS was provided via pharmacological inhibition by DPI in wheat against infestation of *Diuraphis noxia* (Moloi and van der Westhuizen, 2006). Furthermore, increased NADPH oxidase activities are observed in wheat and maize infested with aphids (Sytykiewicz et al., 2014). Several studies have provided direct genetic evidence that both RBOHD and RBOHF influence ROS production and concomitant influence of aphid performance (Miller et al., 2009, Jaouannet et al., 2015). Aphid-induced ROS accumulation in *A. thaliana* may be regulated, in part, by BIK1 (Lei et al., 2014). The *bik1* mutant displayed increased H₂O₂ accumulation relative to wild-type plants, and the increased ROS was correlated with increased resistance to the aphid (Lei et al., 2014), suggesting BIK1 acts as a negative regulator of ROS to aphids. In addition to ROS, calcium bursts are thought to play an important role in plant defence to aphids. A feeding induced, BAK1-

dependent $[Ca^{2+}]_{cyt}$ elevation was identified in *A. thaliana* reporters expressing the GFP-based GCaMP3 reporter (Vincent et al., 2017).

Previous studies have shown that several WRKY family transcription factors have important functions in plant defence to aphids. Silencing the tomato *S*/WRKY72 increased susceptibility to the potato aphid (Bhattarai et al., 2010, Atamian et al., 2013), and *Chrysanthemum morifolium*, *Cm*WRKY53 mediates the sensitivity of chrysanthemum to the *Macrosiphoniella sanborni* aphid via the regulation of secondary metabolites (Zhang et al., 2020b). *A. thaliana* WRKY22 and its homologue, WRKY29 are induced by flg22 treatment and function downstream of MEKK1/MTKMKK4/MKK5-MPK3/MPK6 (Asai et al., 2002). Whilst no significant increase in expression of *At*WRKY22 to *M. persicae* is observed, *wrky22* mutants display increased resistance to the insect and up-regulation in genes involved in SA signalling (Kloth et al., 2016). WRKY22-mediated susceptibility in *A. thaliana* may, therefore, be associated with its suppression of SA signalling in the epidermal and mesophyll tissues (Kloth et al., 2016).

Camalexin and IGSs are thought to be central components of plant defence to aphids. *PAD3* expression is induced during aphid challenge (Zhou et al., 1999, Pegadaraju et al., 2005, Kusnierczyk et al., 2008, Prince et al., 2014), however, the literature is conflicted as to whether *pad3* mutants are altered for aphid resistance. Pegadaraju et al. (2005) found comparable aphid fitness on *pad3* relative to wild-type indicating camalexin is not required for aphid resistance. Similarly, Kim et al. (2008) found no change in fecundity of aphids on *cyp79b2/b3* mutants relative to wild-type plants. However, Kettles et al. (2013) found an increase in *M. persicae* fitness on the *pad3* mutant and *cyp79b2/b3* double mutant relative to wild-type and a similar increase in cabbage aphid fitness was identified on the *A. thaliana pad3* mutant (Kusnierczyk et al., 2008). Interestingly, Prince et al. (2014) found *PAD3* expression in response to *M. persicae* extract was independent of BAK1 suggesting that at least two pathways are required for defence responses in *A. thaliana*.

PAD4, along with its binding partner EDS1, modulates SA biosynthesis (Zhou et al., 1998). PAD4 is also required for camalexin biosynthesis and has been implicated in defence responses to *M. persicae* (Pegadaraju et al., 2005, Dongus et al., 2020).

However, genetic evidence suggests that PAD4-mediated resistance does not require the accumulation of camalexin or SA (Pegadaraju et al., 2005). Herbivory activates the production of JA, SA and ethylene, which regulate the expression of defence genes and production of anti-insect compounds (Erb et al., 2012). JA is thought to play a major role in the outcomes of plant-insect interactions, but sap-feeding insects may induce both JA and SA pathways (Thaler et al., 2012, Johnson et al., 2020). Constitutive activation of JA signalling was shown to contribute to *M. persicae* resistance (Ellis et al., 2002). *M. persicae* feeding induces the expression of SA-related marker genes such as *PR-1* (Moran and Thompson, 2001), and evidence of SA-related JA repression by aphids has been observed in several studies (Kerchev et al., 2013). However, high levels of SA do not necessarily correlate with increased susceptibility (Kerchev et al., 2013). Occasionally, phytohormone concentrations are undetectable during aphid feeding (De Vos et al., 2005a), suggesting that further studies are required to decipher the role of phytohormones in plant defence to aphids (Jaouannet et al., 2014). Furthermore, the upstream signalling components and mechanisms leading to aphid-induced phytohormone signalling, remain largely elusive.

1.5.3 The role of ETI in defence against insect herbivores

Similar to plant pathogens, aphids secrete an arsenal of effector molecules to modulate host cell processes and promote fitness. Several effectors have been functionally characterised from the saliva of piercing-sucking insects (Table 1.2). The majority of functionally characterised effectors display immuno-suppressive function including proteases, detoxifiers and modulators of plant Ca^{2+} and ROS homeostasis (van Bel and Will, 2016). Despite the number of effectors that are predicted to modulate plant immune responses through immunosuppressive functions, very few intracellular receptors of these effectors have been identified in plants.

The aphid-specific effector, C002 has been identified in *M. persicae* (*MpC002*), *A. pisum* (*ApC002*) and *R. padi* (*RpC002*), and is one of the best-studied salivary effectors (Mutti et al., 2008, Bos et al., 2010, Pitino et al., 2013, Elzinga et al., 2014,

Coleman et al., 2015, Escudero-Martinez et al., 2020). Along with PlntO1 (Mp1), and PlntO2 (Mp2), *MpC002* expression in transgenic *A. thaliana* increases *M. persicae* reproduction, suggesting they are not recognised by *A. thaliana* immune receptors (Pitino et al., 2013). Immuno-gold labelling revealed that *MpPlntO1* and *MpC002* are located around the aphid stylet sheaths suggesting these effectors are embedded in the apoplastic space of mesophyll tissue (Mugford et al., 2016). Interestingly, expression of the *A. pisum* orthologs of these effectors did not alter *M. persicae* fitness, suggesting these effectors may promote aphid colonization on specific plant species. In general agreement with this, a transcriptomic study identified effectors whose expression may be modulated depending on host cues (Chen et al., 2020). This might suggest that effector repertoires contribute toward host adaptation or plasticity by the insect.

Several aphid salivary proteins with demonstrable immuno-suppressive function, may perturb aphid colonisation through activation of host immunity. These effectors include *M. persicae* Mp10 and Mp42 (Bos et al., 2010, Rodriguez et al., 2014). Transient expression of the chemosensory protein, Mp10, suppresses the flg22-induced ROS burst and induces chlorosis and local cell death in *N. benthamiana* (Bos et al., 2010). Both Mp10 and Mp42 expression reduces aphid fecundity, however, transient expression of Mp10 but not Mp42 activates SA and JA signalling pathways (Rodriguez et al., 2014). The mechanisms that underlie Mp10-induced chlorosis or the immuno-suppressive function of Mp10, requires further study. However, Mp10 is delivered into the cytosol of plant cells during probing in the pathway phase (Mugford et al., 2016), which may suggest it functions very early in plant-aphid interactions.

The aphid effector, Mp55 suppresses callose deposition and the conversion of I3M to 4MI3M, an indole glucosinolate and effective anti-aphid metabolite in *A. thaliana* (Kim and Jander, 2007, Elzinga et al., 2014). Overexpression of Mp55 increased aphid fecundity and were chosen by aphids in choice test assays, whereas silencing reduced fecundity (Elzinga et al., 2014). In the same screen, three effectors, Mp56, Mp57, and Mp58 were found to inhibit insect reproduction, presumably by activating plant defence responses (Elzinga et al., 2014).

The Arginine rich, mutated in early stage of tumours (Armet) effector is secreted by the silver leaf whitefly (*Bemisia tabaci*), aphids, *M. persicae* and *A. pisum* and the migratory locust (*Locusta migratoria*) into host plants. Armet promotes the accumulation of SA, thereby increasing the resistance of plants to bacterial pathogens, but not to aphids (Cui et al., 2019). Overexpression of *BtArmet* in tobacco also enhances *B. tabaci* performance, and silencing the gene, suppresses performance (Du et al., 2022). *BtArmet* interacts with a cystatin protein, *NtCYS6* to suppress defence and confer whitefly resistance (Du et al., 2022).

Aphids and planthoppers secrete protein disulfide isomerases (PDIs) into host cells to modulate host defence during feeding (Fu et al., 2020). PDI have been identified in insect saliva including from the small brown planthopper (*Laodelphax striatellus*; SBPH), and when secreted into plant cells induce cell death, possibly via the Ca^{2+} , ROS and JA signalling (Carolan et al., 2009, Carolan et al., 2011, Rao et al., 2013, van Bel and Will, 2016, Miao et al., 2018, Huang et al., 2019, Fu et al., 2020). Transient expression of *LsPDI1* impaired *M. persicae* performance (Fu et al., 2020). Another effector from SBPH, the salivary DNase II, with DNA-degrading activity, suppresses ROS accumulation and callose deposition in rice (Huang et al., 2019). Knocking down the expression of *DNase II* results in decreased performance of SBPH reared on rice plants, however, this resistance is independent of SA, JA or ethylene (Huang et al., 2019).

Table 1.2: Immuno-suppressive effectors from piercing-sucking insect herbivores.

Effector	Species	Responsive host	ETS-related response	Reference
Al6	<i>Apolygus lucorum</i>	<i>Nicotiana benthamiana</i>	ROS inhibition	(Dong et al., 2020)
Armet	<i>Acyrtosiphon pisum</i> / <i>Myzus persicae</i>	<i>Vicia fabae</i> / <i>Medicago truncatula</i> / <i>Nicotiana benthamiana</i>	Gene expression / SA production	(Wang et al., 2015b); (Cui et al., 2015)
Bsp9	<i>Bemisia tabaci</i>	<i>Arabidopsis thaliana</i>	Insect fecundity / Gene expression	(Wang et al., 2019b)
Bt56	<i>Bemisia tabaci</i>	<i>Nicotiana tabacum</i> , <i>Gossypium hirsutum</i>	Insect fecundity	(Xu et al., 2019)
Btfer1	<i>Bemisia tabaci</i>	<i>Solanum lycopersicum</i>	Insect fecundity / Insect performance	(Su et al., 2019)
ApC002 / MpC002 / RpC002	<i>Acyrtosiphon pisum</i> / <i>Myzus persicae</i> / <i>Rhopalosiphum padi</i>	<i>Vicia fabae</i> / <i>Nicotiana tabacum</i> / <i>Nicotiana benthamiana</i> / <i>Arabidopsis thaliana</i> / <i>Hordeum vulgare</i>	Insect fecundity	(Mutti et al., 2008); (Bos et al., 2010); (Elzinga et al., 2014); (Coleman et al., 2015); (Escudero-Martinez et al., 2020)
Cathepsin B3	<i>Myzus persicae</i>	<i>Nicotiana tabacum</i>	Insect performance	(Guo et al., 2020)
AcDCXR	<i>Aphis craccivora</i>	<i>Pisum sativum</i>	Insect fecundity	(MacWilliams et al., 2020)
Me10	<i>Macrosiphum euphorbiae</i>	<i>Nicotiana benthamiana</i> / <i>Solanum lycopersicum</i>	Insect fecundity	(Atamian et al., 2013)
Me23	<i>Macrosiphum euphorbiae</i>	<i>Nicotiana benthamiana</i> / <i>Solanum lycopersicum</i>	Insect fecundity	(Atamian et al., 2013)
Me47	<i>Macrosiphum euphorbiae</i>	<i>Nicotiana benthamiana</i> / <i>Solanum lycopersicum</i> / <i>Arabidopsis thaliana</i>	Insect fecundity	(Kettles and Kaloshian, 2016)
MIF	<i>Myzus persicae</i>	<i>Nicotiana benthamiana</i>	Gene expression / HR response	(Naessens et al., 2015)
Mp1	<i>Myzus persicae</i>	<i>Arabidopsis thaliana</i> / <i>Nicotiana benthamiana</i>	Insect fecundity	(Pitino et al., 2013)
Mp2	<i>Myzus persicae</i>	<i>Arabidopsis thaliana</i>	Insect fecundity	(Coleman et al., 2015)
Mp10	<i>Myzus persicae</i>	<i>Nicotiana benthamiana</i> / <i>Arabidopsis thaliana</i>	HR response / ROS suppression / Insect fecundity	(Bos et al., 2010)
Mp42	<i>Myzus persicae</i>	<i>Nicotiana tabacum</i>	HR response / ROS suppression / Insect fecundity	(Bos et al., 2010)
Mp55	<i>Myzus persicae</i>	<i>Arabidopsis thaliana</i> / <i>Nicotiana tabacum</i>	Insect fecundity	(Elzinga et al., 2014)
NIMLP	<i>Nilaparvata lugens</i>	<i>Oryza sativa</i>	HR response / Insect fecundity	(Shangguan et al., 2018)
NcSP75	<i>Nephotettix cincticeps</i>	<i>Oryza sativa</i>	Insect fecundity / Insect performance	(Matsumoto and Hattori, 2018)
NI12	<i>Nilaparvata lugens</i>	<i>Oryza sativa</i> / <i>Nicotiana benthamiana</i>	Gene expression	(Rao et al., 2019)
NI16	<i>Nilaparvata lugens</i>	<i>Oryza sativa</i> / <i>Nicotiana benthamiana</i>	Gene expression	(Rao et al., 2019)
NI28	<i>Nilaparvata lugens</i>	<i>Oryza sativa</i> / <i>Nicotiana benthamiana</i>	Gene expression	(Rao et al., 2019)
NI32	<i>Nilaparvata lugens</i>	<i>Oryza sativa</i> / <i>Nicotiana benthamiana</i>	Gene expression	(Rao et al., 2019)
NISEF1	<i>Nilaparvata lugens</i>	<i>Oryza sativa</i>	Calcium, ROS suppression / Insect fecundity	(Ye et al., 2017)
Rp1	<i>Rhopalosiphum padi</i>	<i>Hordeum vulgare</i>	Insect fecundity	(Escudero-Martinez et al., 2020)
Rp58	<i>Rhopalosiphum padi</i>	<i>Hordeum vulgare</i>	Insect fecundity	(Escudero-Martinez et al., 2020)
Tu28 / Te28	<i>Tetranychus urticae</i> , <i>Tetranychus evansi</i>	<i>Nicotiana benthamiana</i>	Insect fecundity / Gene expression	(Villarroel et al., 2016)
Tu84 / Te84	<i>Tetranychus urticae</i> , <i>Tetranychus evansi</i>	<i>Nicotiana benthamiana</i>	Insect fecundity / Gene expression	(Villarroel et al., 2016)
Vitellogenin	<i>Laodelphax striatellus</i>	<i>Oryza sativa</i>	ROS suppression / Insect fecundity	(Ji et al., 2021)
Ya1	<i>Myzus persicae</i>	<i>Arabidopsis thaliana</i>	Insect fecundity	(Chen et al., 2020)

1.6 This project

1.6.1 Aims of this research

Plant immune responses to aphid-derived elicitors remains a black box despite our increasing understanding of plant defence mechanisms and aphid suppression of plant defence. The aims of this study are to investigate plant immune responses induced by aphid elicitors and the aphid-derived components that trigger these responses. Additionally, to investigate and validate genetic screening approaches to enable accelerated research into aphid-plant interactions.

1.6.2 Summary of thesis content

To investigate the role of MTI to aphids, I developed an activity-led purification strategy to identify elicitors of immune signalling in *A. thaliana*. I utilised two reporters of MTI responses, namely, the *pWRKY33::fLUC* (Kato et al., 2020) transcriptional reporter and GCaMP3 (Tian et al., 2009) calcium reporter to monitor *WRKY33* promoter activity and $[Ca^{2+}]_{cyt}$, respectively. I used biochemical and pharmacological methods to describe the chemical nature of immunoactive elicitors within aphid-derived extracts.

I utilised genetic tools such as *A. thaliana* T-DNA mutants to describe the canonical nature of immune responses to aphid-derived elicitors. Moreover, I assessed the breadth of MTI responses in *A. thaliana* and used forward and reverse genetic approaches to assess the function of gene loci in conferring immune responses to aphid elicitors.

1.6.3 Contribution to thesis

All results presented in this thesis were generated in experiments conducted by me. Some experimental work was carried out by Josh Joyce (JIC, Hogenhout lab) including during insect fecundity assays. Josh Joyce also generated *sobir1-12* x *UBQ10:GCaMP3* and *sobir1-13* x *UBQ10:GCaMP3* that were used in this study. Plant lines and mutant sources are acknowledged in Chapter 2. Jan Sklenar (Menke group, JIC) carried out mass spectrometry.

Chapter 2
Materials and Methods

2.1 Insect rearing conditions

2.1.1 *Myzus persicae* Clone 0

The green peach aphid (*Myzus persicae*) RRes genotype O (Bos et al., 2010), were continuously reared in stock cages of 52 cm³ containing up to six Chinese cabbage plants (*Brassica rapa* subsp. *chinensis*) aged 4-8 weeks with a 14-h-day (90 $\mu\text{mol m}^{-2}\text{sec}^{-1}$ at 18°C) and 10-h-night (15°C) photoperiod.

2.1.2 *Rhopalosiphum padi*

The cherry-oat aphid (*Rhopalosiphum padi*), were continuously reared in stock cages of 24 cm x 54 cm x 47 cm containing up to four oat plants (*Avena sativa*) aged 4-8 weeks with a 14-h-day (90 $\mu\text{mol m}^{-2}\text{sec}^{-1}$ at 18°C) and 10-h-night (15°C) photoperiod.

2.2 Plant growth conditions

2.2.1 *Arabidopsis thaliana* – seedling assays

For *A. thaliana* seedling assays, seeds were surface-sterilised with 1 ml sterilisation solution (0.01% w/v sodium dodecyl sulphate (SDS), 1.6% w/v sodium hypochlorite (NaClO) in sterilised distilled H₂O (dH₂O)) for 10 min with constant end-over-end rotation followed by five times 1 ml dH₂O washes. Surface-sterilised seed were then plated in 12-, 24-, 48- or 96-well plates, depending on the needs of the assay in 0.2 ml – 2 ml half-strength Murashige and Skoog (MS) medium. Plates were closed using a transparent lid and sealed with micropore tape before stratification at 4°C for 3 – 5 days. Seedlings were grown in a controlled environment room (CER) with overhead lighting and a 16-h-day (120 $\mu\text{mol m}^{-2}\text{sec}^{-1}$ at 22°C) and 8-h-night (22°C) photoperiod.

2.2.2 *Arabidopsis thaliana* – soil grown plants

For soil grown *A. thaliana*, seeds were germinated and maintained on Scotts Levington F2 compost (Scotts, Ipswich, UK). Seeds were sown and stratified at 4°C for 5 – 7 days and transferred to a CER with overhead lighting and a 16-h-day (120 $\mu\text{mol m}^{-2}\text{sec}^{-1}$ at 22°C) and 8-h-night (22°C) photoperiod.

2.2.3 *Nicotiana benthamiana* – soil grown plants

For soil grown *N. benthamiana*, seeds were germinated and maintained on Scotts Levington F1 compost (Scotts, Ipswich, UK) and transferred to Scotts Levington F2 compost after 12 days (Scotts, Ipswich, UK) and maintained in a CER with overhead lighting and a 16-h-day (120 $\mu\text{mol m}^{-2}\text{sec}^{-1}$ at 22°C) and 8-h-night (22°C) photoperiod.

2.3 Plant lines

2.3.1 *Arabidopsis thaliana* mutants

A. thaliana ecotype Col-0 was the background for all mutants unless otherwise specified. The *bak1-5* and *bak1-5/bkk1-1* (CS71787) mutants (Schwessinger et al., 2011) were originally provided by Ben Schwessinger (Professor Cyril Zipfel group, The Sainsbury Laboratory (TSL), Norwich, UK). The *bak1-4* / pBAK1:BAK1-eGFP line was provided by Professor Cyril Zipfel (TSL), Norwich, UK). The *mpk3-1* (Wang et al., 2008b), *mpk6-2* (Liu and Zhan, 2004), *mpk11-1* (Kosetsu et al., 2010) and *mpk4-1* (Petersen et al., 2000) mutants were provided by Bruno Ngou (Professor Jonathon Jones group, The Sainsbury Laboratory (TSL), Norwich, UK).

2.3.2 *Arabidopsis thaliana* reporter mutants

For luciferase reporter imaging, *pWRKY33::fLUC* *A. thaliana* seeds were very kindly provided by Professor Ryohei Terauchi and Dr Hiroaki Kato, Iwate University, Japan. M2 EMS-mutagenised *pWRKY33::fLUC* seeds were also provided by Professor Ryohei Terauchi and Dr Hiroaki Kato, Iwate University, Japan.

For cytosolic calcium imaging, *A. thaliana 35S::GCaMP3* (Tian et al., 2009; Vincent et al., 2017) provided by Professor Simon Gilroy (University of Wisconsin, USA) and *UBQ10pro::GCaMP3* (Nguyen et al., 2018) provided by Professor Edward Farmer (University of Lausanne, Switzerland), were used as a background to cross with mutants. The *sobir1-12* x *UBQ10pro::GCaMP3*, *sobir1-13* x *UBQ10pro::GCaMP3* and *bak1-5* x *UBQ10pro::GCaMP3* were generated by Josh Joyce (Hogenhout Lab) and were used in this study with permission.

2.4 Biochemical isolation and characterisation of aphid-derived elicitors

2.4.1 Generation of Aphid Extract Elicitor Filtrate (AEFE)

Myzus persicae Clone 0 aphids, reared on *Brassica rapa*, were collected from stock cages using a brush and flash frozen in LN₃. Frozen aphids were ground to a powder and suspended in extract buffer (50 mM Tris-HCl pH7, 1 mM EDTA) at 0.016 ml mg⁻¹ aphid. All subsequent steps were carried out at 4°C unless otherwise stated. Samples were then briefly sonicated (2 x 20 s) and centrifuged at 10,000 xg for 10 min to remove insoluble material. Supernatants were transferred to a clean eppendorf tube and treated with 60% (v/v) 4.1M ammonium sulphate solution under constant agitation. Samples were agitated on a shaking plate for 1-h before centrifugation at 12,000 xg for 20 min to precipitate protein. Supernatants were discarded and the pellet reconstituted in 1X phosphate buffered saline (PBS) (137 mM NaCl, 2.7 mM KCl, 10 mM

Na₂HPO₄, 1.8 mM KH₂PO₄ 20 mM) at 8 µl mg⁻¹ aphid. Resuspensions were briefly incubated on a shaking plate before rotation on a rotating wheel o/n. Samples were then treated with 80% (v/v) acetonitrile (ACN) and mixed by inversion before incubation for 1-h. Samples were then centrifuged at 12,000 xg for 10 min to precipitate protein. Supernatants were transferred to a fresh eppendorf, flash frozen in LN₃ and lyophilized within a vacuum centrifuge until dehydrated to a powder. Powdered samples were reconstituted briefly on a shaking plate in 1X PBS at 4 µl mg⁻¹ aphid. Samples were then transferred to a < 3kDa molecular weight cut-off filter (pre-cleaned with dH₂O) and centrifuged according to manufacturer's instructions. Filtrates were then treated with 200 µM ml⁻¹ proteinase k (Merck, 70663) and incubated for 2-h at 50°C before deactivation by heat treatment at 95°C for 10 min. The resultant extract was termed *Aphid Extract Filtrate Elicitor* (AEFE) and was stored at 4°C for up to 2 weeks prior to use.

2.4.2 Determination of aphid-derived extract protein concentrations

Protein concentrations of aphid-derived extracts were determined using a Pierce™ BCA Protein Assay Kit (Thermo Scientific; 23227) according to the manufacturer's instructions. Absorption (562 nm) of extracts was measured against a standard curve generated using bovine serum albumin (BSA) standards (Table 2.1) (Fig. 2.1). The slope of the curve was used to determine the protein concentrations (Table 2.2; Fig. 2.1). Protein concentrations used within immuno-assays were determined and used to ascertain specific activity. Activities are defined as *WRKY33* promoter activity in *A. thaliana* seedling stably expressing *pWRKY33::fLUC*. Total activity is calculated as the averaged summed luminescence (LUM) over 600 min minus a control (PBS). Luminescence (LUM) is measured at 30 s intervals and summed to generate a total LUM. Average LUM is presented with standard deviation. Specific activity is calculated as the total activity per µg protein used in the assay.

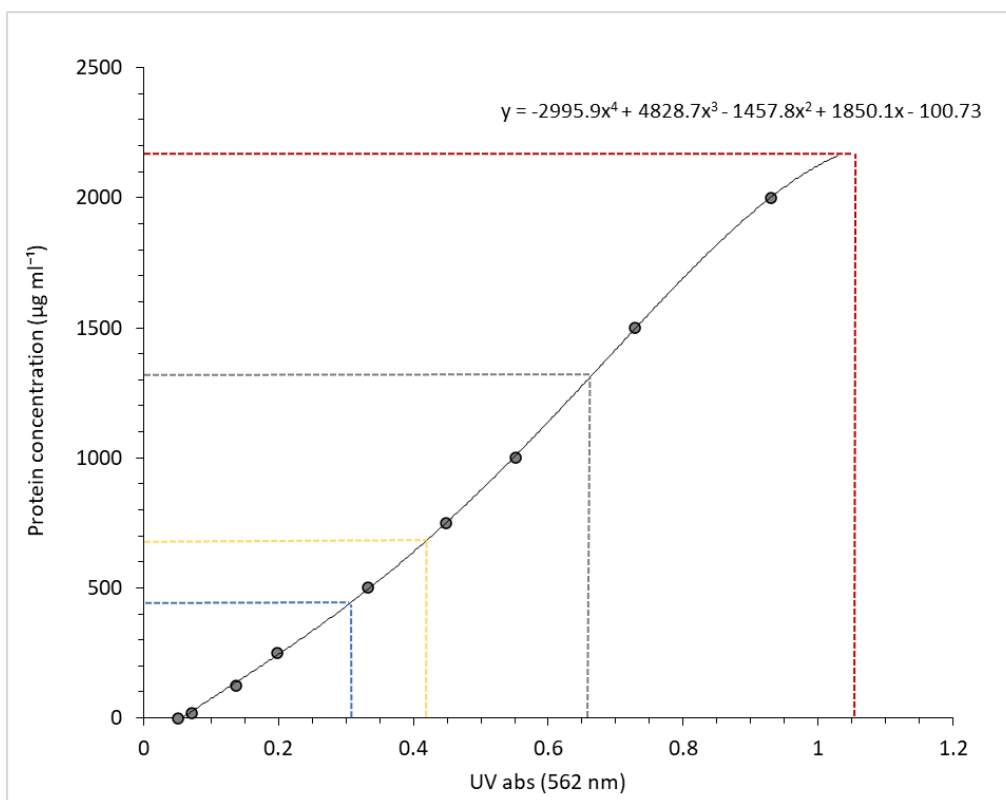


Fig. 2.1: Standard curve of bovine serum albumin (BSA) within a BCA assay to determine aphid extract protein concentrations. Standard curve was generated using the BCA assay (Pierce™ BCA Protein Assay Kit (Thermo Scientific)) according to manufacturer’s instructions. Four aphid-derived extracts (see *Materials and Methods*) were tested for protein concentrations based on the BCA absorption profile at 562 nm. Red = homogenate; Black = AS 60%; Yellow = ACN 80%; Blue = < 3 kDa MWCO.

Table 2.1: Aphid-derived extract sample absorption as determined in a BCA assay.

Repeat	UV absorption (562 nm)			
	homogenate	AS 60%	ACN 80%	<3 kDa MWCO
1	1.166	0.709	0.443	0.313
1	1.205	0.503	0.419	0.307
1	1.040	0.532	0.445	0.222
1	1.123	0.767	0.438	0.224
AVG	1.134	0.628	0.436	0.267
2	1.023	0.648	0.384	0.333
2	0.985	0.678	0.406	0.332
2	1.106	0.744	0.400	0.322
2	1.201	0.763	0.412	0.328
AVG	1.079	0.708	0.401	0.329

3	1.039	0.633	0.448	0.335
3	1.091	0.646	0.439	0.358
3	0.879	0.682	0.398	0.319
3	0.900	0.624	0.407	0.336
AVG	0.977	0.646	0.423	0.337

The absorption (562 nm) of four aphid-derived extracts across four technical repeats and three independent biological repeats are shown. AVG; Average absorption of four technical repeats.

Table 2.2: Protein concentrations of aphid-derived extracts.

Repeat	Protein concentration (mg ml ⁻¹)			
	homogenate	AS 60%	ACN 80%	<3 kDa MWCO
1	2.21	1.22	0.72	0.37
2	2.20	1.44	0.64	0.49
3	2.09	1.27	0.69	0.50
AVG	2.17	1.31	0.68	0.45
SD	0.06	0.10	0.03	0.06

AVG; Average protein concentration of three independent biological repeats. SD; Standard deviation of protein concentration.

2.4.3 Total protein visualisation

To visualise aphid-derived extracts, samples were treated with 1X sample buffer (NuPAGE™ LDS Sample Buffer (4X); 10 mM DTT) and heated to 95°C for 10 min. Subsequently, samples were resolved in SDS-PAGE within a 12% polyacrylamide gel. The gel was then stained using Coomassie ReadyBlue™ protein stain for 30 min. The gel was washed with dH₂O and imaged using ImageQuant™ LAS 500 (GE Lifesciences).

2.4.4 Protease inhibition of aphid-derived extracts

Protease inhibitor treatments of aphid extracts followed the generation of AEFE (described in Section 2.4.1) with some notable differences. Extract buffer (with E-64) contains 50 mM Tris-HCl pH7, 1 mM EDTA and 10 μM E-64 and was used to replace extract buffer previously described (2.4.1). Additionally, 20 mM PBS was treated with 10 μM E-64 and used to reconstitute ammonium sulphate-precipitated protein and reconstitute protein after acetonitrile treatments and subsequent lyophilisation.

Protease inhibitor cocktail (PIC) (Merck, P2714) was obtained as a lyophilised powder and reconstituted as a 1 mM stock in dH₂O. Stocks were stored at -20°C for up to 1 year and used at a working concentration of 10 µM working concentration. PIC treatment was carried out for a minimum of 2-h at 37°C.

E-64 (Sigma-Aldrich, L9783) was obtained as a lyophilised powder. Powder was reconstituted as a 1 mM stock solution in dH₂O and used at a working concentration of 10 µM. Aliquots were stored up to 6 months before use. E-64 treatment was carried out for a minimum of 2-h at 37°C.

4-benzenesulfonyl fluoride hydrochloride (AEBSF) (Sigma-Aldrich, A8456) was purchased as a lyophilized powder and reconstituted as a 100 mM stock in dH₂O. Stocks were stored at -20°C for up to 6 months and used at a working concentration of 1 mM working concentration. AEBSF treatment was carried out for a minimum of 2-h at 37°C.

Leupeptin (Sigma-Aldrich, L9783) was obtained as a lyophilised powder. Leupeptin powder was reconstituted as a 10 mM stock solution in dH₂O and used at a working concentration of 10 µM. Stocks were used immediately upon reconstitution. Leupeptin treatment was carried out for a minimum of 2-h at 37°C.

2.4.4 Enzymatic digestion of aphid-derived extracts

Protease type XIV, pronase (synonyms: PRONASE®) from *Streptomyces griseus* was obtained from Merck (Calbiochem®, 53702) and stored as a lyophilized powder at 4°C. The specific enzymatic activity is ≥45 units/mg dry weight (25 µg of tyrosine per min at 40°C, pH 7.5). PRONASE® powder was reconstituted as a 20 mg/ml stock solution in dH₂O and used at a working concentration of 1 mg/ml. Prior to use, the solution was heated to 56°C for 15 min followed by a 1-h incubation at 37°C to allow for self-cleavage. Aliquots were then stored up to 6 months at 20°C. Pronase treatment was carried out for 2-h at a working concentration of 1 mg/ml followed by heat inactivation at 95°C for 10 min.

Proteinase K (EC 3.4.21.64) from *Tritirachium album limber* was obtained freeze-dried from Merck (70663). The specific enzymatic activity is approximately 30 Anson-U/g (where 1 Anson unit is the amount of enzyme that liberates 1 mmol of Folin-positive amino acids/min at pH 7.5 and 35°C, using haemoglobin as a substrate). Proteinase k powder was reconstituted as a 20 mg/ml stock solution in dH₂O and used at a working concentration of 200 µg/ml. Aliquots were then stored up to 6 months at 20°C. Proteinase k treatment was carried out for a minimum of 2-h at 50°C before heat inactivation at 95°C for 10 min.

Carboxypeptidase b (EC 3.4.12.3) from porcine pancreas was obtained from Merck (C9584), as a lyophilised powder. The specific activity is ~2.350 units/mg protein. Carboxypeptidase b powder was reconstituted as a 1 mg/ml stock solution in dH₂O and used at a working concentration of 10 µg/ml. Aliquots were stored up to 6 months before use. Carboxypeptidase B treatment was carried out for a minimum of 2-h at 37°C before heat inactivation at 95°C for 10 min.

For PBS controls, 1X PBS was treated in accordance with the protocols described above. Samples, such as AEFEE, without protease treatment were diluted with an equivalent quantity of dH₂O and treated in accordance with the protocols above.

2.4.5 Deglycosylation of aphid-derived extracts and RNase B

Peptide-N-glycosylase F (PGNase F) (New England Biolabs Inc, P0704) was used according to the manufacturer's instructions. AEFEE, PBS or RNase B were treated with 1X GlycoBuffer 2 and 2.5 µl PGNase F and mixed by inversion. Samples were incubated at 37°C o/n before heat deactivated at 95°C for 10 min

Endoglycosidase H (Endo H) (New England Biolabs Inc, P0702) was used according to the manufacturer's instructions. AEFEE, PBS or RNase B were treated with 1X GlycoBuffer 3 and 2.5 µl Endo H and mixed by inversion. Samples were incubated at 37°C o/n before heat deactivated at 95°C for 10 min.

Deglycosylation efficiency was assessed via mobility shifts on 12% SDS-PAGE gel electrophoresis. Gels were stained using READYBLUE™ stain (Sigma-Aldrich, RSB) according to manufacturer's instructions. Gels were stained for 1-h at 23°C before 5X washes in dH₂O.

2.4.6 Solid-phase extraction and RP-UHPLC

For solid-phase extraction (SPE), SPE Strata-X-C cartridges (Phenomenex Inc., Macclesfield, UK) were first washed with 100% methanol followed by SPE Solvent B (0.5 M ammonium bicarbonate, 20% ACN). Cartridges were then prepared with SPE Solvent A (0.1% (v/v) trifluoroacetic acid (TFA), 20% ACN). AEFEE was acidified using SPE Solvent A, loaded onto a Strata-X-C cartridge and washed with SPE Solvent A before being eluted with SPE Solvent B. SPE-separated elutes were lyophilized in a SpeedVac centrifuge with cold trap (Thermo Fisher Scientific). Elutes were reconstituted in HPLC high-pH Solvent A (dH₂O and 0.1% TEA), loaded onto a C₁₈ stationary phase (Waters XBridge® Peptide BEH C₁₈, Waters Limited, Wilmslow, UK) and eluted using a linear gradient of high-pH Solvent B (97% (v/v) ACN, 2.9% dH₂O and 0.1% (v/v) TEA) ranging from 3-25% (v/v) at 1.6% min⁻¹ on the Agilent 1290 Infinity II LC System (Agilent). Fractions were collected at 1 min intervals between 0 min and 38 min retention time. Fractions were pooled across four runs. Lyophilised samples were either subject to immuno-activity assays where they were reconstituted in 1X PBS or reconstituted in HPLC low-pH Solvent A (dH₂O and 0.1% (v/v) TFA) for further separation. Samples were loaded onto the same C₁₈ stationary phase and eluted using a linear gradient of HPLC low-pH Solvent B (97% (v/v) ACN, 2.9% dH₂O and 0.1% (v/v) TFA) mobile phase, ranging from 3-16% (v/v) at 0.8% min⁻¹. Samples were collected at 1 min intervals between 0 min and 30 min retention time.

2.4.7 Tandem Mass Tag (TMT) labelling

A total of 3 g aphid (*M. persicae* clone O), reared on *B. rapa* in stock cages were flash frozen in liquid nitrogen and ground to a powder. The powder was suspended in Extract Buffer (50mM Tris-HCl (pH7), 1mM EDTA) with/without E-64 to a concentration of 1600 $\mu\text{l g}^{-1}$ aphid and precipitated with 60% 3.93M ammonium sulphate solution at 4°C. The pellet was reconstituted in 100 μl PBS with 2-hr end-over-end rotation at 4°C. Equal volume 0.1% TFA was used to acidify the sample followed by a clean-up step using the Pierce™ High-pH Reverse-Phased Fractionation column according to manufacturer's instructions. The samples were eluted off the column using 50% acetonitrile and lyophilised. The pellet was reconstituted in 100 μl TEAB. TMT labels were reconstituted in 41 μl acetonitrile, briefly vortexed and centrifuged. Aphid extract and TMT label (TMT126 to +E-64 treated extract; TMT127 to non-treated extract) was combined and incubated at room temperature for 1-hr. To quench the reaction, 8 μl 5% hydroxylamine was added and the sample was incubated for 15 min. The two labels' extracts were combined and precipitated with 80% acetonitrile for 1-hr followed by centrifugation. Samples were lyophilised and reconstituted in 200 μl PBS. Equal volumes of 0.1% TFA was added, and the sample then loaded on the Pierce™ High pH Reverse-Phased Fractionation column. The samples were eluted off the column using 50% acetonitrile, lyophilised, and reconstituted in 100 μl PBS. The resuspension was then passed through a < 3kDa molecular weight cut-off filter and assessed via nanoLC-MS/MS. Extract buffer: 50 mM Tris-HCl (pH7), 1 mM EDTA; Ammonium sulphate buffer: 50 mM Tris-HCl (pH7), 1 mM EDTA, 3.93 M ammonium sulphate.

2.4.8 NanoLC-MS/MS

Trapped ion mobility spectrometry coupled with quadrupole time-of-flight mass spectrometry (timsTOF) was used to identify spectra (Beck et al., 2015). Samples were diluted in Solvent A (0.1% FA in dH_2O) and loaded onto a BrukerFIFTEEN, ReproSil AQ column (0.075mm x 150mm, 1.9 μm , 120A (Bruker)) with attached trap column (C18

PepMap1000.3mm x 5mm, 5µm, 100Å (Thermo) (RT)) and separated with a linear gradient From 2 to 22% Solvent B (0.1% in Acetonitrile) in 48 min, 22% to 34% B in 5 min, 34% to 95% B in 0.5 min, 95% for 4.5 min, flow rate 0.4 µl/min at 50°C. timsTOF, with Parallel Accumulation Serial Fragmentation was used to identify masses in default settings. Peak lists were generated using Data Analysis v6.0 (Bruker Daltonics) from raw mass spectrometry files. No enzyme specificity was used. Precursor ion charge states of +2, +3 and +4 were selected with a mass tolerance of 25 PPM for precursor and fragment masses. Oxidation was included as a variable modification. Masses were searched against the *M. persicae* Clone O proteome sourced from the Bioinformatics Platform for Agroecosystem Arthropods (BIPAA) (genome v2.0 - https://bipaa.genouest.org/sp/myzus_persicae/) (Mathers et al., 2017) and used to predict peptide sequences in Mascot (v2.3.02, Matrix Science). Additionally, a proteomics contaminants database, including human keratin was searched. The decoy database filter could not be used as a small number of true positives were found in highly purified samples.

2.4.9 Candidate elicitor peptide determination and synthesis

Peptides resulting from *M. persicae* Clone O (genome v2.0) database searches using Mascot (v2.3.02, Matrix Science) were imported into excel via Scaffold (v4.0). A pivot table was generated to filter peptides based on three criteria (1) Mascot's peptide spectrum match (PSM) probability modelling from the ion score distribution was used to set an ion score cut-off of at least 45 indicating a 5% false discovery rate. (2) Retention times of 400 - 1080 seconds based on the retention of iRTs during nano-UHPLC. (3) The total number of replicates in which the peptide was identified was at least three of four. The resulting peptides were ascribed the name Candidate Elicitor Peptides (CEPs).

CEPs were synthesised by JPT Peptide Technologies GmbH (Berlin, Germany) as SpikeTides™ peptides and shipped as lyophilised powders in 96-well plates. Peptides

were reconstituted in Reconstitution buffer (0.1X PBS, 0.5% (v/v) DMSO) and placed on a rotating plate for 30 min at 4°C. CEPs were stored at -20°C for up to 3-weeks prior to use in immune-activity assays.

2.5 DNA / RNA extractions

2.5.1 RNA extraction from plants

A total of 3 10-day-old *A. thaliana* seedlings were flash frozen in liquid nitrogen and ground to a powder in a 2 ml eppendorf. The following procedure was carried out at 4°C. The powder was suspended in 500 µl Tri Reagent® (Sigma Aldrich, T9424), and agitated for 10 min on a rotating plate. An aliquot of 100 µl chloroform was added and samples were agitated for 10 min on a rotating plate before centrifugation at 12,000 *xg* for 10 min. The clear upper phase was placed in a new 1.5 ml eppendorf and isopropanol added at a 1:1 ratio. Samples were mixed by inversion and incubated for 15 min. Samples were then centrifuged at 12,000 *xg* for 15 min and the supernatant removed. A clear pellet remained and was washed with 500 µl 70% (v/v) ethanol. Samples were again centrifuged at 12,000 *xg* for 15 min and the ethanol evaporated to leave a clear pellet remaining. The pellet was reconstituted in 20 µl RNase/DNase-free dH₂O and stored at -20°C for up to 24-h before use.

2.5.2 DNA extraction from plants

A single 10-day-old *A. thaliana* seedling was flash frozen in liquid nitrogen and ground to a powder in a 2 ml eppendorf. Powders were reconstituted in 250 µl DNA Extraction Buffer (10 mM Tris-HCl pH7, 1 mM EDTA, 0.4 mM NaCl) and placed on a shaking pate for 30 min at 4°C. Samples were then centrifuged at 12,000 *xg* for 10 min and the supernatant removed. Isopropanol was then added to the sample at a ratio of 1:1, mixed by inversion and placed at -20°C for 30 min. Samples were then centrifuged at 12,000 *xg* for 10 min and the supernatant removed. A clear pellet remained and was

washed with 500 μ l 70% (v/v) ethanol. Samples were again centrifuged at 12,000 xg for 15 min and the ethanol evaporated to leave a clear pellet remaining. The pellet was reconstituted in 50 μ l RNase/DNase-free dH₂O and stored at -20°C for up to 3 months before use.

2.5.3 Genotyping PCR

DNA was isolated from a single *A. thaliana* seedling as described above. PCR reactions using the GoTaq[®] G2 DNA polymerase (Promega) master mix was carried out according to the manufacturer's instructions. Reactions contained 10 μ M forward (LP), reverse (RP) or T-DNA left border (LB) as required and ~250 ng DNA template. Unless otherwise stated, both LP and RP were combined to amplify DNA from wild-type and mutant lines in parallel. Similarly, RP and LB primers were combined to amplify from T-DNA insertion sites within wild-type and mutant lines. The thermocycle consisted of 2 min at 95°C, followed by 35 cycles of 30 s at 95°C, 30 s at 60°C, 30 s at 72°C followed by a final 5 min extension at 72°C. Amplicons were resolved in gel electrophoresis and imaged using the G:BOX gel doc (Syngene).

2.6 Plant immune assays

2.6.1 Immunogenic elicitors

Flg22 and elf18 peptides was obtained from EZBiolab (Carmell, USA) as a lyophilised powder and reconstituted in dH₂O and stored at 1 mM in aliquots at -20°C for up to 2-years before use. Chitin (β -1,4 linked N-acetylglucosamine polymer) from shrimp shell was obtained from Sigma-Aldrich as a lyophilised powder and reconstituted in dH₂O and stored at 10 mg ml⁻¹ in aliquots at -20°C for up to 2-years before use. BcNEP2 peptide (nlp20) from *B. cinerea* was kindly provided by Dr Chris Ridout (Ridout Lab, JIC, UK) in 100 μ M aliquots and stored at -20°C. Flg22 and elf18

were used at a final concentration of 100 nM unless otherwise stated. Chitin was used at a final concentration of 10 $\mu\text{g ml}^{-1}$ and BcNEP2 was used at a concentration of 1 μM .

2.6.2 Luciferase reporter plant assay

Bioluminescence measurements using the transgenic *pWRKY33::fLUC* (Kato et al., 2020) broadly followed previously published protocols (Mohan et al., 2014). Reporter *A. thaliana* seedlings were germinated in white 96-well plates white (Greiner Bio-one; 655074) in 200 μl $\frac{1}{2}$ St MS and grown in a CER with overhead lighting and a 16-h-day (120 $\mu\text{mol m}^{-2}\text{sec}^{-1}$ at 22°C) and 8-h-night (22°C) photoperiod for 10-days. At 5-h prior to imaging, the $\frac{1}{2}$ St MS media was replaced with 50 μM D-Luciferin (Sigma-Aldrich) and incubated in the dark at room temperature until imaging. Treatments were made *in situ* using a multichannel pipette directly before light emission monitoring was conducted using a high-resolution photon counting system (HRPCS218) (Photek) equipped with a 20 mm F1.8 EX DG Aspherical Wide Lens (Sigma). Light capture filtration of 10% was applied and plates were monitored for a minimum of 10-h. Photon counts were retrieved by drawing a ROI around the well and 30 s bins were saved. Data was then imported excel for further analysis including generating time-course graphs and summing photon counts from individual seedlings to generate total luminescence scores.

2.6.3 qRT-PCR

Plant RNA was assessed for RNA concentration using Nanodrop NanoDrop™ One spectrophotometer (Thermo Scientific, UK). A total of 1000 ng RNA was aliquoted for DNase treatment (RQ1 DNase set; Promega) according to manufacturer's instructions. DNase-treated RNA was then used to generate cDNA using RevertAid First Strand cDNA synthesis kit (Thermo Scientific, UK; K1622) according to manufacturer's instructions.

cDNA was diluted 1:4 with dH₂O prior to PCR reactions. Each reaction contained ~25 ng cDNA, 0.5 μg of each primer (Table 2.3) and SYBR Green JumpStart ReadyMix

(Sigma-Aldrich) in a white, 96-well plate (4titude, Azenta Life Sciences). Reactions corresponding to target and reference genes as well as treatments that are used for direct comparisons were placed in a single 96-well plate. The CFX96 Real-Time System with a C1000 Thermal Cycler (Bio-Rad, UK) was used for PCR reactions. The thermocycle consisted of 3 min at 95°C, followed by 40 cycles of 30 s at 95°C, 30 s at 60°C, 30 s at 72°C followed by melt curve analysis of 30 s between 65°C - 95°C at 0.5°C increments.

To calculate relative expression values for target genes, mean C_t values were obtained by averaging two technical repeats per condition per gene. A $2^{-\Delta C_t}$ value was generated by subtracting the target gene C_t value from the reference gene C_t value. Mean $2^{-\Delta C_t}$ values per condition were generated by averaging three biological repeats (three $2^{-\Delta C_t}$ values). Mean $2^{-\Delta C_t}$ values are presented as relative expression values \pm standard error of the mean $2^{-\Delta C_t}$. To test for differences in mean values between conditions, either Student's t-test or a One-Way ANOVA with Tukey HSD (Honestly Significant Differences) post-hoc test was carried out on $2^{-\Delta C_t}$ values within R Studio.

Table 2.3: Primers used for qRT-PCR

Gene name	Primer	Reference
GAPDH	F TCTCGATCTCAATTTTCGCAAAA R CGAAACCGTTGATTCCGATTC	(Czechowski et al., 2005)
WRKY33	F CTCGTGGTAGCGGTTACGCC R CCTTTGCTCTAGAGAATCCACC	(Birkenbihl et al., 2012)
PAD3	F TGCTCCCAAGACAGACAATG R GTTTTGGATCACGACCCATC	(Chassot et al., 2008)
CYP81F2	F AATGGAGAGAGCAACACAATG R ATACTGAGCATGAGCCCTTTG	(Kettles et al., 2013)
CYP79B2	F TCTCCGGTTTATCTCGTTCAGTA R CGTGTCTCATTCTCAGGTAGCTT	(Kettles et al., 2013)
CYP71A13	F ATTCGGATCAGGGAGAAGGATA R CGATACCAATGGCTTCAGTTAGAT	(Birkenbihl et al., 2012)
NHL10	F TTCCTGTCCGTAACCCAAAC R CCCTCGTAGTAGGCATGAGC	(Monaghan et al., 2014)
FRK1	F ATCTTCGCTTGGAGCTTCTC R GCAGCGCAAGGACTAGAG	(Monaghan et al., 2014)
WRKY53	F CGGAAGTCCGAGAAGTGAAG R TCTGACCACTTTGGTAACATCTTT	(Reusche et al., 2013)
At1g51890	F CCAGTTTGTCTGTAATACT R CTAGCCGACTTTGGGCTATC	(Birkenbihl et al., 2012)

FLS2	F ACTCTCCTCCAGGGGCTAAGGAT R AGCTAACAGCTCTCCAGGGATGG	(Monaghan et al., 2014)
EFR	F CGGATGAAGCAGTACGAGAA R CCATTCCTGAGGAGAACTTTG	(Monaghan et al., 2014)
CERK1	F AAGTGGAGGTTTGGGTGGTGCCG R ACAGCCCCAAAACCCACCTTGCCC	(Monaghan et al., 2014)

2.6.4 Immunoprecipitation of BAK1-GFP

Immunoprecipitation was performed according to (Avila et al., 2015). The two lines used in this study were *bak1-4* / pBAK1:BAK1-eGFP (Schwessinger et al., 2011) et al., 2011; (Ntoukakis et al., 2011), and empty-vector GFP. Approximately 500 mg 10-day-old transgenic *A. thaliana* seedlings grown in liquid half-strength MS media were treated with 2.5% (v/v) aphid extract or PBS and incubated for 2 min. Plant tissue was ground in liquid N₂ and further ground in 3 volumes extract buffer (100 mM Tris-HCl pH 8.8; 150 mM NaCl; 1 mM EDTA; 10% glycerol; 20 mM NaF; 1 mM PMSF; 0.1% (v/v) complete protease inhibitor cocktail; 1 mM Na₂MoO₄; 50 mM β-glycerophosphate; 10 mM Na₃VO₄) and sonicated for 10 s. Lysates were centrifuged at 5,000 *xg* for 5 min at 4°C and supernatant transferred to an ultracentrifuge tube and spun at 135,000 *xg* for 30 min at 4°C. The pellet was reconstituted in with 1 volume membrane solubilisation buffer (100 mM Tris-HCl pH 8.8; 150 mM NaCl; 1 mM EDTA; 10% glycerol; 20 mM NaF; 1 mM PMSF; 0.1% (v/v) complete protease inhibitor cocktail; 1% (v/v) Triton X-100) and briefly sonicated. The microsome suspension was then centrifuged at 135,000 *xg* for 30 min at 4°C to remove the insoluble fraction. The supernatant was used in the immunoprecipitation as the membrane input. GFP-Trap®_MA beads (Chromotek) were vortexed and 25 µl bead slurry was washed three times in 500 µl ice-cold wash/dilution buffer (10 mM Tris/Cl pH 7.5; 150 mM NaCl; 0.5 mM EDTA) and incubated with the lysates for 1-h with end-to-end rotation. The beads were immobilized on a magnetic stand and washed three times. After the final wash, the beads were suspended in 100ul 2X sample buffer (NuPAGE™ LDS Sample Buffer (4X); 10 mM DTT) and heated to 95°C for 10 min to dissociate the immunocomplexes. The beads were then magnetically separated, and SDS-PAGE performed with the supernatant.

Proteins were resolved on a 12% polyacrylamide gel SDS-PAGE (NuPAGE®, Invitrogen). The proteins were cut out of gels and digested by trypsin as described previously (Ntoukakis et al., 2009). LC-MS/MS analysis was performed using a LTQ-Orbitrap mass spectrometer (Thermo Scientific) and a nanoflow-HPLC system (nanoAcquity; Waters) as described previously (Ntoukakis et al., 2009). The TAIR10 database was searched (www.Arabidopsis.org) using Mascot (v2.3.02, Matrix Science) and Scaffold (v4) was used to validate MS/MS-detected peptide identification and spectra. Protein IDs and spectral counts of proteins with > 95% confidence were retrieved from Scaffold to be further examined in Excel.

To generate a list of putative BAK1-interactors, total spectral counts of proteins identified in BAK1-GFP and EV-GFP lines were normalized to correct for expression discrepancies. Next, to identify ligand-dependent associations, the difference in total spectral counts of treated to untreated was determined (> 1 indicated enrichment in treated over untreated samples). In parallel, preferential BAK1 interactions were assessed by finding the difference in total spectral counts of BAK1-GFP treated and EV-GFP treated samples. The sum of total spectral counts per protein of putative ligand-dependent associations and BAK1-interaction preference over GFP is presented.

2.6.5 MAPK activation assays

Ten *A. thaliana* seedlings per genotype/condition were snap frozen in liquid nitrogen, and proteins were extracted with Buffer K containing 50 mM Tris-HCl (pH 7.5), 200 mM NaCl, 1 mM EDTA, 10% (v/v) glycerol, 1% tween-20, 1 mM phenylmethylsulfonate fluoride, 1 mM dithiothreitol and 1X protease inhibitor cocktail P9599 (Sigma-Aldrich) and 1X phosphatase inhibitor tablet (Sigma-Aldrich). Samples were vortexed vigorously for 30 s and placed on a shaking plate for 10 min. Samples were then centrifuged at 13,000 *xg* for 30 min at 4°C. Supernatants were then treated with 1X sample buffer (NuPAGE™ LDS Sample Buffer (4X); 10 mM DTT) and heated to 95°C for 10 min. Protein was resolved on a 12% polyacrylamide gel and transferred onto PVDF membrane using the Trans-Blot Turbo Transfer System (Bio-Rad). Membranes were incubated for 1.5-h with agitation at room temperature with

Blocking Buffer (5% Milk, 0.2% Tween-20, 1X TBS; 20 mM Tris-HCl pH and 15 mM NaCl adjusted to pH 7.4 using HCl). The Phospho-p44/42 MAPK (Erk1/2) (Thr202/Tyr204) (Cell Signalling Technologies) primary antibody against phospho-p44/42 MAP kinase was used with horseradish peroxidase-conjugated antirabbit as secondary antibody. Signal detection was performed using SuperSignal™ West Pico PLUS chemoluminescence substrate (Thermo Scientific) and images taken on the ImageQuant™ LAS 500 (GE Lifesciences). Membranes were then stained using Ponceau S stain solution (Sigma-Aldrich) and washed with dH₂O before being imaged on the ImageQuant™ LAS 500.

2.6.6 Seedling growth inhibition

A. thaliana seeds were surface sterilised and germinated on ¼St MS media (see 2.2.1) for 4-days. Four-day-old seedlings were transferred to a transparent 48-well plate (CytoOne®, Starlab) containing either 2.5 % (v/v) (0.5 mM) PBS or 2.5% (v/v) (11 µg ml⁻¹) AEFÉ in ½St liquid MS one seedling per well. Plates were then transferred to a CER with overhead lighting and a 16-h-day (120 µmol m⁻²sec⁻¹ at 22°C) and 8-h-night (22°C) photoperiod for 8-days. Seedlings were then blotted dry on tissue paper for 30 s before seedling mass was recorded.

2.6.7 Calcium reporter imaging of seedlings

Reporter *A. thaliana* seedlings expressing *35:GCaMP3* or *UBQ10:GCaMP3* as indicated, were germinated in 96-well flat-bottomed, transparent plates (Alpha Laboratories) in 200 µl ½MS and grown in a CER with overhead lighting and a 16-h-day (120 µmol m⁻²sec⁻¹ at 22°C) and 8-h-night (22°C) photoperiod for 8-days. After 9-days, the ½MS media was replaced with 150 µl dH₂O and plates were covered and incubated in the dark at room temperature for 24-h. A 30 min pre-treatment baseline was generated using the FLUOstar OMEGA plate reader (BMG LabTech). An aliquot of 50 µl

dH₂O was removed from each well and replaced with 50 µl 3X elicitor solution containing treatments as indicated. Typically, eight seedlings per treatment were used. Plates were imaged for a further 90 min.

Fluorescence, *F* values were obtained through the Omega MARS software (BMG LabTech) and converted into relative fluorescence changes ($\Delta F/F_0$) by utilising the equation $\Delta F/F_0 = (F - F_0)/F_0$ in which *F*₀ is the mean fluorescence over the 30 min baseline period. Mean $\Delta F/F_0$ values were generated per treatment per genotype and are presented with standard error. To test statistical differences, the maximum $\Delta F/F_0$ value per individual were averaged across each treatment/genotype. Comparisons between treatments or genotypes was tested within an ANOVA with Tukey HSD post-hoc test and was carried out only within single plates.

2.7 Insect experimentation

2.7.1 Calcium reporter imaging of live insects

Imaging of live insects was carried out using modified version of previously published protocols (Vincent et al., 2017). Colonies of *Myzus persicae* (Clone O) were maintained in stock cages (see 2.1.1). For real-time imaging, reporter *A. thaliana* stably expressing either the *35S:GCaMP3* (Tian et al., 2009; Vincent et al., 2017) or *UBQ10:GCaMP3* (Nguyen et al., 2008) were used. Crosses including *sobir1-12* x *UBQ10:GCaMP3*, *sobir1-13* x *UBQ10:GCaMP3* were generated by Josh Joyce (Hogenhout Lab, JIC, UK).

A. thaliana reporter lines were grown vertically on ¼ MS media for 15 days. The first or second true leaf was detached from each plant and placed abaxial surface up on 300 µl dH₂O within a well of a flat bottomed, clear 96-well plate (Alpha Laboratories). Plates were wrapped in cling film and kept o/n in the dark at room temperature before use.

Populations of standardized aged *M. persicae* (Clone O) aphids were established by transferring approximately 20 adults from stock plants to four-week-old *A. thaliana* grown in soil (see 2.2.2). Plants were caged using clear plastic tubing (10 cm

r x 30 cm h) for 24-h before the adults were removed. *M. persicae* populations were used 7 days later for real-time imaging experiments.

For imaging, a single insect was transferred to a leaf using a paintbrush. Each insect-occupied leaf was imaged alongside a no insect control leaf. Each insect and control leaf pair represent one biological replicate (n) within the dataset. Plates were then covered with cling film and leaves imaged for approximately 1-h. A feeding event was defined as the aphid being stationary for > 5 min with the feeding site visible, though > 2.5 min would be tolerated. Inappropriate samples were discarded, and the experiment continued until suitable replication had been achieved.

Four leaves (2 x 2 wells) in the 96-well plate were imaged simultaneously using the ZEISS Axio Zoom.V16 epifluorescence microscope, controlled via the ZEN Blue software (ZEISS, Germany). Samples were excited with an LED light source (Lumencor Spectra III light engine). Fluorescence was measured using excitation at 470/40 nm and emission at 525/50 nm wavelengths. Images were captured every 5 s with the LED light source at 15 % with maximum gain and 7X magnification with 1.5 s exposure. All image sequences were exported as CZI. files.

Image files were opened in Fiji Image J 1.52i (National Institutes of Health, USA) with the Bio-Formats 5.9.2 Plugin (Open Microscopy Environment). For signal analysis, extracting fluorescence data at the feeding site was achieved by generating a region of interest (ROI) around the maximum visible signal area. In the absence of any visible response, a ROI, 30 pixels in diameter, was drawn at the aphid feeding site for analysis. ROI were duplicated to equivalent sites on the control leaf. The Time Series Analyzer 3.0 plugin (Department of Neurobiology, UCLA) was used to generate mean ROI intensities (fluorescence, F) for each 5 s frame.

Fluorescence, F values were converted into relative fluorescence changes ($\Delta F/F_0$) by utilising the equation $\Delta F/F_0 = (F-F_0)/F_0$ in which F_0 is the mean fluorescence over a baseline period (Pre-feeding). MTrackJ plugin (1.5.1) was used to measure the average rate of spread of the first visible wave of fluorescence elevation elevations. The Fiji Image J 1.52i measure function was used to record ROI area, leaf area and aphid area. For samples and the corresponding controls to be used in data, samples had 60 frames (5 min) available immediately prior to feeding for F_0 calculations though failing this, they were only discarded if less than 30 were available. Ideally 360 frames (30 min)

would be available after aphid feeding though if not possible, any more than 120 was deemed acceptable. If an insect obstructed or later influenced the ROI recordings, those data points were removed.

2.7.2 Aphid fecundity assay

Approximately 30-50 Col-0, *sobir1-12* or *sobir1-13* *A. thaliana* seeds were sown on Scotts Levington F2 compost (Scotts, Ipswich, UK), stratified at 4°C for 5 – 7 days and transferred to a CER with overhead lighting and a 16-h-day ($120 \mu\text{mol m}^{-2}\text{sec}^{-1}$ at 22°C) and 8-h-night (22°C) photoperiod. After 7 days 12-15 seedlings were transferred to a C15 tray containing Scotts Levington F2 compost, one seedling per pot, and placed in a CER with overhead lighting and a 16-h-day ($120 \mu\text{mol m}^{-2}\text{sec}^{-1}$ at 22°C) and 8-h-night (22°C) photoperiod for 4-weeks.

To establish standardised aged aphids, a single 4-week-old *A. thaliana* plant was used to rear 15-20 adult *M. persicae* (Clone O) aphids from stock cages. After 24-h, the adults were removed leaving 1-day-old nymphs for experimentation. Five-week-old *A. thaliana* plants in C15 pots were transferred to the CER used for insect assays with a 14-h-day ($90 \mu\text{mol m}^{-2}\text{sec}^{-1}$ at 24°C) and 10-h-night (20°C) photoperiod and a humidity of 50%. A single *M. persicae* nymph was placed on each plant. Plants were sealed with a breathable cellophane bag. Counting aphids started on day 7 where all nymphs are removed (if they are present) leaving the single adult. Counting occurs every two days thereafter up to day 13. Nymphs are removed after each count. The experiment was repeated three times.

2.7.3 Aphid survival assay

Aphid survival assays were carried out in a similar way to aphid fecundity assays with some notable differences. The cherry-oat aphid (*R. padi*) was reared in stock cages of 24 cm x 54 cm x 47 cm containing up to four oat plants (*Avena sativa*) aged 4-8 weeks with a 14-h-day ($90 \mu\text{mol m}^{-2}\text{sec}^{-1}$ at 18°C) and 10-h-night (15°C) photoperiod. Between

8 and 10 oat seeds were germinated in 8 cm pots containing Scotts Levington F2 compost and grown in 14-h-day ($90 \mu\text{mol m}^{-2}\text{sec}^{-1}$ at 24°C) and 10-h-night (20°C) photoperiod and a humidity of 60%. Standardised aged aphids were established by placing adult *R. padi* on 7-day-old oat seedlings for 24-h before removing all adults. After four days, 10, aged *R. padi* individuals were placed within a clip cage on a single 4-week-old *A. thaliana* plant leaf. Plants were then placed into a CER with 14-h-day ($90 \mu\text{mol m}^{-2}\text{sec}^{-1}$ at 24°C) and 10-h-night (20°C) photoperiod and a humidity of 60%. Aphids were counted everyday until no aphids remained alive (usually up to 7 days).

2.7.4 Induced resistance assay

To carry out aphid survival assays, *A. thaliana* plants were grown and maintained as stated above. After 4 weeks, *A. thaliana* plants were transferred to a CER with a 14-h-day ($90 \mu\text{mol m}^{-2}\text{sec}^{-1}$ at 24°C) and 10-h-night (20°C) photoperiod and a humidity of 60%. A single 4-week-old *A. thaliana* plant was used to establish a standardised aged population as previously described. A single *A. thaliana* leaf was infiltrated with 2.5% (v/v) PBS or 2.5% (v/v) AEFE 48-h prior to placing a single adult *M. persicae* within a clip cage on the infiltrated leaf. The total number of aphids was counted after 10-days.

Chapter 3

Aphid-derived extracts contain an immunogenic epitope, likely to be a peptide motif

3.1 Introduction

3.1.1 MAMPs, DAMPs and HAMPs during molecular plant-pest interactions

Plants sense microbial pathogens through the receptor-mediated perception of molecular signatures termed microbe-associated molecular patterns (MAMPs) (Ausubel, 2005, Jones and Dangl, 2006, Boller and Felix, 2009). Recognition of MAMPs is performed by surface-localised pattern recognition receptors (PRRs) triggering signalling that converges upon common immune responses such as ion fluxes, production of reactive oxygen species (ROS), activation of phosphorylation cascades and transcriptional reprogramming (Boller and Felix, 2009, Zipfel, 2014). According to this canonical model, plant perception of herbivory occurs via analogous modes. However, in contrast to MAMP PRRs, of which several have been identified, PRRs that perceive herbivore-associated molecular patterns (HAMPs) have largely remained elusive. In fact, only the L-type lectin receptor kinase *LecRK-I.8* that recognises an unknown elicitor within *P. brassicae* egg extract (Gouhier-Darimont et al., 2013, Gouhier-Darimont et al., 2019), and the putative LRR-RLP *INR* that recognises *Vu-In* (inceptin) found in fall armyworm (*Spodoptera frugiperda*) oral secretions (Steinbrenner et al., 2020), have been identified to date. Inceptins are proteolytic fragments, derived from host chloroplastic ATP synthase γ -subunits (Schmelz et al., 2006, Schmelz et al., 2007). Given the origin of inceptins, their action as elicitors is conceptually akin to damage-associated molecular pattern (DAMP)-mediated immune responses and are, therefore, indirect stimulants of defence responses (Schmelz et al., 2006). No HAMP has been identified that is perceived by *LecRK-I.8* although it is unlikely to be proteinaceous (Bruessow et al., 2010, Gouhier-Darimont et al., 2013). Indeed, *LecRK-I.8* was identified as a potential NAD^+ receptor in *A. thaliana* which may suggest that egg extracts contain NAD^+ (Wang et al., 2017). Alternatively, extracts may trigger the release of NAD^+ and immune responses to egg extracts are conferred via a multi-step process (Wang et al., 2017).

Another example of indirect insect recognition by plants is the perception of GroEL produced by the primary aphid endosymbiont, *Buchnera aphidicola* which is secreted into plants during feeding, and triggers host defence (Chaudhary et al., 2014). Currently, no PRR responsible for GroEL perception has been identified but the LRR-RK co-receptor, BAK1 is required for full GroEL-induced immune responses (Chaudhary et al., 2014). Curiously, the *B. aphidicola* genome contains genes encoding flagellin (Maezawa et al., 2006, Schepers et al., 2021), elongation factor-Tu (EF-Tu) and cold shock protein (CSP) (van Ham et al., 2003); three known elicitors of defence responses in plants (Felix and Boller, 2003; Kunze et al., 2004; Chinchilla et al., 2006; Zipfel et al., 2006). Furthermore, in addition to GroEL, flagellin, EF-Tu and CSPs were identified in pea aphid honeydew (Sabri et al., 2013), which may be associated with altered immune responses in *A. thaliana* (Schwartzberg et al., 2014). Similarly, secreted honeydew from the rice brown planthopper elicits immune responses in rice which are associated with microbial constituents (Wari et al., 2019). Whilst there is no indication that *B. aphidicola* flagellin, EF-Tu or CSPs induce plant defence responses, insects contain obligate and facultative microbial symbionts, and should be experimentally controlled for wherever possible. Prince et al. (2014) found that whole-body extracts derived from *M. persicae* induced immune responses in *A. thaliana* independently of PRRs FLS2, EFR or CERK1 suggesting an elicitor other than flagellin, EF-Tu or chitin is responsible for defence induction. Aphid-extract-induced immune responses including a low amplitude, delayed ROS burst and defence gene expression required BAK1, strongly suggesting a HAMP is perceived by a receptor complex (Prince et al., 2014).

3.1.2 Aphid secretome components can both induce and suppress plant immune responses

Aphid saliva is likely to act at the interface between the aphid and plant and thus salivary components may be perceived by plant cells (Will and van Bel, 2006, Bos et al., 2010, Chaudhary et al., 2014, Prince et al., 2014, Jaouannet et al., 2015, Naessens et al., 2015, van Bel and Will, 2016, Vincent et al., 2017). Indeed, aphid saliva has been shown to induce characteristic innate immune responses in *A. thaliana* (De Vos and

Jander, 2009). To characterize aphid secretome content, saliva has been analysed by liquid chromatography coupled to tandem mass spectrometry (LC-MS/MS), identifying several hundred secreted proteins (Harmel et al., 2008, Carolan et al., 2011, Carolan et al., 2009, Cooper et al., 2010, Rao et al., 2013, Rao et al., 2019, Vandermoten et al., 2014, Chaudhary et al., 2014, Thorpe et al., 2016, Boulain et al., 2018, MacWilliams et al., 2020). However, aphid secretome studies are often hindered by the difficulty to induce and separate aphid saliva using artificial diets (Will et al., 2009, Will et al., 2012, van Bel and Will, 2016), and changes in collection and/or clean-up methods may have profound effects on the number of proteins identified (MacWilliams et al., 2020). In addition to saliva, aphid tissues such as mouthparts, feet/legs and secretions other than saliva, such as honeydew, are in direct contact with the plant during feeding and may shed components to promote feeding and suppress or induce immune responses (Schwartzberg et al., 2014, Will and Vilcinskas, 2015).

Plant innate immune responses are mediated by receptor-ligand interactions and thus require physical interactions between plant cells and elicitors. Interestingly, the flg22 epitope is buried in the interior of the flagellum and is not readily accessible for the FLS2 receptor (Samatey et al., 2001, Yonekura et al., 2003). Flagellin likely undergoes several rounds of enzymatic processing before full recognition occurs (Buscaill et al., 2019). The plant-secreted β -GALACTOSIDASE 1 (BGAL1) of *N. benthamiana* promotes hydrolytic release of bioactive flagellin from inactive, glycosylated forms (Buscaill et al., 2019). Furthermore, EF-Tu is not predicted to be readily in contact with the plant cell surface (Zipfel et al., 2006), and understanding of moonlighting functions of Ef-Tu on cell surfaces, where it is a target for proteolytic processing, is emerging (Widjaja et al., 2017).

Predicting elicitor function at the plant-insect interface is particularly challenging. Several proteins identified in the saliva are not detected in the salivary gland (Carolan et al., 2011), and several lack a secretion signal (Harmel et al., 2008, Vandermoten et al., 2014). Predictive or hypothesis-based studies are not aided by the lack of genomic resources available and transcriptome studies can lack tissue-specific data or sufficient depth to uncover gene products acting at the plant-insect interface. Nevertheless, several proteins with putative elicitor-function have been identified

within saliva. Three *M. persicae* salivary proteins, Mp56, Mp57 and Mp58 were shown to reduce aphid fecundity when expressed in *A. thaliana* although the reason for this observation was not tested (Elzinga et al., 2014).

3.1.3 Biochemical isolation of elicitors of plant defence responses

A diverse array of molecules including carbohydrates, lipids and lipid breakdown products, proteins, peptides, glycolipids and glycoproteins may act as MAMPs to elicit plant immune responses (Boller and Felix, 2009, Gust et al., 2012, Abdul Malik et al., 2020). The identification of MAMPs typically relies on detection of robust defence phenotypes followed by development of an activity-led purification strategy. Two extensively studied MAMPs, the flagellin-derived flg22 peptide (*N*-QRLSTGSRINSAKDDAAGLQIA-C) (Gómez-Gómez et al., 1999), and Elongation factor-Thermo unstable (Ef-Tu)-derived elf18 (*N*-SKEKFERTKPHVNVGTIG-C) (Kunze et al., 2004), were purified from soluble fractions of *Pseudomonas syringae* pv *tabaci* (*Pst*) and *Escherichia coli* (*E. coli*) GI826 preparations, respectively. After ion exchange chromatography (IEX), alkalinization of growth media was used as a proxy for bioactive component detection. Subsequent trypsin digestion and analysis for peptide masses by liquid chromatography linked to tandem mass spectroscopy (LC-MS/MS) identified the candidate MAMPs (Gómez-Gómez et al., 1999, Kunze et al., 2004). Interestingly, a second bioactive epitope (Lys176 to Gly225; EFa50) within EF-Tu was isolated that induces MTI in rice (Furukawa et al., 2014). Once again, IEX (Q-Sepharose anion exchange) was used to separate ROS eliciting fractions, which were subsequently analysed by LC-MS/MS (Furukawa et al., 2014). Using similar methods, the bioactive, 13 amino acid peptide, Pep-13 (*N*-VWNQPVRGFKVY-C) was purified from fungal culture filtrates (Nürnberg et al., 1994). The bioactive epitope is derived after release from a 42kDa glycoprotein up on Glu-C proteolysis (Sacks et al., 1995). After proteolytic release, peptides were separated via high-performance, reversed-phase liquid chromatography (RP-HPLC) and amino acid sequence derived via an Edman Degradation assay (Nürnberg et al., 1994).

Recently, the translation initiation factor 1 (IF1) from proteobacteria was isolated from *E. coli* and *R. solanacearum* protein extracts (Fan et al., 2021). Partially purified *E. coli* elicitor was subjected to LC-MS/MS to identify the bioactive motif. IF1, a 71-amino-acid single domain protein, is recognised by the receptor-like protein RLP32 in *A. thaliana* (Fan et al., 2021). As nested peptides spanning intact IF1 are inactive, tertiary structure features rather than primary sequence motifs determine IF1 elicitor activity. Furthermore, IF1 is proteinase k-sensitive and heat unstable (Fan et al., 2021).

In addition to proteinaceous MAMPs, several DAMPs have been biochemically isolated from plant tissue. One of the first purified elicitors was *systemin*, a wound-inducible 18 amino acid peptide (*N*-AVQSKPPSKRDPPKMQTD-C) (Pearce et al., 1991). Several HPLC separations were carried out including orthogonal low-pH/High-pH LC to identify fractions exhibiting protease inhibitor inducing activity (Pearce et al., 1991). Similarly, the *AtPep1* was isolated from leaf material via iterative steps of IEX and RP-HPLC (Huffaker et al., 2006).

Plants are capable of perceiving non-proteinaceous MAMPs. The bacterial and fungal cell wall is a source of several elicitors of immune responses in plants. The lysin motif (LysM) receptor-like proteins/kinases (LysM-RLPs/RLK) perceive carbohydrate ligands such as bacterial peptidoglycan (PGN: alternating β -(1,4)-linked *N*-acetylglucosamine (GlcNAc) and *N*-acetylmuramic acid (MurNAc)), lipopolysaccharide (LPS: lipid A (β -glucosamine-(1,6)-glucosamine-1-phosphate base with fatty acid esters), variable core oligosaccharide, and O antigen)), and fungal chitin (β -1,4-linked *N*-acetylglucosamine) (Braun et al., 2005, Miya et al., 2007, Willmann et al., 2011). One example is the lectin S-domain-1 kinase LORE (*LIPOOLIGOSACCHARIDE-SPECIFIC REDUCED ELICITATION*), that mediates the perception of *Pseudomonas*- and *Xanthomonas*-derived LPS in *A. thaliana* triggering MTI responses (Ranf et al., 2015). LPS purification often follows a conventional hot phenol extraction (HPE) method (Wu et al., 1987). LPS is phase-separated in phenol-water, and the resultant aqueous phase then dialyzed, lyophilised and washed with ethanol. The sample is treated with RNase/DNase and proteinase K to remove nucleic acids and proteins, respectively. Typically, LPS is resolved on a size-exclusion column using fast protein liquid

chromatography (FPLC). Modifications to this original method have been developed (Ahamad and Katti, 2016).

Perception of PGNs and chitin involves the PRR LysM-RLK, CERK1. Chitin-induced *AtCERK1* activation promotes CERK1-LYK5 heterodimerisation, with a minor role for LYK4 (Wan et al., 2012, Cao et al., 2014). Perception is rapidly translated to cellular signalling such as ROS production, cytosolic calcium elevations and phosphorylation cascades (Miya et al., 2007, Liu et al., 2018). Chitin purifications from crustaceans such as shrimp shells often involves demineralisation with mild acidic solutions followed by deproteinization and bleaching (Younes and Rinaudo, 2015). As chitin is generally insoluble in water and many organic solvents, the more readily soluble chitosan is more applicable for immuno-assays. PGN-induced *AtCERK1* associates with the LysM domain RLPs, LYM1 and LYM3 (Willmann et al., 2011). Isolation of PGN involves RNase, DNase and protease treatments followed by mild acidic hydrolysis (Bertsche and Gust, 2017).

3.1.4 Chapter aims

Previous attempts to identify aphid elicitors of plant immune responses revealed that plants are likely to recognize low molecular weight (< 10kDa), proteinaceous components within aphid whole bodies (Prince et al., 2014), and in aphid saliva (De Vos and Jander, 2009, Chaudhary et al., 2014). However, with the notable exception of *B. aphidicola* GroEL (Chaudhary et al., 2014), no bona fide aphid-associated elicitor has been characterised to date. To investigate the bioactive nature of aphid-associated elicitors, here, I exploit the immune responses of transgenic MTI reporter plants to further understand the immunogenic nature of crude extracts derived from *M. persicae*. I present evidence that aphid whole-body extracts induce *WRKY33* promoter activity as well as cytosolic calcium elevations in *A. thaliana* and these proxies may be used to purify bioactive components of extracts. Characterisation of the extract showed that elicitor activity is sensitive to protease treatment, heat insensitive and resistant to deglycosylation treatments. Surprisingly, cysteine protease activity is required for full elicitor activity suggesting that processing of a HAMP is

required. Active components were resolved in RP-HPLC as three distinct peaks, the contents of which were explored using LC-MS/MS. Taken together, these data suggest aphid extract-derived elicitor activity is likely associated with a low molecular weight peptide acting as an immunogenic epitope.

3.2 Results

3.2.1 Activity-guided purification of *Myzus persicae*-derived elicitors from crude aphid extracts

To characterise the immunogenic nature of aphid-derived elicitors, I opted to begin investigations using whole body extracts; an approach that was validated previously (Prince et al., 2014). I developed a bottom-up, activity-led purification pipeline to separate immuno-active peptides from homogenates. The pipeline consisted of five key steps; (I) the solubilisation of *M. persicae* extraction buffer to generate aphid homogenate akin to Prince et al. (2014), (II) an ammonium sulphate (60% (v/v)) precipitation step, (III) an acetonitrile precipitation (80% (v/v)) to deproteinate the supernatant, (IV) a filtration step using a centrifugal, < 3kDa molecular weight cut-off (MWCO) filter and, (V) proteinase k digestion and subsequent heat treatment at 95°C (Fig. 3.1). I chose to name the resultant fraction *aphid extract filtrate elicitor* (AEFE). Aphid homogenates contained approximately 62.5 mg aphid ml⁻¹ or approximately 1.73 mg total protein (~2.17 mg ml⁻¹), whilst fractions, prior to proteinase k digestion, contained approximately 100 µg total protein (~0.45 mg ml⁻¹) (see *Materials and Methods*) (Fig. 3.1A, B; Table 3.2).

During MTI, plants trigger a diverse array of immune responses including extensive transcriptional reprogramming (Tsuda and Somssich, 2015, Bjornson et al., 2021). Luciferase-based transcriptional reporters have become useful tools to monitor MTI-induced gene expression changes (Asai et al., 2002, Feng et al., 2015, Kato et al., 2020). To assess the immunoactivity of fractions after purification steps, I exposed transgenic *A. thaliana* seedlings, stably expressing the firefly luciferase gene (*fluc*) fused to an *AtWRKY33* promoter sequence (*pWRKY33:fluc*), to monitor promoter

activity (Kato et al., 2020). The *WRKY33* promoter was rapidly and transiently activated against aphid extract fractions, peaking at approximately 120 min after exposure (Fig. 3.2A).

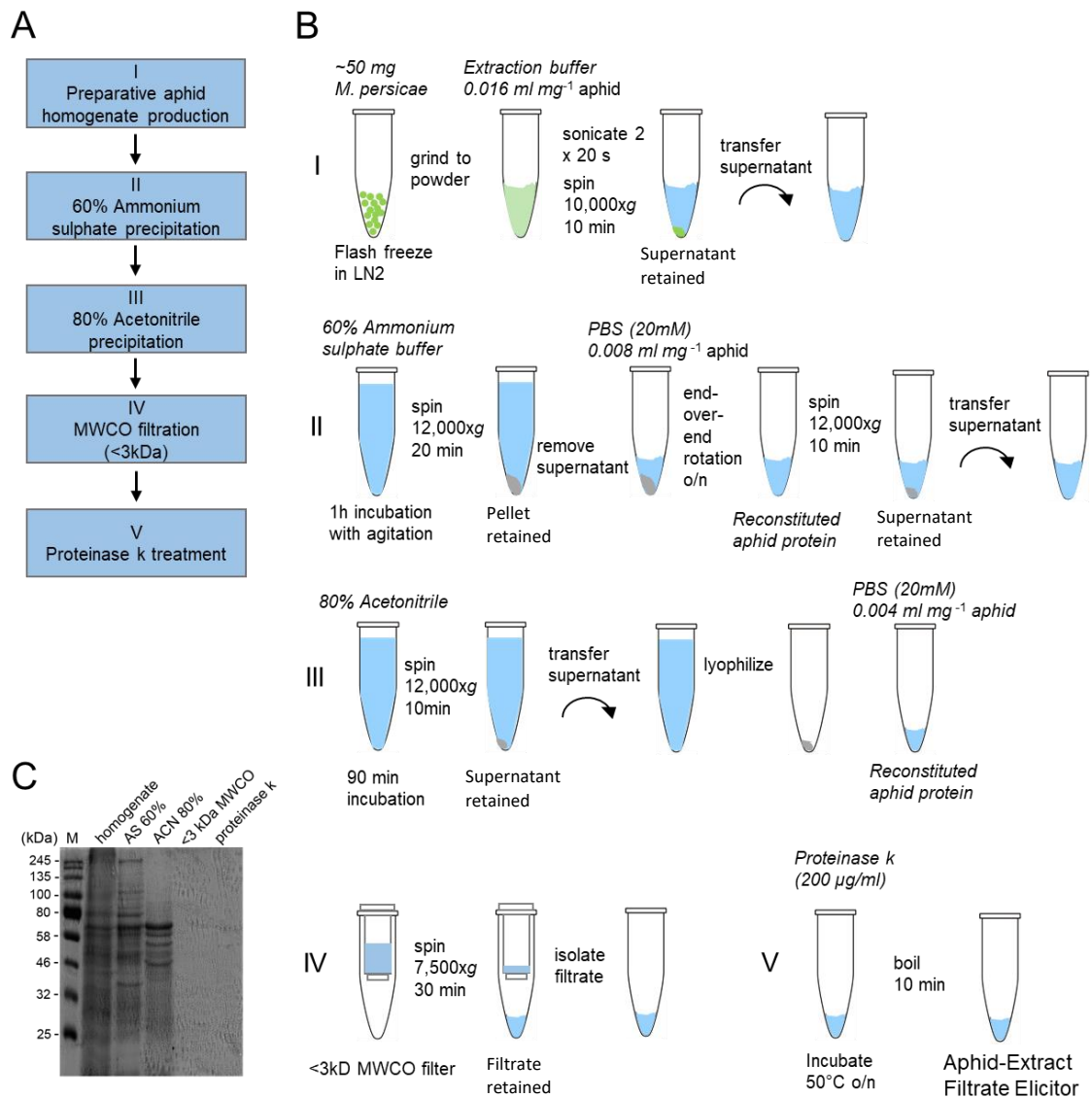


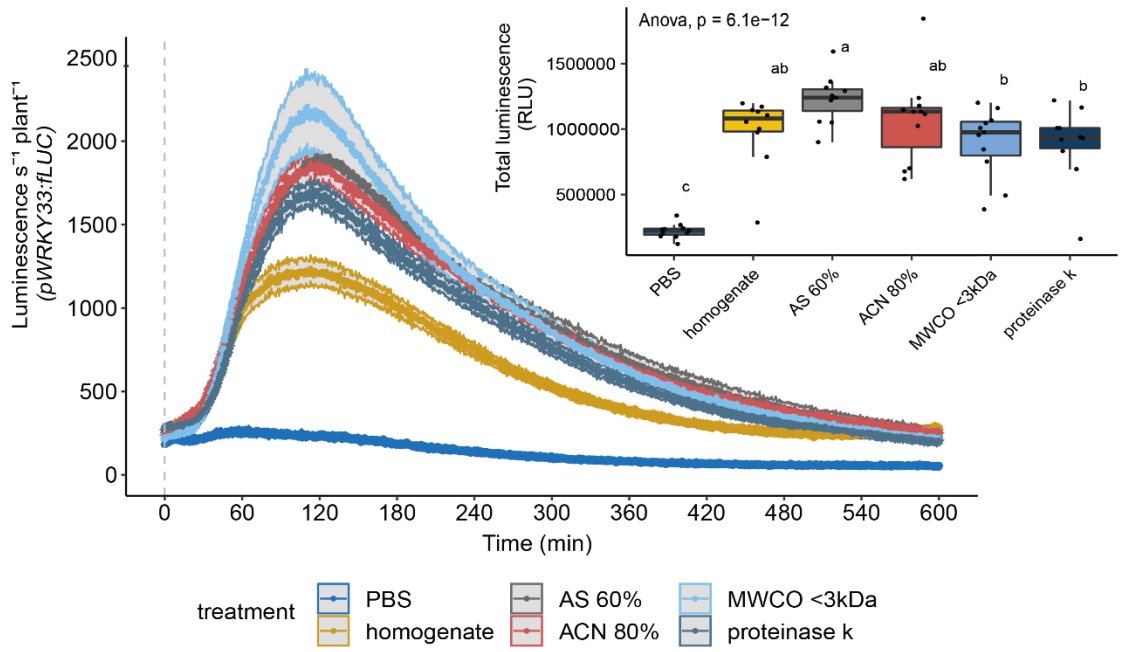
Figure 3.1: Illustrated protocol of aphid extract filtrate elicitor (AEFE)-containing fraction production. **A** Summary flow diagram of key steps (I – V) in the purification procedure. **B** Illustrated method of isolating the AEF E-containing fraction from whole-body *M. persicae*. **C** Coomassie ReadyBlue™ protein stain of *M. persicae* partially purified fractions. Treatment steps are indicated. M: molecular marker; homogenate: soluble fraction of crude aphid extract; AS60%: ammonium sulphate precipitant (60% (v/v)); ACN: acetonitrile precipitant (80% (v/v)); < 3kDa MWCO: molecular weight cut-off filtrate; proteinase k: Proteinase k-treated sample.

Cytosolic calcium ($[Ca^{2+}]_{\text{cyt}}$) elevations are rapidly induced in the plant at the aphid feeding site (Vincent et al., 2017), and is one of the earliest responses in plant cells to environmental stimuli including to MAMPs (Ranf et al., 2008, Thor and Peiter, 2014). To confirm MTI induction against aphid extract fractions, and assess whether $[Ca^{2+}]_{\text{cyt}}$ elevations are induced, I monitored $[Ca^{2+}]_{\text{cyt}}$ elevations in *A. thaliana* seedlings expressing the GFP-based reporter driven by the *Cauliflower Mosaic Virus (35S)* promoter (*35S:GCaMP3*) (Tian et al., 2009, Vincent et al., 2017). $[Ca^{2+}]_{\text{cyt}}$ was rapidly and transiently elevated against extract fractions, peaking at approximately 15 min before returning to a new stable state by approximately 45 min (Fig. 3.2B). The amplitude and duration of transient $[Ca^{2+}]_{\text{cyt}}$ elevations were broadly maintained during the purification process.

Heat tends to denature proteins such that biological activity is lost upon boiling; a process linked to loss of hydrogen bond integrity and water ingress (Mirsky and Pauling, 1936). I assessed the effect of heat treatment by boiling aphid-derived extracts as an integrated step during the purification process to heat-inactivate proteinase k (tested further in Fig. 3.3). Heat treatment did not alter extract-induced *WRKY33* promoter activity or $[Ca^{2+}]_{\text{cyt}}$ elevations, indicating that heat denaturation does not perturb AEF activity (Fig. 3.2).

To determine whether sequential purification steps resulted in a tendency toward purifying an elicitor of MTI, I concomitantly measured total protein and immuno-activity. The immunoactivity was broadly conserved despite a global reduction in protein concentration which results in an increase in *specific activity* (the activity (relative luminescence) per unit of total protein) (Table 3.1). Together, these results suggest that sequential purification steps results in enrichment of an elicitor, or elicitors, likely of a low molecular weight (< 3kDa) that induce *WRKY33* promoter activity and $[Ca^{2+}]_{\text{cyt}}$ elevations.

A



B

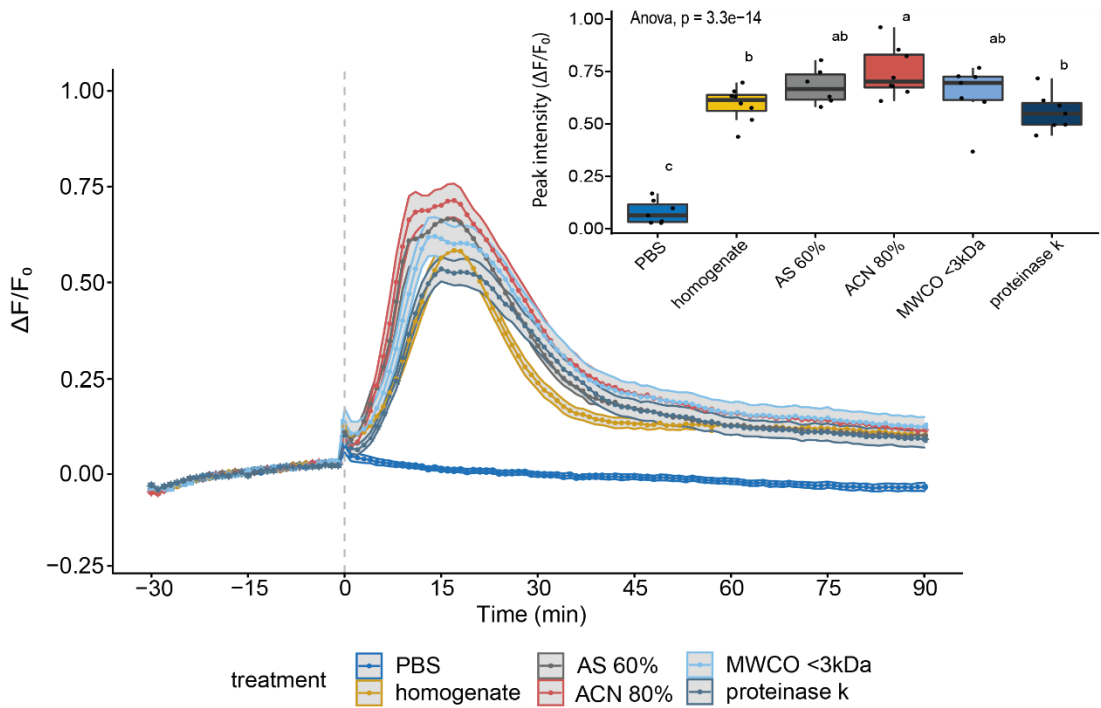


Figure 3.2: Aphid-derived elicitors induce MAMP-triggered immune responses in *A. thaliana*.

A *WRKY33* promoter activity in *A. thaliana* *pWRKY33::fLUC* seedlings during step-wise, activity-guided enrichment of aphid-derived elicitors. Reporter plants were exposed to 2.5% (v/v) per treatment. Bioluminescence from each seedling was monitored with real-time bioluminescence monitoring every 30 s. Data are shown as mean \pm SE from at least seven seedlings per treatment. [Inset graph] Data is replicated as mean of the summed luminescence between 0- and 600-min post-treatment. Whiskers represent lowest and highest score excluding outliers. Biological repeat values are shown as black dots. Letters indicate significant differences ($p < 0.05$) between treatments (ANOVA; $df = 5,58$, $F = 21.06$, $p = 6.14^{-12}$).

B Cytosolic calcium $[Ca^{2+}]_{\text{cyt}}$ elevations in *A. thaliana* seedlings expressing *GCaMP3* driven by the *Cauliflower Mosaic Virus (35S)* promoter (*35S::GCaMP3*; Tian et al., 2009, Vincent et al., 2017) upon challenge against aphid-derived elicitor fractions. GFP fluorescence was monitored every 60 s and normalised according to the equation $\Delta F/F_0 = (F - F_0)/F_0$, where F is the fluorescence emission (at 525/50 nm) and F_0 is the mean baseline (pre-treatment) fluorescence calculated from the mean of F over the first 15 frames (15 min). Mean $\Delta F/F_0$ ($n = 7-16$) is displayed \pm SE (gray shading). [Inset graph] displays the mean of the peak intensity ($\Delta F/F_0$). Letters indicate significant differences ($p < 0.05$) between treatments (ANOVA; $df = 5,37$, $F = 41.64$, $p = 3.35^{-14}$).

Table 3.1: Specific activity of partially purified, aphid-derived extracts.

Purification step	Volume (ml)	Total activity ^a (LUM s ⁻¹ plant ⁻¹) ($\times 10^4$ \pm SD)	Protein per assay ($\mu\text{g ml}^{-1}$)	Specific activity ^b (Relative LUM μg^{-1}) ($\times 10^2 \pm$ SD)	Purification factor	Protein yield (%)
<i>pWRKY33::fLUC</i>						
homogenate	0.8	73.2 \pm 3.1	108.4 \pm 2.8	56 \pm 9	1.0	100.0
AS 60%	0.4	102.3 \pm 1.5	65.4 \pm 4.8	193 \pm 34	3.4	20.0
acetonitrile 80%	0.2	93.6 \pm 8.5	34.2 \pm 1.7	296 \pm 2	6.4	5.2
<3kDa MWCO	0.2	87.3 \pm 19.6	22.5 \pm 3.1	369 \pm 104	10.1	3.4

Activities are defined as *WRKY33* promoter activity in *A. thaliana* seedling stably expressing *pWRKY33::fLUC*. Luminescence (LUM) is measured at 30 s intervals and summed to generate a total LUM. Averages are presented \pm standard deviation.

^a Total activity is calculated as the averaged summed luminescence (LUM) over 600 min minus a control (PBS).

^b Specific activity is calculated as the total activity per μg protein used in the assay.

3.2.2 AEF E activity is sensitive to protease treatment, resistant to deglycosylation and is concentration-dependent

A wide array of proteinaceous and non-proteinaceous MAMPs elicit innate immune responses in plants (Newman et al., 2013). To further assess the nature of the elicitor(s) responsible for AEF E-associated MTI, I treated the AEF E fraction with three non-specific proteases: carboxypeptidase b (Merck, C9584), pronase (Merck Calbiochem®, 53702) and proteinase K (Merck, 70663) followed by enzyme deactivation by heat treatment at 95°C. *WRKY33* promoter activity was significantly reduced ($p < 0.05$) against pronase-treated AEF E whereas carboxypeptidase b or proteinase k treatments had no effect on AEF E-induced *WRKY33* promoter activity (Fig. 3.3A). Given that proteinase K digestion preserved AEF E immunoactivity, I used proteinase K digestion to further purify elicitors within the aphid-derived extracts (as shown in Fig. 3.1; 3.2).

Pronase is a mixture of serine-type proteases, Zn²⁺ endopeptidases, Zn²⁺-leucine aminopeptidases and Zn²⁺ carboxypeptidase isolated from the extracellular fluid of *Streptomyces griseus* (Narahashi and Yanagita, 1967). To further assess the specificity of pronase-mediated proteolysis of aphid-derived elicitors, I treated p*WRKY33:fluc* reporter seedlings with flg22 and the polysaccharide polymer, chitin (β -(1–4)-poly-*N*-acetyl-D-glucosamine). Pronase treatment of flg22 abolished flg22-induced *WRKY33* promoter activity but had no effect on chitin-induced activity (Fig. 3.3B). Given that flg22 activity is conferred by its amino acid sequence (Naito et al., 2008), and cleavages are likely to reduce or abolish flg22 activity, it is likely that pronase can digest flg22, rendering it inactive. In contrast, chitin remains bioactive and there is no evidence of glycosidase activity within pronase.

To test whether pronase protease constituents are responsible for pronase-mediated proteolysis of AEF E, I treated pronase with a protease inhibitor cocktail (PIC) (Sigma-Aldrich, P2714) or leupeptin (*N*-acetyl-L-leucyl-L-leucyl-L-argininal) (Sigma-Aldrich, L9783), a serine and cysteine protease inhibitor. Treatment of pronase with PIC but not leupeptin prior to AEF E treatment abolished the pronase mediated loss of *WRKY33* promoter activity (Fig. 3.3C). Furthermore, treatment of seedlings with PIC- or leupeptin-treated AEF E did not affect AEF E-induced *WRKY33* promoter activity suggesting that PIC inhibits a pronase-derived protease, other than a serine or cysteine protease, to avoid cleavage of the elicitor(s) (Fig. 3.3C). Additionally, neither PIC nor leupeptin can inhibit AEF E activity by inhibiting a protease within AEF E itself. These results strongly suggest a proteinaceous elicitor within AEF E can induce *WRKY33* promoter activity.

MAMPs represent a broad range of molecules which include proteins, peptides, carbohydrates, lipids, glycolipids and glycoproteins (Boller and Felix, 2009, Trouvelot et al., 2014). Next, I wanted to determine whether glycoproteins may contribute to AEF E-mediated immune induction by treating AEF E with deglycosylases Peptide-N-glycosylase F (PGNase F) or Endoglycosidase H (Endo H). Neither PGNase F- nor Endo H-treatment significantly ($p > 0.05$) altered AEF E-mediated *WRKY33* promoter activity (Appendix I.IA). To control for altered PGNase F activity by AEF E components, I treated the glycoprotein, RNase B (NEB, P7817S) with PGNase F to visualise RNase B deglycosylation via an SDS-PAGE mobility-shift assay with and without AEF E. RNase B contains a single *N*-linked glycosylation site thus is cleaved to generate a low molecular weight product up on PGNase F treatment. Deglycosylation of RNase B occurred both in the presence of AEF E and without suggesting AEF E does not alter PGNase F-mediated deglycosylation (Appendix I.IB).

flg22- and *elf18*-triggered ROS production and defence gene expression are dose-dependent and typical of responses that are dependent on ligand sensing by receptors (Felix and Boller, 2003, Kunze et al., 2004, Zipfel et al., 2006, Denoux et al., 2008). To assess whether AEF E-triggered *WRKY33* promoter activation or $[Ca^{2+}]_{cyt}$ elevations are dose-dependent, I exposed reporter seedlings to dilutions of AEF E. The

AEFE fraction, both with respect to *WRKY33* expression and $[Ca^{2+}]_{cyt}$ elevations, displays dose-responsive activity with concentrations as low as 0.01% (v/v) (~9 $\mu\text{g/ml}$) and 0.001% (v/v) (~0.9 $\mu\text{g/ml}$), respectively, sufficient to elicit responses (Appendix I.II).

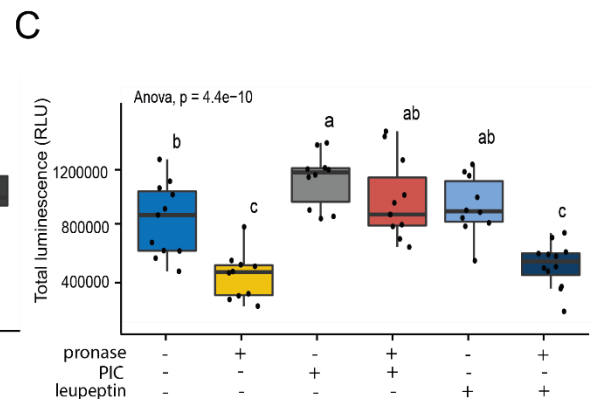
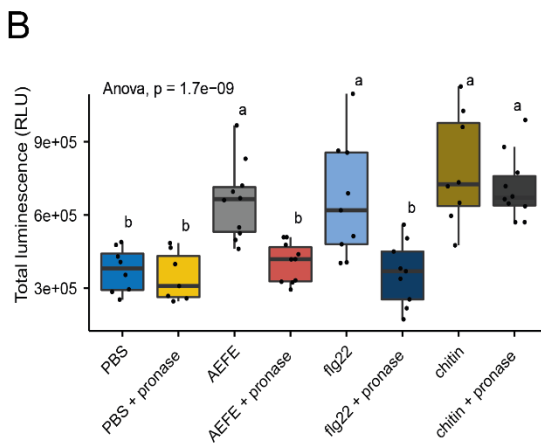
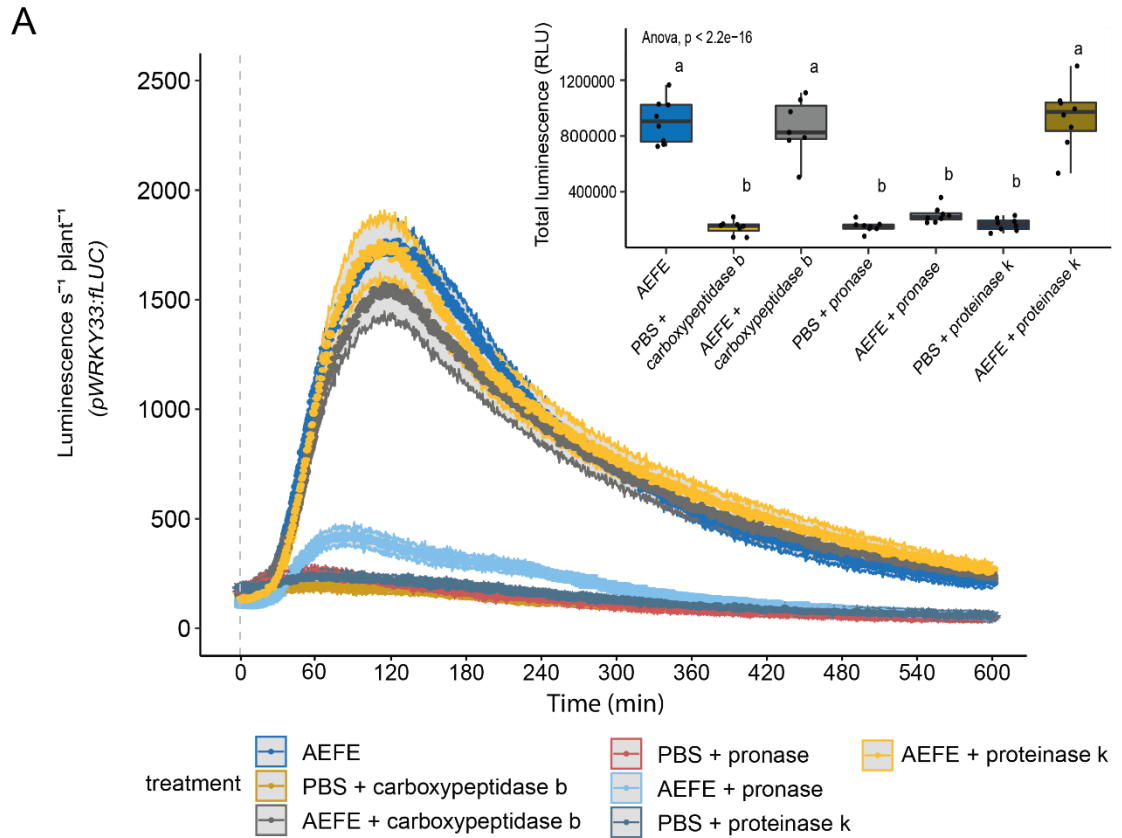


Figure 3.3: Elicitor activity of aphid-derived extract (AEFE) is sensitive to pronase treatment.

A Luminescence time-course of 10-day-old *pWRKY33::fLUC A. thaliana* seedlings treated as displayed. AEFE was generated from whole-body *M. persicae* (see text for details) and treated with carboxypeptidase b (Merck (C9584); 10 µg/ml), pronase (Calbiochem® (53702); 1 mg/ml) or proteinase k (Merck (70663); 100 µg/ml). AEFE and protease-treated AEFE were used at concentrations of 2.5% (v/v) (~22.5 µg/µl). Seedlings were treated with PBS or protease-treated PBS at a concentration of 2.5% (v/v) as a control. Proteases within AEFE and PBS samples were heat-deactivated prior to seedling treatments. Bioluminescence from each seedling was monitored with real-time bioluminescence monitoring every 30 s. Data are shown as mean ± SE from at least seven seedlings per treatment. [Inset graph] Data is replicated as mean of the summed luminescence between 0- and 600-min post-treatment. Whiskers represent lowest and highest score excluding outliers. Biological repeat values are shown as black dots. Letters indicate significant differences ($p < 0.05$) between treatments (ANOVA; $df = 5,48$, $F = 66.86$, $p = 6.14 \cdot 10^{-12}$).

B AEFE- and flg22- but not chitin-induced *WRKY33* promoter activity is inhibited by pronase treatments. Total luminescence showing the mean ± SE of the summed luminescence between 0- and 600-min post-treatment. Seedlings were treated with PBS (2.5% (v/v)), AEFE (2.5% (v/v); ~22.5 µg/µl), flg22 (100nM) or chitin (25 µg/ml) with/without pre-treatment with pronase protease. Biological repeat values are shown as black dots. Letters indicate significant differences ($p < 0.05$) between treatments (ANOVA; $df = 7,62$, $F = 4.97$, $p = 0.000166$).

C Inhibition of pronase-mediated loss of AEFE activity is sensitive to Protease Inhibitor Cocktail (PIC) treatment but not leupeptin treatment. *pWRKY33::fLUC* seedlings were exposed to AEFE pre-treated with pronase with/without PIC or leupeptin pre-treatment or AEFE treated with leupeptin or PIC directly. Differences in mean luminescence between treatments was assessed via an ANOVA with Tukey post-hoc analysis. Letters indicate significant differences ($p < 0.05$) between treatments ($df = 5,58$, $F = 16.45$, $p = 4.41 \cdot 10^{-10}$).

3.2.3 Proteolytic activity within extract is required for full AEFE-induced immune response

I have shown that induction of immune responses by AEFE is likely conferred by LMW components that are sensitive to pronase-mediated proteolysis. To further assess the nature of LMW components of AEFE, I treated crude aphid extracts with protease inhibitor cocktail (PIC), a broad protease inhibitor, E-64 or AEBSF, a cysteine and serine protease inhibitor, respectively (Hanada et al., 1978, Nakabo and Pabst, 1996). Extracts were then purified to generate the AEFE fraction following the protocol illustrated (Fig. 3.1) and *WRKY33* promoter activity assessed. Treatment of AEFE at an early stage (step I) of purification with PIC or E-64 but not AEBSF significantly reduces ($p < 0.05$) AEFE-induced *WRKY33* promoter activity (Fig. 3.4). Addition of E-64 to AEFE

after purification (after step V), or to flg22 or elf18, does not alter defence induction against these MAMPs (Fig. 3.4B). These results suggest that proteolytic processing, likely mediated by a cysteine protease, takes place during the purification process to generate an elicitor of immune responses.

To further delineate the class of cysteine proteases required for elicitor function, I treated crude extracts with the methyl ester E-64 derivative, CA-074-Me or the caspase-3 inhibitor, Ac-DEVD-CHO (*N*-Ac-Asp-Glu-Val-Asp-CHO) (Garcia-Calvo et al., 1998, Danon et al., 2004). Treatment with CA-074-Me but not Ac-DEVD-CHO abolished AEF2-mediated *WRKY33* promoter activity (Fig. 3.4C). Although it is not known that CA-074-Me or Ac-DEVD-CHO can inhibit aphid cysteine proteases, this result suggests that CA-074-Me can inhibit at least one member of aphid cysteine proteases involved in the liberation of an aphid-derived elicitor. I cannot rule out the possibility E-64 or CA-074-Me acts indirectly on a protease that doesn't directly process an elicitor. Additionally, I cannot rule out the possibility that the aphid has ingested a protease substrate or a cysteine protease from the plant host (*B. rapa*) that is targeted by a protease or inhibited by an inhibitor, respectively.

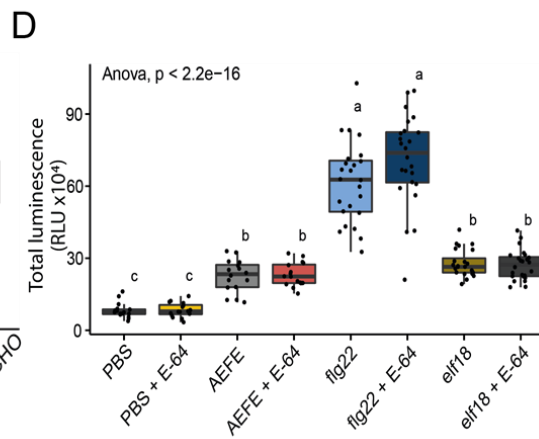
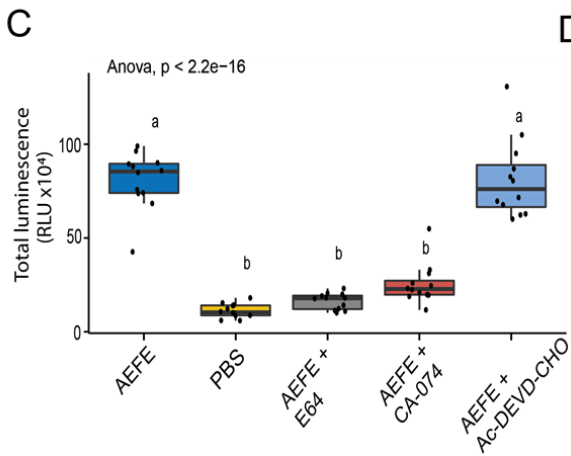
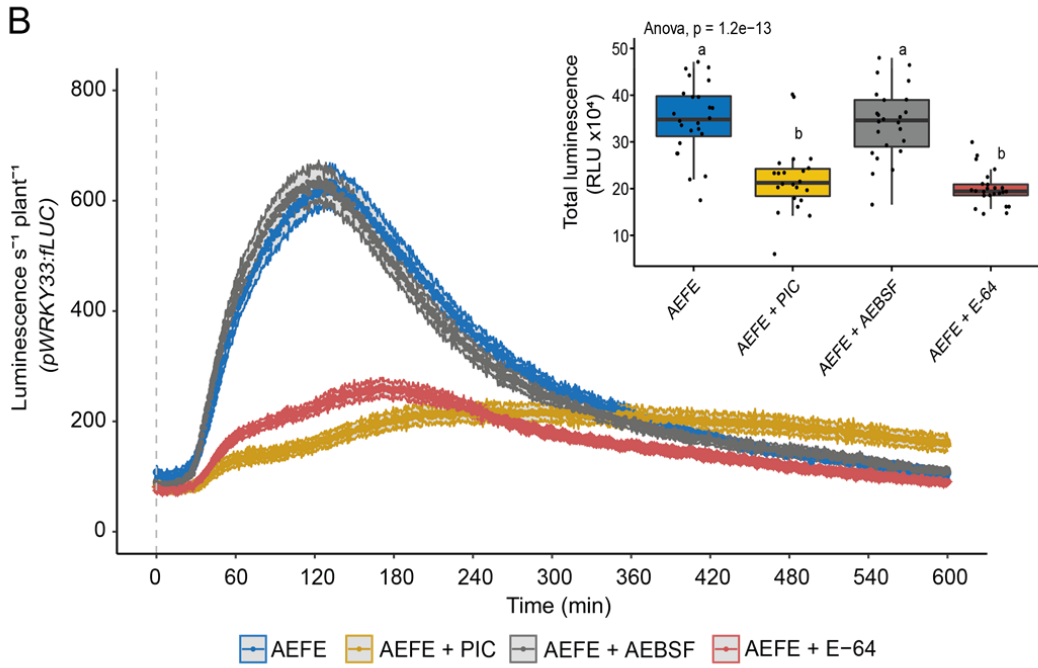
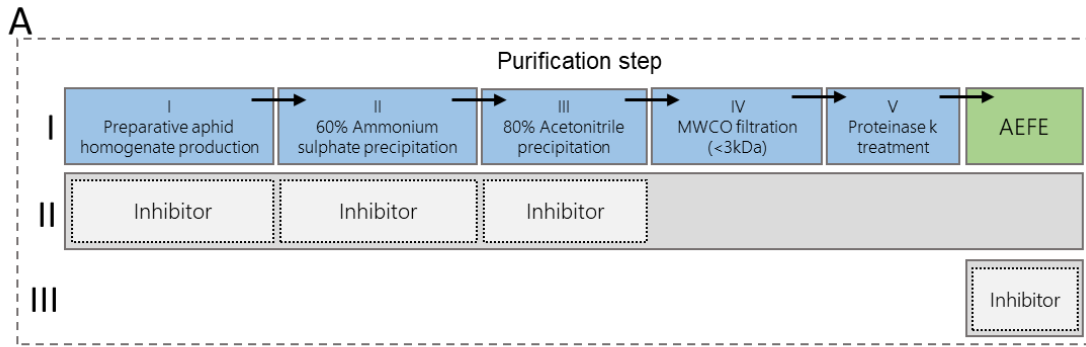


Figure 3.4: Elicitor activity of aphid-derived extract (AEFE) requires cysteine proteases. A Illustration of protease inhibitor treatments of aphid-derived extracts. Inhibitor treatments followed protocol II, where inhibitors (E-64) are present in buffers throughout the extraction process (I). Where inhibitors were added late in the extraction process, protocol III was followed. **B** Early addition (II) of a protease inhibitor cocktail (PIC) or E-64, but not AEBSF results in reduced bioactivity of AEFE. Luminescence time-course of 10-day-old *pWRKY33::fLUC A. thaliana* seedlings treated as displayed. [Inset graph] Data is replicated as mean of the summed luminescence between 0- and 600-min post-treatment. Whiskers represent lowest and highest score excluding outliers. Biological repeat values are shown as black dots. Letters indicate significant differences ($p < 0.05$) between treatments ($df = 3,90$, $F = 30.36$, $p = 1.19 \cdot 10^{-13}$). **C** Early addition (II) of E-64 and CA-074, but not Ac-DEVD-CHO results in reduced bioactivity of AEFE. Boxes represent mean of the summed luminescence between 0- and 600-min post-treatment. Letters indicate significant differences ($p < 0.05$) between treatments ($df = 3,44$, $F = 72.59$, $p < 2 \cdot 10^{-16}$). **D** Late addition (III) of E-64 to PBS (2.5 % (v/v)) or elicitors AEFE ($\sim 22.5 \mu\text{g}/\mu\text{l}$), flg22 (100 nM) or elf18 (100nM) had no effect on luminescence output of *pWRKY33::fLUC A. thaliana* seedlings. Boxes represent mean of the summed luminescence between 0- and 600-min post-treatment. Letters indicate significant differences ($p < 0.05$) between treatments ($df = 7,152$, $F = 96.81$, $p < 2 \cdot 10^{-16}$).

3.2.5 Purifying aphid-derived elicitors using three-dimensional liquid chromatography

Crude extracts, derived from cell cultures or insect pests, have proven useful materials to decipher MAMP-PRR dynamics and may act as a starting point to isolate novel elicitors of MTI in plants (Prince et al., 2014). To further purify aphid-derived elicitors from AEFE, I opted to separate AEFE components via several, chromatographical steps. Firstly, I subjected AEFE to solid phase extraction (SPE) using a strong cation exchanger (¹D) prior to orthogonal high-pH (²D), low-pH (³D) reversed-phase, ultra-high performance liquid chromatography (RP-UHPLC) steps (Fig. 3.5). During ²D and ³D separation elutes were fractionated into 1 min fractions and subsequently lyophilised and reconstituted in PBS solution to test for induction of *WRKY33* promoter activity. UV absorption at 254 nm and 280 nm was monitored to indicate sample complexity during purification steps.

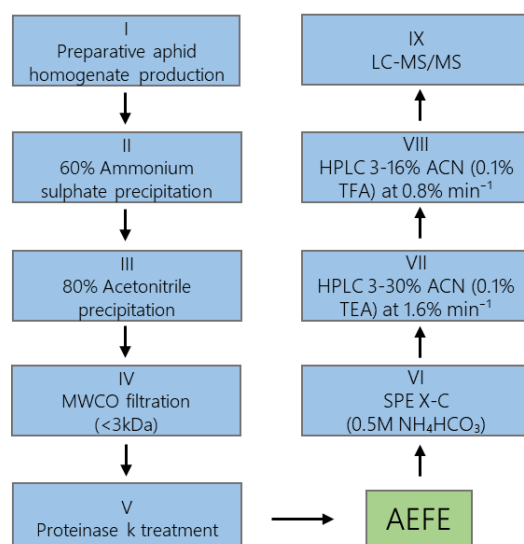


Figure 3.5: Illustrated protocol of purification steps towards the identification of candidate elicitor peptides Summary flow diagram of key steps (I – IX) in the purification procedure. Illustrated method of isolating the AEFE-containing fraction from whole-body *M. persicae*. AEFE were subject to strong cation exchange chromatography (SPE X-C) to clean-up and concentrate prior to orthogonal (high pH/low pH), reverse-phase UHPLC. Fraction constituents were measured by mass spectroscopy (LC-MS/MS).

For SPE separation, AEFE was acidified with 0.1% (v/v) trifluoroacetic acid (TFA), loaded onto a Strata™-X-C column (Phenomenex® Ltd, Macclesfield, UK) and eluted with SPE Solvent B (20% (v/v) ACN and 0.1% (v/v) triethylamine (TEA)). Due to acidic carry-over, I was unable to confirm immuno-activity directly after strong cation exchange separation. Despite this, UV absorption of X-C-separated samples indicated elutes were less complex post SPE and remained amenable to reversed-phase UHPLC where immuno-activity could be readily assessed. Lyophilized X-C-separated elutes were reconstituted in UHPLC high-pH Solvent A (dH₂O and 0.1% TEA), loaded onto a C₁₈ stationary phase (Waters XBridge® Peptide BEH C₁₈, Waters Limited, Wilmslow, UK) and eluted using a linear gradient of high-pH Solvent B (97% (v/v) ACN, 2.9% dH₂O and 0.1% (v/v) TEA) ranging from 3-25% (v/v) at 1.6% min⁻¹. Fractions were collected at 1 min intervals between 0 - 38 min retention times, lyophilised and concomitantly assessed for their ability to induce *WRKY33* promoter activity and reconstituted in UHPLC low-pH Solvent A (dH₂O and 0.1% (v/v) TFA) for downstream separation.

Under high-pH conditions (²D), immuno-active components elute as a major peak with a retention time of approximately 12 min (fraction 12), which is associated

with a rapid increase in 254 nm and 280 nm absorption (Fig. 3.6A, B). Two fractions, eluting at 26 min and 29 min also exhibit weak immuno-activity relative to fraction 12 but induce *WRKY33* promoter activity significantly above a buffer control ($p < 0.05$). Furthermore, two additional fractions, eluting at 11 min and 24 min exhibit very weak ability to induce *WRKY33* promoter activity ($p < 0.05$). In addition to flow-through (fractions 1 and 2) (data not shown), all other 1 min fractions, eluting between 3 min and 38 min exhibited activity not different to a PBS control treatment ($p > 0.05$), suggesting that bioactive components of aphid-derived extracts bind to the C_{18} column and are retained for varying periods during mobile phase elution.

To carryout sub-fractionation of the immuno-active ²D Fraction 12, I reconstituted in low-pH Solvent A (dH₂O and 0.1% (v/v) TFA), loaded onto the same C_{18} stationary phase and eluted using a linear gradient of low-pH Solvent B (97% (v/v) ACN, 2.9% dH₂O and 0.1% (v/v) TFA) ranging from 3-16% (v/v) at 0.8% min⁻¹ (³D). Immuno-active components eluted within a single fraction with a retention time of approximately 25 min ($p < 0.05$) (Fig. 3.6C, D). Further separations identified two additional immuno-active peaks flanking the 25 min fraction with retention times of approximately 21-22 min and 29-31 min. In the illustrated example separation, the 29 min fraction displayed elevated immuno-activity but is not significant relative to a PBS control ($p > 0.05$).

To further resolve the region of retention times encompassing fractions exhibiting major and minor immuno-activity, I conducted four independent ³D separations, collecting Fractions 21 to 32 to assess their ability to induce *WRKY33* promoter activity. Immuno-activity could be consistently and robustly identified as a major peak at 25 and 26 min, and two minor peaks; a later peak at 30 and 31 min and an early peak at 21 and 22 min (Fig. 3.7). Due to lack of robustness and amplitude of the minor early peak, I opted not to further assess these fractions.

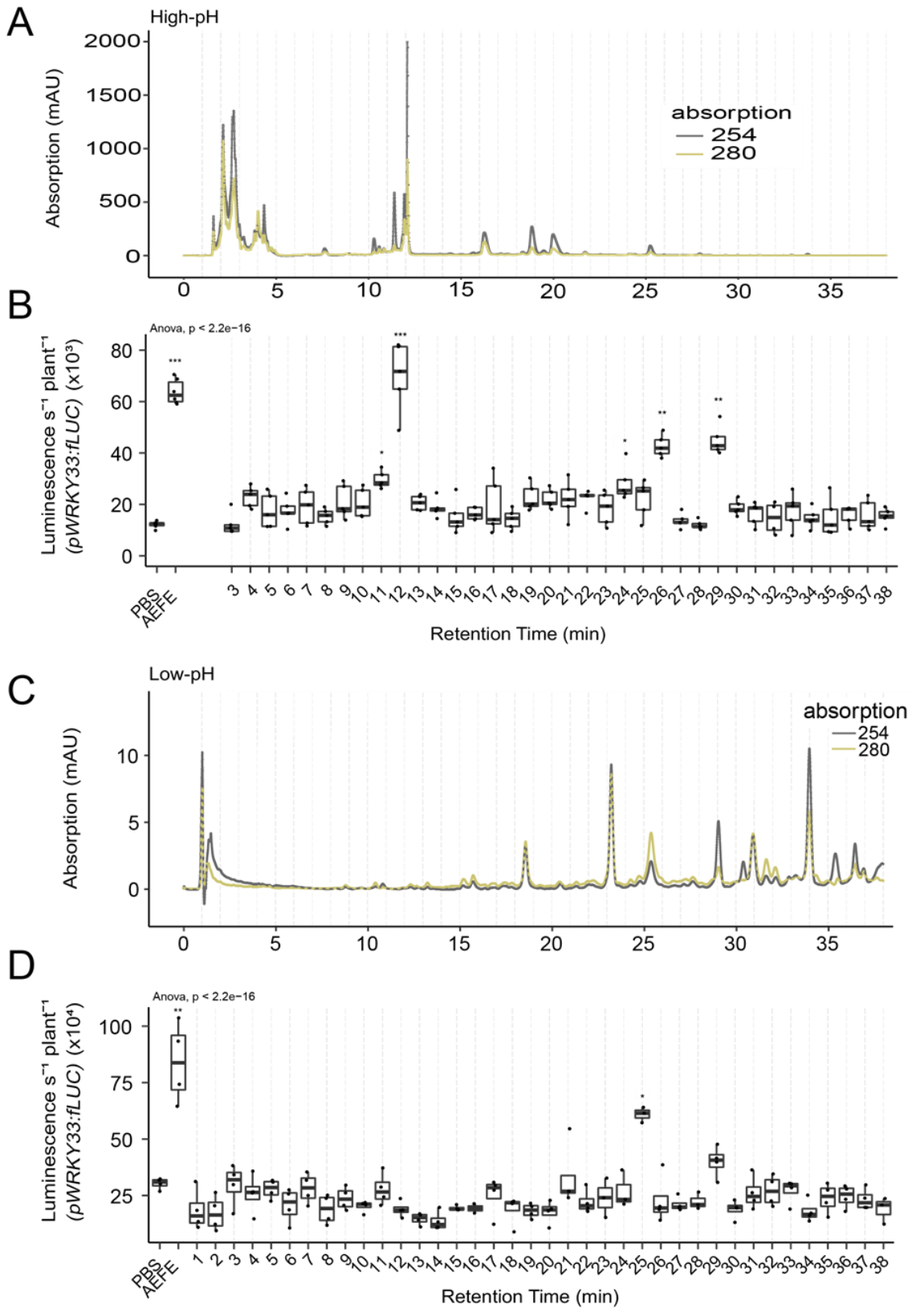


Figure 3.6: Elicitor activity of aphid-derived extract (AEFE) elutes as discrete fractions in ³D-UHPLC. **A** Solid-phase extracted (SPE X-C) AEFE was resuspended in high pH buffer A, injected onto a reverse-phase, X-bridge C₁₈ column (Waters) and eluted in a mobile phase (solvent B) of ACN + 0.1% (v/v) TEA with a linear gradient (1.2 ml min⁻¹), using the Agilent 1290 Infinity II LC system. Absorbance at 254 nm and 280 nm were monitored between 3-30% solvent B. Vertical, light grey bars are fraction boundaries collected every 1 min. **B** Eluting fractions were assessed for their ability to induce luminescence output in *pWRKY33:flUC A. thaliana* seedlings. Boxes represent mean of the summed luminescence between 0- and 600-min post-treatment. Asterisks indicate significant differences ($p < 0.05$) between treatments. **C** After high-pH RP-UHPLC, the 12 min retention peak was collected, lyophilized and reconstituted with low-pH solvent A (low pH). The fraction was injected and eluted with low pH solvent B (ACN + 0.1% (v/v) TFA) with a linear gradient (0.8 ml min⁻¹). Absorbance at 254 nm and 280 nm were monitored between 3-16% solvent B. **D** Eluting fractions were assessed for their ability to induce luminescence output in *pWRKY33:flUC A. thaliana* seedlings as described above.

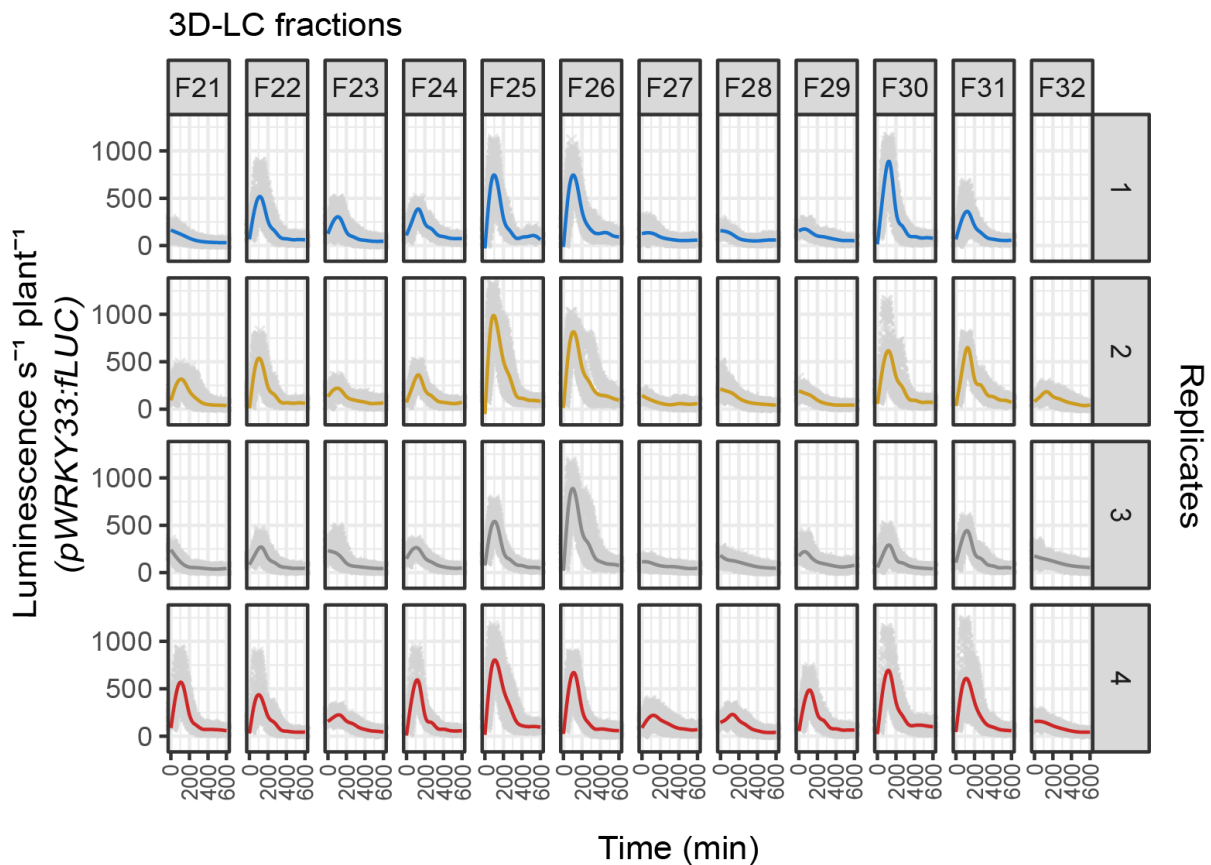


Figure 3.7: Luminescence of ³D-UHPLC separated fractions of aphid-derived extracts reveals consistent peaks of immune-activity across biological repetitions. Ultra-high performance liquid chromatography (UHPLC) Agilent 1290 Infinity II LC System as described. ³D fractions were assessed for their ability to induce luminescence output in *pWRKY33::fLUC A. thaliana* seedlings. Luminescence was monitored 0 - 600 min post-treatment. Coloured lines represent average luminescence per seedling. All biological repeats are shown in grey shading.

3.2.6 UHPLC-separated immune-active peaks are pronase-sensitive

Previously, I showed that pronase treatment of aphid-derived extracts abolished immuno-activity (Fig. 3.3). To test whether bioactive components of 3D-UHPLC-separated samples remained sensitive to pronase treatment, I combined active fractions 24 and 25 as well as active fractions 30 and 31 and treated these samples with pronase for 2-hr prior to heat inactivation. To control for indirect effects of treatment, fractions 25/26 and 30/31 were treated with an equivalent aliquot of dH₂O and incubated under similar conditions. Pronase treated fractions 25/26 or fractions 30/31

were unable to induce *WRKY33* promoter activity ($p < 0.05$) whereas untreated fractions remained active (Appendix I.III). Pronase treatment of PBS did not alter its inability to induce *WRKY33* promoter activity in the plant.

Previously, I demonstrated that the addition of E-64 during aphid-extract processing results in the loss of bioactivity (Fig. 3.4). This result suggests that the action of cysteine protease(s) is required for the liberation of an immuno-active component within extracts. I hypothesised that the protease-mediated action may lead to quantitative differences between of an immuno-active component between E-64-treated and untreated samples. To exploit this characteristic, I opted to carry out *N*-terminal, isobaric stable isotope labelling using tandem mass tags (TMTs). TMT labelling results in a hydrophobic shift on RP-HPLC as the characteristics of labelled peptides is altered. Unfortunately, no evidence of a shift in activity was detected and this line of investigation was not pursued further.

3.2.7 UHPLC-separated immune-active peaks are pronase-sensitive

To further reduce the complexity of ³D-separated samples, I next opted to separate indexed retention time (iRT) peptides (Zolg et al., 2018), to use their retention time to serve as a proxy for immuno-activity on nano-LC. The iRTs retentions on semi-preparative UHPLC and nanoLC characteristic were compared. Given that the relationship between immuno-activity and iRT retention could be established on UHPLC, this enabled signposting of the activity for nanoLC. Three 11-mer iRT peptides; SYASDFGSSAK, LSSGYDGTSYK and FLASSEGGFTK were chosen as they display moderate to high hydrophilicity, predictably separate on a C₁₈ stationary phase, and are not found in nature (Zolg et al., 2018). iRT peptides were synthesised (Pepmic Co. Ltd, Suzhou, China) and separated utilising the low-pH UHPLC method. Each synthetic iRT preparation contained at least one peptide derivative that were identified as *N*-terminal truncations in LC-MS/MS analysis. By utilizing each iRT and iRT derivative, the

retention time on nano-LC of immunoactive components could be placed between 400 and 1080 s. For example, retention of the major bioactive peak (Fraction 25 and 26) is closely followed by the elution of SSGYDGTSYK during ³D-UHPLC. Retention of the later peak (Fraction 30 and 31) was closely preceded by SYASDFGSSAK and closely followed by FLASSEGGFTK during ³D-UHPLC.

³D-fractionated samples were subject to nano-ultra-high performance liquid chromatography coupled to tandem mass spectroscopy (nano-UHPLC-MS/MS) to obtain mass spectra. Spectra were searched against the *M. persicae* Clone O (genome v2.0 - https://bipaa.genouest.org/sp/myzus_persicae/) (Mathers et al., 2020) proteome to predict peptide sequences in Mascot. Peptide predictions were subsequently filtered using three characteristics: (1) Mascot ion score cut-off of > 45 indicating a 5% false discovery rate. (2) Retention times of between 400 - 1080 seconds based on the retention of iRTs during nano-UHPLC. (3) The total number of replicates in which the peptide was identified was at least three of four.

A total of 443 unique peptides were identified in all samples after applying filters for Mascot ion score (> 45) and retention time (400s - 1080s). The total number of unique peptides occurring in multiple experimental replicates is listed in Appendix I.IV. Of these peptides, a total of 68 peptides were selected for synthesis, 59 from fractions 25 and 26 (Table 3.2), and 9 from samples 30 and 31 (Table 3.3), based on their characteristics.

The candidate elicitor peptides (CEPs) were 6-11 amino acids in length with a mean length of 8.2. The CEPs were comprised of 23.1% (128/555) proline, 14.2% (79/555) lysine, 5.9% (33/555) valine, 5.8% (32/555) arginine and glutamic acid and 45.2% (251/555) other residues. No cysteine or tryptophan residues were present in any CEP (Table 3.3, Table 3.4).

Peptides that satisfy the selection characteristics were synthesised as SpikeTides™ (JPT Peptide Technologies, Berlin, Germany) peptide candidates (Schnatbaum et al., 2011). Peptides were reconstituted in peptide reconstitution buffer (see *Materials and Methods*) and used to treat *A. thaliana pWRKY33::fLUC* seedlings.

No peptide candidate induced *WRKY33* promoter activity above background levels suggesting that synthetic peptide candidates are not immunoactive (Fig. 3.8).

Table 3.2: Candidate elicitor peptides (CEPs), identified in LC-MS/MS of fractions 25 and 26 and satisfying selection characteristics.

ID	Peptide	Protein accession	Peptide mass (AMU)	Retention time (s)	Fraction 25		Fraction 26	
					MIS (max)	Rep count	MIS (max)	Rep count
P1_A4	YAPKKPIG	MYZPE13164_O_Elv2.1_0247760.1	1001.6	807 - 854	43.3	4	53.2	4
P1_A5	GNRPKPPVE	MYZPE13164_O_Elv2.1_0167610.1	993.5	774 - 948	46.9	4	52.2	4
P1_A6	FPKPGGGDK	MYZPE13164_O_Elv2.1_0268960.1	902.5	757 - 969			51.8	4
P1_A7	GNKFEPAPK	MYZPE13164_O_Elv2.1_0252480.1	1088.6	777 - 834	24.2	4	61.5	3
P1_A8	IIDAPGHRD	MYZPE13164_O_Elv2.1_0146250.2	993.5	830 - 879	53.9	4	58.8	3
P1_A9	IKVPNQEQ	MYZPE13164_O_Elv2.1_0268960.1	955.5	1027 - 1080	30.5	4	28.8	3
P1_A10	TKFPER	MYZPE13164_O_Elv2.1_0306860.1	777.4	727 - 779	32.8	3	36.6	4
P1_A11	IIRDPAM	MYZPE13164_O_Elv2.1_0180410.1	831.4	991 - 1057	30.5	3	33.7	3
P1_A12	VNPPKYE	MYZPE13164_O_Elv2.1_0327430.1	974.5	1037 - 1077	48.2	3	49	3
P1_B1	QKPEPPLK	MYZPE13164_O_Elv2.1_0370090.1	936.6	815 - 852	23.4	3	43.3	3
P1_B2	FVHRPTE	MYZPE13164_O_Elv2.1_0221860.1	884.4	695 - 726	35.3	3	37	3
P1_B3	mLPDPKN	MYZPE13164_O_Elv2.1_0357130.1	830.4	872 - 1079	40.4	4	42.9	4
P1_B4	GSRHPDMPR	MYZPE13164_O_Elv2.1_0253230.1	1051.5	575 - 661	50.9	3	52.6	3
P1_B5	GVGTVPDSPHK	MYZPE13164_O_Elv2.1_0179290.1	1092.5	901 - 934	51.5	3	40	3
P1_B6	SHFQPSPA	MYZPE13164_O_Elv2.1_0140840.1	869.4	972 - 1019	42.6	3	46.8	3
P1_B7	AGPPPLTK	MYZPE13164_O_Elv2.1_0219310.1	780.5	1043 - 1078	69.7	4		
P1_B8	FKNGKPID	MYZPE13164_O_Elv2.1_0368240.1	917.5	720 - 819	41.6	4		
P1_B9	IKVPNQEQ	MYZPE13164_O_Elv2.1_0268960.1	955.5	1027 - 1080	30.5	4	28.8	3
P1_B10	IQKPKVE	MYZPE13164_O_Elv2.1_0262390.1	840.5	727 - 812	36	4		
P1_B11	IRPIEH	MYZPE13164_O_Elv2.1_0106610.1	764.4	697 - 926	32.2	4		
P1_B12	ISKPKVE	MYZPE13164_O_Elv2.1_0273600.1	799.5	714 - 772	35.2	4		
P2_A1	KNPADLPK	MYZPE13164_O_Elv2.1_0180790.2	882.5	795 - 832	34.8	4	30.9	1
P2_A2	KTPSTPKVE	MYZPE13164_O_Elv2.1_0225020.1	986.6	786 - 829	47.6	4		
P2_A3	KVPAmPTEPR	MYZPE13164_O_Elv2.1_0347860.1	1141.6	843 - 894	48.6	4		
P2_A4	LPVKHPE	MYZPE13164_O_Elv2.1_0283820.1	818.5	723 - 784	48	4		
P2_A5	LQPNDRP	MYZPE13164_O_Elv2.1_0227360.1	936.5	1016 - 1073	48.3	4		
P2_A7	NKFEPAPK	MYZPE13164_O_Elv2.1_0252480.1	1088.6	728 - 828	44.2	4		
P2_A8	NKPKPTR	MYZPE13164_O_Elv2.1_0164980.1	839.0	794 - 864	25.5	4		
P2_A9	NRPKPPVE	MYZPE13164_O_Elv2.1_0167610.1	993.5	749 - 828	41.3	4		
P2_A10	NVPKPIEK	MYZPE13164_O_Elv2.1_0307590.1	924.6	792 - 854	39.6	4	27.4	1
P2_A11	NVSAKQVPS	MYZPE13164_O_Elv2.1_0358820.1	928.5	918 - 1061	20.5	4		
P2_A12	REPKIVN	MYZPE13164_O_Elv2.1_0206110.1	926.5	711 - 748	39	4		
P2_B1	RPPPPYSS	MYZPE13164_O_Elv2.1_0164730.1	997.5	1020 - 1078	51.8	4		
P2_B2	SVVPSPK	MYZPE13164_O_Elv2.1_0244590.1	713.4	986 - 1080	57.6	4		
P2_B3	VPPEIK	MYZPE13164_O_Elv2.1_0335660.3	681.0	985 - 1080	28.9	4	36	3
P2_B4	VTDKGPLQ	MYZPE13164_O_Elv2.1_0034880.2	857.5	959 - 1048	46.9	4		
P2_B5	AAPKPANPY	MYZPE13164_O_Elv2.1_0318050.1	928.4	1017 - 1075	54.9	4	58.7	4
P2_B6	DRAPIVKPK	MYZPE13164_O_Elv2.1_0185200.1	1138.7	718 - 747			49.6	4

P2_B7	EQRPIPKPGPN	MYZPE13164_O_Elv2.1_0270680.1	1232.7	946 - 1006			64.6	4
P2_B8	FGDKPISK	MYZPE13164_O_Elv2.1_0134490.2	891.5	787 - 828			51.8	4
P2_B9	FKDKGSPLD	MYZPE13164_O_Elv2.1_0135720.1	1005.5	822 - 872			26.9	4
P2_B10	ITDKPYPR	MYZPE13164_O_Elv2.1_0087470.1	989.5	827 - 861			42.2	4
P2_B11	KVRTDPNYPAG	MYZPE13164_O_Elv2.1_0360450.1	1217.6	828 - 934			56.7	4
P2_B12	KYLPAEH	MYZPE13164_O_Elv2.1_0204710.1	857.5	806 - 1074	21.1	2	22.4	4
P3_A1	LGKKPIPKET	MYZPE13164_O_Elv2.1_0287120.2	1239.7	624 - 673			46.2	4
P3_A2	LNGPKGPEPTR	MYZPE13164_O_Elv2.1_0256570.1	1165.6	865 - 897			76.6	4
P3_A3	NAPPSRPL	MYZPE13164_O_Elv2.1_0228000.1	851.5	1015 - 1055			41.1	4
P3_A4	NNIAPK	MYZPE13164_O_Elv2.1_0357120.1	769.5	1041 - 1077	23.6	1	35.8	4
P3_A5	PKPANPY	MYZPE13164_O_Elv2.1_0318050.1	786.4	879 - 1063			27.8	4
P3_A6	PKPGGGDK	MYZPE13164_O_Elv2.1_0268960.1	902.5	786 - 851			36.5	4
P3_A7	PNSIPTTA	MYZPE13164_O_Elv2.1_0359550.1	799.4	848 - 1066	19.9	2	21.4	4
P3_A8	TGKDIINR	MYZPE13164_O_Elv2.1_0287120.2	915.5	754 - 807			66.8	4
P3_A9	TGNRPKPPVE	MYZPE13164_O_Elv2.1_0167610.1	1094.6	803 - 866	18.5	1	41.2	4
P3_A10	TKPDTPLPKDK	MYZPE13164_O_Elv2.1_0339060.1	1239.7	748 - 819			74.6	4
P3_A11	TTLPQPK	MYZPE13164_O_Elv2.1_0289910.1	784.5	1054 - 1080			40	4
P3_A12	VDNPINKR	MYZPE13164_O_Elv2.1_0252920.1	955.6	806 - 919			67	4
P3_B1	VFEPGTR	MYZPE13164_O_Elv2.1_0208790.1	805.4	1022 - 1078			36.4	4
P3_B2	VTPRRPYE	MYZPE13164_O_Elv2.1_0350710.1	1017.5	780 - 908			27.9	4
P3_B3	YELKGGK	MYZPE13164_O_Elv2.1_0242070.2	833.5	820 - 879	35.9	2	34.1	4

MIS: Mascot ion score of peptide exhibiting maximum MIS.

Rep: Number of replicate samples the peptide was identified in.

Table 3.3: Candidate elicitor peptides (CEPs), identified in LC-MS/MS of fractions 30 and 31 and satisfying selection characteristics.

ID	Peptide	Protein accession	Peptide mass (AMU)	Retention time (s)	Fraction 30		Fraction 31	
					MIS (max)	Rep count	MIS (max)	Rep count
P3_B4	EDQPTKRPNVIR	MYZPE13164_O_Elv2.1_0248020.1	1452.8	858 - 934	41.2	4	57.4	4
P3_B5	EPVIIKK	MYZPE13164_O_Elv2.1_0300660.1	826.5	936 - 1001	54.7	4	48.5	3
P3_B6	VPDPKIR	MYZPE13164_O_Elv2.1_0288350.1	824.4	960 - 1077	56.1	4	36.5	3
P3_B7	IAPPERKY	MYZPE13164_O_Elv2.1_0272380.2	973.5	964 - 1052	49.7	3	61.8	4
P3_B8	TPmPKTPDA	MYZPE13164_O_Elv2.1_0339060.1	1087.5	941 - 984	45.9	3	45.4	3
P3_B9	NSEAHPLPVK	MYZPE13164_O_Elv2.1_0137590.2	1091.6	973 - 1000	62.6	3	41.3	3
P3_B10	KRPTVDY	MYZPE13164_O_Elv2.1_0154920.1	878.5	819 - 953	26	3	29.1	4
P3_B11	APPERKY	MYZPE13164_O_Elv2.1_0246220.2	860.5	973 - 1031	30.6	3	37.4	4
P3_B12	FKDVKY	MYZPE13164_O_Elv2.1_0250210.1	798.4	849 - 1046	35.7	3	40.2	4

MIS: Mascot ion score of peptide exhibiting maximum MIS.

Rep: Number of replicate samples the peptide was identified in.

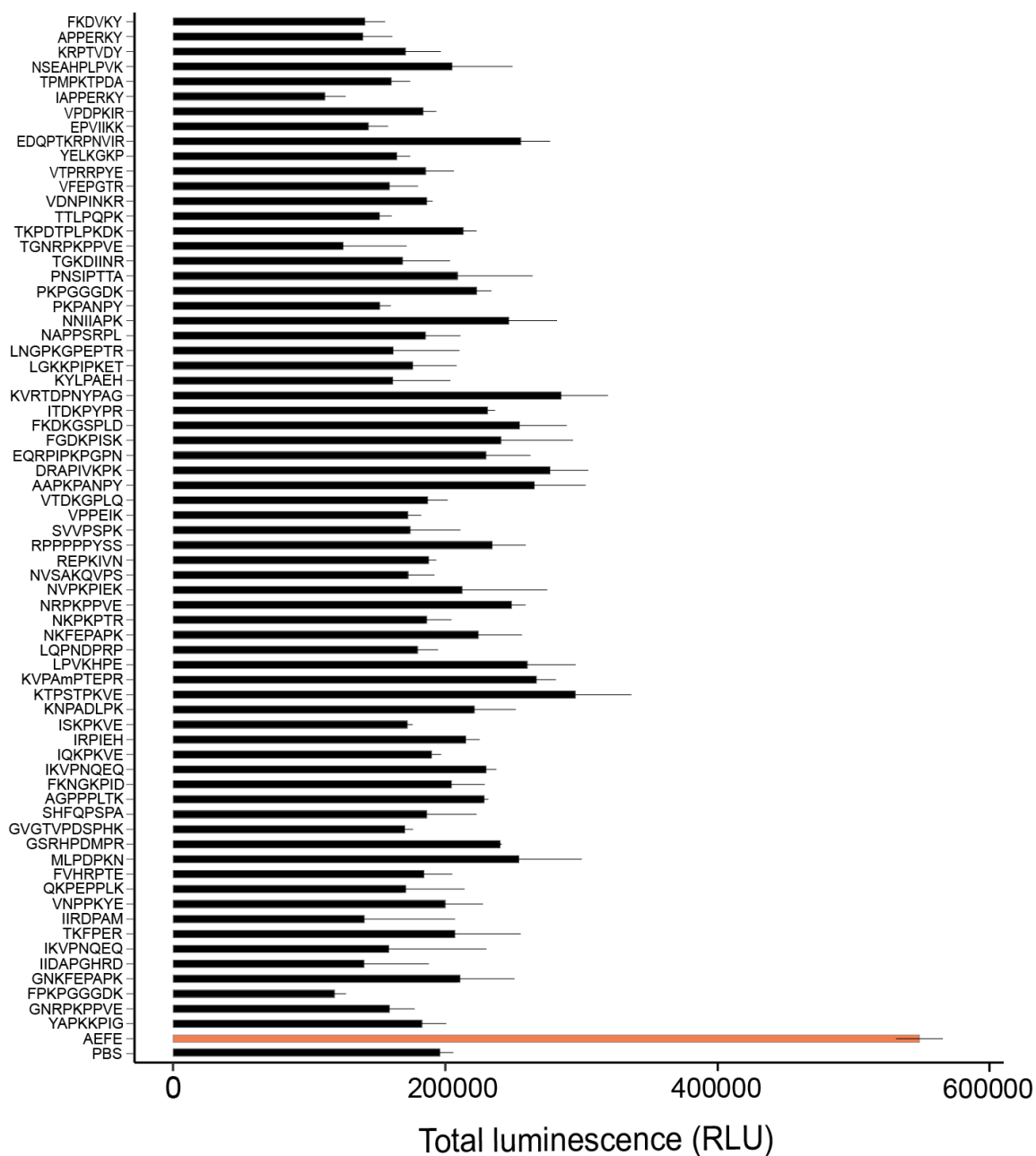


Figure 3.8: Candidate elicitor peptides (CEPs) do not induce *WRKY33* promoter activity in *A. thaliana*. Aphid-derived peptides, identified in LC-MS/MS were synthesised as SpikeTides™ (JPT Peptide Technologies, Berlin, Germany) (Schnatbaum et al., 2011) and used to treat *A. thaliana* seedlings expressing the transcriptional reporter *pWRKY33::fLUC*. Amino acid sequences are displayed from N- to C-terminal. Bioluminescence from each seedling was monitored with real-time bioluminescence monitoring every 30 s. Bars represent the mean ± SE of the summed luminescence between 0- and 600-min post-treatment of at least three seedlings. AEFE (~22.5 µg/µl) and PBS (2.5 % (v/v)) were used as controls.

3.3 Discussion

3.3.1 *M. persicae*-derived homogenates as bioactive extracts to uncover novel defence mechanisms

Previous studies have implicated low molecular weight (LMW), aphid-derived components as bioactive elicitors of MTI responses (De Vos and Jander, 2009, Prince et al., 2014), but the identity of these elicitors is unknown. The use of whole-body aphid homogenates, or aphid secretions, such as saliva or honeydew have been useful to unravel defence mechanisms during plant-aphid interactions (Schwartzberg et al., 2014, Prince et al., 2014, De Vos and Jander, 2009). Here, I exploited the induction of *WRKY33* promoter activity by aphid-derived extracts to further characterise the bioactive components that may play a role in MTI to aphids. I isolated immuno-active fractions via 3D-chromatography and identified candidate elicitor peptides (CEPs) via LC-MS/MS. However, synthesised peptides within active fractions were not found to be bioactive and thus aphid extract-derived elicitors of plant innate immune responses remain elusive.

Exposure of *A. thaliana* seedlings, stably expressing *pWRKY33::fLUC* (Kato et al., 2020), resulted in rapid, transient increases in bioluminescence, suggesting *WRKY33* expression is induced in *A. thaliana* against aphid-derived extracts (Fig. 3.2A). *WRKY33* plays a vital role as a master regulator of innate immune responses in plants (Liu and Zhan, 2004, Mao et al., 2011, Li et al., 2012, Yang et al., 2020b). This, and previous studies, indicate that *WRKY33* is a key modulator of plant defences to aphids. *WRKY33* is expressed during aphid feeding (Gioli, M. 2019), and *wrky33* mutants show increased susceptibility to *M. persicae* (Kettles, 2013). The coregulation of *WRKY33* by *MPK3/6* and *CPK5/6* suggests converging immune signalling pathways to regulate defence responses (Yang et al., 2020a).

WRKY transcription factors comprise a large family of DNA-binding proteins found in all plants (Eulgem and Somssich, 2007). In general, *WRKYs* regulate gene expression through binding W-box *cis*-elements in gene promoters with the core

sequence TGAC, although some WRKYs recognize *cis*-elements without this core sequence (Ulker and Somssich, 2004, Liu et al., 2015, O'Malley et al., 2016, Birkenbihl et al., 2017). WRKY proteins are important regulators of growth and development as well as biotic and abiotic stress responses and interact with other proteins, such as receptors, kinases, and other transcription factors for their function (Ishihama and Yoshioka, 2012). Besides WRKY33, several other WRKY transcription factors have been implicated in plant immunity to herbivores (Bhattarai et al., 2010, Li et al., 2015b). *AtWRKY22* may modulate the interplay between SA and JA pathways in response to aphid infestation (Kloth et al., 2016), and heterologous expression of *SbWRKY86* in *N. benthamiana* and *A. thaliana* results in reduced *M. persicae* fecundity (Poosapati et al., 2022). Similarly, several tomato WRKYs, *SlWRKY72* and *SlWRKY80* mediate MTI and *Mi-1*-mediated ETI against root-knot nematodes (*M. javanica*) and potato aphids (*M. euphorbiae*) (Bhattarai et al., 2010, Atamian et al., 2012). Notwithstanding these studies, the role of transcription factors and key modulators of innate immunity to aphids is unclear particularly in light of the extensive transcriptional changes evoked by aphids in plants (Jaouannet et al., 2015, Kloth et al., 2016).

Aphid feeding induces the production of the secondary metabolites IGS and camalexin, with the final step in camalexin biosynthesis, mediated by a P450 enzyme encoded by *PAD3* (Schuhegger et al., 2006, Kusnierczyk et al., 2008, Kettles et al., 2013). Furthermore, *PAD3* and other phytoalexin biosynthesis genes are expressed during aphid feeding (Pegadaraju et al., 2007, Bednarek et al., 2011, Kettles et al., 2013, Piaseck et al., 2015). However, regulation of plant phytoalexin biosynthesis gene expression to aphids, and subsequent metabolite production, are not well understood. In *A. thaliana*, *PAD3* promoter sequences are targeted by *WRKY33* driving *PAD3* expression and subsequent camalexin production against *B. cinerea* (Schuhegger et al., 2006, Mao et al., 2011). During *B. cinerea* infection, *WRKY33* is a substrate of activated MPK3/6 and CPK5/6 and acts on IGS and camalexin biosynthesis gene clusters to promote secondary metabolite production and resistance (Andreasson et al., 2005, Mao et al., 2011, Zheng et al., 2006). The requirement of *WRKY33* to mediate aphid resistance via camalexin or other secondary metabolites has not been explored. *PAD4* also regulates the synthesis of both SA and camalexin in *A. thaliana* (Tsuji et al., 1992),

and is required for plant defence against *M. persicae* (Louis et al., 2012, Dongus et al., 2020). However, PAD4-mediated defence against the aphid does not involve SA or camalexin metabolism (Pegadaraju et al., 2005), suggesting alternative sources of plant resistance are important during plant-aphid interactions.

Another apparent physiological feature of MTI to aphid-derived extracts revealed in this study is rapid, transient $[Ca^{2+}]_{cyt}$ elevations (Fig. 3.2B). $[Ca^{2+}]_{cyt}$ elevations were monitored in *A. thaliana* seedlings in expressing the GFP-based reporter *35S:GCaMP3*, which was previously used to monitor aphid feeding-mediated $[Ca^{2+}]_{cyt}$ elevations (Vincent et al., 2017). Aphid feeding may induce $[Ca^{2+}]_{cyt}$ elevations due to recognition of chemical cues or other biotic or abiotic stimuli, for example, cell damage. Transient $[Ca^{2+}]_{cyt}$ elevations due to aphid feeding are partially dependent on the co-receptor BAK1 which may indicate the involvement of a PRR receptor complex upstream of calcium signalling (Vincent et al., 2017). $[Ca^{2+}]_{cyt}$ elevations are often coupled with ROS production, and a number of studies have identified ROS bursts (within 1-h) after aphid infestation (Argandona et al., 2001, Xu et al., 2021), or slow ROS burst kinetics after treatments with aphid extracts (Prince et al., 2014). $[Ca^{2+}]_{cyt}$ elevations may be essential in regulating MTI responses to aphid-derived extract and will be explored in more depth herein (Chapter 4).

3.3.2 *M. persicae*-derived proteinaceous elicitor is likely to be liberated by a cysteine protease

Treatments of aphid-derived extracts during purification of elicitors with a PIC or E-64, resulted in a significant reduction in extract-induced *WRKY33* promoter activity (Fig. 3.6). Similar reductions in extract-induced $[Ca^{2+}]_{cyt}$ elevations were also identified (data not shown). Interestingly, protease inhibitor treatment of extracts after partial purification has no effect on extract-induced bioactivity. Furthermore, CA-074-Me, which is the methyl ester E-64 derivative and selective inhibitor of cathepsin B/Ls (CathB/L) (Ge et al., 2016), had an inhibitory effect on the bioactivity of aphid-derived extracts (Fig. 3.6C). Interactions between a cysteine proteases and a substrate may only occur during elicitor purification and not in a biological context, though cysteine-

protease activity occurs very early during the purification process as late addition of the inhibitors has no effect on elicitor activity (Fig. 3.4D). Taken together, these results suggest that a cysteine protease, endogenous to the aphid, may process a substrate to liberate an immunogenic peptide.

Aphid secretion of saliva into the host tissue during probing and feeding leads to the perturbation of host defence responses and promotes aphid colonisation (Elzinga et al., 2014). Proteins belonging to the cathepsin B (CathB) protease family have been identified in the aphid saliva and are known to be deposited into the plant during feeding (Thorpe et al., 2016; Guo et al., 2020). Moreover, members of the CathB family genes are uni-directionally, up- or downregulated upon aphid host swaps depending on the plant species (Mathers et al., 2017, Chen et al., 2020). CathB contributes to *M. persicae* fitness in a host-dependent manner as knocking down the expression of these genes reduces *M. persicae* fitness on *A. thaliana* but not *N. benthamiana* (Mathers et al., 2017). Guo et al. (2020) found that CathB3 interacts with the MAPKKK, EDR1-like protein to promote EDR1-like ROS production. Silencing *CathB3* resulted in increased performance of non-adapted *M. persicae* on *N. tabacum* (Guo et al., 2020), suggesting that CathB3 itself, or peptide fragments of CathB3 acts as an elicitor of plant immunity. Indeed, CathB peptides were identified in *R. padi* saliva (Thorpe et al., 2016). Alternatively, actions resulting from CathB presence in the cell may give rise to an ETI-like response in the plant. Whether *M. persicae* CathBs that are present in aphid saliva have cysteine protease activity and are responsible for cleaving an extract substrate to liberate an immunogenic peptide is an area for further investigation. Peptide fragments derived from the CathB proteins themselves may also have elicitor activities, although this is unlikely given that E-64 and its derivatives inhibit activity of these proteases by binding their active sites, and data herein indicates that protease activity is required for extract bioactivity. Given that aphids used in the elicitor extraction procedure were collected from plants (*B. rapa*), it cannot be entirely ruled out that the aphid has ingested the substrate for proteolytic release of the elicitor or active cysteine proteases from these plant hosts.

The immunogenicity of proteinaceous MAMPs such as flg22 and elf18 is conferred by their amino acid sequence. As such, their biological activity is

compromised by protease-mediated hydrolysis (Kunze et al., 2004). Interestingly, I found that the AEFE-mediated activity was not altered by proteinase k or carboxypeptidase B treatments, whereas sample treatments with pronase almost entirely abolished activity (Fig. 3.3A). Pronase is a mixture of serine-type proteases, Zn²⁺ endopeptidases, Zn²⁺ aminopeptidases and Zn²⁺ carboxypeptidases (Hiramatsu and Ouchi, 1963). As expected, pronase treatment also abolishes the biological activities of flg22 and EF-Tu, but not that of chitin (Kunze et al., 2004). I found that pronase-mediated hydrolysis of AEFE was lost in the presence of PIC but not leupeptin, indicating that proteases other than serine/cysteine proteases are responsible for pronase-mediated hydrolysis of bioactive AEFE constituents.

It is possible that EDTA contamination within AEFE inhibits carboxypeptidase B leading to an appearance of bioactive AEFE component resistance. Carboxypeptidase B specifically hydrolyses basic amino acids including lysine and arginine from the C-terminal end of polypeptides (Tan and Eaton, 1995), and as a metalloprotease, the enzyme is competitively inhibited by metal chelating agents such as EDTA (Hook and Loh, 1984). However, whereas extract buffers used in this study contain 1 mM EDTA, the reconstitution buffers used for the extractions do not, and removal of the majority of EDTA is expected during ammonium sulphate precipitation. Additionally, metalloproteases within pronase are likely responsible for pronase-mediated inhibition of AEFE bioactivity and are unaffected by buffer constituents. Therefore, EDTA contamination is unlikely to have affected carboxypeptidase B activity.

Peptides/proteins that are resistant to cleavage by proteinase k are extremely rare, notwithstanding proteinase k itself which is proteinase k-resistant (Kushnirov et al., 2020). Proteinase k is a serine protease with a broad substrate specificity and a preference for cleavage at aliphatic or aromatic amino acid residues in position P1 or immediately N-terminal to the cleavage site (Keil, 1987). A recent study of proteinase k treatments of the yeast Sup35 prion showed that all fragments were digested at the C-termini of all amino acids, with the exception of after prolines (Kushnirov et al., 2020). Indeed, of the 68 candidate elicitor peptides (CEPs) presented, all but two contained at least one Pro residue, with CEPs comprised of 23.1% Pro residues. Proline is abundant in many biologically active peptides and is known to protect against

proteolysis (Aldridge et al., 2009). Studies have shown that two adjacent prolines possess a high degree of resistance to proteolytic enzymes when they are not positioned terminally (Vanhoof et al., 1995, Walker et al., 2003).

Insect cell wall-associated components, such as collagens, contain high proportions of proline residues. Interestingly, collagen fragments are known to induce insect innate immunity where they may act as DAMPs during infection (Altincicek and Vilcinskas, 2006, Berisha et al., 2013). Insect collagen disintegration and fragmentation from wound sites is also associated with protease activity of effectors of fungal and bacterial pathogens of entomopathogenic nematodes (Leger et al., 1997, Cabral et al., 2004). Whether AEF E bioactivity is derived from a collagen-like peptide remains to be investigated.

3.3.3 The elusiveness of *M. persicae*-derived bioactive components

Overall, 163 unique CEPs were identified in active AEF E fractions. These CEPs were synthesised and tested for their ability to induce *WRKY33* promoter activity. Of these peptides, 68 CEPs are described in the results presented in Chapter 3 (Fig. 3.8, Fig. 3.9). 3D-chromatography and identification via LC-MS/MS revealed that the CEPs comprise sequences between 7 and 11 amino acids in length (Table 3.3, Table 3.4). Unfortunately, none of the CEPs identified and synthesised in this study induced *WRKY33* promoter activity.

False-positive identifications (type I errors) and false-negative identifications (type II errors) contribute to two major sources of error in shotgun proteomic studies within LC-MS/MS datasets (Bogdanow et al., 2016). Both sources of error could have prevented the identification of bioactive peptides here. In addition, potential sources of error in the following three stages of the identification process are further discussed: (1) The mass spectra for the corresponding peptide(s) were not generated in MS; (2) The masses did not correspond to amino acid sequences within the *M. persicae* Clone 0 (genome v2.0) (Mathers et al., 2017) database; and (3) Bioactive peptides did not pass the parameters used to filter matched peptides.

1. Protonated analyte molecules within samples are generated during electrospray ionization (ESI), resulting in positively charged ions precursors essential for detection in MS (Ho et al., 2003). However, ionization efficiencies can vary between peptides, and in the most extreme cases, some may not ionize at all (King et al., 2000). Given that peptide sequences and lengths are likely to be diverse in the AEFE immunoactive samples, some peptides may not have undergone ionization and would have therefore remained obscure. Studies have shown that hydrophobic residues may increase ionization efficiency, whereas the positive charge derived from basic arginine (Arg) and Lys has a strong negative effect on the efficiency (Mallick et al., 2007, Sanders et al., 2007). Identified CEPs in the AEFE immunoactive samples contained an overrepresentation of hydrophobic proline (Pro) residues (23.1%), and lysine (Lys) residues (14.2%), resulting in typically hydrophobic or basic peptides. Hence, there is no evidence that ionization efficiency has detrimentally affected identification of the CEPs in AEFE.

Divalent $[M+2H]^{2+}$ and trivalent $[M+3H]^{3+}$ precursor ions were selected for MS2 fragmentation as ESI of peptides typically generates multiple-charge ion precursors (Ho et al., 2003). However, single-charge peptide moieties can occur but were not considered in this study. This is due to the complexity and diversity of singularly charged moieties that may occur within samples. I cannot rule out the possibility of immuno-active being single-charge peptides.

Another possible cause of poor, missing or suppressed spectra is the suppression of the signals of less abundant moieties by those of highly abundant moieties within samples. Whilst peptide quantitation was not conducted, peptide counts did not reveal an obvious presence of highly abundant moieties within samples. However, the abundance of immunoactive peptides may be low relative to other moieties given that few ligands are needed to activate the highly sensitive plant ligand receptors.

2. The chromosome-scale *M. persicae* Clone 0, (genome v2.0 - https://bipaa.genouest.org/sp/myzus_persicae/) (Mathers et al., 2020), reference was used to generate a list of peptide-spectrum matches (PSMs) to identify individual peptides through Mascot (Matrix Science, London, UK). The use of this database in

solitude reduces the risk of false positives as the search space remains a manageable size and peptide assignment thresholds may be maintained at a stringent, but also inclusive level (Dupree et al., 2020). I chose to further assess spectra against additional databases of the plant host, *B. rapa*, and aphid primary and secondary endosymbiotic bacteria and entomopathogenic fungi. Relatively few peptide spectra matched constituents of these databases compared to the aphid genome, and the few peptides occurring in active fractions, and matching these auxiliary databases, were synthesised but found not to be bioactive. The success of bottom-up proteomics using a restricted search space relies on an assumption that all protein-coding gene sequences are known and are present in the database. However, it is possible that genomes corresponding to the bioactive peptides have not yet been sequenced, are misassembled or not (properly) annotated.

Proteins are highly susceptible to modifications that, in a physiological context, diversify the molecular structures of proteins and regulate their functions. Around half of false positive hits may be derived from modified peptides (Bogdanow et al., 2016). Typically, searches use narrow-window mass tolerances to accurately identify peptides. However, these parameters cannot account for mass changes due to modifications. Such modifications may arise through physiological or artificial means by biologically meaningful post-translational modifications (PTMs), such as phosphorylation and acetylation, or during the sample processing prior to MS, respectively. If a peptide is modified, these peptides will no longer be identified in a database search unless the specific modification has been considered. However, allowing multiple modifications in a database search leads to a combinatorial expansion that dramatically increases the search space, limiting the robustness of matched peptides (Ahrne et al., 2010). Some search algorithms may allow for variable modifications of peptides, such as MSfragger (Kong et al., 2017), enabling the identification of peptides with unknown alterations. Future approaches may consider such open search strategies.

Another consideration is that specific modifications of the peptide(s) are required for biological activity. As a part of investigations, I tested the potential that activity is conferred by a glycopeptide. However, the use of deglycosylases that remove

N-linked glycans from peptides had no effect on extract activity. Other modification may confer activity however, and in this scenario, one or more CEPs may be required for extract-induced defence induction, but may occur as a modified form. For example, the endogenous plant elicitor, hydroxyproline-rich glycopeptide systemin (HypSys), undergoes both hydroxylation and glycosylation, is wound inducible and activates defence-related genes in response to herbivore attacks (Pearce and Ryan, 2003). Modifications may also amplify the bioactivity of elicitors. One such example is the elongation factor Tu N-terminal elf18 is acetylated; a modification that increases the specific activity by ~20-fold relative to unmodified elf18 (Kunze et al., 2004).

Typically, shotgun proteomic approaches utilise trypsin to generate predictable C-termini, usually consisting of a basic residue such as Arg or Lys. The use of trypsin was not feasible in this study. Firstly, the use of proteinase k to digest samples will have generated small peptides, as reflected in CEPs, the majority of which would not have been substrates for trypsin. Secondly, in applying filters to find tryptic peptides, many peptides without trypsin cleavage sites would have likely been excluded.

3. In this study, CEPs were selected for synthesis based on three characteristics; I) a peptide minimum Mascot ion score of 45 in any one sample, II) a peptide retention time in nano-UHPLC of between 400s and 1080s, and III) identification of peptide in a minimum of three biological replicates (out of four total replicates). Mass spectrometric data contain precursor masses and MS2 fragment masses. The Mascot ion score is a statistical score describing how well the MS masses match the reference database sequence (Koenig et al., 2008). I chose to focus investigations on fraction 25 and fraction 26 as these fractions consistently induced *WRKY33* promoter activity (Fig. 3.9), and this activity was significantly reduced upon pronase treatments (Fig. 3.10). Fractions 25/26 contained relatively few peptides with each of these fractions including four replicates and 29 peptides when filtered for Mascot ion scores > 45 (Table 3.2). Five of the peptides occurred in both 25 and 26. Therefore, several spectra were examined manually and the filtering parameters were made less conservative to incorporate some peptides that occurred in only 3 of the 4 replicates and had Mascot ion scores below 45.

Based on the retention of iRTs during nano-UHPLC, a window of interest was highlighted between 400s and 1080s. Several iRTs were used to signpost activity within nano-UHPLC to reduce the retention time window within which to search spectra against *M. persicae* reference database. Retention times were compared to analytical RP-UHPLC where iRT retention and bioactivity were demarcated.

3.3.4 Recommendations for future biochemical purification of *M. persicae*-derived elicitors

I purified the bioactive components via orthogonal, chromatographical steps including ion exchange chromatography and sequential RP-UHPLC (high-/low-pH) at 1-min intervals. In future experiments, the fractionation window could be reduced as most peptides are likely to elute from a C₁₈ column over 15-30s. This fine-fractionation would enable closer scrutiny of spectra by examining the extracted ion chromatograms (EICs) of masses that occur in active fine-fractions.

I used isobaric, *N*-terminal modification of peptides via tandem mass tag (TMT) labelling to enable the differentiation and relative quantification of peptides in the same MS₂ scan (Zecha et al., 2019). I conducted TMT labelling on crude extracts with and without E-64-mediated activity inhibition, but did not identify a TMT-conferred hydrophobic shift in activity. The TMT labelling was unsuccessful likely because the reagent was consumed by competing primary amines. Future experimentation using TMT may focus on less complex extract mixtures, such as orthogonally separated samples, to reduce impurities that may compete with isobaric labels.

Further improvement on the current study may be achieved by additional biochemical processing of fractions 25/26 with specific enzymes such as chitinases, deacetylases, dephosphorylases etc. The use of these enzymes may identify modifications that confer biological activity and aid in the identification of future CEPs.

Chapter 4

The receptor-like protein *AtSOBIR1* and SERK-family kinases *AtBAK1* and *AtBKK1* regulate immune signalling to aphid-derived elicitors

4.1 Introduction

4.1.1 Plant perception of piercing-sucking insects

Plants are constantly under threat by pests and pathogens and, accordingly, have evolved intricate strategies to overcome microbial and herbivorous threats. One component of the multifaceted defence response is innate immunity – the perception of molecular patterns or chemical cues that are recognised by the plant through receptor-mediated perception (Boller and Felix, 2009). Plants perceive insect herbivores through touch, damage and herbivore-associated molecular patterns (HAMPs), triggering an array of constitutive and inducible defence responses for protection (Howe and Jander, 2008). Insect oral secretions (OS) and/or saliva contain chemical cues that may potentiate wound-induced signalling during feeding and probing of plant tissue (Schmelz et al., 2006, Howe and Jander, 2008, De Vos and Jander, 2009). Unlike chewing insects, piercing-sucking hemipterans inflict minimal damage upon their host plants and are thus termed *stealthy* feeders (De Vos et al., 2005a, Leitner et al., 2005). Aphids may ingest phloem sap without eliciting the phloem sieve elements' occlusion response to injury (Tjallingii et al., 2006). A consequence of limiting consumption and inflicting a subdued wound response is that aphid feeding, and colonisation, can be well tolerated by most plant hosts. Whereas plant responses to chewing insects is dominated by JA-mediated wound signalling, aphids induce the differential regulation of fewer JA-related genes (De Vos et al., 2005a, Leitner et al., 2005, Schmelz et al., 2006, Wunsche et al., 2011). Indeed, aphids may minimise the effects of wounding through the secretion of sheath (gelling) saliva to seal damaged sites as well as sabotage plant phloem occlusion through the introduction of calcium-binding proteins during probing and feeding (Tjallingii, 2006, Will et al., 2007, Zhu-Salzman et al., 2004).

Despite their stealthy feeding habits, aphids induce an array of detectable responses in the plant (Will et al., 2007, Jaouannet et al., 2014, Snoeck et al., 2022). The degree to which aphids, chewing insects or microbial pathogens are analogous as

inducers of plant immunity, however, remains to be fully appreciated. For example, the mechanisms that link insect perception to downstream responses in the plant is poorly understood, particularly in the context of plant-aphid interactions.

4.1.2 The role of BAK1 during insect perception

In its role as a co-receptor in MTI, BRASSINOSTEROID INSENSITIVE 1 (BRI1)-associated receptor kinase 1 (BAK1/SERK3), forms ligand-dependent, bipartite complexes with LRR receptor kinases (RKs) in their role as pattern recognition receptors (PRRs). Two well characterised examples are the PRRs ELONGATION FACTOR-TU RECEPTOR (EFR) and FLAGELLIN SENSING2 (FLS2), which interact with BAK1 upon elf18 or flg22 perception, respectively (Gomez-Gomez and Boller, 2000, Zipfel et al., 2006, Chinchilla et al., 2007, Heese et al., 2007, Roux et al., 2011). Moreover, BAK1 is required for perception of MAMPs by an alternative group of receptors, the LRR-receptor protein (RPs), which form tripartite complexes with the LRR-RK SOBIR1 and LRR-RP PRRs (van der Burgh et al., 2019). Not limited to MAMP perception, BAK1 also interacts with RK-PRRs, PEPR1 and PEPR2, upon perception of endogenous pro-peptide (PROPEP) family elicitors (Halkier and Gershenzon, 2006, Yamaguchi et al., 2006, Schulze et al., 2010, Yamaguchi et al., 2010, Roux et al., 2011, Tintor et al., 2013). The tonoplast-localised precursor PROPEP undergoes metacaspase (MC)-mediated processing to release the *so-called* danger-associated molecular patterns (DAMPs) upon membrane disintegration (Yamaguchi and Huffaker, 2011, Shen et al., 2019). In accordance with its central role in plant innate immunity, several type III secreted pathogen virulent factors bind to, and suppress the activity of BAK1 including the HopF2, and HopB1 effectors of *P. syringae* (Zhou et al., 2014, Wu et al., 2020). In addition, the *P. syringae* effectors AvrPto and AvrPtoB suppress PRR-BAK1 complex formation thereby suppressing plant immune responses downstream of receptor complex activation (Abramovitch et al., 2006, He et al., 2006, Gohre et al., 2008, Shan et al., 2008, Gimenez-Ibanez et al., 2009, Xiang et al., 2011).

Several studies have linked BAK1 to insect-induced wound and HAMP perception and downstream signalling during plant-herbivore interactions. In

Nicotiana attenuata, silencing the BAK1 homolog, *NaBAK1* partially reduces wound- and OS-induced accumulation of JA and JA-Ile (Yang et al., 2011). Interestingly, silencing *NaBAK1* did not impair wound- or OS-induced activation of mitogen-activated protein kinases (MAPKs) suggesting these pathways are independent (Yang et al., 2011). Caterpillar feeding on *Vigna unguiculata* results in the production of the inceptin peptide HAMPs such as Vu-In in OS (Schmelz et al., 2006, Schmelz et al., 2007). Recently, it was shown that Vu-In induces the inceptin receptor (INR), a LRR-RP PRR, to associate with BAK1 and other SERKs as well as SOBIR1, leading to defence signalling (Steinbrenner et al., 2020). Crude extracts derived from *M. persicae* were shown to induce BAK1-dependent responses in *A. thaliana* as well as *N. benthamiana* (Prince et al., 2014, Drurey, 2015,). Furthermore, the endosymbiont-derived chaperonin protein GroEL induced BAK1-dependent immune responses and was found in aphid saliva suggesting it may be secreted into plant tissue during feeding (Chaudhary et al., 2014). BAK1 has also been directly implicated in defence signalling during aphid feeding. The cytosolic calcium elevations induced by aphid feeding and probing events are dependent on BAK1 (Vincent et al., 2017). Taken together, these studies implicate BAK1 as a regulator in receptor-mediated signalling during aphid wound and/or elicitor-induced responses. The precise role of BAK1 in this context, however, remains undetermined and currently no PRR has been identified that interacts with BAK1 to mediate these responses.

4.1.3 Signalling downstream of receptor complexes during plant-insect interactions

Upon MAMP recognition, BAK1 mediates the rapid phosphorylation of the receptor-like cytoplasmic kinase (RLCK) BOTRYTIS-INDUCED KINASE1 (BIK1) as well as its homolog PBL1, and is thereby released from the receptor complex (Lin et al., 2014, Rao et al., 2018). BIK1 then positively regulates immune signalling by phosphorylating the plasma membrane NADPH oxidase RBOHD, resulting in the production of reactive oxygen species (ROS) (u et al., 2010, Kadota et al., 2014, Li et al., 2014b).

ROS accumulation is believed to play a role in plant resistance to invading aphids by providing direct phytotoxicity and regulating downstream immune responses (Lei et al., 2014, Shoala et al., 2018). *In vivo* inhibition of NADPH oxidase by DPI resulted in the concomitant inhibition of H₂O₂ production in wheat against infestation of the Russian wheat aphid *Diuraphis noxia* (Moloi and van der Westhuizen, 2006). Similarly, elevated accumulation of H₂O₂ was observed in aphid-resistant sorghum (HN16) (Shao et al., 2019), pepper (Sun et al., 2020) and sugarcane (Pant and Huang, 2021). H₂O₂ accumulation was observed in locally infested *A. thaliana* leaves upon *M. persicae* infestation; accumulation that was earlier and stronger in *bik1* mutant plants compared to wild-type and correlated to increased resistance to the aphid (Lei and Zhu-Salzman, 2015). Interestingly, aphid fecundity was enhanced on the *rbohD* mutant impaired in the production of apoplastic ROS accumulation (Miller et al., 2009), whilst higher levels of NADPH oxidase activities were observed in wheat and maize infested with aphids (Sytykiewicz, 2016). Moreover, disrupting RBOHF expression benefits aphid species that have compatible and incompatible interactions with *A. thaliana* (Jaouannet et al., 2015). Similarly, *M. persicae* displays enhanced fecundity on an *A. thaliana* CATALASE 2 (CAT2) mutant, which is impaired in detoxification of H₂O₂ in the peroxisomes (Rasool et al., 2020). In general agreement with these studies, it was recently reported that aphid infestation induces a rapid, short-lived oxidative burst, and a more persistent intracellular oxidative response involving ROS generation in the peroxisomes (Xu et al., 2021).

Ca²⁺ ions are profoundly important in biotic stress signalling. Ca²⁺ act in coordination with ROS and are potent second messengers during innate immunity (Gilroy et al., 2016). BIK1 and its paralog in rice (*OsBIK1*) can phosphorylate several cyclic nucleotide-gated channels (CNGCs) to positively regulate Ca²⁺ influx during abiotic stress (Tian et al., 2019). [Ca²⁺]_{cyt} elevations activate immune responses by directly regulating several calcium sensors such as CDKs, CDPKs, calmodulin-binding proteins and calcium-dependent metacaspases (Romeis et al., 2001, Ranf et al., 2014, Hander et al., 2019, Shen et al., 2019, Huang et al., 2020). Aphid feeding induces transient [Ca²⁺]_{cyt} elevations in *N. tabacum* (Ren et al., 2014), and *A. thaliana* (Vincent et al., 2017). In response to *M. persicae*, differentially regulated genes involved in Ca²⁺

and ROS signalling appear overrepresented, although their role during aphid-plant interactions has seldom been empirically tested (Kusnierczyk et al., 2008, Kerchev et al., 2013, Ren et al., 2014, Jaouannet et al., 2015). It is proposed that an important role of Ca²⁺ during plant-insect interactions is to promote phloem occlusion (Will and van Bel, 2006, Furch et al., 2015). Indeed, aphid saliva contains Ca²⁺ binding proteins that may act to chelate phloem Ca²⁺ preventing occlusion, and thus aid feeding (Will et al., 2007, Carolan et al., 2009, Rao et al., 2013).

MAPK cascades are rapidly activated upon MAMP perception including modules, MAPKKK3/5-MKK4/5-MPK3/6 and MEKK1-MKK1/2-MPK4 (Asai et al., 2002). The involvement of MAPK signalling during plant-aphid interactions remains unclear (Hettenhausen et al., 2015). The tomato *Mi-1* gene confers salicylic acid-dependent resistance to potato aphids (*Macrosiphum euphorbiae*) (Vos et al., 1998, Li et al., 2006). Silencing plants for MAPK kinase, *LeMKK2* and MAPKs, *LeMPK2*, *LeMPK1* or *LeMPK3* resulted in the loss of *Mi-1*-mediated aphid resistance suggesting at least one MAPK module is required for *Mi-1* function (Li et al., 2006). Whilst wounding itself can induce MAPK activation (Seo et al., 1995), the addition of herbivore OS may amplify the response, implicating HAMPs in MAPK activation (Wu et al., 2007). During MTI, MAPKs target several transcription factors (TFs) including WRKY-domain TFs involved in immunity (Adachi et al., 2015). For example, flg22 perception leads to the induction of *WRKY29* and *FRK1* transcription through the activation of a MAPK signalling cascade (Asai et al., 2002).

A downstream consequence, and integral part of MTI, is transcriptional reprogramming. Aphid-induced transcriptional reprogramming has been comprehensively studied (Kusnierczyk et al., 2008, Kerchev et al., 2013, Jaouannet et al., 2015, Foyer et al., 2015, Thorpe et al., 2016, Mathers et al., 2017). Notable amongst two transcriptional studies, one short-term (hours) (Giolai, 2019) and one long-term (weeks) (Hohenstein et al., 2019), are the significant induction of defence-related genes and particularly those involved with MTI. In particular, *WRKY33* or its ortholog in soybean was found to be significantly expressed upon aphid challenge (Giolai, 2019, Hohenstein et al., 2019). Furthermore, these studies both indicated that 'response to chitin' was an overrepresented GO term in plants exposed to aphids, highlighting the

considerable overlap of responses to aphids and pathogens (Giolai, 2019, Hohenstein et al., 2019).

Another gene expressed during aphid challenge is *PHYTOALEXIN DEFICIENT4* (*PAD4*) (Pegadaraju et al., 2005, Pegadaraju et al., 2007, Louis et al., 2010; Lei et al., 2014). Insect fecundity is increased on *pad4* mutants suggesting a key role for PAD4 in resistance to aphids (Pegadaraju et al., 2005, Pegadaraju et al., 2007). In the context of defence to aphids, as opposed to its role in *P. syringae*-mediated defence, PAD4 acts independently of EDS1 or SA (Jirage et al., 1999, Pegadaraju et al., 2005, Pegadaraju et al., 2007). Moreover, PAD4-mediated defence against *M. persicae* does not involve camalexin (Pegadaraju et al., 2005). Recent studies suggest that the PAD4LLD is sufficient for limiting *M. persicae* fecundity, but the C-terminal PAD4 EP domain is dispensable offering novel insights into PAD4 function in immunity more widely (Dongus et al., 2020).

4.1.5 Chapter aims

The aim of this chapter is to investigate the extent of *A. thaliana* MTI responses to a partially purified, whole-body *M. persicae* extract (AEFE), shown in the previous chapter to be bioactive. I demonstrate that AEFE-induced immune signalling likely occurs via a canonical MTI pathway, requiring receptor-like kinases *AtBAK1*, *AtSOBIR1* and to a lesser extent, *AtBKK1*. MTI to AEFE includes the expression of camalexin biosynthesis genes and AEFE-induced $[Ca^{2+}]_{cyt}$ elevations are likely upstream of both AEFE-induced MAPK activation and gene expression. The putative role of *AtSOBIR1* may offer novel insights into the recognition of aphid-derived HAMPs. The perturbed aphid feeding-induced $[Ca^{2+}]_{cyt}$ bursts in the *sobir1* mutant provides increased biological relevance to this finding.

4.2 Results

4.2.1 Aphid Extract Filtrate Elicitor (AEFE) induces innate immune responses in *A. thaliana*

In Chapter 3, I demonstrated that partially purified, aphid-derived extracts induce rapid both transient $[Ca^{2+}]_{\text{cyt}}$ elevations and induction of *WRKY33* promoter activity. To study the extent of AEFE-induced canonical MTI responses in *A. thaliana*, I challenged seedlings with AEFE or a PBS mock treatment and subsequently monitored $[Ca^{2+}]_{\text{cyt}}$ elevations, posttranslational activation of mitogen activated protein kinase (MAPK) cascades, defence gene expression and plant growth inhibition (Gómez-Gómez et al., 1999, Boller and Felix, 2009). I used the peptide flg22 to activate RLK-mediated MTI responses to contrast AEFE-mediated responses.

Broadly, I found that AEFE induces an array of MTI responses typical of bioactive peptides such as flg22 (Fig. 4.1). In wild-type (Col-0) plants, both AEFE and flg22 elicit a single-phase $[Ca^{2+}]_{\text{cyt}}$ elevation within 90 min of treatment (Fig. 4.1A). AEFE-induced $[Ca^{2+}]_{\text{cyt}}$ elevations initiate at approximately 4 min post-treatment, peaking between 15- and 20-min post-treatment. Flg22, by contrast, elicited $[Ca^{2+}]_{\text{cyt}}$ elevations within 1 min of treatment and peaked between 4- and 10-min post-treatment. Neither AEFE- nor flg22-induced $[Ca^{2+}]_{\text{cyt}}$ elevation returned to full resting state within the 90-min recorded. In order to assess AEFE-induced MAPK activation, I utilised the p44/42 MAPK (Erk1/2) antibody to detect endogenous levels of total p44/42 MAP kinase (Erk1/Erk2) protein from AEFE-treated seedlings. As expected, flg22 rapidly induced MAPK cascades in *A. thaliana* (Fig. 4.1B), in agreement with published results (Asai et al., 2002, Navarro et al., 2004). AEFE induced MPK3/6 as well as MPK4/11, suggesting that AEFE perception leads to the induction of rapid and transient activation of the canonical MAPK cascades, MAPKKK3/5-MKK4/5-MPK3/6 and MEKK1-MKK1/2-MPK4 (Fig. 4.1B).

In Col-0 plants, MAMP treatments activate immune responses via cognate receptors, diverting metabolic resources toward defence over growth, leading to

growth inhibition (Huot et al., 2014). To test whether AEFÉ induces seedling growth inhibition, I treated individual Col-0 plants with/without elicitor (as displayed) and measured fresh weight. Both flg22 and AEFÉ induce seedling growth inhibition relative to their controls water and PBS, respectively (Fig. 4.1C). Compared to flg22, which is a very potent inhibitor of growth, AEFÉ mildly but nonetheless significantly ($p < 0.05$) reduced growth. Therefore, AEFÉ likely induces defence responses in the seedling leading to growth inhibition, but the induction of these defences may be reduced compared to those induced by flg22.

In *A. thaliana*, the biosynthetic pathways responsible for the production of tryptophan-derived indole glucosinolates (IGSs) are well studied (Glawischnig et al., 2004) (Fig. 4.1D). IGSs such as camalexin are critical to plant immunity in response to several pathogens (Tsuji et al., 1992, Thomma et al., 1999, Bednarek et al., 2009) and *M. persicae* (Kettles et al., 2013). To test the AEFÉ-mediated induction of IGS biosynthesis genes, I assessed expression of several pathway members including *CYTOCHROME P450 FAMILY83:B1 (CYP83B1)*, *CYTOCHROME P450 FAMILY79:B2 (CYP79B2)*, *CYTOCHROME P450 FAMILY71:A13 (CYP71A13)* and *PHYTOALEXIN DEFICIENT3 (PAD3)* via RT-qPCR. AEFÉ strongly induced the expression of all IGS biosynthesis genes tested in *A. thaliana* relative to control treatments (Fig. 4.1E). Secondly, I tested the expression of four routinely analysed MAMP-responsive marker genes: *WRKY DNA-BINDING PROTEIN53 (WRKY53)*, *WRKY DNA-BINDING PROTEIN33 (WRKY33)*, *AT1G51890* and *FLG22-INDUCED RECEPTOR-LIKE KINASE1 (FRK1)*. With the notable exception of *FRK1*, AEFÉ induced the expression of each MTI marker gene tested within 90-min of treatments relative to control treatments (Fig. 4.1F).

Immunogenic ligands form specific interactions with their cognate receptors leading to the initiation of immune responses that counteract specific threats. Previously, Prince et al. (2014) showed that MTI responses to a crude aphid extract were independent of PRR receptor-like kinases FLS2, EFR and CERK1. In order to determine whether AEFÉ induces MTI independently of these receptors, I assessed gene expression and MAPK activation in *fls2*, *efr* and *cerk1* mutants. Expression of *WRKY33* was similar in Col-0, *fls2*, *efr* and *cerk1* mutants suggesting that these RLK PRRs

are unlikely to be involved in AEFE-induced transcriptional reprogramming (Appendix II.I).

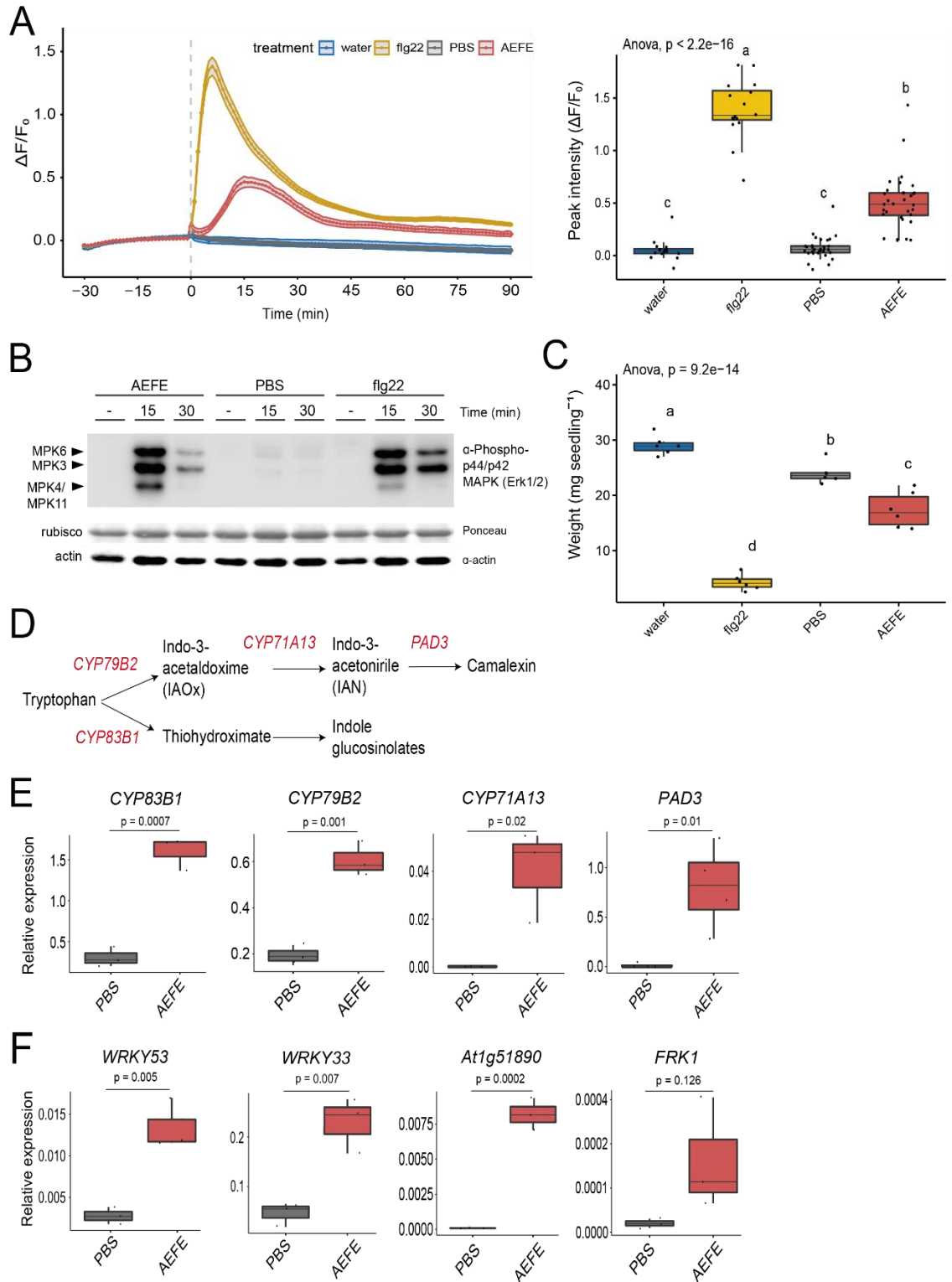


Figure 4.1: Aphid-derived extracts (aphid extract elicitor filtrate, AEFE) induces innate immune responses in *A. thaliana*. **A** Normalised GFP fluorescence ($\Delta F/F$) kinetics in 10-day-old Col-0 35S:GCaMP3 seedlings after elicitation with AEFE (0.25% (v/v); $\sim 2.3 \mu\text{g}/\mu\text{l}$), mock PBS treatment at 0.25% (v/v) or flg22 (20nM), mock water treatment. Lines represent mean values with upper and lower lines representing the standard error of the mean. Data are from a minimum of six biological replicates. Data is replicated as peak mean GFP fluorescence ($\Delta F/F$) for clarity. Interquartile range is coloured. Whiskers represent lowest and highest score excluding outliers. Biological repeat values are shown as black dots. Letters indicate significant differences between treatments ($p < 0.05$). **B** MAPK activation during AEFE-induced MTI. Ten 10-days-old *A. thaliana* seedlings were elicited per treatment per time point. Seedlings were treated with AEFE (2.5% (v/v); $\sim 22.5 \mu\text{g}/\mu\text{l}$), mock PBS treatment at 2.5% (v/v) or flg22 (100nM) and flash frozen in LN₂ after an elapsed time as displayed. Mock (-) seedlings remained untreated. Activated MAPKs, MPK3/6/4/11 were detected by immunoblot using anti-p44/42 MAPK. Actin was detected using anti-actin antibody and ponceau S staining of membranes are shown as loading controls. The experiment was repeated at least three times with similar results. Data shown is a representative example. **C** AEFE-induced seedling growth inhibition. Individual *A. thaliana* seedlings, germinated on 1/4St MS were transferred to liquid MS with treatments as indicated. Seedlings were dried and weighted after 8-days. Data are from a minimum of six biological replicates. Letters indicate significant differences between treatments ($p < 0.05$). **D** Tryptophan-derived secondary metabolites represent key anti-insect molecules. Pathway intermediates/products are shown in black. Genes key to the production of each metabolite are shown in red. Adapted from Glawischnig et al. (2004). **E** Transcriptional profiling of tryptophan-derived secondary metabolite pathway genes and, **F** MTI marker genes by quantitative reverse transcription-PCR (qRT-PCR). Three 10-day-old *A. thaliana* Col-0 plants were elicited with 2.5% (v/v) PBS (mock) or 2.5% (v/v) $\sim 22.5 \mu\text{g}/\mu\text{l}$ AEFE and flash frozen after 1.5-h. Relative expression ($2^{\Delta\text{CT}}$) of the indicated genes is shown normalized to the *GAPDH* transcript (p -values were obtained in a Student's *t*-test). Data are from three biological replicates.

4.2.2 [Ca²⁺]_{cyt} elevations are upstream of AEFE-induced MAPK activation and defence gene expression

Pharmacological approaches have shown that Ca²⁺ signalling acts upstream of MAPK pathways during MTI (Lebrun-Garcia et al., 1998, Romeis et al., 2001, Lecourieux et al., 2002) and that Ca²⁺ signalling is also required for ROS production generated by RBOHs (Blume et al., 2000, Marcec and Tanaka, 2021). To further assess the canonical nature of AEFE-induced MTI, I inhibited Ca²⁺ signalling by preincubating *A. thaliana* seedlings with the calcium chelator, EGTA or calcium channel blocker, lanthanum

chloride (LaCl₃) and assessed AEFÉ-induced MAPK activation and transcription levels of the AEFÉ-responsive gene *NDR1/HIN1-LIKE PROTEIN 10 (NHL10)*. Treatments of both EGTA and LaCl₃ abolished AEFÉ-induced [Ca²⁺]_{cyt} elevations (Fig. 4.2A). Concomitantly, MAPK activation was reduced and *NHL10* transcript levels was significantly reduced in EGTA- and LaCl₃-treated seedlings relative to untreated samples (Fig. 4.2B,C). Taken together, these data suggest an important role for Ca²⁺ signalling upstream of MAPK activation and defence gene expression to AEFÉ.

4.2.3 AEFÉ pre-exposure does not alter aphid fecundity

A commonly observed consequence of PRR-mediated defence activation is enhanced cross-reactivity against a spectrum of pathogens (Nie et al., 2017, Gong et al., 2019), as well as a ‘memory’ where future MAMP/DAMP exposure results in amplified defence signalling (Conrath et al., 2015). Previously, it was reported that aphid infestation can confer induced resistance against future aphid colonisation (Vincent, 2016). To assess whether pre-exposure of plants to AEFÉ confers protection to the insect, I infiltrated a single *A. thaliana* leaf with AEFÉ or PBS and scored aphid fecundity from 48-h post-infiltration to 10-days post-infiltration. The mean numbers of offspring per adult were highly variable among the plants in each experiment and the offspring production was more often lower on the AEFÉ- versus the PBS-treated plants, though differences were not found significant ($p > 0.05$) in any of the three independent experiments. Therefore, there was no consistent induction of AEFÉ-mediated induced resistance to the aphid (Fig. 4.3). Experimental methods may need to be further optimized to reduce variation among the plants.

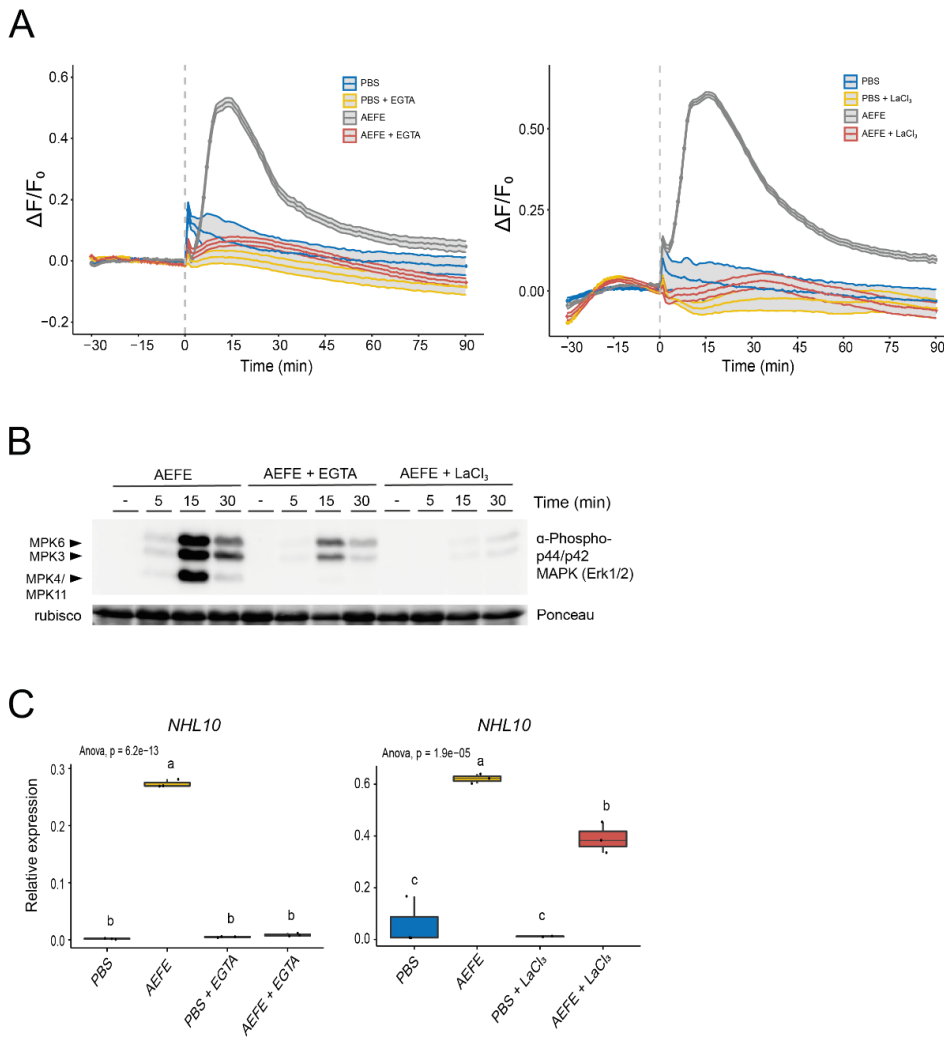


Figure 4.2: Cytoplasmic calcium elevations are required for full AEF E-induced immune responses in *A. thaliana*. **A** Normalised GFP fluorescence ($\Delta F/F_0$) kinetics in 10-day-old Col-0 35S:GCaMP3 seedlings, pre-incubated for 1-h with 5 mM glycol-bis(β -aminoethyl ether)-*N,N,N',N'*-tetraacetic acid (EGTA) or 1 mM lanthanum chloride (LaCl_3) after elicitation with AEF E (0.25% (v/v); $\sim 2.3 \mu\text{g}/\mu\text{l}$) or PBS treatment at 0.25% (v/v). An equal volume of dH_2O was used in untreated samples to eliminate dilution effects. Lines represent mean values with upper and lower lines representing the standard error of the mean. Data are from a minimum of six biological replicates. **B** AEF E-induced MAPK activation in treated (EGTA or LaCl_3) or untreated (dH_2O) in *A. thaliana* seedlings. Pharmacological inhibition of *A. thaliana* seedlings by EGTA and LaCl_3 was carried out as above. Samples contain protein extracted from ten *A. thaliana*, grown in $\frac{1}{2}$ St liquid MS in 24-well plates and elicited at 10-days-old. Mock (-) seedlings remained untreated. Activated MAPKs, MPK3/6/4/11 were detected by immunoblot using anti-p44/42 MAPK. Ponceau S staining of the membrane is shown as loading controls. **C** Transcriptional profiling of *NDR1/HIN1-LIKE PROTEIN 10* (*NHL10*) by quantitative reverse transcription-PCR (qRT-PCR). Pharmacological inhibition of *A. thaliana* seedlings by EGTA and LaCl_3 was carried out as above. Three 10-day-old *A. thaliana* Col-0 plants were elicited with 2.5% (v/v) $\sim 22.5 \mu\text{g}/\mu\text{l}$ AEF E or 2.5% (v/v) PBS (mock) and harvested after 1.5-h. Relative expression of the indicated genes is shown normalized to the *GAPDH* transcript. Data are from three biological replicates.

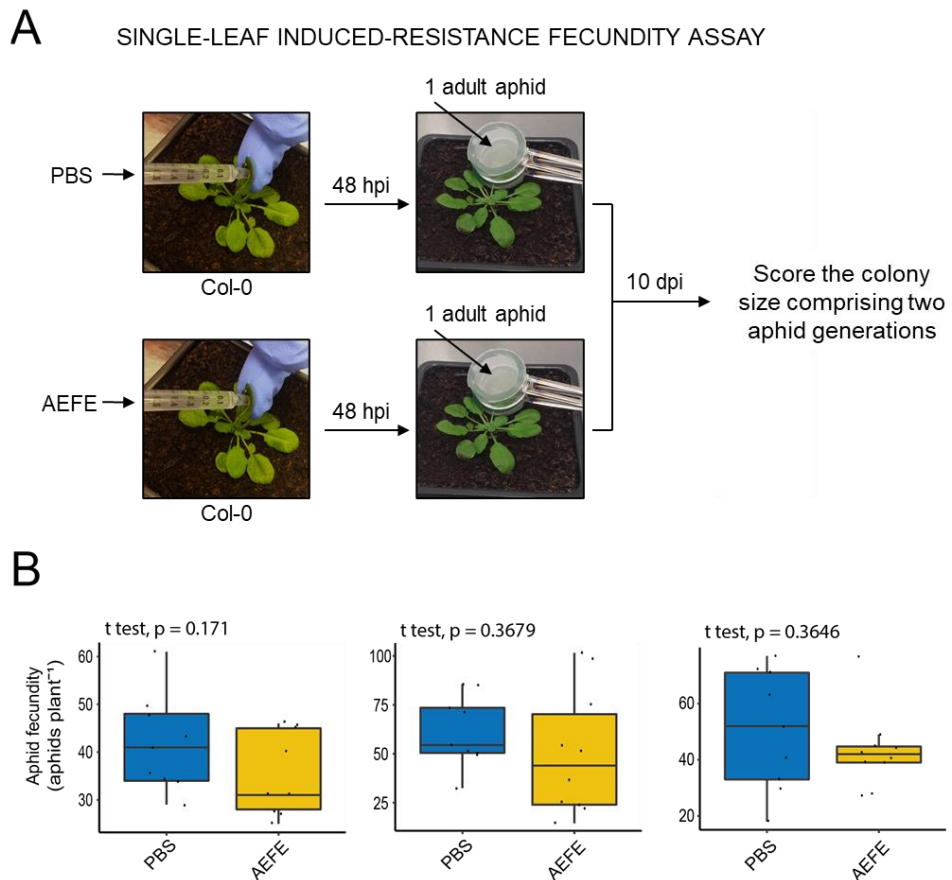


Figure 4.3: Aphid-derived extracts (aphid extract elicitor filtrate, AEFE) does not confer induced resistance to future aphid fecundity. **A** Illustrated method to score induced resistance to aphids in *A. thaliana*. Treatments, AEFE (2.5% (v/v); ~22.5 $\mu\text{g}/\mu\text{l}$) or PBS (mock) treatment at 2.5% (v/v) were infiltrated into a single 4-week-old *A. thaliana* leaf. After 48-h post-infiltration (hpi), a single 5-day-old adult *M. persicae* was clip caged on the treated leaf. Aphid fecundity was scored at 10-days post-infiltration (dpi). Images supplied by Matteo Gravino. **B** Total number of aphids at 10 dpi. To compare means between treatments, a Student's *t*-test was conducted and a *p*-value obtained. The results of three independent experiments are shown.

4.2.4 Receptor-like kinases *AtBAK1* and *AtBKK1* are required for AEFÉ-induced defence response

The *A. thaliana* SERK family receptor-like kinase and co-receptor *AtBAK1* forms a ligand-dependent complex with *AtFLS2* and *AtEFR* (Chinchilla et al., 2007; Roux et al., 2011). *BAK1* also interacts with *AtRLP23*, *AtRLP32* and *AtRLP42* to regulate RLP-mediated signalling (Albert et al., 2015; Fan et al., 2021; Zhang et al., 2022). Furthermore, previous studies have implicated *AtBAK1* in MTI responses to aphids (Chaudhary et al., 2014, Prince et al., 2014, Vincent et al., 2017).

The *Atbak1-5* mutant allele, containing the missense mutation C408Y, leads to compromised immune signalling without effecting *BRI1*-mediated signalling (Schwessinger et al., 2011). Given its prominent role in MTI, I tested *Atbak1-5* for its ability to induce AEFÉ-mediated MTI along with a second SERK family kinase mutant, *Atbkk1-1*, which is also implicated in flg22-triggered immune signalling (Roux et al., 2011). AEFÉ-triggered $[Ca^{2+}]_{cyt}$ burst was impaired in the *GCaMP3:UBQ10* x *bak1-5* mutant and MAPK activation was mildly altered in the single *bak1-5* mutant, unaltered in the *bkk1-1* mutant but more severely impaired in the *bak1-5 bkk1-1* double mutant (Fig. 4.4A,B). Furthermore, both AEFÉ- and flg22-induced growth inhibition were lost in the *bak1-5* and *bak1-5 bkk1-1* double mutant but not in the *bkk1-1* single mutant (Fig. 4.4C). AEFÉ-induced *WRKY33* and *PAD3* expression were impaired in *bak1-5* and *bak1-5 bkk1-1* double mutant plants (Fig. 4.4D). These results suggest that *BAK1* is required for full AEFÉ-triggered immunity and may act together with *BKK1* to regulate downstream responses. *BKK1* alone is insufficient to regulate AEFÉ-mediated MTI.

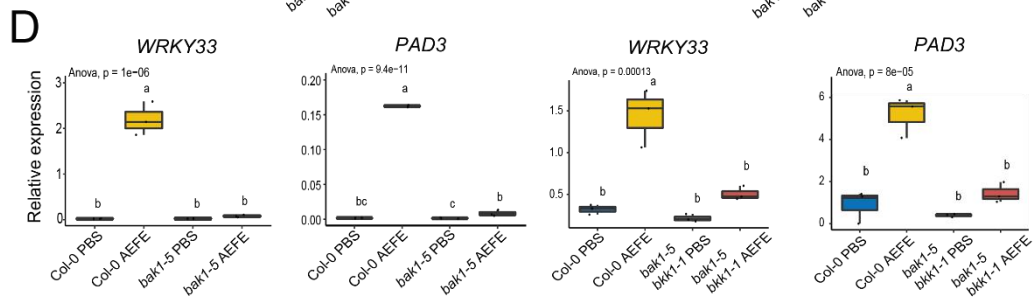
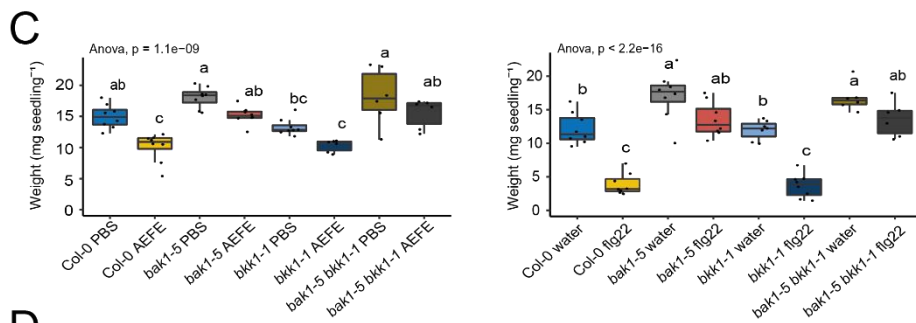
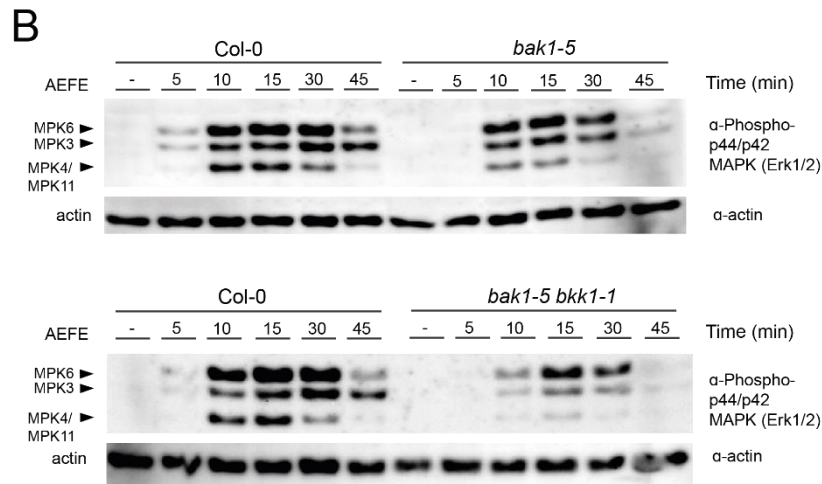
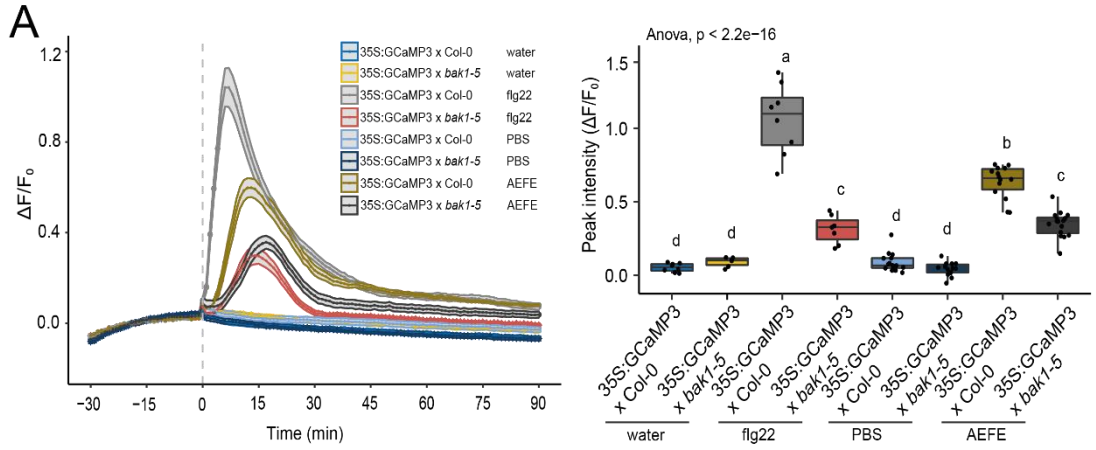


Figure 4.4: SERK family kinases *BAK1* and *BKK1* act as positive regulators of AEFÉ-induced immune signalling. **A** Normalised GFP fluorescence ($\Delta F/F$) kinetics in 10-day-old Col-0 35S:GCaMP3 or 35S:GCaMP3 x *bak1-5* seedlings after elicitation with AEFÉ (0.25% (v/v); ~2.3 $\mu\text{g}/\mu\text{l}$), mock PBS treatment at 0.25% (v/v) or flg22 (20nM), mock water treatment as indicated. Lines represent mean values with upper and lower lines representing the standard error of the mean. Data are from a minimum of six biological replicates. Data is replicated as peak mean GFP fluorescence ($\Delta F/F$) for clarity. Letters indicate significant differences between treatments ($p < 0.05$). **B** MAPK activation during AEFÉ-induced MTI. Ten 10-days-old Col-0, *bak1-5* or *bak1-5 bkk1-1* *A. thaliana* seedlings were elicited per treatment per time point. Seedlings were treated with AEFÉ (2.5% (v/v); ~22.5 $\mu\text{g}/\mu\text{l}$) and flash frozen in LN₂ after an elapsed time as displayed. Mock (-) seedlings remained untreated. Activated MAPKs, MPK3/6/4/11 were detected by immunoblot using anti-p44/42 MAPK. Actin was detected using anti-actin antibody and shown as loading controls. The experiment was repeated at least twice with similar results. Data shown is a representative example. **C** AEFÉ-induced seedling growth inhibition. Individual Col-0, *bak1-5*, *bkk1-1* or *bak1-5 bkk1-1* *A. thaliana* seedlings were germinated on ¼St MS and transferred to liquid MS with treatments as indicated. Seedlings were dried and weighted after 8-days. Data are from a minimum of six biological replicates. Letters indicate significant differences between treatments ($p < 0.05$). **D** Transcriptional profiling of MTI marker genes by quantitative reverse transcription-PCR (qRT-PCR). Three 10-day-old *A. thaliana* Col-0 or *bak1-5 bkk1-1* plants were elicited with AEFÉ (2.5% (v/v); ~22.5 $\mu\text{g}/\mu\text{l}$), mock PBS treatment at 2.5% (v/v) and flash frozen after 1.5-h. Relative expression ($2^{\Delta\text{CT}}$) of the indicated genes is shown normalized to the *GAPDH* transcript (p -values were obtained in an ANOVA with Tukey HSD). Data are from three biological replicates.

Given its demonstrable role in AEFÉ-mediated immune signalling, I opted to pull-down GFP-tagged BAK1 from *A. thaliana bak1-4* mutants (*BAK1p:BAK1-GFP bak1-4*). To ensure receptor complex components that associate with BAK1 in aphid-derived ligand-specific manner, I treated BAK1-GFP and EV-GFP expressing plants with AEFÉ or PBS. Several proteins, enriched in AEFÉ-treated samples were identified I tested for GFP expression by resolving membrane and immunoprecipitated samples via gel electrophoresis and probed blots using α -GFP antibody as previously described (Schwessinger et al., 2011) (Appendix II.II). Several known interactors of BAK1 were identified including BRI1-ASSOCIATED KINASE 1 (BAK1)-INTERACTING RECEPTOR-LIKE KINASE 2/3 (BIR2/BIR3) (Table 4.1). However, very few leucine-rich repeat containing proteins were identified as AEFÉ-dependent BAK1 interactors, hence these putative interactors were not examined further.

Table 4.1: Proteins detected in LC-MS/MS samples as putative interactors of BAK1. See *Methods* (2.6.4) for details.

Protein	Gene ID	Protein size	Sum of normalized spectral counts
BIR3	AT1G27190.1	65 kDa	13.7
DCL3	AT3G43920.2	177 kDa	13.2
PEN3	AT1G59870.1	165 kDa	10.2
	AT3G62360.1 (+1)	133 kDa	9.6
TUB5	AT1G20010.1	50 kDa	8.1
FTSH8	AT1G06430.1 (+2)	73 kDa	8.0
	AT2G27730.1 (+3)	12 kDa	7.6
	AT2G16380.1 (+1)	63 kDa	7.5
HIR2	AT3G01290.1	31 kDa	7.3
ATPC1	AT4G04640.1	41 kDa	7.3
CURT1C	AT1G52220.1 (+1)	17 kDa	7.2
	AT3G11510.1	16 kDa	6.7
SIF3	AT1G51805.1 (+1)	98 kDa	6.2
ATP3	AT2G33040.1	35 kDa	5.4
	AT1G07920.1 (+8)	50 kDa	4.9
	AT5G10360.1	28 kDa	4.6
	AT5G37360.1	33 kDa	4.5
BIP2	AT5G42020.1 (+2)	74 kDa	4.2
RPS27AA	AT1G23410.1 (+3)	18 kDa	4.2
LETM1	AT3G59820.1 (+2)	86 kDa	4.2
NPQ4	AT1G44575.1 (+1)	28 kDa	4.0
PGRL1A	AT4G22890.1 (+3)	36 kDa	3.9
ATP1	ATMG01190.1	55 kDa	3.7
ATPD	AT4G09650.1	26 kDa	3.7
	AT5G23890.1 (+1)	104 kDa	3.7
PHT1	AT3G54700.1 (+1)	58 kDa	3.7
ATSMC2	AT3G47460.1 (+1)	132 kDa	3.2
	AT2G34357.1	142 kDa	3.0
	AT4G10930.1 (+1)	130 kDa	2.9
STP1	AT1G11260.1	58 kDa	2.9
PDE334	AT4G32260.1	24 kDa	2.9
	AT1G09640.1	47 kDa	2.6
CAT3	AT1G20620.1 (+2)	57 kDa	2.6
	AT1G22520.1	10 kDa	2.3
BIR2	AT3G28450.1	67 kDa	2.2
ZAR1	AT2G01210.1	78 kDa	2.1
PSAE-2	AT2G20260.1	15 kDa	1.8
AVP1	AT1G15690.1	81 kDa	1.4
	AT2G24090.1	16 kDa	1.2
PGLCT	AT5G16150.1 (+2)	57 kDa	1.2

4.2.5 Receptor-like kinase *AtSOBIR1* is required for AEFÉ-induced defence response

During LRR-RP-mediated MTI in *A. thaliana*, LRR-RLP-type PRRs constitutively interact with SOBIR1 and recruit BAK1 into a receptor complex in a ligand-dependent manner (Albert et al., 2015, Postma et al., 2016, Domazakis et al., 2018, van der Burgh et al., 2019). To assess whether *AtSOBIR1* is required for AEFÉ-mediated MTI, I treated *Atsobir1-12* mutant with AEFÉ and measured $[Ca^{2+}]_{cyt}$ elevations, MAPK activation, defence gene expression and plant growth inhibition. Interestingly, the *sobir1-12* mutant was compromised for AEFÉ-mediated $[Ca^{2+}]_{cyt}$ elevations, MAPK activation and defence gene expression ($p < 0.05$) (Fig. 4.5). Furthermore, the *sobir1-12* mutant lost the AEFÉ-induced growth inhibition phenotype suggesting that *AtSOBIR1* is required for AEFÉ-mediated MTI responses. Similar experiments were conducted on the *sobir1-13* mutant with similar results (Appendix II.III).

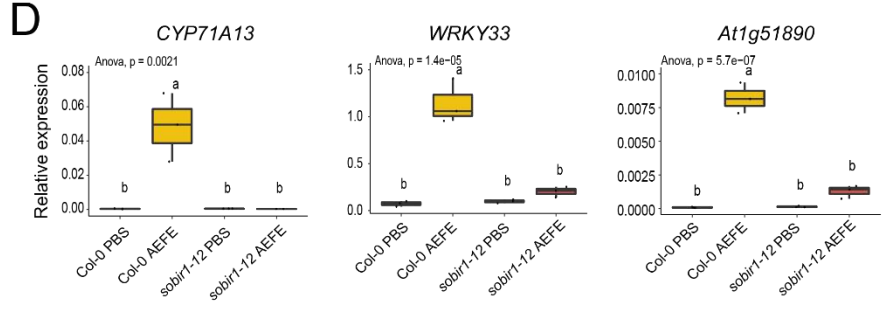
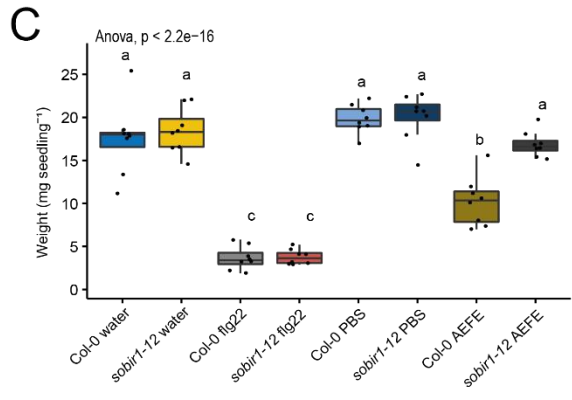
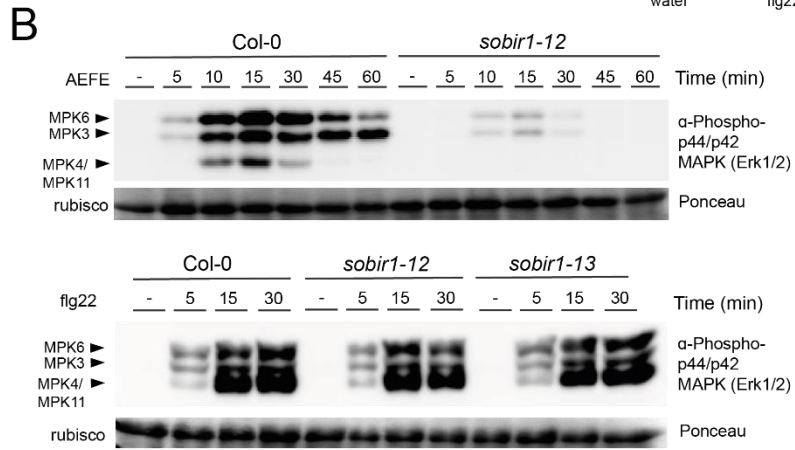
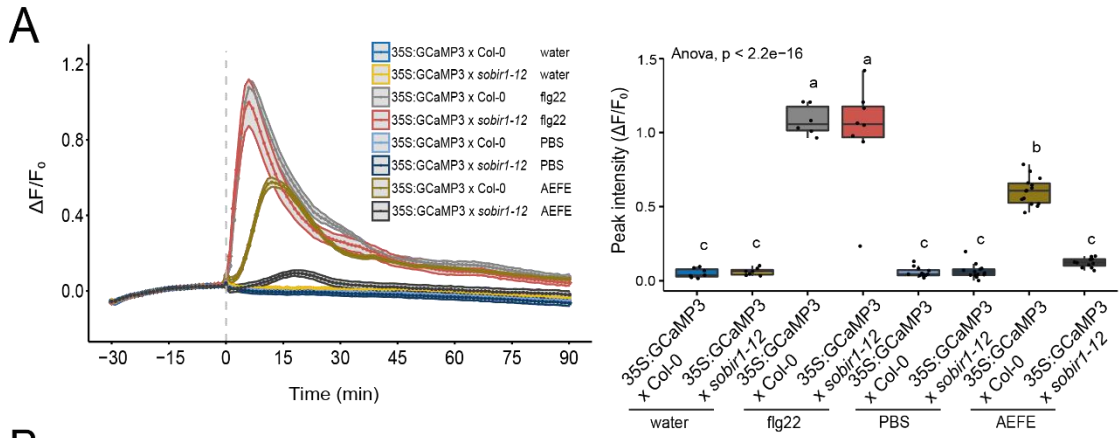


Figure 4.5: SUPPRESSOR OF BRASSINOSTEROID-ASSOCIATED KINASE 1-ASSOCIATED RECEPTOR 1 (SOBIR1) is a positive regulator of AEF E-induced defence signalling. **A** *A. thaliana sobir1-12* mutant is compromised for AEF E-induced $[Ca^{2+}]_{cyt}$ elevations. Normalised GFP fluorescence ($\Delta F/F$) kinetics in 10-day-old Col-0 35S:GCaMP3 or 35S:GCaMP3 x *sobir1-12* seedlings after elicitation with AEF E (0.25% (v/v); $\sim 2.3 \mu\text{g}/\mu\text{l}$), mock PBS treatment at 2.5% (v/v) or flg22 (20nM), mock water treatment as indicated. Lines represent mean values with upper and lower lines representing the standard error of the mean. Data are from a minimum of six biological replicates. Data is replicated as peak mean GFP fluorescence ($\Delta F/F$) for clarity. Letters indicate significant differences between treatments ($p < 0.05$). **B** MAPK activation during AEF E-induced MTI. Ten 10-days-old Col-0, *sobir1-12* *A. thaliana* seedlings were elicited per treatment per time point. Seedlings were treated with AEF E (2.5% (v/v); $\sim 22.5 \mu\text{g}/\mu\text{l}$), or flg22 (100nM) and flash frozen in LN₂ after an elapsed time as displayed. Mock (-) seedlings remained untreated. Activated MAPKs, MPK3/6/4/11 were detected by immunoblot using anti-p44/42 MAPK. Ponceau S staining of membranes are shown as loading controls. The experiment was repeated at least three times with similar results. Data shown is a representative example. **C** AEF E-induced seedling growth inhibition. Individual Col-0 or *sobir1-12* *A. thaliana* seedlings were germinated on ¼St MS and transferred to liquid MS with treatments as indicated. Seedlings were dried and weighted after 8-days. Data are from a minimum of six biological replicates. Letters indicate significant differences between treatments ($p < 0.05$). **D** Transcriptional profiling of MTI marker genes by quantitative reverse transcription-PCR (qRT-PCR). Three 10-day-old *A. thaliana* plants were elicited with AEF E (2.5% (v/v); $\sim 22.5 \mu\text{g}/\mu\text{l}$), mock PBS treatment at 2.5% (v/v) and flash-frozen after 1.5-h. Relative expression ($2^{\Delta\Delta CT}$) of the indicated genes is shown normalized to the *GAPDH* transcript (p -values were obtained in an ANOVA with Tukey HSD). Data are from three biological replicates.

4.2.6 *M. persicae* fecundity is not altered on *Atsobir1* mutant plants

In this study (Fig. 4.3), and previous studies, BAK1 was found to contribute to *aphid extract*-induced defence signalling and is required for feeding-induced defence signalling (Prince et al., 2014; Vincent et al., 2017). The vacuolar calcium-permeable channel TWO-PORE CHANNEL1 (TPC1) has also been implicated in aphid-feeding induced $[Ca^{2+}]_{\text{cyt}}$ elevations (Vincent et al., 2017). However, aphid fecundity is unaltered on *bak1-5* or *tpc1-2* mutants (Prince et al., 2014; Vincent et al., 2017). Given its putative role as a positive regulator of AEF2-mediated defence signalling, *AtSOBIR1* may act in a defence pathway against aphids and reduce *M. persicae* fecundity despite the interaction of *M. persicae* and *A. thaliana* being compatible. Moreover, *AtSOBIR1* may act during the defence response in incompatible circumstances, for instance when an aphid species cannot typically colonise the plant. To test these hypotheses, I scored *M. persicae* fecundity on *A. thaliana* Col-0 and *sobir1-12*, *sobir1-13* mutant lines. I also scored *Rhopalosiphum padi* (*R. padi*), a specialist aphid with preference for monocotyledon plants, particularly of the Gramineae family, for survival on *A. thaliana* wild-type and *sobir1-12*, *sobir1-13* mutant lines. There were no differences in the numbers of *M. persicae* offspring produced among the *A. thaliana* genotypes (Fig. 4.6A). Similarly, I identified no change in *R. padi* survival on *A. thaliana* wild-type and *sobir1-12*, *sobir1-13* mutant lines (Fig. 4.6B). Taken together, these results suggest that loss of *SOBIR1* has no obvious effects on the performances of compatible and incompatible aphids on *A. thaliana*.

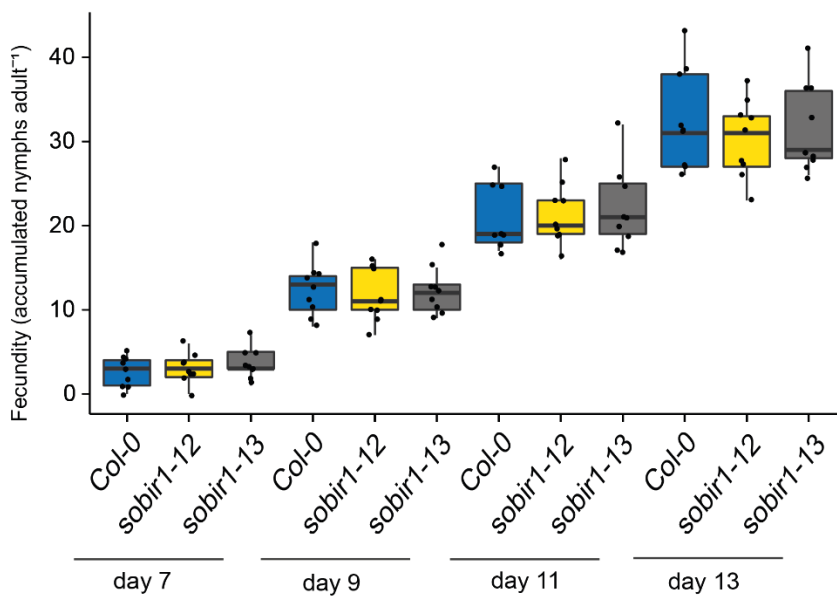
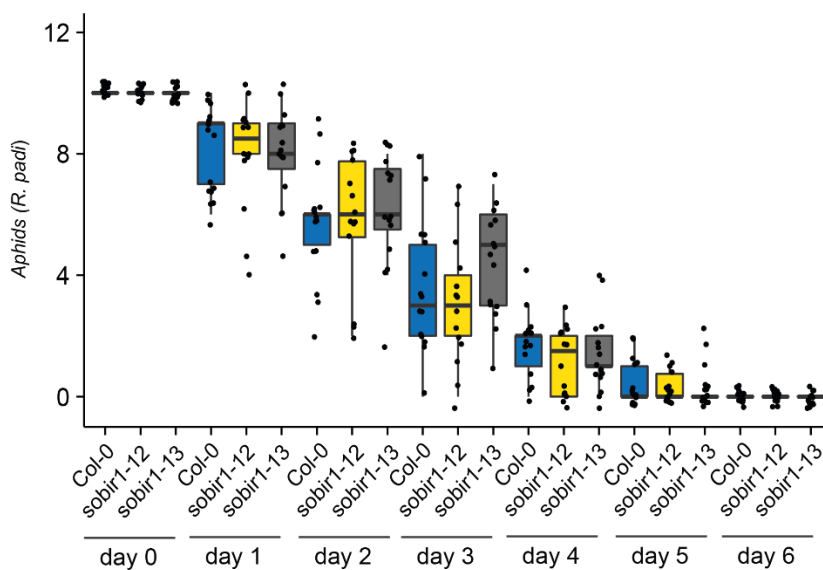
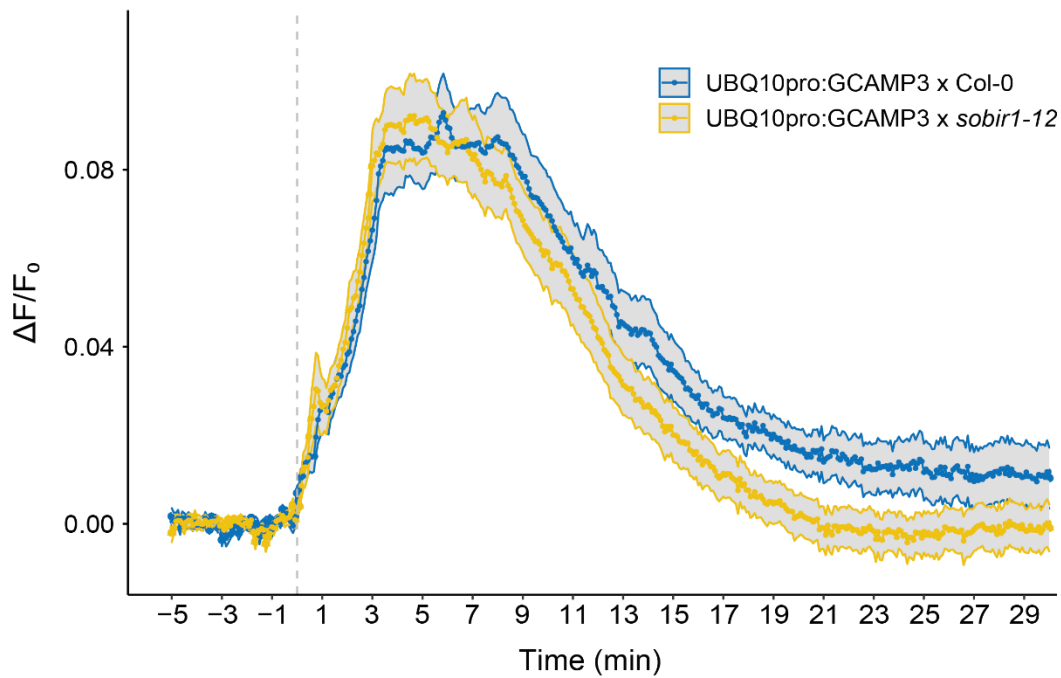
A**B**

Figure 4.6: Aphid performance is unaltered on the *A. thaliana* *sobir1* mutants. **A** Accumulated *M. persicae* fecundity scored over 13 days on 4-week-old Col-0, *sobir1-12* or *sobir1-13* mutant plants. Nymphs were scored at 7-, 9-, 11- and 13-days with nymphs being removed after each count. Data represent mean values of at least 10 plants per genotype. The experiment was repeated three times with similar results. Accumulated totals were tested for significant differences in an ANOVA with no significant differences between genotypes and within counts identified ($p > 0.05$). **B** *R. padi* survival on 4-week-old Col-0, *sobir1-12* or *sobir1-13* mutant plants. Ten 5-day-old *R. padi*, reared on oats, were transferred to and contained in a single-leaf clip cage on *A. thaliana*. Their survival was assessed daily. Data represent mean values of at least 12 plants per genotype. *R. padi* counts were tested for significant differences in an ANOVA with no significant differences between genotypes and within counts identified ($p > 0.05$). The experiment was repeated three times with similar results.

4.2.7 **AtSOBIR1 may alter $[Ca^{2+}]_{cyt}$ elevations in plants during feeding**

Aphids induce rapid, transient $[Ca^{2+}]_{cyt}$ elevations in plants during feeding and probing events (Vincent et al., 2017). $[Ca^{2+}]_{cyt}$ elevations are highly localised to the feeding site and are likely associated with epidermal- and mesophyll cell-perception of elicitors (Vincent et al., 2017). In agreement with this hypothesis, aphid feeding-induced $[Ca^{2+}]_{cyt}$ elevations were reported to partially depend on BAK1 (Vincent et al., 2017), and thus likely to be a signalling component of aphid-induced, BAK1-regulated MTI. To investigate whether SOBIR1 contributes to aphid-induced $[Ca^{2+}]_{cyt}$ elevations, the *35S:GCaMP3* reporter was crossed with the *sobir1-12* null mutant and the resultant reporter mutant was exposed to aphids. Aphid feeding-induced $[Ca^{2+}]_{cyt}$ elevations may return to basal levels (pre-exposure levels) more rapidly in *sobir1-12* plants relative to Col-0 (Fig. 4.7A). However, differences between the genotypes could not be explained by analysing signal area, peak intensity or the rate of $[Ca^{2+}]_{cyt}$ elevation spread (Fig. 4.7B).

A



B

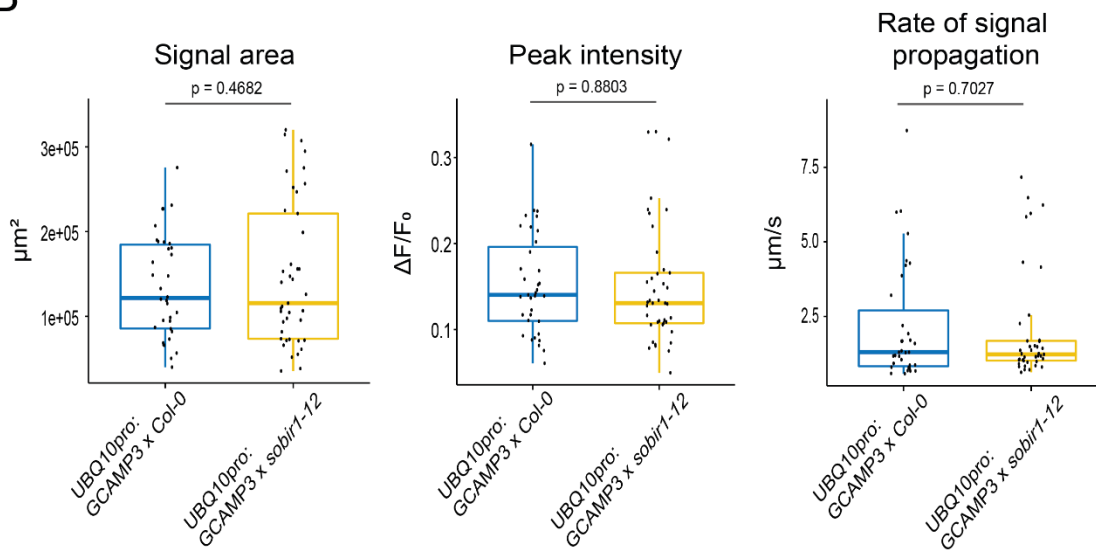


Figure 4.7: Cytosolic calcium influxes ($[Ca^{2+}]_{\text{cyt}}$) are altered on *Atsobir1* mutant plants. A A single adult *M. persicae* aphid was placed on an excised, 10-day-old *UBQ10:GCaMP3* x *Col-0* or *UBQ10:GCaMP3* x *sobir1-12* leaf floating in 200 μl dH_2O in a 96-well plate (Vincent et al., 2017). Fluorescence imaging was conducted and an F value obtained per 5s frame. Plots were generated by assessing the difference between F values and an F_0 (a pre-feeding average F between 30 and 60 frames). No aphid control leaves were simultaneously imaged and the F values $((F-F_0)/F)$ were subtracted from aphid treatment leaves to reduce experimental noise. Data represent the mean $(F-F_0)/F \pm \text{SE}$ ($n =$ minimum of 30 feeding events per genotype). **B** Data has been replicated from (A) for clarity. $[Ca^{2+}]_{\text{cyt}}$ elevations (as described above) were assessed for metrics such as signal area, peak intensity and rate of signal propagation. Data were analysed by a Student's *t*-test.

4.3 Discussion

4.3.1 AEFE induces MTI in *A. thaliana* and requires *BAK1*, *BKK1* and *SOBIR1*

MAMP-triggered immunity (MTI) is considered the first line of inducible defence in plants (Ausubel, 2005; Jones and Dangl, 2006). It was previously reported that aphid-associated feeding (Vincent et al., 2017), salivary components (de Vos and Jander, 2005; Chaudhary et al., 2014), and crude extracts (Prince et al., 2014), induce characteristic MTI responses in *A. thaliana*. Here, the breadths of AEFE-induced MTI responses were assessed. Plant responses to AEFE strongly overlapped with flg22-induced MTI in *A. thaliana* (Fig. 4.1). AEFE- and flg22-induced immunity appear to share PRR complex components, including a major role for BAK1 and minor role for BKK1 (Roux et al., 2011) (Fig. 4.4). Moreover, both elicitors induced immune signalling events including rapid, transient $[Ca^{2+}]_{cyt}$ elevations and MAPK activation. Furthermore, both flg22 and AEFE induce a growth inhibition phenotype in *A. thaliana* seedling after exposure suggesting reallocation of resources toward defence over growth. Growth inhibition induced by AEFE was less pronounced than the potent growth inhibitor flg22, but, nevertheless, was significant ($p < 0.05$) relative to a control (Fig. 4.1C).

A notable divergence in the plant response to AEFE- and flg22-induced MTI is the apparent role of adapter RK, SOBIR1 in AEFE-induced MTI but not to flg22. Mutants of SOBIR1, *sobir1-12* and *sobir1-13* were compromised for AEFE-induced $[Ca^{2+}]_{cyt}$ elevations, MAPK activation and defence gene expression, but not for flg22-induced responses (Fig. 4.5). Additionally, the *sobir1-12* and *sobir1-13* mutants rescued AEFE-induced seedling growth inhibition (Fig. 4.5C). Several RLPs constitutively associate with SOBIR1 and recruit BAK1 in a ligand-dependent manner (Liebrand et al., 2013; Steinbrenner et al., 2020). Given the strong inhibition of immune responses in *sobir1* KO mutants, and the apparent role of BAK1, it is tempting to speculate that SOBIR1, BAK1 and an unknown receptor-like protein (RLP) mediate AEFE-induced signalling. Indeed, five RLPs, RLP1, RLP23, RLP30, RLP32 and RLP42 require BAK1 and SOBIR1 for full function in the defence response against various pathogens (Jehle et al., 2013,

Zhang et al., 2013, Zhang et al., 2014, Albert et al., 2015, Fan et al., 2022). Where characterised, these RLPs mediate signalling in a tripartite, two-stage process; by first recognising ligands via RLP-SOBIR1 bimolecular complexes and second, recruiting BAK1 after ligand binding leading to complex activation (Liebrand et al., 2013; van der Burgh et al., 2019). Receptor complex activation is likely conferred by SOBIR1 trans-autophosphorylation as well as SOBIR1 and BAK1 transphosphorylation (van der Burgh et al., 2019). Accordingly, both SOBIR1 kinase activity and BAK1 are likely to be essential for SOBIR1 function in immunity (Liebrand et al., 2013; Wu et al., 2018; van der Burgh et al., 2019). Overexpression of SOBIR1 in *A. thaliana* as well as transient expression of *AtSOBIR1* in *N. benthamiana* or *N. tabacum* induced constitutive immunity, consistent with a model that places SOBIR1 as a key activator of RLP-mediated defence (Gao et al., 2009; Jamieson et al., 2018).

BAK1 pull-downs from *bak1-4* / *pBAK1:BAK1-eGFP* plants (Ntoukakis et al., 2011; Schwessinger et al., 2011), with or without AEF2, did not identify SOBIR1, or a putative PRR that fits the profile of an RLP (Table 4.1; Appendix II.II). Whilst tagged BAK1 variants still form ligand-dependent complexes with FLS2, they are not fully functional in MTI responses (Ntoukakis et al., 2011), thus caution should be applied when drawing conclusions from these data. However, it has been postulated, given the transphosphorylation requirements of BAK1 and SOBIR1, that BAK1-SOBIR1 complexes occur at low levels, are quickly degraded and are tightly controlled by negative regulators of immunity such as BIR1 (Gao et al., 2009; Liu et al., 2016). Indeed, SOBIR1 was first discovered in a suppressor screen for loss of autoimmunity in *bir1-1* (Gao et al., 2009). BAK1 is also required for *bir1-1* autoimmunity and BAK1-SOBIR1 complexes were only identified upon co-expression of BAK1 and SOBIR1 in *bir1-1* mutants (Lui et al., 2016). BIR1, together with its close homologs, BIR2 and BIR3 are thought to negatively regulate MTI by sequestering BAK1 (Halter et al., 2014, Imkampe et al., 2017). Consistent with these studies, all three BIRs were identified in BAK1 pull-downs (Table 4.1). BAK1 sequestration by BIRs may have prevented the identification of BAK1-binding partners in immuno-precipitations although the ligand-dependent dissociation of BAK1-BIRs should have enabled BAK1-RLP/SOBIR1 associations (Lui et al., 2016). Notwithstanding the *bir1-1* autoimmune phenotype, future immunoprecipitation

studies may benefit from being conducted in the *bir1-1* mutant background to improve BAK1 availability.

Previous studies have identified a key role for PAD4 in resistance to aphids, and this protection is independent of EDS1, SA or camalexin (Pegadaraju et al., 2005, Couldridge et al., 2007, Pegadaraju et al., 2007, Louis et al., 2010, Lei et al., 2014). Furthermore, PAD4-mediated resistance requires only PAD4 lipase domain to limit aphid fecundity, indicating novel PAD4 function during immune responses (Dongus et al., 2020). Recently, PAD4 was shown to be implicated in MTI responses directly (Pruitt et al., 2021). Both the *pad4* as well as *eds1* are impaired in RLP23-mediated MTI (Pruitt et al., 2021). Moreover, the authors identified a molecular interaction between SOBIR1 and ACTIVATED DISEASE RESISTANCE 1 (ADR1) (Pruitt et al., 2021), the helper NLR, required for PAD4-EDS1-ADR1-mediated ETI (Bonardi et al., 2011, Qi et al., 2018). These data suggest that the PAD4-EDS1-ADR1 node may act at the conduit of MTI and ETI in plants. Interestingly, and surprisingly, the autoimmune phenotype in *bir1-1* is not only dependent on BAK1 and SOBIR1, but is partially dependent on PAD4, which is suggestive of PAD4 regulation by BIR1 (Liu et al., 2016). Given the role of PAD4 in aphid resistance and link to MTI, as well as the putative role of SOBIR1 in perception of aphid-derived elicitors (Fig. 4.5), it is possible that the PAD4-EDS1-ADR1 node plays a role in AEFEE-induced MTI.

The MTI marker gene, *FRK1* is responsive to a number of MAMPs and is strongly expressed after 1-h upon flg22 treatment (Asai et al., 2002; Shan et al., 2008; Ma et al., 2021). *FRK1* expression is thought to be downstream of MPK3 and MPK6 activation in *A. thaliana* (Asai et al., 2002). Here, I showed that AEFEE only weakly induces *FRK1* expression after 90 min and that the transcript accumulation was not significantly different to control plants (Fig. 4.1E). Interestingly, previous studies have demonstrated that both aphid saliva (Chaudhary et al., 2014) and aphid extracts (Prince et al., 2014), induce *FRK1* expression. In contrast, aphid infestation did not induce the expression of *FRK1* (Jaouannet et al., 2015), and other MAMPs such as chitin may only marginally induce *FRK1* expression after only 1-h (Ma et al., 2021). To further resolve AEFEE-responsive gene induction, time-resolved data would be more informative. Such analyses have been employed to assess *FRK1* responsiveness during aphid challenge

and, interestingly, feeding induces a downregulation of *FRK1*, suggesting any initial induction is suppressed by the aphid (Bricchi et al., 2012). The prospect of AEFÉ not inducing *FRK1*, however, is surprising given AEFÉ-induced MAPK activation and $[Ca^{2+}]_{cyt}$ elevations; responses previously linked to *FRK1* induction during MTI (Boudsocq et al., 2010; Ranf et al., 2011).

Seedling growth inhibition (SGI) was observed after flg22 or elf18 treatment (Gómez-Gómez and Boller, 2000, Zipfel et al., 2006), but not after nlp20-treatment (Böhm et al., 2014b), suggesting RLK- and RLP-mediated responses apply differing metabolic needs on the plant (Wan et al., 2019). Here, I show that AEFÉ does induce SGI that is dependent on BAK1 and SOBIR1 (Fig. 4.1C, Fig. 4.4C, Fig. 4.5C). As expected, the *bak1-5* mutant but not the *sobir1-12* mutant partially rescues flg22-induced SGI highlighting the dual role of BAK1 in RLK- and RLP-mediated MTI but no involvement of SOBIR1 in flg22-induced responses.

4.3.2 Phytoalexin, downstream of *WRKY33* during MTI to aphids

Amongst the notable MTI responses to AEFÉ was the strong expression of phytoalexin biosynthesis pathway genes as well as the *WRKY*-domain transcription factor, *WRKY33* (Fig. 4.1D, E). AEFÉ induced the expression of all phytoalexin biosynthesis genes tested in this study, and furthermore, their expression was dependent on BAK1 and SOBIR1 in all instances (Fig. 4.4, Fig. 4.5). Interestingly, a previous study found *PAD3* induction in response to *M. persicae* extract is unaltered in the *bak1-5* mutant (Prince et al., 2014). This contrasting data may suggest that differing elicitors have been partially purified between the two studies. Indeed, BAK1 may differentially contribute to responses induced by MAMPs flg22 and elf18 (Ranf et al., 2011), and striking differences between RLK- and RLP-mediated signalling, with respect to camalexin biosynthesis gene expression, has been previously acknowledged (Wan et al., 2019).

The cytochrome P450 monooxygenase, CYP81F2 is responsible for the accumulation of modified indole glucosinolates in *A. thaliana* and contributes to resistance against *M. persicae* (Pfalz et al., 2009, Kettles et al., 2013). Whilst expression of *CYP81F2* was not directly tested in this study, upstream *CYP79B2* and *CYP83B1* (Glawischnig et al., 2004), were both expressed during AEF challenge (Fig. 4.1D). The P450 monooxygenase, CYP79B2 acts redundantly with CYP79B3 from which several branches diverge to generate indole glucosinolates (indole GSs), camalexin and indole-3-carboxylic acid (ICA) in *A. thaliana* (Zhao et al., 2002). In addition to displaying anti-herbivory characteristics, IGSs and camalexin are key anti-microbial, -fungal and -oomycete compounds (Bednarek et al., 2009). The *cyp79b2/cyp79b3* double mutant displays increased susceptibility to *M. persicae* suggesting that these compounds are also toxic to aphids (Kettles et al., 2013). Indeed, camalexin has been identified in aphids feeding on plants with elevated levels (de Vos and Jander, 2009). The final catalytic step of camalexin biosynthesis is regulated by *PAD3*, the expression of which during aphid challenge has been extensively studied (Zhou et al., 1999; Kusnierczyk et al., 2008; Prince et al., 2014). Furthermore, a common feature of RLP-mediated signalling appears to be enhanced transcript accumulation of camalexin biosynthesis genes and subsequent camalexin production (Zhang et al., 2013; Wan et al., 2019). AEF challenge induces *PAD3* expression, which is in general agreement with these studies and others that have considered phytoalexin biosynthesis gene expression to MAMPs (Frerigmann et al., 2016). These results indicate that both indole GSs and camalexin may be important components of aphid elicitor-induced plant defence responses.

In addition to phytoalexin biosynthesis gene expression, *WRKY33* has been shown to directly contribute to resistance against *M. persicae* (Kettles, 2011). *WRKY33* is a substrate for CPK5/CPK6 and MPK3/MPK6 and regulates camalexin biosynthesis in response to fungal pathogens, *B. cinerea* and *A. brassicicola* in *A. thaliana* (Ren et al., 2008; Mao et al., 2011; Birkenbihl et al., 2012; Yang et al., 2020). Challenge with flg22 leads to the activation of MPK4 (Andreasson et al., 2005). Subsequently, complexes with MKS1 and *WRKY33* are released from MPK4, and *WRKY33* targets the promoter of *PAD3* (Qiu et al., 2008). The role of *WRKY33* is poorly studied in the context of plant-aphid interactions, but *WRKY33* transcript accumulation

was recently identified in a short-term (0-h to 24-h) transcriptional study in *A. thaliana* upon aphid challenge (Giolai, M. 2019). Furthermore, *wrky33* mutant plants are more susceptible to *M. persicae* (Kettles, 2011). A long-term (21-days) study highlighted increased expression of an ortholog of *AtWRKY33* (*Glyma.01G128100*) in soybean (*Glycine max*) to soybean aphid (*Aphis glycines*) (Hohenstein et al., 2019). Moreover, *TaWRKY53*, the wheat ortholog of *AtWRKY33* is expressed during aphid infestation, and silencing results in increased susceptibility to aphid infestation (Van Eck et al., 2010). Consistent with these studies, *WRKY33* also contributes to whitefly resistance and is targeted by a secreted effector, Bsp9 (Wang et al., 2019b). The precise role of *WRKY33* in the context of aphid-plant interactions remains poorly characterised. Future studies may attempt to identify the targets of *WRKY33* during MTI to aphids, as well as identify the kinases for which it is a substrate.

4.3.3 [Ca²⁺]_{cyt} elevations are integral signalling events during MTI to aphids

I have presented evidence that [Ca²⁺]_{cyt} elevations are upstream of AEF2-induced MAPK activation and defence gene expression (Fig. 4.2). These findings are consistent with previous studies that have used pharmacological inhibition of Ca²⁺ channels to MAMP-induced ROS production and MAPK activation (Lebrun-Garcia et al., 1998, Romeis et al., 2001, Lecourieux et al., 2002, Marcec and Tanaka, 2021). Previous studies have identified BAK1-dependent [Ca²⁺]_{cyt} elevations during aphid feeding (Vincent et al., 2017), suggesting that aphid perception via PRR complexes during feeding events, leading to immune responses in the plant. AEF2-induced [Ca²⁺]_{cyt} elevations are partially dependent on BAK1 and SOBIR1 suggesting that these RLKs are part of a receptor complex that regulate rapid signal transduction after MAMP perception. Surprisingly, SOBIR1-dependent [Ca²⁺]_{cyt} elevations have not been demonstrated to the knowledge of this author. I found that BcNEP (nlp20) also induces SOBIR1-dependent [Ca²⁺]_{cyt} elevations in *A. thaliana* (data not shown). These findings may offer new opportunities to uncover novel RLP-mediated defence mechanisms. More specifically, how calcium signals are decoded and relayed by Ca²⁺-binding

proteins such as CaMs, CaM-like proteins and CDPKs. Ca^{2+} binds elongation factor (EF)-hand domains of CDPKs that are subsequently activated (Ludwig et al., 2005, Xie et al., 2014). Further experimentation might explore the role of CDPKs during AEFÉ-induced MTI. In *A. thaliana* CPK4, CPK5, CPK6, and CPK11 are positive regulators of the MAMP-induced responses (Boudsocq et al., 2010), and several CDPKs phosphorylate RBOHD and regulate its activity (Dubielia et al., 2013, Kadota et al., 2014).

$[\text{Ca}^{2+}]_{\text{cyt}}$ elevations during aphid feeding was perturbed in the *sobir1-12* mutant reporter (Fig. 4.7A), although differences were subtle and not due to signal area, peak intensity and rate of signal propagation (Fig. 4.7B). Instead, feeding induced $[\text{Ca}^{2+}]_{\text{cyt}}$ elevations were less prolonged in *sobir1-12* mutant lines relative to wild-type (Col-0). The apoplast, vacuole, mitochondria, peroxisomes and the endoplasmic reticulum are sources of Ca^{2+} (Stael et al., 2012). Two cyclic nucleotide-gated channels (CNGC2 and CNGC4) are likely key candidates for Ca^{2+} influx during flg22-triggered signalling (Tian et al., 2019). The removal of Ca^{2+} occurs against an electrochemical gradient by Ca^{2+} -ATPases and $\text{Ca}^{2+}/\text{H}^+$ exchangers (jointly known as Ca^{2+} -extruding systems), and is directly regulated by $[\text{Ca}^{2+}]_{\text{cyt}}$ elevations (Corry et al., 2001, Demidchik et al., 2018). Mutants of P2B-type ATPases, or autoinhibited calcium ATPases (ACAs), show impaired defence and attenuated flg22-induced Ca^{2+} signals (Geisler et al., 2000; Frei dit Frey et al., 2012). *aca4/11* mutants show elevated basal Ca^{2+} and an increased Ca^{2+} signal in response to flg22 (Hilleary et al., 2020), but their regulation by other MTI components remains unclear. Given our findings, and the contribution of ACAs to MTI, studies assessing the role of these ATPases in defence to aphids may be valuable.

ROS production in plants could enhance aphid resistance (Shoala et al., 2018), while impairment of ROS production reduces aphid resistance (Lei et al., 2014). Whether AEFÉ induces ROS bursts remains to be determined. *rbohD rbohF* double mutants were unaffected in AEFÉ-induced $[\text{Ca}^{2+}]_{\text{cyt}}$ elevations (data not shown), in agreement with $[\text{Ca}^{2+}]_{\text{cyt}}$ elevations being placed upstream of ROS and/or ROS production not being a factor in AEFÉ-induced MTI. RBOHD alone is sufficient to MAMP-triggered ROS (Mersmann et al., 2010). However, MAPK activation and seedling growth inhibition was not affected in *RbohD* mutants suggesting that ROS production is insufficient to trigger MAPK activation and is not a proxy for growth inhibition in all

circumstances (Mersmann et al., 2010). Treatment with MAMPs, *M. persicae* extracts and the bacterial GroEL protein present in aphid saliva induces extracellular ROS accumulation via BAK1 (Chaudhary et al., 2014; Prince et al., 2014). Although we cannot be conclusive on AEFÉ-induced ROS production, we might expect AEFÉ to induce ROS via BAK1 and SOBIR1 and similarly to nlp20, which induces ROS production in *A. thaliana* with a lag phase (Wan et al., 2019).

4.3.4 Aphid fecundity remains unaffected despite MTI perturbations

Challenging plants with aphids after MTI induction with AEFÉ did not significantly alter aphid fecundity (Fig. 4.3), suggesting that *M. persicae* is capable of overcoming MTI induced by this fraction. Aphid performance phenotypes have typically been studied in the context of modulation of plant defences by aphid secretion of virulence factors or effectors. Aphids deliver effectors in their saliva to modulate MTI and promote fitness (Mutti et al., 2006, Bos et al., 2010, Mutti et al., 2008, Pitino et al., 2013, Kettles and Kaloshian, 2016, Mugford et al., 2016, Chen et al., 2020, MacWilliams et al., 2020). However, previous studies have shown that induced resistance conferred by GroEL (Chaudhary et al., 2014), or aphid extract (Prince et al., 2014), can reduce aphid fitness on *A. thaliana*. Moreover, induced resistance conferred by crude aphid extract appeared to be dependent on BAK1 as well as camalexin production as the *cyp79b2/cyp79b3* and *pad3* mutants did not show an induced resistance phenotype (Prince et al., 2014).

In addition to the absence of AEFÉ-induced induced resistance, *M. persicae* fecundity was unaffected on *sobir1* mutants across the experimental period (days 7 – 13) assessed (Fig. 4.6A). Similarly, *M. persicae* fecundity is unaltered on *bak1-5* plants (Prince et al., 2014), indicating that the aphid may overcome BAK1-mediated defence during compatible interactions. In addition, I tested the role of SOBIR1 in incompatible interactions but *R. padi* survival was not altered on *sobir1* mutants suggesting that SOBIR1 does not strongly contribute to non-host resistance in *A. thaliana* (Fig. 4.6B). Given that camalexin biosynthesis genes are expressed in a SOBIR1-dependent manner

(Fig. 4.5), it is surprising that no *sobir1* fecundity phenotype was observed in these experiments. Furthermore, *A. pisum* survival was improved on *bak1-5* mutant plants suggesting that BAK1 does contribute to non-host resistance to this aphid in *A. thaliana* (Prince et al., 2014). Testing SOBIR1 overexpression lines may reveal altered aphid performance. However, overexpression of *A. thaliana* SOBIR1 induces constitutive activation of cell death and defence responses (Gao et al., 2009), which may alter morphology in older plants and hinder performance measurements.

Chapter 5

Forward- and reverse-genetic approaches to uncover
receptors mediating aphid perception

5.1 Introduction

5.1.1 Chapter aims

In the previous chapter, I presented evidence that the RLK adaptor protein *AtSOBIR1* as well as the co-receptor, BAK1 are required for full AEFEE-induced immune responses in *A. thaliana*. Both BAK1 and SOBIR1 have been implicated in LRR-RLP-mediated immunity where they form tripartite complexes to perceive immunogenic patterns and relay stimuli into cellular responses (Liebrand et al., 2013; Albert et al., 2015). The aims of this chapter are to examine whether pattern recognition receptors play a role in plant responses to aphid elicitors by screening plant material harbouring natural and induced variation for altered responses to AEFEE.

5.1.2 Receptor-like proteins mediate MAMP responses within receptor complexes

Plants deploy a large number of RLKs and RLPs as pattern recognition receptors (PRRs), which act to perceive MAMPs as well as endogenous DAMPS to induce defence responses (Boller and Felix, 2009). The highly variable ectodomain (ECD) of RLKs and RLPs provide the means to recognize a wide range of ligands that activate the receptor upon binding (Jones and Dangl, 2006, Boller and Felix, 2009, Macho and Zipfel, 2014, Breiden and Simon, 2016). PRR ECDs can contain leucine-rich repeats (LRRs), lysine motifs (LysMs), lectin motifs, or epidermal growth factor (EGF)-like domains to recognise bioactive patterns (Macho and Zipfel, 2014, Tang et al., 2017). Ligand binding can induce the formation of multimeric complexes involving activated receptors, co-receptors and intracellular kinases resulting in induced MTI (Couto and Zipfel, 2016). According to the prevailing model, constitutive RLP-SOBIR1 complexes are functional equivalents of RLKs that require the recruitment of BAK1 to activate RLP-SOBIR1 complexes (Jones et al., 1994, Gust and Felix, 2014, Liebrand et al., 2014, Bi et al., 2016). Intracellular outcomes are similar as those resulting from RLK PRR recruitment of BAK1.

Of the 57 annotated RLPs in *A. thaliana*, eight are experimentally validated to be associated with defence functions (*AtRLP1*, *AtRLP3*, *AtRLP23*, *AtRLP30*, *AtRLP32*, *AtRLP42*, *AtRLP51* and *AtRLP52*) (Zhang et al., 2010, Zhang et al., 2013, Zhang et al., 2014, Jehle et al., 2014b, Albert et al., 2015, Fan et al., 2021). Of these RLPs, *AtRLP1*, *AtRLP23*, *AtRLP30*, *AtRLP32* and *AtRLP42* form constitutive heterodimers with *AtSOBIR1* (Zhang et al., 2013, Zhang et al., 2014, Jehle et al., 2014b, Albert et al., 2015). Additionally, several RLPs in tomato, including *Ve1*, *Cf-2*, *Cf-4* and *Cf-9*, associate with *S/SOBIR1* and *S/SOBIR1*-like, which are two *SOBIR1* homologs with putatively redundant functions to mediate resistance against several fungal and oomycete pathogens (Liebrand et al. 2013; Peng et al. 2015; Zhang et al. 2014). Moreover, activated *Cf* receptors recruit *BAK1* to the receptor complex, a process that has been shown to regulate effector-triggered endocytosis of the activated *Cf* PRR and is required for resistance of tomato against *C. fulvum* (Liebrand et al., 2013; Postma et al. 2016). *Cf-4*-mediated signalling results in *SOBIR1* phosphorylation and activation of *BAK1* transphosphorylation (van Burgh et al., 2019). Expression of *AtSOBIR1* with signal-incompetent *AtBAK1* in *N. benthamiana* results in reduced phosphorylation levels of *SOBIR1* suggesting that *BAK1*, in turn, transphosphorylates *SOBIR1* to regulate specific responses (van Burgh et al., 2019).

In *A. thaliana*, currently only *AtRLP23* (Albert et al., 2015), *AtRLP30* (Zhang et al., 2013) and *AtRLP32* (Fan et al., 2021) are known to mediate defence signalling via *BAK1*. *AtRLP23* mediates recognition of a 20-amino-acid peptide motif (*nlp20*), which is derived from the necrosis and ethylene-inducing peptide 1 (*Nep1*)-like proteins (*NLPs*) that are found in various bacteria, fungi, and oomycetes (Bohm et al., 2014). The *RLP23-nlp20* PRR-ligand pair represents the most comprehensively studied LRR-RLP-type defence response (Bohm et al., 2014, Oome et al., 2014, Albert et al., 2015). Ligand perception is mediated via the *RLP23* ECD and is required for *BAK1* recruitment upon activation (Albert et al., 2019). Additionally, *SOBIR1* is required for *RLP23*-mediated signalling (Albert et al. 2015). Constitutive *RLP23-SOBIR1* association is mediated by the *GXXXG* protein dimerization motif in the *AtRLP23* transmembrane domain and a stretch of negatively charged residues in the extracellular juxtamembrane domain of the receptor (Albert et al., 2019). *Nlp20*-triggered *MTI* responses include *RLP23-*

dependent ROS and ethylene production, weak MAPK activation and defence gene expression (Albert et al., 2015, Wan et al., 2019). Moreover, ectopic expression of AtRLP23 in potato confers nlp20 recognition and enhanced immunity to several fungal and oomycete pathogens (Albert et al., 2015).

In *A. thaliana*, the bacterial pathogen *Ralstonia solanacearum* induces MTI independently of flg22- or elf18-triggered responses, suggesting additional MAMPs are perceived from *R. solanacearum* (Pfund et al., 2004). Recently, Fan et al. (2022) identified the proteobacterial protein translation initiation factor 1 (IF1) of *R. solanacearum* that triggers MTI in *A. thaliana* and some related Brassicaceae species. IF1 perception is mediated by AtRLP32-SOBIR1 complexes that recruit BAK1 upon activation (Fan et al., 2022). Accordingly, *bak1* mutants are insensitive to IF1 treatment and no longer display IF1-mediated resistance (Fan et al., 2022).

The proteinaceous elicitor called SCLEROTINIA CULTURE FILTRATE ELICITOR1 (SCFE1) from the fungal pathogen *Sclerotinia sclerotiorum* induces MTI via its receptor RLP30, as well as SOBIR1 and BAK1 in *A. thaliana* (Zhang et al., 2013). The SCFE1 fraction induces characteristic MTI responses including ROS production and MAPK activation (Zhang et al., 2013). To identify AtRLP30, the authors utilised natural variation for SCFE1 in *A. thaliana* accessions, finding several insensitive accessions amongst the panel (Zhang et al., 2013). The elicitor(s) within SCFE1 is currently unknown. In another study, several necrosis-inducing effectors that also require the plant BAK1 and SOBIR1 for the induction of necrosis were identified from *S. sclerotiorum* (Seifbarghi et al., 2020). However, AtRLP30 is not required for immune responses to necrosis-inducing effectors and thus *S. sclerotiorum* induces several independent immune pathways that require BAK1 and SOBIR1 (Seifbarghi et al., 2020).

AtRLP1/ReMAX (RECEPTOR of eMAX) can detect the ENIGMATIC MAMP OF XANTHOMONAS (eMAX) and requires AtSOBIR1 for full sensitivity (Jehle et al., 2013). In contrast with most MAMPs, eMAX is heat labile suggesting its secondary structure is important for its perception by RLP1 (Jehle et al., 2013). Interestingly, RLP1 has no ortholog in *N. benthamiana* and transient expression of AtRLP1 does not confer eMAX sensitivity (Jehle et al., 2013), suggesting that defence components outside of SOBIR1 and BAK1, and absent in *N. benthamiana* are likely required for eMAX signalling.

Pathogens secrete cell wall degrading enzymes (CWDEs) to promote virulence in their host (Kubicek et al., 2014). Some CWDEs induce innate immune responses in plants either directly, or indirectly through the release of cell wall elicitors (Benedetti et al., 2015). Fungal CWDE, polygalacturonase (PG) can be recognized as MAMPs by AtRLP42 (Zhang et al., 2014). Intriguingly, co-immunoprecipitation assays showed that AtRLP42 interacts with SOBIR1 but not with BAK1, suggesting an alternative RLK regulates downstream signalling to PGs (Zhang et al., 2014). Another hydrolytic enzyme, ethylene-inducing xylanase (EIX), is perceived by the tomato LRR-RLP LeEIX2 to induce HR (Ron and Avni, 2004). The *LeEIX2* homolog in *N. benthamiana*, Response to XEG1 (RXEG1), has evolved to recognise a distinct MAMP, the glycoside hydrolase 12 protein XEG1 to induce HR (Wang et al., 2018). Recently, a novel EIX-like protein from *Verticillium dahlia*, *VdEIX3*, was found to elicit immune responses in *N. benthamiana* (Yin et al., 2021). *VdEIX3* is perceived by the LRR-RLP, *NbEIX2* to induce ROS production, expression of defence genes and increased resistance to oomycete and fungal pathogens (Yin et al., 2021).

Interestingly, two RLPs, AtRLP10/CLAVATA2 (CLV2) and AtRLP17/TOO MANY MOUTHS (TMM), have been implicated in both developmental as well as immune function (Pan et al., 2016). AtRLP17 forms complexes with ERECTA-family genes (ERf) paralogs ER-like 1 (ERL1) and ERL2 to regulate stomatal patterning upon the perception of EPF1 and EPF2 (Lin et al., 2017). Furthermore, AtRLP17-ERL complexes associate with BAK1 to modulate pathogen resistance (Pan et al., 2016).

LRR-containing proteins are often involved in protein-protein and protein-ligand interactions (Kobe and Deisenhofer, 1994). *A. thaliana* LRR-RLPs contain between 16 and 28 repeats with an extracellular LRR motif containing a 22- to 25-amino acid conserved consensus sequence, LxxLxxLxLxxNxLSGxIPxxLGx in which “L” is Leu, Ile, Val, or Phe, “N” is Asn, Thr, Ser, or Cys, and “C” is Cys, Ser or Asn (Fritz-Laylin et al., 2005, Matsushima et al., 2010).

The plant-specific LRR-RLPs are divided into domains A through G (Jones and Jones, 1997). At the N-terminal, Domain A comprises a putative signal peptide, and Domain B, which forms the N terminus of the mature protein, contains a cysteine-rich region. Domain C is the primary extracellular LRR (eLRR) domain that is generally

thought to mediate ligand perception (Kobe and Deisenhofer, 1994). This LRR-containing domain is subdivided into three domains in which the non-LRR “loop-out” or “island” C2 domain interrupts the C1 and C3 LRR regions (Jones and Jones, 1997). Domain D is termed a spacer region whilst the juxtamembrane domain, Domain E contains several glutamic acid residues Domain F contains the transmembrane domain comprising a conserved GxxxG motif. Domains E and F are thought to contribute to RLP-SOBIR1 interactions (Albert et al., 2019). Finally, Domain G comprises a small, C-terminal cytoplasmic region (Jones and Jones, 1997).

5.1.3 Divergent LRR-RLPs

Phylogenetic analyses, of *A. thaliana*, tomato, rice and *B. rapa* LRR-RLPs has shown little conservation of sequence and as such LRR-RLPs tend to cluster by plant species (Fritz-Laylin et al., 2005, Jamieson et al., 2018). It has been proposed that the lack of intracellular kinase makes LRR-RLPs relatively more predisposed to neofunctionalization when compared to LRR-RLKs for example (Jamieson et al., 2018). Indeed, a comparative genetic approach to identify PUTATIVE DEVELOPMENTAL ORTHOLOGS (PDOs) in *A. thaliana* and rice only identified four putative orthologs (Fritz-Laylin et al., 2005). The lack of orthologous genes between species results in MTI responses that are restricted to individual plant families such as *AtRLP1*-, *AtRLP23*-, *AtRLP32*- and *AtRLP42*-mediated MTIs that are limited to members of the Brassicaceae family (Jehle et al., 2013, Albert et al., 2015, Fan et al., 2021, Zhang et al., 2021). Similarly, genus-specific distribution has been noted, such as the tomato EIX2 receptor for fungal xylanase (Ron and Avni, 2004).

5.1.4 Forward genetics to uncover regulators of immunity in plants

Several genetic approaches have been used to identify causal genes underlying MAMP sensitivity in plants. Typically, these approaches rely on natural or induced variation and assessment of altered MAMP-induced phenotypes. Furthermore, these approaches use map-based cloning or a combination of map-based cloning and whole-genome sequencing (WGS) to identify causal genes.

The PRR RLK, FLS2 was identified by assessing the flg22-induced seedling growth inhibition phenotype (Gómez-Gómez et al., 1999), from an EMS mutagenized population of flg22-sensitive La-er seedlings (Gómez-Gómez and Boller, 2000). Prior to this study, a screen for flagellin sensitivity was conducted using a panel of *A. thaliana* accessions and identified the FLS1 locus underlying flagellin-insensitivity in Ws-0 (Gómez-Gómez et al., 1999).

In addition to PRRs, downstream signalling components are often identified in forward genetic screens. Boutrot et al. (2010) utilised a genome-wide T-DNA library of mutagenised *A. thaliana* seedlings (Alonso et al., 2003) to isolate approximately two-dozen flagellin-insensitive (*fin*) mutants impaired in flg22-induced ROS burst. Validating the approach, the authors identified FLS2 (*fin1*) and BAK1 (*fin2*) in the screen, but also ethylene-signalling protein EIN2 (*fin3*) and the chloroplastic enzyme ASPARTATE OXIDASE (AO) (*fin4*) (Boutrot et al., 2010, Macho et al., 2012). T-DNA-mediated mutagenesis often leads to missense mutations, and as such several *fin* mutants often carried small (1- or 2-bp) deletions (Boutrot et al., 2010).

Ranf et al. (2012) screened EMS-mutagenized *A. thaliana* aequorin transgenic line to identify mutants altered for $[Ca^{2+}]$ responses to flg22. Approximately three-dozen lines were analysed and several novel *fls2* and *bak1* alleles were identified. Despite only modest reductions in $[Ca^{2+}]$ responses, likely owing to considerable redundancy in calcium influx mechanisms, other regulators of MAMP-triggered $[Ca^{2+}]$ responses were identified, including PBL1 and BIK1 (Ranf et al., 2014).

Li et al. (2014) reported a novel screening system with EMS-mutagenised, transgenic *A. thaliana* stably expressing the promoter sequence of flg22-responsive *FRK1* fused to the firefly luciferase reporter (fLUC) termed *Arabidopsis genes governing immune gene expression* (aggie). The screen revealed enhanced immune gene activation in aggie1 and aggie3, two mutants of *RNA POLYMERASE II C-TERMINAL DOMAIN* (CTD) *PHOSPHATASE-LIKE 3* gene (Li et al., 2014a) as well as aggie2, a mutant of *POLY(ADP-RIBOSE) GLYCOHYDROLASE 1* (PARG1) was found to be compromised in defence gene expression (Feng et al., 2015).

Several studies have utilised NGS and natural variation within *A. thaliana* accessions to identify genes underlying RLK- or RLP-mediated MTI. The PRR regulating *S. sclerotiorum*-derived elicitor (SCFE1)-triggered ethylene responses is RLP30 in *A. thaliana* (Zhang et al., 2013). Of the 70 accessions screened, five (Br-0, Lov-1, Lov-5, Mt-0 and Sq-1) were fully insensitive to SCFE1 (Zhang et al., 2013). F2 populations from the insensitive Lov-1 × sensitive Col-0 cross showed a Mendelian segregation ratio of 3:1 suggesting that the insensitivity to SCFE1 is controlled by a single recessive gene. Fine-mapping identified a ~2.3 Mb loci containing four RLPs (RLP30 to RLP33), which were tested using T-DNA insertion lines (Zhang et al., 2013). Similarly, the loci underlying IF1 elicitor insensitivity was revealed by screening 106 accessions for ethylene production, identifying three insensitive accessions (Dog-4, ICE21, and ICE73). Subsequent fine mapping using newly generated DNA markers by restriction site-associated DNA sequencing (RAD-seq) identified a ~2.3 Mb region containing RLP32 (Fan et al., 2021). In a separate study, *A. thaliana* accessions were screened for eMax responsiveness (Jehle et al., 2013). Shakh dara (Sha), an eMAX insensitive accession, was crossed with the sensitive Ler-0 or Bay-0 to generate recombinant inbred lines to allow mapping of *AtRLP1* (Jehle et al., 2013).

Several contemporary next-generation sequencing (NGS)-based methods have enabled rapid identification of causal genes underlying immune phenotypes. Examples include *Next Generation Mapping* (NGM) (Austin et al., 2011) *MutMap* (Abe et al., 2012), and *Needle in the k-stack* (NIKS) (Nordstrom et al., 2013). *MutMap* relies on knowledge of MAMP-responsive defence gene expression and real-time monitoring to screen EMS-mutagenize an *A. thaliana* line stably expressing a luciferase reporter fused

to a MTI promoter which is activated upon MAMP challenge (Abe et al., 2012). Mapping the causal loci is carried out by generating an F₂ segregating population, scoring individuals for MAMP responsiveness and detecting single-nucleotide polymorphisms (SNPs) and insertion-deletions (indels) between mutant and wild-type phenotypes (Abe et al., 2012). Among the F₂ progeny, the majority of SNPs will segregate in a 1:1 mutant:wild-type ratio. SNPs that are unlinked to the SNP responsible for the mutant phenotype would show 50% mutant and 50% wild-type sequence reads. A causal SNP and closely linked SNPs should show 100% mutant and 0% wild-type reads. Defining a SNP index as the ratio between the number of reads of a mutant SNP and the total number of reads corresponding to the SNP, the index would equal 1 near the causal gene and 0.5 for the unlinked loci (Abe et al., 2012).

5.1.5 Hypotheses and Approach

In the previous chapter I presented evidence that the RLK adaptor protein AtSOBIR1 as well as the co-receptor, BAK1 are required for full AEFEE-induced immune responses in *A. thaliana*. Because BAK1 and SOBIR1 have been implicated in LRR-RLP-mediated immunity, where they form tripartite complexes to perceive immunogenic patterns and relay stimuli into cellular responses (Liebrand et al., 2013; Albert et al., 2015), I hypothesised that an RLP may be involved in recognition of AEFEE. Therefore, I conducted a reverse genetic screen for altered MAPK activation to AEFEE by utilising a panel of *Atrlp* mutant lines. However, the role of BAK1 and SOBIR1 in plant defence to aphids is not fully understood, and it is possible that BAK1 and SOBIR1 mediate as yet unknown processes to contribute toward aphid-induced responses. To address this, I also aimed at validating forward genetic approaches to enable future identification of components governing AEFEE perception and signalling. This was achieved by conducting a forward screen of EMS-mutagenised *pWRKY33::fLUC* *A. thaliana* seedlings to identify lines with altered AEFEE-induced *WRKY33* promoter activation. Moreover, given the previous success of screens of natural variation to identify RLP PRRs, I assessed a panel of *A. thaliana* accessions for altered AEFEE-induced SGI. Taken together, I have explored and validated a number of forward and reverse genetic

approaches that may be used to determine plant components that underlie plant immune responses to aphid elicitors.

5.2 Results

5.2.1 Receptor-like proteins do not regulate AEFE-induced MAPK activation in *A. thaliana*

The cytoplasmic kinase domain of RLKs transduce extracellular stimuli into intracellular signalling, whilst RLPs depend on regulatory RLKs to achieve this signalling (Albert et al., 2015, Couto and Zipfel, 2016, Tang et al., 2017, van Burgh et al., 2019). Two RLKs shown to regulate RLP-mediated MTI are adaptor protein SOBIR1 and co-receptor BAK1 (Liebrand et al., 2013, Zhang et al., 2013, Jehle et al., 2014b, Liebrand et al., 2014, Zhang et al., 2014, Albert et al., 2015, Fan et al., 2021). In the previous chapter, I presented evidence that AEFE induces BAK1- and SOBIR1-dependent MAPK activation in *A. thaliana*. These data suggest that components within AEFE may be perceived by a tripartite receptor complex composing BAK1, SOBIR1 and an RLP. There are 57 RLPs annotated in the *A. thaliana* genome and *AtRLP* domain composition consists of domains A-F, where C3-F are the most highly conserved regions (Jones and Jones, 1997; Fritz-Laylin et al., 2005; Wang et al., 2008). Sequence alignments of the C3-F region can be arranged into a phylogenetic tree (Fig. 5.1A) (Fritz-Laylin et al., 2005; Wang et al., 2008).

To test whether an LRR-RLP is responsible for AEFE perception, I accumulated a library of the 53 of the 57 *A. thaliana* RLP T-DNA mutants in *A. thaliana* (Wang et al., 2008a), and genotyped each mutant line to confirm T-DNA mutant allele homozygosity (Fig. 5.1B). Due to lack of germination, some mutant lines were genotyped from segregating populations and several alternative alleles and primers were chosen (Table 5.1). Unfortunately, homozygous mutants could not be confirmed in 4 lines (RLP19, RLP36, RLP47, RLP49). Allele names are consistent with and run contiguous to Wang et al. (2008). To assess the role of LRR-RLPs in AEFE-perception, each *rlp* mutant was treated with AEFE and MAPK activity monitored at 15- and 30-min post-elicitation.

Despite the loss of AEF E-induced MAPK activation in the *sobir1-12* mutant (Fig. 5.2A), none of the *Atrlp* mutants tested displayed altered AEF E-induced MAPK activation relative to wild-type (Col-0) (Fig. 5.2B), suggesting that mutation of any single *AtRLP* is insufficient to alter MPK3/6 activation in *A. thaliana*.

MAPK cascades, MAPKKK3/5-MKK4/5-MPK3/6 and MEKK1-MKK1/2-MPK4 are rapidly activated upon MAMP perception (Asai et al., 2002). To ensure the AEF E-induced MAPK activation occurred via MPK3/6 and the labelling of these MPKs is specific, I tested the *mpk3* and *mpk6* mutants for AEF E-induced MAPK activation. Importantly, bands corresponding to MPK3/6 activation were lost in the respective *mpk3* and *mpk6* mutant lines, confirming MPK3/6 activation to AEF E (Appendix III.I).

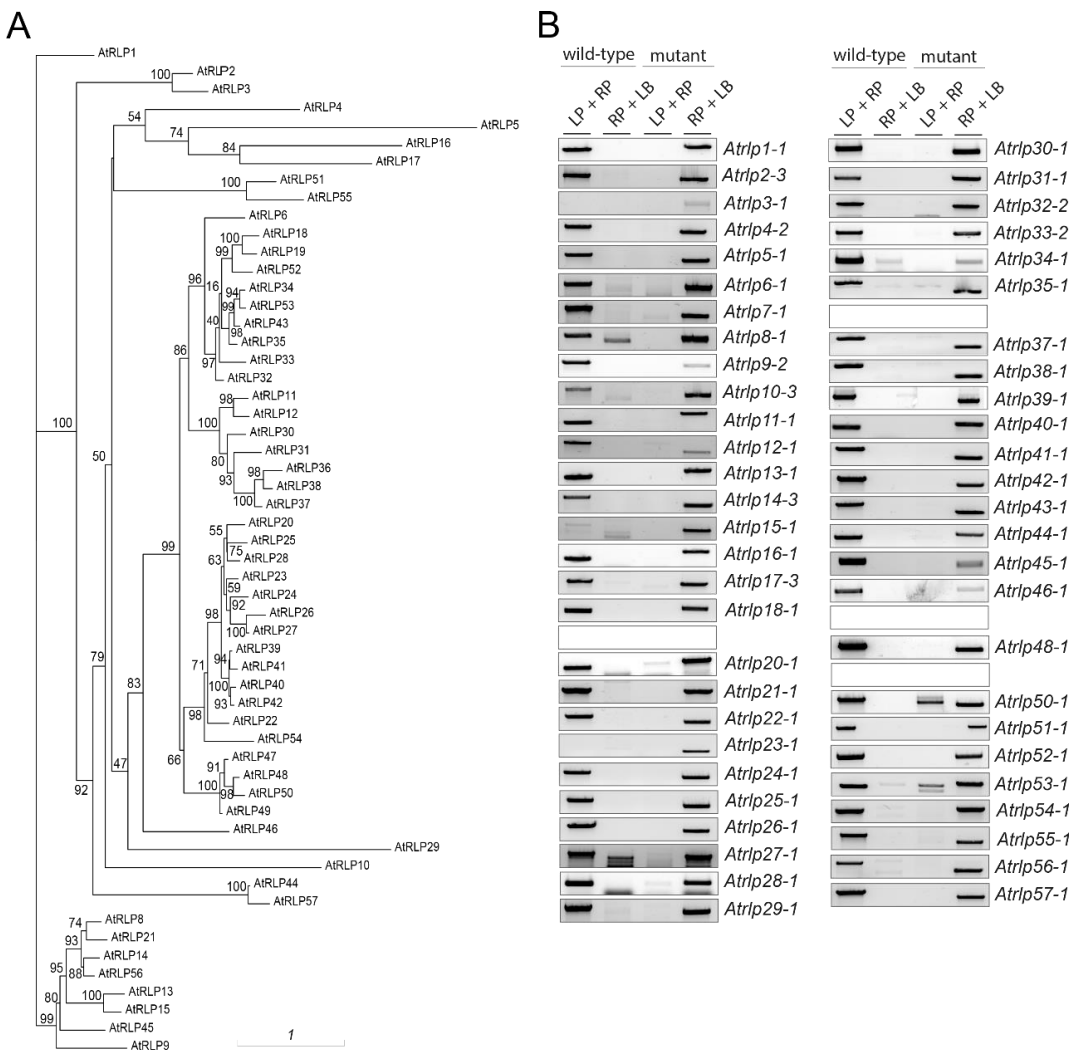


Figure 5.1: *A. thaliana* receptor-like proteins (AtRLPs). **A** Maximum likelihood (W-IQ-TREE; Trifinopoulos et al., 2016) phylogeny of *A. thaliana* RLPs based on the alignment of C3-F domains of all AtRLPs with 1000 bootstrap support values as indicated on the branches (Wang et al., 2008). Sequences were retrieved from NCBI and aligned in MEGA (v.7.0.26) using Multiple Sequence Alignment Comparison by Log-Expectation (MUSCLE). The scale bar represents an amino acid substitution per site. **B** Genotyping of *Atrlp* T-DNA mutant alleles. T-DNA insertion lines were retrieved from the Nottingham Arabidopsis Stock Centre (NASC) and genotyped from homozygous lines or segregating populations as required. Published primers were used (as indicated in Appendix III.II; Wang et al., 2008) and novel primers designed using <http://signal.salk.edu/>. Four amplification reactions were generated per T-DNA mutant line – left- and right- primer (LP and RP), amplifying from wild-type (Col-0) DNA and T-DNA mutant allele DNA, and RP and left border (LB) amplifying from wild-type and mutant DNA. All T-DNA insertion mutants are in Col-0 background with the exception of *Atrlp18-1* (Col-3) and *Atrlp54-1* (Col-3). See Appendix III.II for further information. Note that the *Atrlp36* line was not obtained and *Atrlp19*, *Atrlp47* and *Atrlp49* were not confirmed as homozygous mutants.

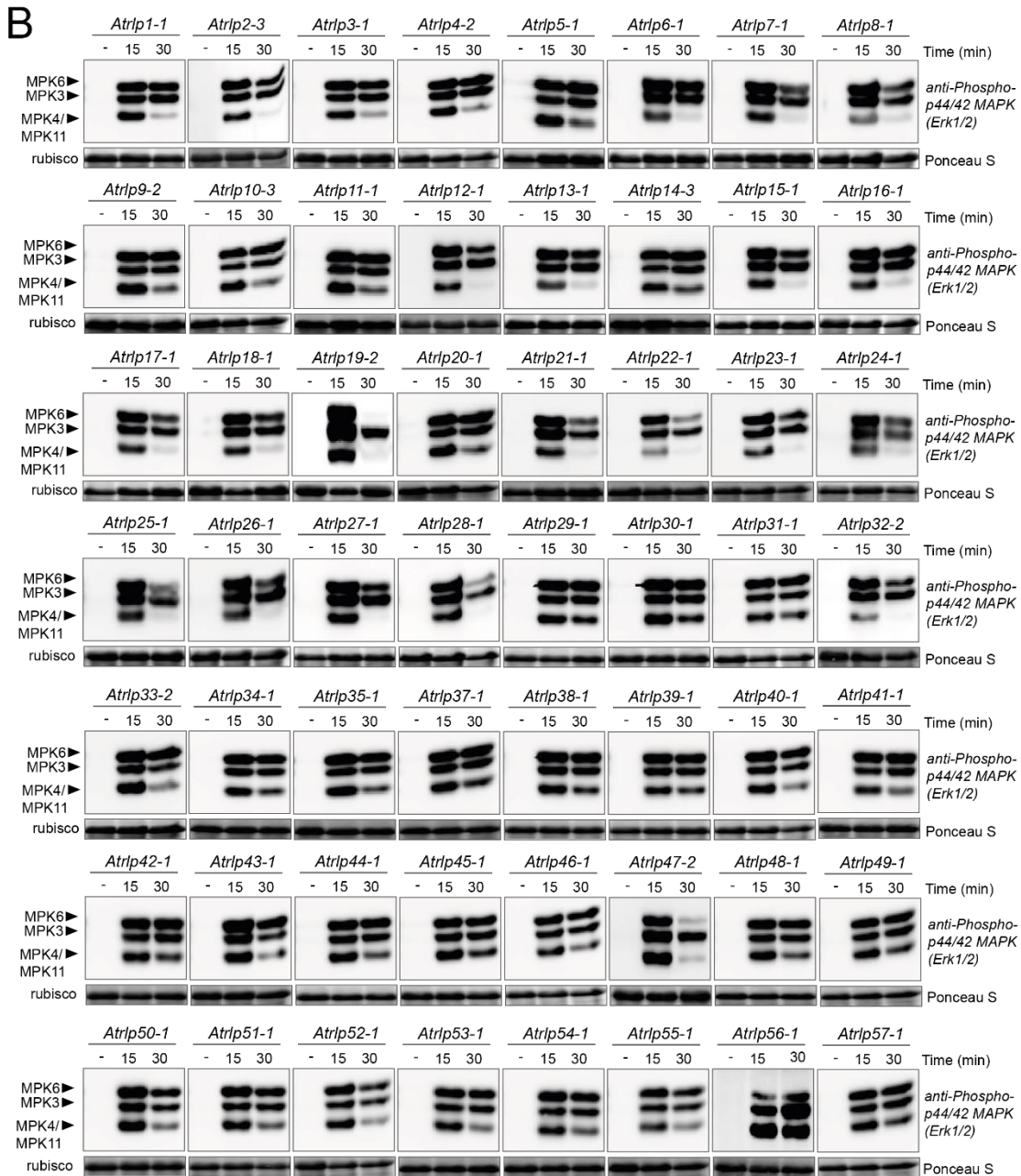
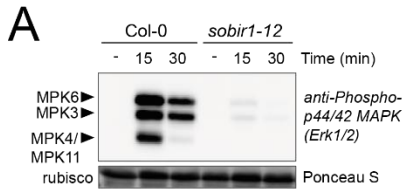


Figure 5.2: MAPK activation screen of *A. thaliana* receptor-like protein mutants (*Atrlp*) during AEF E-induced MTI. Ten 10-days-old *A. thaliana* **A** Col-0 and *sobir1-12* seedlings, or **B**, *atrlp* T-DNA insertion mutant seedlings were treated with AEF E (2.5% (v/v); ~22.5 µg/µl) and flash frozen in LN₂ after an elapsed time as displayed. Mock (-) seedlings remained untreated. Activated MAPKs, MPK3/6/4/11 were detected by immunoblot using anti-p44/42 MAPK. Ponceau S staining of membranes are shown as loading controls. The experiment was repeated at least twice per T-DNA insertion line with similar results. Data shown is a representative example. Note that *Atrlp36* was not tested and *Atrlp19*, *Atrlp47* and *Atrlp49* were not confirmed as homozygous mutants.

5.2.2 Forward genetic screen reveals hyposensitive and hypersensitive variation in AEF E-responsiveness

Previously, I have shown that AEF E induces rapid *WRKY33* promoter activity that can be visualised by the production of firefly luciferase within a *pWRKY33:fLUC* reporter plant (Fig. 3.2). Next, I opted to investigate the signalling networks regulating *WRKY33* promoter activity via a genetic screen with an ethyl methanesulfonate (EMS)-mutagenized population of *A. thaliana pWRKY33:fLUC* transgenic plants (Kato et al., 2020).

To identify mutants showing altered response to AEF E, I screened 5,984 M₂ EMS-mutagenized seedlings of the *pWRKY33:fLUC* reporter using real-time, bioluminescence monitoring (Kato et al., 2020). Mutant lines with altered morphological phenotypes were excluded from the analysis leaving 2,795 M₂ individuals. M₂ individuals were compared to AEF E-treated, wild-type *pWRKY33:fLUC* to generate a z-score (Fig. 5.3A). For a single recessive trait, M₂ individuals will contain non-segregating alleles and subsequent selfing will result in the maintenance of these alleles. In total, 84 M₂ mutant individuals were rescued, selfed and assessed as an M₃ population for AEF E-responsiveness. Two mutant lines named *3g 5-7* and *6c 2-8* displayed consistent reduction of AEF E-induced luminescence relative to wild-type seedlings ($p < 0.05$) (Fig. 5.3B). Several lines, including *2c 6-7* displayed reduced AEF E-induced luminescence as an M₂ individual but did not display consistently reduced luminescence in the next generation (Appendix III.III).

To uncover the underlying, casual genetic loci responsible for the reduction of AEFÉ-induced luminescence in mutants *3g 5-7* and *6c 2-8*, these lines were backcrossed to the parental, wild-type *pWRKY33:fluc* line with a view to carry out a MutMap analysis (Abe et al., 2012). However, despite several attempts, I was unable to successfully cross *3g 5-7* and wild-type reporter plants. Several crosses of *6c 2-8* were successful and F₁ plants were allowed to self-pollinate to generate F₂ segregating populations. Unfortunately, no clear segregation of AEFÉ-responsiveness within F₂ populations could be identified (Fig. 5.3B). Hence, this avenue of investigations was not taken forward.

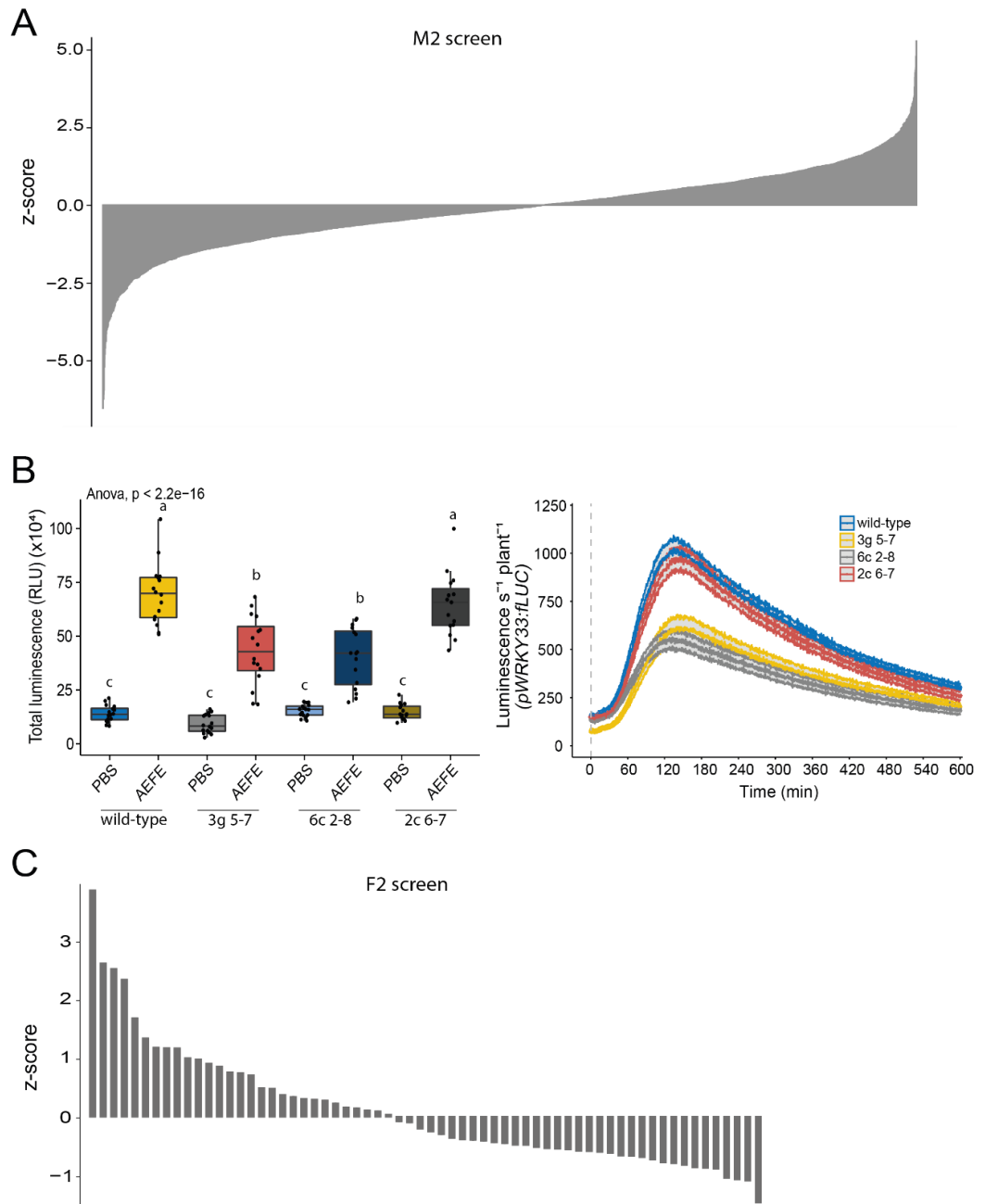


Figure 5.3: EMS-mutagenised *pWRKY33:fLUC A. thaliana* seedlings exposed to aphid-derived extract, AEF E. **A** Bioluminescence was monitored in M₂ EMS-mutagenised *pWRKY33:fLUC* individuals. A z-score for each individual was determined by the relationship of the individuals' AEF E response relative to a *wild-type* mean value over 600 min post-treatment. A total of 2,795 M₂ individuals are displayed. **B** Total luminescence of three candidate lines in the M₃ generation. Boxes represent mean luminescence of summed data between 0 and 600 min after treatment. Whiskers represent lowest and highest score excluding outliers. Luminescence of individuals are shown as black dots. Means are generated from at least 8 individuals per genotype. Letters indicate significant differences between treatments ($p < 0.05$). [Right] Data is replicated as a time-course. Lines represent mean \pm SE. **C** Bioluminescence of F₂ individuals (60 individuals represented). z-score was generated as above.

5.2.3 Natural variation for AEF E-sensitivity in *A. thaliana*

Several studies of receptor-mediated immunity in *A. thaliana* have utilised natural variation for MAMP sensitivity to identify the underlying locus conferring perception and subsequent cellular signalling (Gómez-Gómez and Boller, 2000; Vetter et al., 2012; Jehle et al., 2013; Zhang et al., 2013; Zhang et al., 2014; Fan et al., 2022). AEF E was previously found to induce SOBIR1- and BAK1-dependent SGI (Fig. 4.1, Fig. 4.3, Fig. 4.4). These experiments were all conducted in the Col-0 background. To test whether there is natural variation for AEF E-responsiveness, AEF E-induced SGI was assessed in 44 *A. thaliana* accessions. Seedlings were transferred to ¼MS media containing either AEF E (11 ug ml⁻¹) or PBS (0.5 mM) and weighed after 8-days. SGI was calculated as a percentage difference between treatments. Variation for AEF E-induced SGI was observed between accessions and ranged between ~4% ± 1.4% (NFA-8) and 38% ± 4.5% (Se-0) (Fig. 5.4). SGI of Col-0 seedlings was approximately 27% (Fig. 5.4).

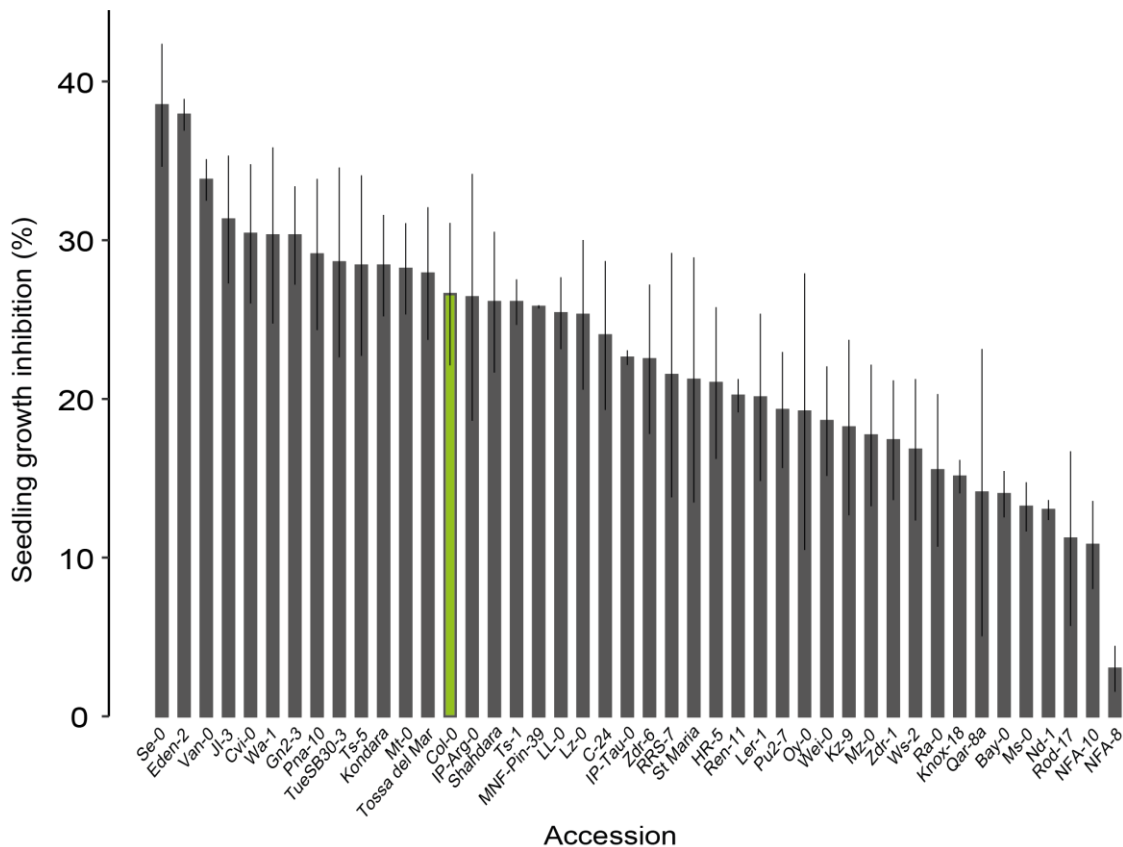


Figure 5.4: Natural variation for AEFÉ-induced seedling growth inhibition (SGI) within *A. thaliana* ecotypes. *A. thaliana* seeds were germinated on solid ½MS and transferred to AEFÉ- or PBS-containing liquid ¼MS for 8-days. The weight of AEFÉ-treated seedlings relative to PBS-treated seedling was used to determine the seedling growth percentage. Bars represent mean % (\pm SE) of at least two independent experiments, consisting of a minimum of three seedlings per treatment. Col-0 is coloured green.

5.3 Discussion

5.3.1 Receptor-like proteins are unlikely to contribute to AEFÉ perception

LRR-RLPs are cell-surface-localised receptors lacking an intracellular kinase domain, and thus require a kinase adapter protein to transduce extracellular stimuli into cellular responses (Gust and Felix, 2014). Given the putative role of the LRR-RLK, SOBIR1 in AEFÉ-induced defence signalling (Fig. 4.4), I tested a library of *Atrlp* mutants for AEFÉ-sensitivity. However, AEFÉ-induced MAPK activation was not observably perturbed in any *Atrlp* mutant assessed suggesting that *A. thaliana* LRR-RLPs are not required for AEFÉ perception (Fig 5.1). Several LRR-RLP-SOBIR1 heterodimers have been implicated in defence to various stimuli including *A. thaliana* LRR-RLPs, *AtRLP1*-, *AtRLP23*-, *AtRLP30*-, *AtRLP42*-SOBIR1 and tomato LRR-RLPs *Ve1*-, *Cf-2*-, *Cf-4*- and *Cf-9*-SOBIR1 (Liebrand et al. 2013, Zhang et al., 2013, Zhang et al., 2014, Jehle et al., 2014, Albert et al., 2015, Bi et al., 2016, Huang et al., 2020). Whilst these complexes might be thought of as prototypical bimolecular receptors, which are mechanistic equivalents to LRR-RLKs (Gust and Felix 2014), much remains to be clarified about LRR-RLP receptor-mediated signalling and the functions of many *A. thaliana* LRR-RLPs. Currently, no putative PRR outside of the LRR-RLPs is known to interact with SOBIR1 in *A. thaliana*, and SOBIR1 does not act in solitude to recognise patterns within the canonical understanding of its role in MTI.

One possible explanation for the lack of perturbed MAPK activation in *Atrlp* mutants may be due to functional redundancy of the LRR-RLP gene family in *A.*

thaliana. Redundancy within the LRR-RLP/RLK gene families may obscure phenotypes within genetic screens, and has been previously reported (Wang et al., 2008; Wang et al., 2010). Many *AtRLPs* appear to have originated from gene duplication events and the lack of functional assignment to many *AtRLPs* may be explained by redundancy among *AtRLP* genes (Fritz-Laylin et al., 2005, Wang et al., 2008, Jamieson et al., 2018). Such redundancy within the LRR-RLPs has been previously demonstrated. *AtRLP10/CLAVATA2 (CLV2)* is involved in both developmental as well as immune functions (Reddy and Meyerowitz, 2005, Pan et al., 2016). Expression of *AtRLP2* or *AtRLP12* under the *AtRLP10/CLV2* promoter was found to functionally complement the *clv2-3* mutant, although this was likely attributable to expression patterns (Wang et al., 2010). Additionally, overexpression of *AtRLP11* and *AtRLP3* rescued the *clv2-1* mutant with respect to carpel number, and *AtRLP10/CLV2* exhibited overlapping expression patterns with *AtRLP2*, *AtRLP3*, *AtRLP11* and *AtRLP12*, suggesting these LRR-RLPs may have overlapping function with *AtRLP10/CLV2* (Wu et al., 2016). Given these observations, it is a possibility that multiple *AtRLP* are involved in perceiving aphid-derived elicitors within AEF; a scenario that is likely to hinder forward genetic screens as it does reverse screens.

Another possible explanation of wild-type responses in *Atrlp* mutants to AEF, may be due to the complexity of AEF itself. The fraction may contain multiple elicitors, other than flagellin, EF-Tu and chitin that are unlikely to be present based on absence of phenotypes in *fls2*, *efr* and *cerk1* mutants. Furthermore, downstream of the receptor complexes, MAPK cascades are modules at which RLK and RLP signalling pathways converge (He et al., 2018). In the scenario that multiple elicitors induce several pathways, these responses would not be discriminated at the point of MAPK activation. For example, both flg22 and nlp20, induce MAPK activation within minutes of receptor activation via FLS2 and RLP23, respectively (Wan et al., 2019).

5.3.2 Forward genetic screens offer promise to uncover novel aphid elicitor receptors

To uncover components of AEFÉ-induced immune signalling, I took advantage of AEFÉ-induced *WRKY33* promoter activity and conducted a screen of EMS-mutagenised *pWRKY33::fLUC* seedlings. Several individuals within mutagenised M₂ and M₃ populations displayed reduced *WRKY33* promoter activity relative to the wild-type progenitor line (Fig. 5.3). Unfortunately, the phenotype was lost in the F₂ population after back-crossing to the progenitor and no clear segregation of phenotypes could be distinguished. Despite this, the identification of two individuals with compromised responses to aphid-derived elicitors validated the screening method. A population of 50,000 EMS-mutagenised *A. thaliana* plants contain transitions in almost every G-C pair of the genome (Till et al., 2003). At this mutagenesis rate, a sample of around 1000 mutagenised plants, whilst not exhaustive, should be sufficient to validate a screening method (Gillmor and Lukowitz, 2020). In this screen, two mutants with approximately 60% wild-type luminescence were identified and may be used in future studies to uncover genes underlying aphid-derived elicitor-induced immunity.

Within the MutMap pipeline, a phenotype caused by a single recessive mutation should result in an F₂ population segregating 3:1 wild-type:mutant (Fekih et al, 2013). Homozygous mutants are likely selected for during the M₂ screen and fixed in the M₃ population (Abe et al., 2012). If heterozygotes were selected in the M₂ screen, the M₃ population would be segregating. If an error was made during M₂ screening, the M₃ population would contain only wild-type individuals and this would be reflected in their phenotype. However, there was no evidence for segregating or wild-type phenotypes within the M₃ screen. The F₁ individuals are heterozygous and if tested, should display wild-type phenotypes. However, too few seeds were recovered from crosses to test this generation. This step would represent an important sanity check, and a future cross would ensure this expected phenotype is observed in the F₁.

The forward screen is subject to similar ambiguous phenotype determination as the reverse screen conducted previously. The use of AEFÉ, a heterogeneous fraction, may contain multiple elicitors and further increased the risk of inducing several

immune pathways within mutant lines, although there is no evidence that this occurred.

5.3.3 Natural variation for AEFÉ-induced SGI in *A. thaliana*

The identification of natural variation for pattern-sensitivity in *A. thaliana* accessions has enabled the identification of several LRR-RLK/RLPs mediating pattern sensitivity (Gómez-Gómez and Boller, 2000, Vetter et al., 2012, Jehle et al., 2013, Zhang et al., 2013, Zhang et al., 2014, Fan et al., 2022). Here, I analysed 44 *A. thaliana* accessions to uncover quantitative differences in AEFÉ-induced SGI and validate the approach for follow-up studies. Accessions such as NFA-8, NFA-10 and Rod-17 with weaker SGI phenotypes may be less sensitive to AEFÉ, suggesting that immune components are either absent or compromised in those lines. In contrast, accessions exhibiting strong SGI phenotypes, such as Se-0 and Eden-2 are likely hypersensitive to AEFÉ.

During plant immunity, metabolic resources are diverted toward defence over growth, leading to growth inhibition (Huot et al., 2014). Both flg22 and elf18 treatments lead to SGI in *A. thaliana* which is associated with FLS2- and EFR-mediated signalling, respectively (Gómez-Gómez et al., 1999; Gómez-Gómez and Boller, 2000; Zipfel et al., 2006). Binding of radiolabelled flg22 (Bauer et al., 2001), is positively associated with SGI in *A. thaliana* and, in accordance, reduced flg22 binding is associated with increased bacterial proliferation (Vetter et al., 2012). Additionally, flg22-induced SGI is correlated with elf18-induced SGI within *A. thaliana* accessions, suggesting common pathway components likely contribute to SGI to these elicitors (Vetter et al., 2012). Further experimentation would use another MAMP such as flg22 or nlp20 to induce LRR-RLK/RLP-mediated immune signalling to test whether insensitivity to aphid elicitors was due to a general defect in defence activation. It was recently reported that IF1 sensitivity was not linked to AtRLP32 protein sequence polymorphisms between *A. thaliana* accessions (Fan et al., 2022). AtRLP32 recognises the bacterial pattern, IF1 to mediate defence responses in Brassicaceae, including

ethylene production (Fan et al., 2022). IF1-hypersensitive *A. thaliana* accessions, however, when treated with flg22 or nlp20 patterns also showed increased levels of ethylene production and transient expression of *AtRLP32* alleles in *N. benthamiana* resulted in similar levels of ethylene production (Fan et al., 2022).

Sequence polymorphisms within relatively small panels of *A. thaliana* accessions have been exploited to uncover characteristics underlying plant immunity (Vetter et al., 2012; Zhang et al., 2013). For example, Zhang et al. (2013) identified 5 of 70 (7.1%) accessions to be insensitive to SCFE1 and subsequently identified the *AtRLP30* gene as the underlying genetic loci responsible for SCFE1 perception (Zhang et al., 2013).

To identify causal genes or polymorphisms conferring pattern perception or mediated downstream responses, crosses between accessions are typically performed to produce nonuniform F₂ progeny (Weigel, 2012). Enabled by WGS data, phenotypes are then associated with segregating genetic markers that distinguish the contributions from the parental genomes. An alternative approach that may be exploited with improving genomic resources and a more comprehensive SGI screen, is a genome-wide association study (GWAS). A GWA approach would obviate the need for crossing and extensive phenotyping burden but would rely on reliable and sufficient phenotypic diversity within the panel (Myles et al., 2009).

Chapter 6
Discussion

6.1 LRR-RLKs mediate aphid-derived elicitor induced signalling in *A. thaliana*

Plants perceive aphid-derived elicitors resulting in rapid, transient immune signalling. Cellular responses to aphid-derived elicitors include $[Ca^{2+}]_{cyt}$ elevations, activation of MPK3/6/4/11 and defence gene expression and results in SGI (Fig. 4.1). Aphid elicitor-induced immune responses are attenuated in the *bak1-5* and *sobir1-12* and *sobir1-13* mutants suggesting the co-receptor BAK1 and the adaptor kinase SOBIR1 are required for aphid elicitor-mediated signalling in *A. thaliana* (Fig. 4.4, Fig. 4.5). Furthermore, *bak1-5 bkk1-1* double mutants displayed compromised AEFEE-induced MAPK activation relative to wild-type, and *bak1-5* plants, suggesting that both SERK family kinases are required for full signalling to aphid-derived elicitors (Fig. 4.4). This is in agreement with previous reports that show BAK1 and BKK1 act cooperatively during MTI (Roux et al., 2011), and BR signalling (He et al., 2007). BAK1 has also been implicated in defence to aphids where it may mediate signalling after perception of the aphid-secreted *B. aphidicola* protein, GroEL (Chaudhary et al., 2014). Furthermore, BAK1 is required for aphid feeding induced $[Ca^{2+}]_{cyt}$ elevations (Vincent et al., 2018), and to regulate immune responses to crude aphid extracts (Prince et al., 2014). Whether SOBIR1 is required for GroEL-induced immune responses is unknown and the identity of the PRR perceiving GroEL also remains unknown (Chaudhary et al., 2014).

Prior to this study, SOBIR1 had not been implicated in plant defence responses to piercing-sucking insects. Here, SOBIR1 was found to be required for aphid elicitor-induced $[Ca^{2+}]_{cyt}$ elevations, MAPK activation, defence gene expression and SGI (Fig. 4.5). Importantly, *sobir1* mutants did not display altered flg22-induced immune responses, suggesting that attenuation of aphid elicitor-induced immunity was not due to a general effect (Fig. 4.5). LRR-RLKs, BAK1 and SOBIR1 are known to interact with LRR-RLPs to mediate immune responses to a variety of immunogenic patterns (Liebrand et al., 2013, Zhang et al., 2013, Jehle et al., 2014, Liebrand et al., 2014, Zhang et al., 2014, Albert et al., 2015, Fan et al., 2021). However, notwithstanding the 4 lines (RLP19, RLP36, RLP47, RLP49) that were not confirmed as mutants, a screen of *Atrlp*s failed to identify an *Atrlp* compromised for aphid-derived elicitor-induced MAPK activation (Fig. 5.1, Fig. 5.2), so the putative role of LRR-RLPs in the perception of aphid

elicitors requires further examination. Given the high degree of multifunctionality across several physiological responses and cases of observed redundancy between LRR-RLPs (Wang et al., 2010), it is possible that there is functional redundancy within AtRLPs to perceive and transduce external stimuli into cellular responses (Jamieson et al., 2018). Redundancy between AtRLPs may also explain the lack of functional characterisation of AtLRR-RLP family genes, many of which have no assigned function despite genome-wide studies and availability of mutant lines (Wang et al., 2008, Wang et al., 2010). Many AtRLPs have arisen by tandem duplication and occur in genetic clusters across the genome (Fritz-Laylin et al., 2005, Jamieson et al., 2018). It has been proposed that RLPs involved in development show higher levels of conservation than those with immune function (Jamieson et al., 2018). A future investigation into the role of AtRLPs in perception of aphid-derived elicitors may generate higher order mutants, combining mutants of close homologs or mutants of AtRLPs with known function in immunity. An alternative approach might seek to identify suppressors of the *sobir1-12/sobir1-13* mutant phenotype. Indeed, *SOBIR1* was identified in a screen for suppressors of the *bir1-1* mutant phenotype (Gao et al., 2009).

Issues surrounding redundancy are not limited to MAMP receptors and downstream signalling components but also arise with the use of a crude extract. Without purifying elicitors to homogeneity or synthesising an immunoactive ligand, the activation of multiple immune pathways by multiple elicitor contaminants may occur. Similar concerns have been raised in the context of LPS purification from Gram-negative bacterial cells (Zipfel et al., 2005). Isolation of active patterns from aphid extracts might also cause unspecific stress to plants with increasing concentrations of amphiphilic constituents.

In *A. thaliana*, RLK- and RLP-mediated signalling converge on similar defence modules but are under pathway-specific regulation. Several RLCK-VII clade members are required for RLP-mediated signalling, including BIK1 as a negative regulator (Wan et al., 2019), and PBL31 as a positive regulator (Pruitt et al., 2021). Interestingly, negative regulation of RLP signalling by BIK1 is in contrast to its role as a positive regulator of RLK-mediated signalling (Wan et al., 2019). Similarly, SOBIR1 interacts with PBL31 and members of the EDS1-PAD4-ADR1 node to form a constitutive, intracellular

complex that positively regulates RLP-, but not RLK-mediated signalling (Pruitt et al., 2021). Intriguingly, PAD4, but not EDS1 or SAG101 mediates aphid resistance independently of SA signalling and camalexin production (Pegadaraju et al., 2005, 2007, Dongus et al., 2020). Furthermore, the PAD4 lipase-domain (PAD4^{L^{LD}}) alone is sufficient to confer resistance to *M. persicae* but not to microbial pathogens such as *P. syringae* pv. *tomato* (Dongus et al., 2020). Loss of BIK1 adversely impacts aphid performance suggesting BIK1 negatively regulates plant defence to aphids and BIK1-conferred aphid susceptibility occurs through its suppression of *PAD4* expression (Lei et al., 2014).

Defence signalling to aphids appears to align within RLP-mediated responses involving BIK1 as a negative regulator and BAK1 and PAD4 as positive regulators. The role of SOBIR1 within this pathway remains to be determined but evidence presented in this study indicates it too positively influences immune signalling to aphid-derived elicitors (Fig. 4.5). Given that none of the *At*RLPs tested in this study showed altered immune responses to aphid-derived elicitors, it may suggest that more than one receptor can mediate MTI to aphid elicitors. To ascertain whether aphid elicitor-induced and aphid feeding-induced MTI responses are related, and if canonical RLP signalling is induced, the role of BIK1 may be further explored. BIK1 phosphorylation and dissociation from receptor complexes is ligand-dependent (Lu et al., 2010, Lin et al., 2014), but whether these responses are detected during aphid-induced defence signalling remains to be determined.

In RLP-mediated signalling, BAK1 and SOBIR1, along with an LRR-RLP form tripartite complexes to mediate MTI (Zhang et al., 2013, Jehle et al., 2014, Zhang et al., 2014, Albert et al., 2015; Fan et al., 2021). In this study, no evidence of ETI-like responses were observed such as HR, characterised by cell death. However, both BAK1 and SOBIR1 have been implicated in HR, a response associated with ETI rather than PTI/MTI. For example, BAK1 and SOBIR1 are required for Cf-4-mediated HR in tomato and *Leptosphaeria maculans* Resistance 3 (LepR3)-mediated ETI in *B. napus* (Liebrand et al., 2013, Postma et al., 2016). Furthermore, BAK1 and SOBIR1 are required for the activation of cell death to necrosis-inducing effectors from *S. sclerotiorum* (Seifbarghi et al., 2020), as well as cell death in the *bir1-1* mutant (Gao et al., 2009; Liu et al., 2016).

Moreover, Ve-1 and Cf-4 signalling in tomato results in ETI-like responses requiring BAK1 and EDS1 (Fradin et al., 2009).

6.2 *AtWRKY33* as a key regulator of immune responses to aphids

This study contributes to a growing body of evidence that points to WRKY33 as an important regulator of defence responses to aphids. Aphid-derived elicitors induced transient *WRKY33* promoter activity in plants stably expressing *pWRKY33::fLUC* (Kato et al., 2020) (Fig. 3.2). Aphid elicitor-induced increase in *WRKY33* transcripts was also confirmed in qRT-PCRs and increases in *WRKY33* expression was dependent on BAK1 and SOBIR1 (Fig. 4.1, Fig. 4.4, Fig. 4.5), implicating WRKY33 in MTI to aphids. In a previous study exploring spatio-temporal expression patterns to crude aphid extracts and aphid feeding, WRKY33 was found to be rapidly expressed at the aphid feeding site (Gioli, M. 2019). Additionally, *wrky33* mutants were more susceptible to *M. persicae* suggesting WRKY33 positively regulates defence to aphids (Kettles, G. 2013). The coregulation of WRKY33 by MPK3/6 and CPK5/6 suggests immune signalling pathways converge on WRKY33 to regulate defence responses (Mao et al., 2011; Yang et al., 2020). A feature of aphid elicitor-induced immune signalling presented in this study, was the activation of MAPKs, MPK3/6/4/11 which showed similar amplitude and temporal activation as flg22 (Fig. 4.1). Moreover, aphid elicitor induced MAPK activation required RLKs BAK1 and SOBIR1 (Fig. 4.4, Fig. 4.5).

WRKY33 can bind to and activate the PAD3 promoter, driving its expression and subsequent camalexin biosynthesis (Kusnierczyk et al., 2008). In non-stimulated cells, MKS1 forms complexes with MPK4 and WRKY33 (Andreasson et al., 2005, Qiu et al., 2008). During MTI, phosphorylation of MKS1 results in MKS1 release thereby releasing WRKY33 to bind target promoter sequences (Qiu et al., 2008). Several studies have reported camalexin biosynthesis genes, including *PAD3*, are expressed during aphid feeding (Pegadaraju et al., 2007, Bednarek et al., 2012, Kettles et al., 2013, Piasecka et al. 2015), and when plants are challenged with aphid-derived extracts (this study) (Prince et al., 2014). WRKY33 is required for camalexin biosynthesis during MTI (Qiu et

al., 2008), but it is not clear whether aphid induction of MTI and subsequent WRKY33 release is required for *PAD3* expression and camalexin production. Interestingly, *PAD3* expression is also regulated by *PAD4* (Zhou et al., 1999), which therefore, also regulates the synthesis of camalexin in *A. thaliana* (Tsuji et al., 1992), and is required for plant defence against *M. persicae* (Louis et al., 2012; Dongus et al., 2020). However, *PAD4*-mediated defence against the aphid does not involve camalexin or SA metabolism (Pegadaraju et al., 2005), suggesting the role of *PAD4* in mediating aphid resistance is contrary to its role as an essential component of EDS1-*PAD4*-ADR1-triggered SA responses and in protection against pathogens (Cui et al., 2019, Dongus et al., 2020). The MAMP-triggered activation of MPK3/6 is upstream of *PAD3*, but independent or downstream of *PAD4* (Ren et al., 2008). In light of the recent report of *PAD4* interacting with PRR complex members such as SOBIR1 and PBL31 (Pruitt et al., 2021), future studies may seek to investigate whether SOBIR1-*PAD4* interactions mediate *PAD4*-dependent aphid resistance.

It is likely that a suite of WRKY transcription factors regulate responses to aphids both positively and negatively. Notwithstanding the evidence presented in favour of WRKY33 regulating responses, WRKY22 (Kloth et al., 2016), *SbWRKY86* in sorghum (Poosapati et al., 2022) and several tomato WRKYs, *SlWRKY72* and *SlWRKY80* (Bhattarai et al., 2010; Atamian et al., 2012), mediate plant responses to aphids. The role of WRKYs in defence responses to aphids may be further explored through experiments that identify transcription factor binding sequences (Mundade et al., 2014), or through the use proximity labelling approaches (Mair et al., 2019), to uncover novel plant defence mechanisms to aphids.

6.3 SOBIR1-dependent $[Ca^{2+}]_{cyt}$ elevations are essential for aphid elicitor-derived immune responses

Previously, Vincent et al. (2017) linked aphid feeding to plant MTI responses by demonstrating that feeding-induced $[Ca^{2+}]_{cyt}$ elevations are BAK1-dependent. *bak1* mutants are defective in MAMP-triggered Ca^{2+} responses (Ranf et al., 2011), and BAK1 directly regulates calcium channels including CNGC20 in *A. thaliana* (Yu et al., 2019). In

this study, pharmacological inhibition of $[Ca^{2+}]_{cyt}$ elevations, using the Ca^{2+} channel blocker $LaCl_3$ or the Ca^{2+} chelator EGTA, resulted in attenuated elicitor-induced MAPK activation and *NHL10* expression (Fig. 4.2), indicating $[Ca^{2+}]_{cyt}$ elevations are a prerequisite for aphid elicitor-induced MTI responses. This is in general agreement with previous studies that have used pharmacological and genetic evidence to show Ca^{2+} signalling is required for MAMP-induced immune responses (Lebrun-Garcia et al., 1998, Romais et al., 1999, Lecourieux et al., 2002, Boudsocq et al., 2010, Ranf et al., 2011, Ranf et al., 2012, Marcec and Tanaka, 2021). Boudsocq et al. (2010) utilised the flg22-induced expression of *NHL10*, and $LaCl_3$ to show that *NHL10* expression is highly dependent on Ca^{2+} influx. $LaCl_3$ prevents influx of external calcium into the cytosol (Price et al., 1994), and EGTA restricts Ca^{2+} entry into the cytosol by reducing the pool of free apoplastic Ca^{2+} (Ward and Schroeder, 1994). The calcium channels required for aphid-mediated Ca^{2+} influx have been partially resolved as the *A. thaliana glr3.3/3.6* double mutant is defective in feeding-induced $[Ca^{2+}]_{cyt}$ elevations relative to wild-type plants (Vincent et al., 2017). However, the same mutant was unaffected in aphid elicitor-induced $[Ca^{2+}]_{cyt}$ elevations (data not shown), therefore, the mechanisms mediating Ca^{2+} influx to aphid elicitors appear to be different to those required for aphid feeding. One explanation for this discrepancy is the lack of wound-induced response evoked by application of elicitors. Wounding induces systemic Ca^{2+} signalling in distal leaves but this response is partially attenuated in the *glr3.3 glr3.6* mutant (Kiep et al., 2015, Toyota et al., 2018). The Ca^{2+} response appears to mimic wound-induced systemic membrane depolarization, which is also limited to nearby cells in the *glr3.3/3.6* mutant (Mousavi et al., 2013). Furthermore, systemic signalling may be obsolete when plants are homogeneously exposed to large quantities of elicitor as every exposed cell should respond to the elicitor directly rather than via intermediaries. This may, in part, contribute to the difficulty of identifying Ca^{2+} channels mediating MTI. Another possible explanation of the lack of *glr3.3/3.6* phenotype to aphid elicitors might be explained by *GLR3.3* expression patterns which appears to be in phloem and stomal guard cells as well as trichome base cells (Nguyen et al., 2018). Herbivore feeding, whether it is conducted by piercing-sucking insects, or chewing insects, is more likely to impact on phloem-specific responses than general elicitors would.

Surprisingly little is known about SOBIR1- or RLP-mediated Ca^{2+} signalling. Only that the Ca^{2+} -dependent kinase, *NbCPK2* is required for Cf-4- and Cf-9-triggered HR (Romeis et al., 2001). This is in contrast to BAK1 which contributes to Ca^{2+} influxes to several MAMPs (Ranf et al., 2011), and interacts with and phosphorylates the calcium-permeable channel, CNGC20 and likely CNGC19, promoting their destabilisation and preventing cell death (Yu et al., 2019). In this study, $[\text{Ca}^{2+}]_{\text{cyt}}$ elevations were attenuated in the *sobir1* mutants as well as in the *bak1-5* mutant (Fig. 4.4, Fig.4.5). Interestingly, the *sobir1-12 UBQ10:GCaMP3* mutant displays altered Ca^{2+} responses to aphid feeding that could not be explained by signal area, rate of signal propagation or peak intensity (Fig. 4.7). However, feeding-induced $[\text{Ca}^{2+}]_{\text{cyt}}$ appeared to return to basal levels more rapidly than those in Col-0 *UBQ10:GCaMP3* plants, suggesting $[\text{Ca}^{2+}]_{\text{cyt}}$ may be sequestered more efficiently in the *sobir1* mutant. It is thought that the removal of Ca^{2+} from the cytosol where excesses are cytotoxic, is regulated by Ca^{2+} -extruding systems such as Ca^{2+} -ATPases and $\text{Ca}^{2+}/\text{H}^+$ exchangers (Corry et al., 2001, Demidchik et al., 2018). Interestingly, mutants of some P2B-type ATPases, or autoinhibited calcium ATPases (ACAs) are impaired in defence responses and attenuated flg22-induced Ca^{2+} signals (Geisler et al., 2000, Bousiac et al., 2010, Frei dit Frey et al., 2012, Hilleary et al., 2020). For example, *aca4/11* mutants show elevated basal Ca^{2+} and an increased Ca^{2+} signal in response to flg22 (Hilleary et al., 2020).

Interestingly, *rbohD rbohF* double mutants were unaffected in AEFEE-induced $[\text{Ca}^{2+}]_{\text{cyt}}$ elevations (data not shown), in agreement with studies that place $[\text{Ca}^{2+}]_{\text{cyt}}$ elevations upstream of ROS during MTI (Ranf et al., 2011). RBOHD alone is sufficient to generate MAMP-triggered ROS (Zhang et al., 2007), but does not fully explain MAMP-triggered MAPK activation or SGI responses as these physiological markers occur in the *rbohD* mutant (Mersmann et al., 2010). Additionally, BIK1 and PBL1 play a positive role in the RBOHD-dependent ROS production, but similarly, are not required for MAPK activation (Zhang et al., 2010). These studies indicate that ROS production is not a prerequisite for MTI. I did not measure aphid-elicitor induced ROS bursts in this study because AEFEE interfered with flg22-induced ROS accumulation, likely by interfering with luminol reagents. However, future studies may pursue alternative methods for ROS measurements such as DAB staining (Daudi et al., 2012).

6.4 Aphid fitness is not altered on *sobir1* mutants

Despite the demonstrable role of SOBIR1 in mediating MTI to aphid-derived elicitors, aphid fitness was not altered on *sobir1-12* or *sobir1-13* mutants (Fig.4.6). As a polyphagous species, *M. persicae* is capable of colonising many plant species including *A. thaliana*. In situations where MTI is artificially attenuated, such as is in *sobir1* mutant plants, it may be predicted that *M. persicae* will become more fecund. However, aphids secrete virulence factors to modulate plant defence and promote fitness (Mutti et al., 2006, Mutti et al., 2008, Bos et al., 2010, Pitino et al., 2013, Wang et al., 2015, Kettles and Kaloshian, 2016, Mugford et al., 2016, Rodriguez et al., 2017, Chaudhary et al., 2019, Chen et al., 2020, MacWilliams et al., 2020). Virulence factors may therefore be the primary determinants of plant-aphid interaction outcomes in many cases. Indeed, *M. persicae* fecundity is unaltered on *bak1-5* plants (Prince et al., 2014), indicating that the aphid may overcome BAK1-mediated defence during compatible interactions. In contrast, *A. pisum* survival was improved on *bak1-5* mutant plants suggesting that BAK1 does contribute to non-host resistance to this aphid in *A. thaliana* (Prince et al., 2014). However, *R. padi* survival was not altered on *sobir1* mutants suggesting that SOBIR1 does not strongly contribute to non-host resistance in *A. thaliana* (Fig. 4.6B). This finding is surprising in light of the findings herein that link SOBIR1 with downstream defence components such as WRKY33 and camalexin biosynthesis genes. Camalexin has been shown to mediate plant defence to *M. persicae* (Kettles et al., 2013) and induced resistance conferred by crude aphid extract appeared to be dependent on genes involved in camalexin production such as the *cyp79b2/cyp79b3* double mutant and *pad3* mutant (Prince et al., 2014). Results here suggest SOBIR1 does not influence aphid-plant outcomes, which is in contrast with reports of increased susceptibility to *S. sclerotiorum* and the related fungus *B. cinerea* (Zhang et al., 2013). It is worthwhile noting however, that the *bak1-5* mutant plants were also more susceptible to these pathogens suggesting that BAK1 function in plant-fungi and plant-aphid interactions are not directly comparable (Zhang et al., 2013). The role of SOBIR1 in plant-aphid interactions requires further investigation. Whether SOBIR1 influences camalexin biosynthesis by regulating upstream components remains to be determined and may shed light on aphid fecundity outcomes. Interestingly, *nlp20* triggers

camalexin accumulation in contrast to flg22 signalling which, through its induction of miR393, blocks transcripts encoding camalexin biosynthetic enzymes (Robert-Seilaniantz et al., 2011, Wan et al., 2019).

Aphid-derived elicitors induce an array of immune responses including $[Ca^{2+}]$ elevations, MAPK activation and defence gene expression (Fig. 4.1). Surprisingly, pre-exposure of *A. thaliana* leaves to aphid elicitors had no effect ($p > 0.05$) on *M. persicae* fitness (Fig. 4.3), suggesting MTI induction did not confer protection against the insect. It is worthwhile noting that whilst significant differences were not observed, a consistent reduction in mean fecundity was scored in these experiments. The lack of a notable protection to *M. persicae* conferred by aphid-derived extracts is in contrast to GroEL induced aphid resistance or previous studies with crude extracts that also conferred a protective effect on *A. thaliana* to *M. persicae* (Chaudhary et al., 2014, Prince et al., 2014). A possible explanation for this contrasting result might be that the timing and longevity of MTI was not sufficient to offer a protective effect. Here, a 48-h window between treatment and aphid application was adopted. However, a systematic approach, testing shorter and later incubation periods may have revealed optimal MTI-mediated protection.

6.5 Aphid-derived, proline-rich peptides may induce MTI responses in *A. thaliana*

An activity-led purification strategy was employed to isolate CEPs within aphid-derived, whole-body extracts (Fig. 3.1). Components inducing *WRKY33* promoter activity were purified via 3D-chromatography (XIC-UHPLC^{highpH}-UHPLC^{lowpH}), identified in nanoLC-MS/MS, and synthesised. (Table 3.3, Table 3.4). A total of 68 unique CEPs were identified and ranged between 6-11 amino acids in length (Table 3.2, 3.3). However, CEPs did not induce *WRKY33* promoter activity within *pWRKY33::fLUC* expressing plants, suggesting that CEPs are not immunoactive (Fig. 3.9).

Identified CEPs were small, proline-rich peptides with 44/68 peptides containing at least two proline residues. Proline-rich peptides likely became enriched

in aphid-derived fractions due to the use of proteinase k which may be blocked from accessing small peptides with tight turns conferred by proline conformation. Proline is abundant in many biologically active peptides and is known to protect proteins/peptides against proteolysis (Vanhoof et al., 1995, Walker et al., 2003). In conventional studies, proteinase k, and other non-specific proteases, are used to determine whether a bioactive elicitor is proteinaceous as they cleave peptides into small, inactive fragments (Kunze et al., 2004). Here, proteinase k treatments undermined convention as bioactivity was not lost upon its addition (Fig. 3.3).

At this stage, there is no evidence directly linking aphid-derived proline-rich peptides with MTI responses. Future experimentation may focus on the possibility of modifications to peptides, particularly the hydroxylation of proline given the abundance of proline residues within CEPs (Table 3.2, 3.3). One interesting source of hydroxyproline-rich peptides that might hold promise as candidate elicitors are insect cell wall-associated collagens. Collagen fragments are known to induce insect innate immunity where they may act as DAMPs during infection (Altincicek et al., 2006, Berisha et al., 2013). Intriguingly, another DAMP, plant systemin peptides contain a conserved proline or hydroxyproline-rich central domain (Ryan and Pearce, 2003), which may also preserve systemins in protease-containing environments. However, currently it is not known whether insect collagens are detected by plants and bottom-up strategies for future identification of elicitors remains the best approach to identify aphid-derived elicitors.

Elicitor activity within aphid extracts is likely conferred by a proteinaceous motif. Bioactivity of fractions was lost upon treatment of fractions with pronase, a non-specific mixture of proteases, strongly suggesting a proteinaceous element is required for immunogenicity conferred by aphid-derived fractions (Fig. 3.3). As expected, pronase abolished flg22-induced immune responses but not chitin-induced responses. The activity of an unknown cysteine protease is required for aphid elicitor-induced MTI (Fig. 3.4). Metalloproteases within pronase are the most likely candidate proteases that can abolish bioactivity of aphid-derived extracts (Fig. 3.3).

The cysteine protease E-64 abolished aphid-extract induced immune responses but only when it was added early in the purification procedure. This result strongly

suggests an aphid-derived cysteine protease liberates an immunogenic peptide. Furthermore, CA-074-Me, which is a selective inhibitor of CathB/L (Ge et al., 2016), also had an inhibitory effect on the bioactivity of aphid-derived extracts (Fig. 3.4), suggesting that a cathepsin family cysteine protease may be required for elicitor processing. Proteins belonging to the CathB protease family have been identified in the aphid saliva and in plant cells probed by aphids, suggesting CathB may function as an effector to promote insect colonisation (Cui et al., 2012, Thorpe et al., 2016, Guo et al., 2020). Interestingly, modulation of aphid CathB gene expression levels between *A. thaliana* and *N. benthamiana* contributes to the ability of *M. persicae* to colonise these plant species (Mathers et al., 2017, Chen et al., 2020). Guo et al. (2020) found that CathB3 interacts with the MAPKKK, EDR1-like protein to promote EDR1-like-dependent ROS production. Silencing *CathB3* resulted in increased performance of non-adapted *M. persicae* on *N. tabacum* that may indicate a reduction of ETI (or ETI-like) triggered responses in the plant (Guo et al., 2020). Another possibility is that CathB acts as an elicitor, and may be recognised by cell-surface localised receptors. Indeed, CathB peptides were identified in *R. padi* saliva (Thorpe et al., 2016). CathB represents a good candidate for the cysteine protease responsible for liberating an immunogenic peptide within aphid-derived fractions.

6.6 Validating screening methods for future aphid-derived elicitor investigations

The identification of natural variation for pattern-sensitivity in *A. thaliana* accessions has enabled the identification of several LRR-RLK/RLPs mediating pattern sensitivity (Gómez-Gómez and Boller, 2000, Vetter et al., 2012, Jehle et al., 2013, Zhang et al., 2013, Zhang et al., 2014, Fan et al., 2022). Here, I analysed 44 *A. thaliana* accessions to uncover quantitative differences in AEF-induced SGI. Accessions displayed a range of SGI phenotypes from ~4% (NFA-8) to ~37% (Se-0 and Eden-2). Several accessions displayed a degree of insensitivity to aphid-derived fractions suggesting they are compromised in MTI responses. Interestingly, two of these lines, NFA-8 and NFA-10 were originally sourced from a similar location (Bershire, UK) and

may be more genetically similar to one another than to other accessions. In contrast, accessions exhibiting strong SGI phenotypes, such as Se-0 and Eden-2 are likely hypersensitive to aphid-derived elicitors and are predicted to induce strong (greater amplitude or longevity) MTI. Responses to AEFE appeared to be quantitative rather than qualitative as accessions displayed a wide-ranging and continuous degree of SGI. With improving genomic resources and a more comprehensive SGI screen, including additional *A. thaliana* accessions, a GWA study may reveal the genetic loci underlying such quantitative traits (Myles et al., 2009).

I took advantage of AEFE-induced *WRKY33* promoter activity and conducted a screen of EMS-mutagenised *pWRKY33::fLUC* seedlings (Kato et al., 2020). The phenotype of mutant candidates was relatively minor, and no loss-of-function mutant was identified. However, several individuals displayed hyposensitive responses inducing around 60% of wild-type bioluminescence to AEFE (Fig. 5.3). These lines may be re-backcrossed in the expectation that the phenotype can be recovered in the F2 generation. Future experiments may also examine upstream (to *WRKY33* promoter activity) responses to help deduce the source of impaired immune responses in these lines.

6.7 Conclusion

Herein, I have presented evidence that aphid-derived extracts trigger an array of immune responses in *A. thaliana* that appear to be analogous to, but distinct from PTI/MTI responses to microbial pathogens. These results add to a growing body of evidence that piercing-sucking herbivores are perceived by plasma-membrane-associated PRRs and likely trigger a specific response in the plant (de Vos and Jander, 2009, Chaudhary et al., 2014, Prince et al., 2014). Amongst the findings presented herein, the putative role of the LRR-RLK SOBIR1 in regulating MTI to aphids may be of particular importance as SOBIR1 has previously been implicated as a co-receptor during MTI (Liebrand et al., 2013, Zhang et al., 2013, Jehle et al., 2014, Liebrand et al., 2014, Zhang et al., 2014, Albert et al., 2015, Fan et al., 2021). A screen of *AtRLP* mutants did

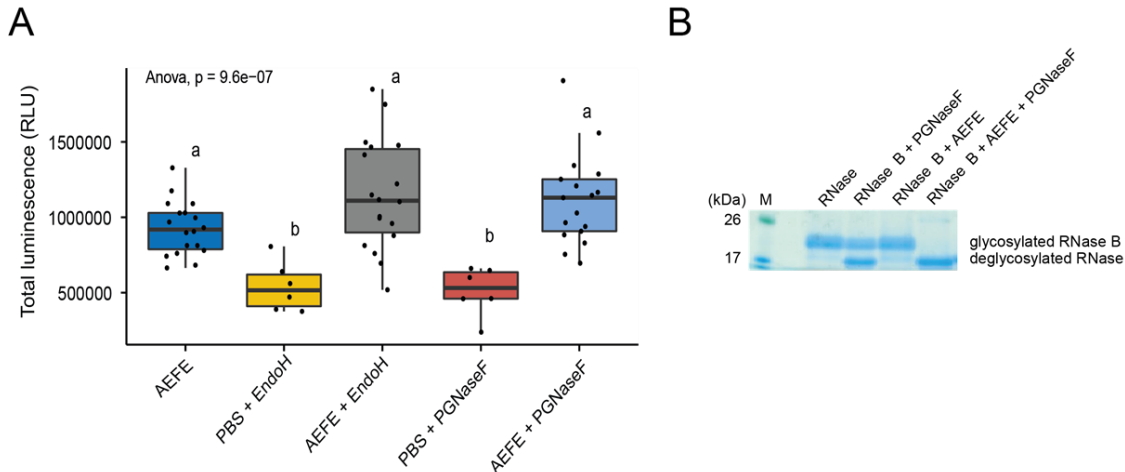
not reveal an *Atrlp* mutant with a clear phenotype, hence the PRR to aphid elicitors remains elusive. This finding presents the possibility that SOBIR1 acts to regulate a novel mechanism during immune responses to aphids.

The aphid-derived elicitors, partially purified in this study, are likely to be proteinaceous as they show sensitivity to proteolysis and require the activity of a cysteine protease to confer immunogenicity. I have demonstrated that elicitors could be separated from the lysate through rounds of protein precipitation and solid-phase extraction techniques. Unfortunately, I was unable to identify the aphid-derived elicitor as no peptide identified and synthesised in this study displayed immuno-activity. Future experimentation may focus on methods to reduce false positive and false negative identification of aphid components during purification, mass spectroscopy and subsequent database searches. Approaches may include the allowance of variable modifications and additional peptide charge states.

Forward and reverse genetics may aid in the identification of causal genes conferring pattern perception in plants to herbivorous insects. Here, I validated both approaches by identifying variation in aphid elicitor-triggered responses in an EMS-mutagenised population of *pWRKY33:flUC A. thaliana* plants and between *A. thaliana* accessions. Materials isolated in these screens may provide a start point for future characterisation of causal genes or may be expanded to utilise genome-wide association methods.

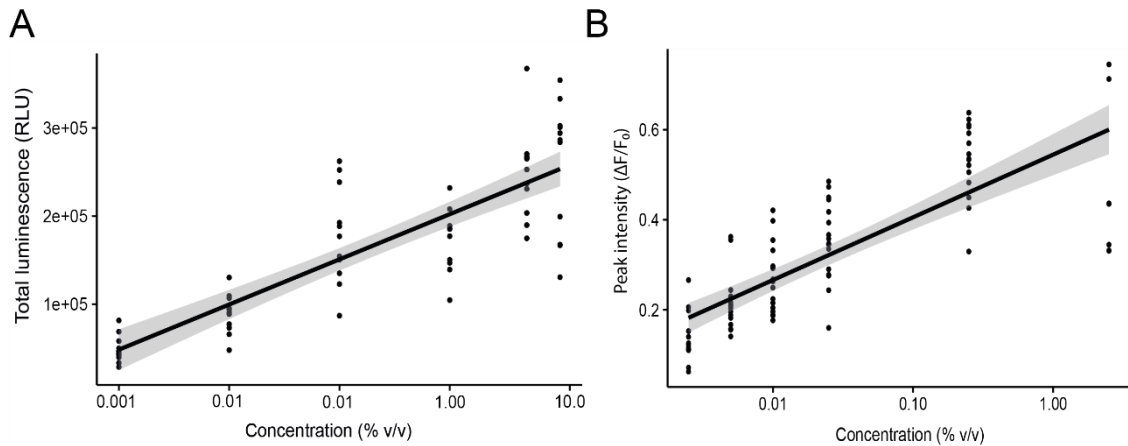
Appendices

Appendix I.I



Appendix I.I: Elicitor activity of aphid-derived extract (AEFE) is insensitive to deglycosylases Endo H or PGNase F. **A** Total Luminescence of 10-day-old *pWRKY33::fLUC A. thaliana* seedlings treated as displayed. Means were generated as the summed luminescence between 0- and 600-min post-treatment. Luminescence was recorded every 30 s. AEFE, PBS or RNase B were treated with GlycoBuffer 2 and PGNase F or GlycoBuffer 3 and Endo H. Letters indicate significant differences ($p < 0.05$) between treatments ($df = 4,60$, $F = 10.97$, $p = 9.63 \cdot 10^{-7}$). **B** RNase B is deglycosylated in AEFE by PGNaseF. Deglycosylation efficiency of RNase B was assessed via SDS-PAGE mobility shifts on 12% SDS-PAGE gel electrophoresis after treatment with PGNase F. Gels were stained using READYBLUE™ stain.

Appendix I.II



Appendix I.II: Aphid Extract Filtrate Elicitor (AEFE)-induced defence activation is dose-dependent. **A** Total Luminescence of 10-day-old *pWRKY33::fLUC* *A. thaliana* seedlings treated as displayed. Means were generated as the summed luminescence between 0- and 600-min post-treatment and plotted as dots. Luminescence was recorded every 30s. **B** Cytosolic calcium $[Ca^{2+}]_{cyt}$ elevations in *A. thaliana* seedlings expressing *GCaMP3* driven by the *Cauliflower Mosaic Virus (35S)* promoter (*35S::GCaMP3*; Tian et al., 2009, Vincent et al., 2017). GFP fluorescence was monitored every 60 s and normalised according to the equation $\Delta F/F_0 = (F - F_0)/F_0$, where F is the fluorescence emission (at 525/50 nm) and F_0 is the mean baseline (pre-treatment) fluorescence calculated from the mean of F over the first 15 frames (15 min). Dots represent the peak (maximum) intensity ($\Delta F/F_0$).

Appendix I.III

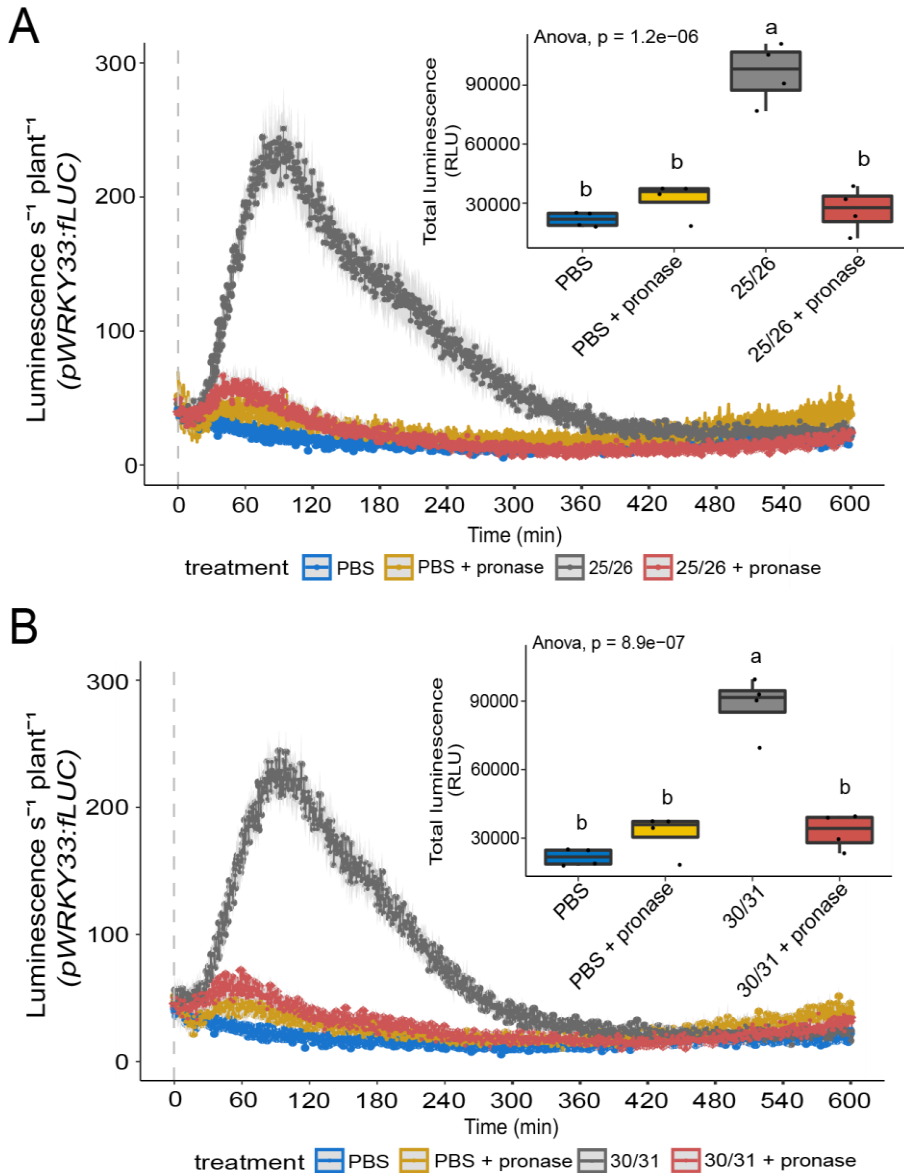


Figure 3.8: Ultra-high performance liquid chromatography (UHPLC)-separated, bioactive, aphid-derived extracts are pronase-sensitive. Extracts were separated on Agilent 1290 Infinity II LC System using an X-bridge® Peptide BEH C₁₈ column stationary phase (Waters Limited, Wilmslow, UK). **A.** *thaliana* *pWRKY33::fLUC* seedlings were exposed to **A** fractions 25 and 26 (25/26) or **B** fractions 30 and 31 (30/31) eluted off the column using a linear gradient mobile phase (97% v/v ACN, 2.9% dH₂O and 0.1% v/v TFA). Luminescence was monitored from 0 – 600 min post treatment. [Inset] Total Luminescence of 10-day-old *pWRKY33::fLUC* *A. thaliana* seedlings treated as displayed. Means \pm SE were generated as the summed luminescence between 0- and 600-min post-treatment. Luminescence was recorded every 30s. Letters indicate significant differences ($p < 0.05$) between treatments.

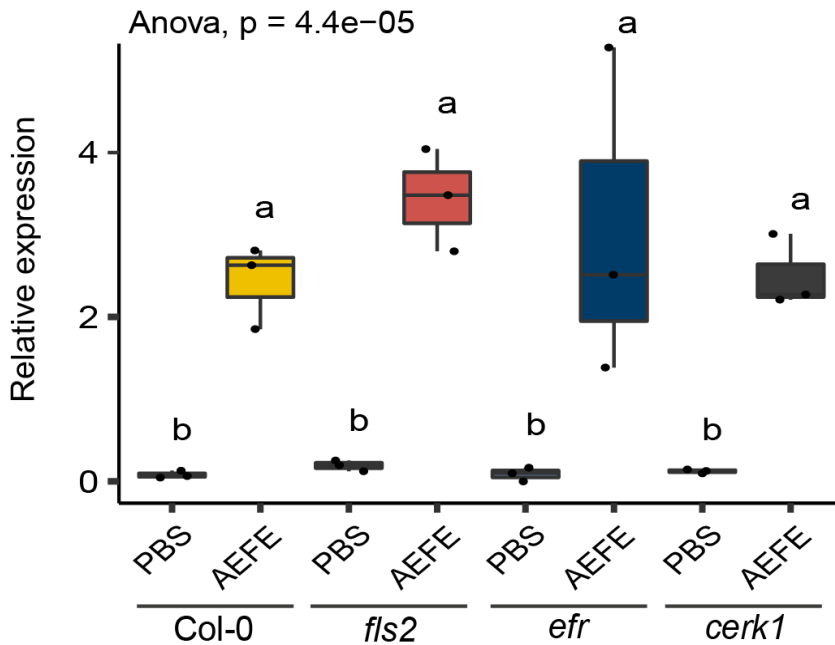
Appendix I.IV

Appendix I.IV: Total number of unique peptides within UHPLC-separated, aphid-derived extract fractions.

Mascot Ion Score	Fraction 25				Fraction 26			
	Total distinct count of rep				Total distinct count of rep			
	>1	>2	>3	4	>1	>2	>3	4
0	1925	296	86	29	1473	317	103	29
45	76	59	34	16	93	60	40	14
	Fraction 30				Fraction 31			
	>1	>2	>3	4	>1	>2	>3	4
0	1306	280	90	27	1124	203	71	26
45	65	51	32	15	59	49	28	11

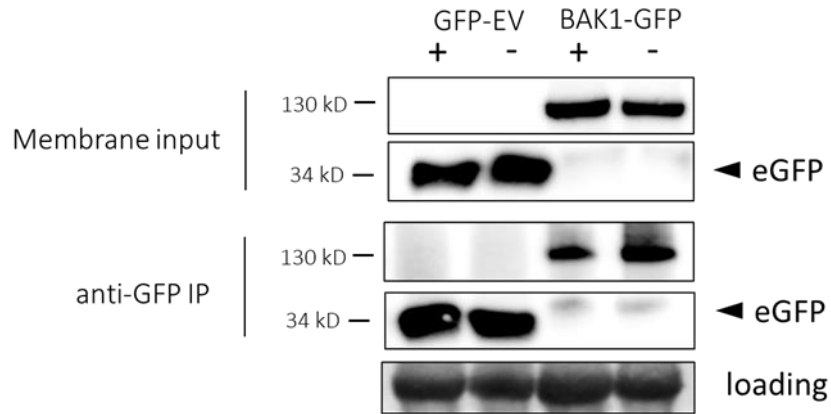
Appendix II.I

WRKY33



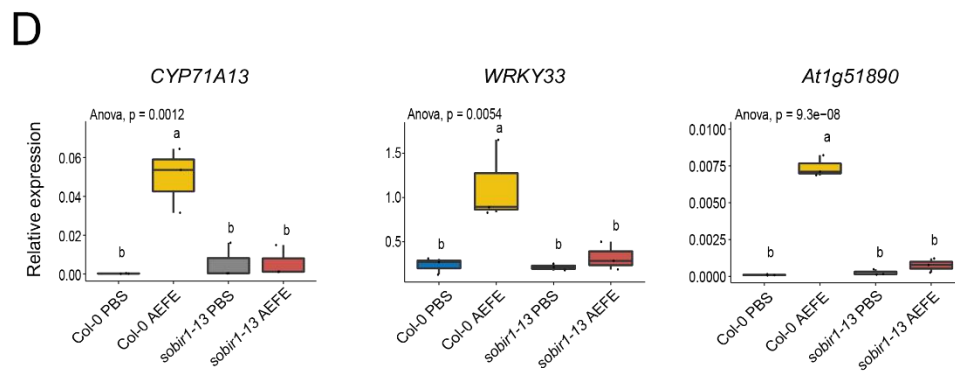
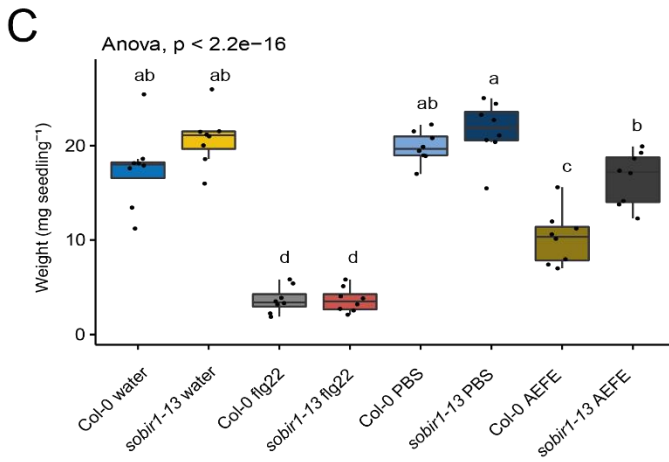
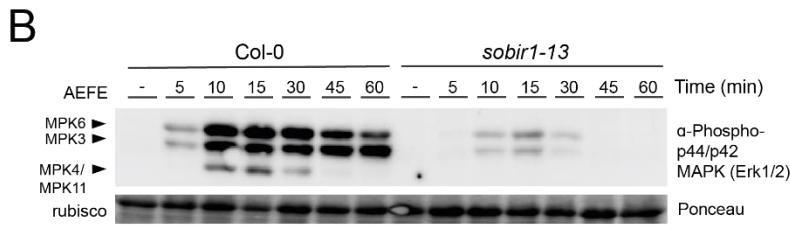
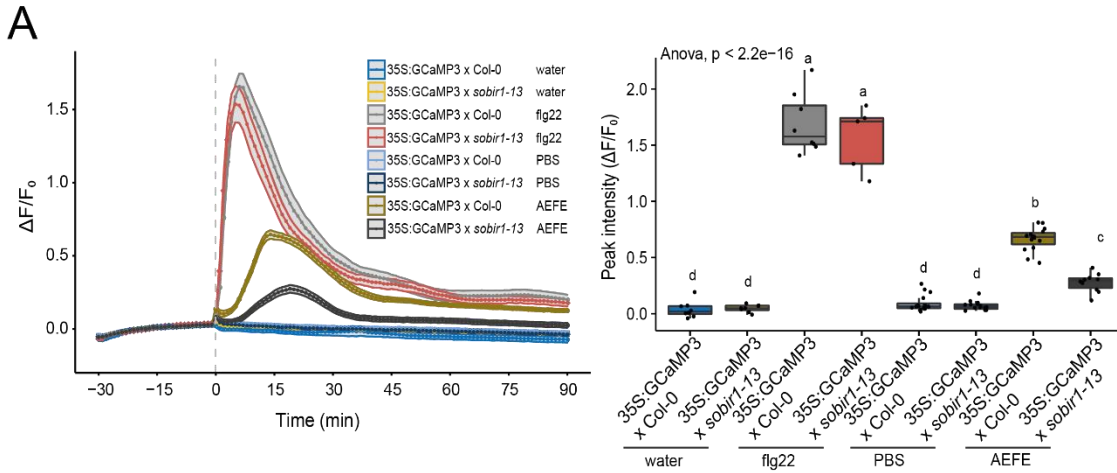
Appendix II.I: *M. persicae*-derived extract, aphid extract filtrate elicitor (AEFE) induces MTI via an unknown pattern recognition pathway, independent of PRRs EFR, FLS2 and CERK1 in *A. thaliana*. Transcriptional profiling of MTI marker gene *WRKY33* by quantitative reverse transcription-PCR (qRT-PCR). Three seedlings of 10-day-old *Arabidopsis* Col-0, *efr1-2*, *fls2-1* and *cerk1-2*, plants were elicited with 2.5% v/v PBS (mock) or 2.5% v/v (~22.5 $\mu\text{g}/\mu\text{l}$) AEFEl and flash frozen at 1.5-h post-elicitation. Relative expression of *AtWRKY33* is shown normalized to the *GAPDH* transcript. Data are from a single experiment containing three biological replicates. Differences in mean expression was analysed via ANOVA with Tukey post-hoc test. Letters indicate significant differences ($p < 0.05$) (df = 7, F-value = 11.04, p-value = 4.41^{-5}).

Appendix II.II



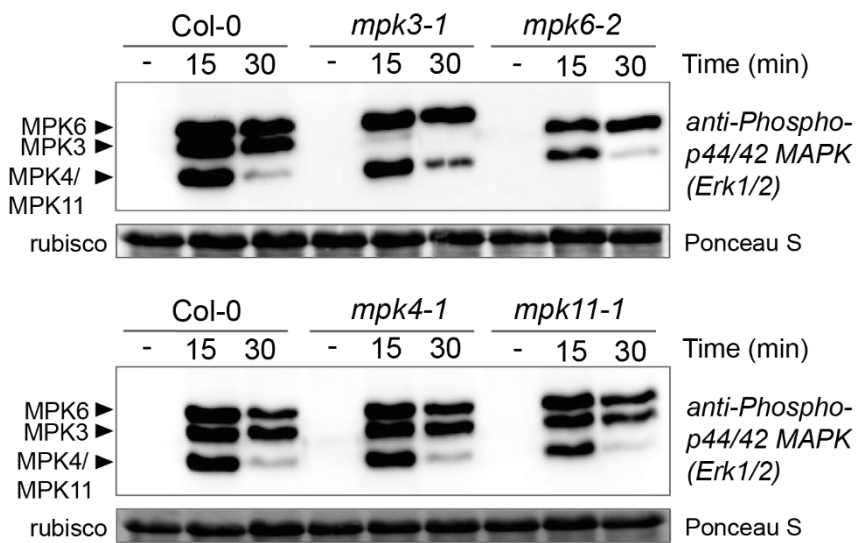
Appendix II.II: BAK1 immunoprecipitation from *bak1-4 pBAK1:eGFP A. thaliana*. BAK1 pull-downs from *bak1-4 / pBAK1:BAK1-eGFP* plants (Ntoukakis et al., 2011; Schwessinger et al., 2011). Immunoprecipitations were carried out as previously described (Schwessinger et al., 2011).

Appendix II.III



Appendix II.III: SUPPRESSOR OF BRASSINOSTEROID-ASSOCIATED KINASE 1-ASSOCIATED RECEPTOR 1 (SOBIR1) is a positive regulator of AEFEE-induced defence signalling. **A** *A. thaliana sobir1-13* mutant is compromised for AEFEE-induced $[Ca^{2+}]_{cyt}$ elevations. Normalised GFP fluorescence ($\Delta F/F$) kinetics in 10-day-old Col-0 35S:GCaMP3 or 35S:GCaMP3 x *sobir1-13* seedlings after elicitation with AEFEE (0.25% (v/v); $\sim 2.3 \mu\text{g}/\mu\text{l}$), mock PBS treatment at 2.5% (v/v) or flg22 (20nM), mock water treatment as indicated. Lines represent mean values with upper and lower lines representing the standard error of the mean. Data are from a minimum of six biological replicates. Data is replicated as peak mean GFP fluorescence ($\Delta F/F$) for clarity. Letters indicate significant differences between treatments ($p < 0.05$). **B** MAPK activation during AEFEE-induced MTI. Ten 10-days-old seedlings were elicited per treatment per time point. Seedlings were treated with AEFEE (2.5% (v/v); $\sim 22.5 \mu\text{g}/\mu\text{l}$), or flg22 (100nM) and flash frozen in LN₂ after an elapsed time as displayed. Mock (-) seedlings remained untreated. Activated MAPKs, MPK3/6/4/11 were detected by immunoblot using anti-p44/42 MAPK. Ponceau S staining of membranes are shown as loading controls. The experiment was repeated at least three times with similar results. Data shown is a representative example. **C** AEFEE-induced seedling growth inhibition. Individual Col-0 or *sobir1-13* *A. thaliana* seedlings were germinated on ¼St MS and transferred to liquid MS with treatments as indicated. Seedlings were dried and weighted after 8-days. Data are from a minimum of six biological replicates. Letters indicate significant differences between treatments ($p < 0.05$). **D** Transcriptional profiling of MTI marker genes by quantitative reverse transcription-PCR (qRT-PCR). Three 10-day-old *A. thaliana* plants were elicited with AEFEE (2.5% (v/v); $\sim 22.5 \mu\text{g}/\mu\text{l}$), mock PBS treatment at 2.5% (v/v) and flash-frozen after 1.5-h. Relative expression ($2^{\Delta CT}$) of the indicated genes is shown normalized to the *GAPDH* transcript (p -values were obtained in an ANOVA with Tukey HSD). Letters indicate significant differences ($p = < 0.05$) between treatments. Data are from three biological replicates.

Appendix III.I



Appendix III.I AEF E-induced MAPK activation is dependent on MPK3 and MPK6. Activated MAPKs, MPK3/6/4/11 were detected by immunoblot using anti-p44/42 MAPK. Ponceau S staining of the membrane is shown as loading controls.

Appendix III.II

Appendix III.II: List of *A. thaliana* receptor-like proteins (AtRLPs), T-DNA insertion mutant lines and corresponding genotyping primers used in this study.

Gene name	AGI code	T-DNA line	Mutant name	Gene-specific primer pair		T-DNA primer	Primer reference ^a	Reference
				Left Border (LB)	Right Border (RB)			
AtRLP1	at1g07390	SALK_059920b	<i>Atrlp1-1</i>	TGCGTTCATCATATTCTACAGTTC	CTCCGCCGTCTCTTCCAGTC	TGGTTCACGTAGTGGGCCATCG	Wang et al., 2008	Wang et al., 2008
AtRLP2	at1g17240	SALK_006696	<i>Atrlp2-3</i>	TGAATCATCGCAGGTAATTCC	TTATTTACAATGGCTGCCACTG	TGGTTCACGTAGTGGGCCATCG	This study	NASC ^b
AtRLP3	at1g17250	SALK_051677	<i>Atrlp3-1</i>	ATGGGTTTGCTCACTATGCTG	GCCGTGATCTTGCTGTCCAAC	TAGATTTGTCCACAACCAGC	This study	Wang et al., 2008
AtRLP4	at1g28340	SALK_004404	<i>Atrlp4-2</i>	CTGTGCTTCTACAACCAAGG	TCCTCCACGAATGTTGTTTTTC	TGGTTCACGTAGTGGGCCATCG	This study	NASC
AtRLP5	at1g34290	SALK_112291	<i>Atrlp5-1</i>	TCACAGTTTTGCCCTCGTATC	TGCGTGTTGACTCTACATGC	TGGTTCACGTAGTGGGCCATCG	This study	Wang et al., 2008
AtRLP6	at1g45616	SALK_080898	<i>Atrlp6-1</i>	ATGTGAGACGAATCTTCTGGG	CGAAGAGTGAAACAGAGCTGC	TGGTTCACGTAGTGGGCCATCG	This study	Wang et al., 2008
AtRLP7	at1g47890	SALK_030269	<i>Atrlp7-1</i>	ACTAGCGATACGACGACATCG	TGGTTTGGATTCCTCAGTTG	TGGTTCACGTAGTGGGCCATCG	This study	Wang et al., 2008
AtRLP8	at1g54480	SM_3_38632	<i>Atrlp8-1</i>	CTTCTCATTTGATCCACTCGC	GCTGCCTTGACATAGATCCTG	TACGAATAAGAGCGTCCATTTTAGAGTGA	This study	Wang et al., 2008
AtRLP9	at1g58190	SALK_023419	<i>Atrlp9-2</i>	CTTTGGCAGGACTTTGTCAAC	GGTAAGTTCGCCGAGAAGTTG	TGGTTCACGTAGTGGGCCATCG	Wang et al., 2008	Wang et al., 2008
AtRLP10	at1g65380	SALK_060804	<i>Atrlp10-3</i>	ACTGACCAACCTGAGACAACG	TTCGATTTAGGTGCTGAATCG	TGGTTCACGTAGTGGGCCATCG	This study	NASC
AtRLP11	at1g71390	SALK_013218	<i>Atrlp11-1</i>	CTTTGGTAGGTGAAGTTCCAGC	GGCAACATCTAACAGTACGAGG	TGGTTCACGTAGTGGGCCATCG	Wang et al., 2008	Wang et al., 2008
AtRLP12	at1g71400	SALK_151456	<i>Atrlp12-1</i>	TCTAGTGTTCCAACCACGTCC	TCATGGTTGGAATCTCTACCG	TGGTTCACGTAGTGGGCCATCG	This study	Wang et al., 2008
AtRLP13	at1g74170	SALK_020984	<i>Atrlp13-1</i>	GGCTCCATACCAACACAAG	ATATTTTTCCATGGGCAAGTCC	TGGTTCACGTAGTGGGCCATCG	Wang et al., 2008	Wang et al., 2008
AtRLP14	at1g74180	GABI_380E04	<i>Atrlp14-3</i>	ATGGCCAATATTATCAGGGAGCAC	TTGCATTTAGGTGCCTATGTAGCA	CCCATTTGGACGTGAATGTAGACAC	This study	NASC
AtRLP15	at1g74190	SALK_041143	<i>Atrlp15-1</i>	GATGAACCTCCGGAATCTTTCC	TCGAACAAATTAACGGGACG	TGGTTCACGTAGTGGGCCATCG	This study	Wang et al., 2008
AtRLP16	at1g74200	SALK_032150	<i>Atrlp16-1</i>	TGCTTGACATTTCGAACAA	GCGAGGAATACTGCCTGTTAAA	TGGTTCACGTAGTGGGCCATCG	Wang et al., 2008	Wang et al., 2008
AtRLP17	at1g80080	SALK_057932	<i>Atrlp17-3</i>	AACTGCATCAGACGGCTGTAC	CAAGGCTTTGAGGTGTTTGAG	TGGTTCACGTAGTGGGCCATCG	This study	NASC
AtRLP18	at2g15040	SAIL_400_H02d	<i>Atrlp18-1^c</i>	CAGTGTTCGACAGCAG	CGACTTTTCTCAACGGTC	TTCATAACCAATCTCGATACAC	Wang et al., 2008	Wang et al., 2008
AtRLP19	at2g15080	SALK_065907	<i>Atrlp19-2</i>	GCTTCGTAGTATTTAGGGGCC	AACTCTGGGTAAATTTGGCC	TGGTTCACGTAGTGGGCCATCG	This study	NASC

AtRLP20	at2g25440	SALK_130147	<i>Atrlp20-1</i>	TCTATACTAGAATCACTGAAGC	GAGACACAACAAAGTAAGAGTAGC	TGGTTCACGTAGTGGGCCATCG	Wang et al., 2008	Wang et al., 2008
AtRLP21	at2g25470	SAIL_693_F05	<i>Atrlp21-1</i>	GGCTCTCTGGTGCTATTCC	GCCTATCAATGCGGTCAC	TTCATAACCAATCTCGATACAC	Wang et al., 2008	Wang et al., 2008
AtRLP22	at2g32660	SALK_125231	<i>Atrlp22-1</i>	TCACATTAGCGAAAGACATCGGA	CAAAGGAAACGTTCTGATTGGA	TGGTTCACGTAGTGGGCCATCG	Wang et al., 2008	Wang et al., 2008
AtRLP23	at2g32680	SALK_034225	<i>Atrlp23-1</i>	ACAACAGAATTGAAGATACGTTTCC	CCAGTTCACAAAGTAGTTTGGTGG	TGGTTCACGTAGTGGGCCATCG	Wang et al., 2008	Wang et al., 2008
AtRLP24	at2g33020	SALK_046236	<i>Atrlp24-1</i>	AGTTTGCCCTTTCTAGATGCC	TTGGCTACAATCGACTAACC	TGGTTCACGTAGTGGGCCATCG	This study	Wang et al., 2008
AtRLP25	at2g33030	SALK_048434	<i>Atrlp25-1</i>	TTCAAATGAGGATTTGGTGG	TATTTACCCACCTTGAAGG	TGGTTCACGTAGTGGGCCATCG	Wang et al., 2008	Wang et al., 2008
AtRLP26	at2g33050	SALK_104127	<i>Atrlp26-1</i>	CGAACTCCAAGAAGTCCTTCC	TGACGTAACGATGATGACAATTC	TGGTTCACGTAGTGGGCCATCG	Wang et al., 2008	Wang et al., 2008
AtRLP27	at2g33060	SALK_029443	<i>Atrlp27-1</i>	GCCAAATCTAAAAGCCTCAC	CACATCATACTCGGCTTCTCC	TGGTTCACGTAGTGGGCCATCG	This study	Wang et al., 2008
AtRLP28	at2g33080	SM_3_1740	<i>Atrlp28-1</i>	CCTCGATCTTCCGGTAACAGT	CCGAGAGAAGGCTTTGATAGA	TACGAATAAGAGCGTCCATTTAGAGTGA	Wang et al., 2008	Wang et al., 2008
AtRLP29	at2g42800	SALK_022220	<i>Atrlp29-1</i>	CCACACGTGTCACTTTCAGTC	CTACACCTTCCGGGATTCTTC	TGGTTCACGTAGTGGGCCATCG	This study	Wang et al., 2008
AtRLP30	at3g05360	SALK_122528	<i>Atrlp30-1</i>	TCAATTATTGGTCCAAGTGGG	CAAGGTTTAGATCCCAAAGCC	TGGTTCACGTAGTGGGCCATCG	This study	Wang et al., 2008
AtRLP31	at3g05370	SALK_058586	<i>Atrlp31-1</i>	TGGGACGTTGTATCAACC	CAATCCACAGACGACACCAGG	TGGTTCACGTAGTGGGCCATCG	Wang et al., 2008	Wang et al., 2008
AtRLP32	at3g05650	SALK_032167	<i>Atrlp32-2</i>	TGGGTGTAACGACAATCTCATG	AATCAAGATGCCTTTCCACC	TGGTTCACGTAGTGGGCCATCG	This study	NASC
AtRLP33	at3g05660	SALK_087631	<i>Atrlp33-2</i>	TTTTAAAGGAGAAGCAAAACCTCA	CAAGAGTGCCGCTGAGTTGGT	TGGTTCACGTAGTGGGCCATCG	Wang et al., 2008	Wang et al., 2008
AtRLP34	at3g11010	SALK_067155	<i>Atrlp34-1</i>	GTCTAAGGTCGCTTGATGTCG	TGCGAAAACGAAAGATCAAAG	TGGTTCACGTAGTGGGCCATCG	This study	Wang et al., 2008
AtRLP35	at3g11080	SALK_096171	<i>Atrlp35-1</i>	CGGATGAACCTTGATTG	GGACGGGATTTGACCTGAA	TGGTTCACGTAGTGGGCCATCG	Wang et al., 2008	Wang et al., 2008
AtRLP36	at3g23010	GABI_706H01	<i>Atrlp36-2</i>	CCTAAACCAACTAGAGTC	TTAAACTGTGGGATGTCC	CCCATTGGACGTGAATGTAGACAC	This study	NASC
AtRLP37	at3g23110	SALK_041785	<i>Atrlp37-1</i>	GCGATTTGGGTGTCTGAGAAC	GGTCCTTGAGGGAAATTTGAGC	TGGTTCACGTAGTGGGCCATCG	Wang et al., 2008	Wang et al., 2008
AtRLP38	at3g23120	SALK_017819	<i>Atrlp38-1</i>	ATCTACAAGGATTCGTGCCACG	TGCCGTGAGATTTCAAGTCCAG	TGGTTCACGTAGTGGGCCATCG	Wang et al., 2008	Wang et al., 2008
AtRLP39	at3g24900	SALK_126505	<i>Atrlp39-1</i>	TAGGTCCTGTAACAACCTTG	TAGGTCCTGTAACAACCTTG	TGGTTCACGTAGTGGGCCATCG	This study	Wang et al., 2008
AtRLP40	at3g24982	GABI_564D03	<i>Atrlp40-1</i>	CTGGGTCTATATATGGTATATG	TTGTGTTCTTGTGGTATTTCAACAA	CCCATTGGACGTGAATGTAGACAC	Wang et al., 2008	Wang et al., 2008
AtRLP41	at3g25010	SALK_024020	<i>Atrlp41-1</i>	TGGTCTCTATCTCCTCAA	GCCTTCCAGTTCAACACTTGTTCCTG	TGGTTCACGTAGTGGGCCATCG	Wang et al., 2008	Wang et al., 2008
AtRLP42	at3g25020	SALK_080324b	<i>Atrlp42-1</i>	GTCCGAAGGGAATCTCTTTG	TGGAGTGTTACTTGGATTGGC	TGGTTCACGTAGTGGGCCATCG	Wang et al., 2008	Wang et al., 2008
AtRLP43	at3g28890	SALK_041685	<i>Atrlp43-1</i>	ATTCCTTGTGGGTGCATTATG	AGAATCAATGACACGTTTCCG	TGGTTCACGTAGTGGGCCATCG	This study	Wang et al., 2008
AtRLP44	at3g49750	SALK_097350i	<i>Atrlp44-1</i>	GTTTGGATCGGCGGTGGTTA	GCTTGTGATTGGGCTTTACA	TGGTTCACGTAGTGGGCCATCG	Wang et al., 2008	Wang et al., 2008
AtRLP45	at3g53240	GABI_620G05	<i>Atrlp45-1</i>	GCATGGAACCATTCCCTC	CCCTCTAGATAACTCCAG	CCCATTGGACGTGAATGTAGACAC	Wang et al., 2008	Wang et al., 2008
AtRLP46	at4g04220	SALK_048207i	<i>Atrlp46-1</i>	TCTTTGGAAGGCGAACTAGCG	TTCGAGAATGGAGACATGTAGA	TGGTTCACGTAGTGGGCCATCG	Wang et al., 2008	Wang et al., 2008

AtRLP47	at4g13810	SALK_105921	<i>Atrlp47-2</i>	TGGTTATGGAGTCTGCCAGAG	TGGTTATGGAGTCTGCCAGAG	CCCATTGGACGTGAATGTAGACAC	This study	NASC
AtRLP48	at4g13880	SALK_036842	<i>Atrlp48-1</i>	GTTCAACTCTCAGCTTCCCTCAG	CCAGCTCCATATTTAATCCTTTGT	TGGTTCACGTAGTGGGCCATCG	Wang et al., 2008	Wang et al., 2008
AtRLP49	at4g13900	SALK_067372	<i>Atrlp49-1</i>	ACTGATTGCTGTTCTTGGGATGGT	GGTGAGGGAAGACTGACGTTGA	TGGTTCACGTAGTGGGCCATCG	Wang et al., 2008	Wang et al., 2008
AtRLP50	at4g13920	SALK_070876i	<i>Atrlp50-1</i>	TTGGCTGCGGTGTGGTGTG	TCGGGGCTGGGATAGAGAA	TGGTTCACGTAGTGGGCCATCG	Wang et al., 2008	Wang et al., 2008
AtRLP51	at4g18760	SALK_143038	<i>Atrlp51-1</i>	CGAAGTGTCAAATCGGTGGA	CCAGGCTGGATCTTTGATGGA	TGGTTCACGTAGTGGGCCATCG	Wang et al., 2008	Wang et al., 2008
AtRLP52	at5g25910	SALK_107922	<i>Atrlp52-1</i>	CCCATTGATGATGGGATGTGG	CACCGGAGAAATCCCAGAGTC	TGGTTCACGTAGTGGGCCATCG	Wang et al., 2008	Wang et al., 2008
AtRLP53	at5g27060	SALK_124008	<i>Atrlp53-1</i>	TTATGGCCGACATCAAGAGAC	CTCATCTCACCCTCTCAGCC	TGGTTCACGTAGTGGGCCATCG	This study	Wang et al., 2008
AtRLP54	at5g40170	SAIL_306_E09d	<i>Atrlp54-1^c</i>	TCTGTTGCGTCTTTGTGACCAG	GGCAGAGTCCATAAACAACCTCAG	TTCATAACCAATCTCGATACAC	Wang et al., 2008	Wang et al., 2008
AtRLP55	at5g45770	SALK_139161b	<i>Atrlp55-1</i>	TGGTTGAATGCTAGATTTGGG	TGAATCAACTAAACGGAACCG	TGGTTCACGTAGTGGGCCATCG	This study	Wang et al., 2008
AtRLP56	at5g49290	SALK_129306	<i>Atrlp56-1</i>	AAATTCATTAGTCCGTGGGC	TTTATCATTGGACTGGCGAG	TGGTTCACGTAGTGGGCCATCG	This study	Wang et al., 2008
AtRLP57	at5g65830	SALK_077716	<i>Atrlp57-1</i>	AATGAACCCTCCCTATTGCTG	ATGAAAGCTCTATAATGCGCG	TGGTTCACGTAGTGGGCCATCG	This study	Wang et al., 2008

^a Where *This study* is referenced, left border (LB) and right border (RB) primers were generated via <http://signal.salk.edu/>.

^b NASC – Nottingham Arabidopsis Stock Centre.

^c T-DNA insertion is in Col-3 background.

Appendix III.III

Appendix III.III: EMS-mutagenised *pWRKY33:fluc* reporter seedlings exposed to aphid-derived extract, AEFE.

Mutant line	M ₂ score	M ₃ repeat 1			M ₃ repeat 2			M ₃ repeat 3		
		% of WT response	<i>n</i>	<i>p</i> -value	% of WT response	<i>n</i>	<i>p</i> -value	% of WT response	<i>n</i>	<i>p</i> -value
2c 6-07	-2.53	-28.1	16	***	-29.9	10	***	-9.3	14	ns
6c 2-08	-3.26	-27.5	16	***	-42.5	15	****	-27.8	16	***
3g 5-07	-3.39	-19.7	16	*	-36.5	13	****	-37.8	16	****

References

- AARTS, N., METZ, M., HOLOB, B., STASKAWICZ, B. J., DANIELS, M. & PARKER, J. E. 1998. Different requirements for EDS1 and NDR1 by disease resistance genes define at least two R gene-mediated signaling pathways in Arabidopsis. *Proc. Natl. Acad. Sci. USA*, 95, 10306–10311.
- ABDUL MALIK, N. A., KUMAR, I. S. & NADARAJAH, K. 2020. Elicitor and Receptor Molecules: Orchestrators of Plant Defense and Immunity. *Int J Mol Sci*, 21.
- ABE, A., KOSUGI, S., YOSHIDA, K., NATSUME, S., TAKAGI, H., KANZAKI, H., MATSUMURA, H., YOSHIDA, K., MITSUOKA, C., TAMIRU, M., INNAN, H., CANO, L., KAMOUN, S. & TERAUCHI, R. 2012. Genome sequencing reveals agronomically important loci in rice using MutMap. *Nat Biotechnol*, 30, 174-8.
- ABRAMOVITCH, R. B., JANJUSEVIC, R., STEBBINS, C. E. & MARTIN, G. B. 2006. Type III effector AvrPtoB requires intrinsic E3 ubiquitin ligase activity to suppress plant cell death and immunity. *Proc Natl Acad Sci U S A*, 103, 2851-6.
- ACEVEDO, F. E., RIVERA-VEGA, L. J., CHUNG, S. H., RAY, S. & FELTON, G. W. 2015. Cues from chewing insects - the intersection of DAMPs, HAMPs, MAMPs and effectors. *Curr Opin Plant Biol*, 26, 80-6.
- ADACHI, H., NAKANO, T., MIYAGAWA, N., ISHIHAMA, N., YOSHIOKA, M., KATOU, Y., YAENO, T., SHIRASU, K. & YOSHIOKA, H. 2015. WRKY Transcription Factors Phosphorylated by MAPK Regulate a Plant Immune NADPH Oxidase in *Nicotiana benthamiana*. *Plant Cell*, 27, 2645-63.
- AHAMAD, N. & KATTI, D. S. 2016. A two-step method for extraction of lipopolysaccharide from *Shigella dysenteriae* serotype 1 and *Salmonella typhimurium*: An improved method for enhanced yield and purity. *J Microbiol Methods*, 127, 41-50.
- AHRNE, E., MULLER, M. & LISACEK, F. 2010. Unrestricted identification of modified proteins using MS/MS. *Proteomics*, 10, 671-86.
- ALBERT, I., BOHM, H., ALBERT, M., FEILER, C. E., IMKAMPE, J., WALLMERTH, N., BRANCATO, C., RAAJMAKERS, T. M., OOME, S., ZHANG, H., KROL, E., GREFFEN, C., GUST, A. A., CHAI, J., HEDRICH, R., VAN DEN ACKERVEN, G. & NURNBERGER, T. 2015. An RLP23-SOBIR1-BAK1 complex mediates NLP-triggered immunity. *Nat Plants*, 1, 15140.
- ALBERT, I., ZHANG, L., BEMM, H. & NURNBERGER, T. 2019. Structure-Function Analysis of Immune Receptor AtRLP23 with Its Ligand nlp20 and Coreceptors AtSOBIR1 and AtBAK1. *Mol Plant Microbe Interact*, 32, 1038-1046.
- ALHORAIBI, H., BIGEARD, J., RAYAPURAM, N., COLCOMBET, J. & HIRT, H. 2019. Plant Immunity: The MTI-ETI Model and Beyond. *Curr Issues Mol Biol*, 30, 39-58.
- ALTINCICEK, B. & VILCINSKAS, A. 2006. Metamorphosis and collagen-IV-fragments stimulate innate immune response in the greater wax moth, *Galleria mellonella*. *Dev Comp Immunol*, 30, 1108-18.
- ANDREASSON, E., JENKINS, T., BRODERSEN, P., THORGRIMSEN, S., PETERSEN, N. H., ZHU, S., QIU, J. L., MICHEELSEN, P., ROCHER, A., PETERSEN, M., NEWMAN, M. A., BJORN NIELSEN, H., HIRT, H., SOMSSICH, I., MATTSSON, O. & MUNDY, J. 2005. The MAP kinase substrate MKS1 is a regulator of plant defense responses. *EMBO J*, 24, 2579-89.
- ANSTEAD, J. A., MALLET, J. & DENHOLM, I. 2007. Temporal and spatial incidence of alleles conferring knockdown resistance to pyrethroids in the peach-potato aphid, *Myzus persicae* (Hemiptera: Aphididae), and their association with other insecticide resistance mechanisms. *Bulletin of Entomological Research*, 97, 243 - 252.
- ARGANDONA, V. H., CHAMAN, M., CARDEMIL, L., MUNOZ, O., ZUNIGA, G. E. & CORCUERA, L. J. 2001. Ethylene production and peroxidase activity in aphid-infested barley. *J Chem Ecol*, 27, 53-68.

- ASAI, T., TENA, G., PLOTNIKOVA, J., WILLMANN, M. R., CHIU, W. L., GOMEZ-GOMEZ, L., BOLLER, T., AUSUBEL, F. M. & SHEEN, J. 2002. MAP kinase signalling cascade in Arabidopsis innate immunity. *Nature*, 415, 977-83.
- ATAMIAN, H. S., CHAUDHARY, R., CIN, V. D., BAO, E., GIRKE, T. & KALOSHIAN, I. 2013. In planta expression or delivery of potato aphid *Macrosiphum euphorbiae* effectors Me10 and Me23 enhances aphid fecundity. *Mol. Plant Microbe Interact*, 26, 67–74.
- ATAMIAN, H. S., EULGEM, T. & KALOSHIAN, I. 2012. SIWRKY70 is required for Mi-1-mediated resistance to aphids and nematodes in tomato. *Planta*, 235, 299-309.
- AUSTIN, R. S., VIDAURRE, D., STAMATIOU, G., BREIT, R., PROVART, N. J., BONETTA, D., ZHANG, J., FUNG, P., GONG, Y., WANG, P. W., MCCOURT, P. & GUTTMAN, D. S. 2011. Next-generation mapping of Arabidopsis genes. *Plant J*, 67, 715-25.
- AUSUBEL, F. M. 2005. Are innate immune signaling pathways in plants and animals conserved? *Nat Immunol*, 6, 973-9.
- AVILA, J. R., LEE, J. S. & TORII, K. U. 2015. Co-Immunoprecipitation of Membrane-Bound Receptors. *Arabidopsis Book*, 13, e0180.
- BAR, M., SHARFMAN, M., RON, M. & AVNI, A. 2010. BAK1 is required for the attenuation of ethylene-inducing xylanase (Eix)-induced defense responses by the decoy receptor LeEix1. *Plant J*, 63, 791-800.
- BASS, C., PUINEAN, A. M., ANDREWS, M., CUTLER, P., DANIELS, M., ELIAS, J., PAUL, V. L., CROSTHWAITE, A. J., DENHOLM, I., FIELD, L. M., FOSTER, S. P., LIND, R., WILLIAMSON, M. S. & SLATER, R. 2011. Mutation of a nicotinic acetylcholine receptor b subunit is associated with resistance to neonicotinoid insecticides in the aphid *Myzus persicae*. *BMC Neuroscience*, 12.
- BASS, C., PUINEAN, A. M., ZIMMER, C. T., DENHOLM, I., FIELD, L. M., FOSTER, S. P., GUTBROD, O., NAUEN, R., SLATER, R. & WILLIAMSON, M. S. 2014. The evolution of insecticide resistance in the peach potato aphid, *Myzus persicae*. *Insect Biochem Mol Biol*, 51, 41-51.
- BASU, S., VARSANI, S. & LOUIS, J. 2018. Altering Plant Defenses: Herbivore-Associated Molecular Patterns and Effector Arsenal of Chewing Herbivores. *Mol Plant Microbe Interact*, 31, 13-21.
- BAUER, Z., GOMEZ-GOMEZ, L., BOLLER, T. & FELIX, G. 2001. Sensitivity of different ecotypes and mutants of Arabidopsis thaliana toward the bacterial elicitor flagellin correlates with the presence of receptor-binding sites. *J Biol Chem*, 276, 45669-76.
- BECK, M., ZHOU, J., FAULKNER, C., MACLEAN, D. & ROBATZEK, S. 2012. Spatio-temporal cellular dynamics of the Arabidopsis flagellin receptor reveal activation status-dependent endosomal sorting. *Plant Cell*, 24, 4205-19.
- BECKERS, G. J., JASKIEWICZ, M., LIU, Y., UNDERWOOD, W. R., HE, S. Y., ZHANG, S. & CONRATH, U. 2009. Mitogen-activated protein kinases 3 and 6 are required for full priming of stress responses in Arabidopsis thaliana. *Plant Cell*, 21, 944–53.
- BECKINGHAM, C., PHILLIPS, J., GILL, M. & CROSTHWAITE, A. J. 2013. Investigating nicotinic acetylcholine receptor expression in neonicotinoid resistant *Myzus persicae* FRC. *Pestic Biochem Physiol*, 107, 293-8.
- BEDNAREK, P., PIŚLEWSKA-BEDNAREK, M., SVATOŠ, A., SCHNEIDER, B., DOUBSKÝ, J., MANSUROVA, M., HUMPHRY, M., CONSONNI, C., PANSTRUGA, R., SANCHEZ-VALLET, A., MOLINA, A. & SCHULZE-LEFERT, P. 2009. A glucosinolate metabolism pathway in living plant cells mediates broad-spectrum antifungal defense. *Science* 323, 101-106.
- BEDNAREK, P., PIŚLEWSKA-BEDNAREK, M., VER, L. V. T. E., MADDULA, R. K., SVATOŠ, A. & SCHULZE-LEFERT, P. 2011. Conservation and clade-specific diversification of pathogen-inducible tryptophan and indole glucosinolate metabolism in Arabidopsis thaliana relatives. *New Phytol.*, 192, 713-726.
- BENEDETTI, M., PONTIGGIA, D., RAGGI, S., CHENG, Z., SCALONI, F., FERRARI, S., AUSUBEL, F. M., CERVONE, F. & DE LORENZO, G. 2015. Plant immunity triggered by engineered in

- vivo release of oligogalacturonides, damage-associated molecular patterns. *Proc Natl Acad Sci U S A*, 112, 5533-8.
- BERISHA, A., MUKHERJEE, K., VILCINSKAS, A., SPENGLER, B. & ROMPP, A. 2013. High-resolution mass spectrometry driven discovery of peptidic danger signals in insect immunity. *PLoS One*, 8, e80406.
- BERTSCHE, U. & GUST, A. A. 2017. Peptidoglycan Isolation and Binding Studies with LysM-Type Pattern Recognition Receptors. In: SHAN, L. & HE, P. (eds.) *Plant Pattern Recognition Receptors: Methods and Protocols*. New York, NY: Springer New York.
- BHATTARAI, K. K., ATAMIAN, H. S., KALOSHIAN, I. & EULGEM, T. 2010. WRKY72-type transcription factors contribute to basal immunity in tomato and Arabidopsis as well as gene-for-gene resistance mediated by the tomato R gene Mi-1. *The Plant Journal*, 63, 229–240.
- BI, G., LIEBRAND, T. W., BYE, R. R., POSTMA, J., VAN DER BURGH, A. M., ROBATZEK, S., XU, X. & JOOSTEN, M. H. 2016. SOBIR1 requires the GxxxG dimerization motif in its transmembrane domain to form constitutive complexes with receptor-like proteins. *Mol Plant Pathol*, 17, 96-107.
- BI, G., SU, M., LI, N., LIANG, Y., DANG, S., XU, J., HU, M., WANG, J., ZOU, M., DENG, Y., LI, Q., HUANG, S., LI, J., CHAI, J., HE, K., CHEN, Y. H. & ZHOU, J. M. 2021. The ZAR1 resistosome is a calcium-permeable channel triggering plant immune signaling. *Cell*, 184, 3528-3541 e12.
- BI, G., ZHOU, Z., WANG, W., LI, L., RAO, S., WU, Y., ZHANG, X., MENKE, F. L. H., CHEN, S. & ZHOU, J. M. 2018. Receptor-Like Cytoplasmic Kinases Directly Link Diverse Pattern Recognition Receptors to the Activation of Mitogen-Activated Protein Kinase Cascades in Arabidopsis. *Plant Cell*, 30, 1543-1561.
- BICKFORD, D., LOHMAN, D. J., SODHI, N. S., NG, P. K., MEIER, R., WINKER, K., INGRAM, K. K. & DAS, I. 2007. Cryptic species as a window on diversity and conservation. *Trends Ecol Evol*, 22, 148-55.
- BIRKENBIHL, R. P., DIEZEL, C. & SOMSSICH, I. E. 2012. Arabidopsis WRKY33 is a key transcriptional regulator of hormonal and metabolic responses toward Botrytis cinerea infection. *Plant Physiol*, 159, 266-85.
- BIRKENBIHL, R. P., KRACHER, B., ROCCARO, M. & SOMSSICH, I. E. 2017. Induced Genome-Wide Binding of Three Arabidopsis WRKY Transcription Factors during Early MAMP-Trigged Immunity. *Plant Cell*, 29, 20-38.
- BJORNSON, M., PIMPRIKAR, P., NURNBERGER, T. & ZIPFEL, C. 2021. The transcriptional landscape of Arabidopsis thaliana pattern-triggered immunity. *Nat Plants*, 7, 579-586.
- BLACKMAN, R. L. & EASTOP, V. F. 2007. *Aphids as crop pests.*, UK, CAB International.
- BLANCO, F., GARRETON, V., FREY, N., DOMINGUEZ, C., PEREZ-ACLE, T., VAN DER STRAETEN, D., JORDANA, X. & HOLUIGUE, L. 2005. Identification of NPR1-dependent and independent genes early induced by salicylic acid treatment in Arabidopsis. *Plant Mol Biol*, 59, 927-44.
- BLUME, B., NÜRNBERGER, T., NASS, N. & SCHEEL, D. 2000. Receptor-Mediated Increase in Cytoplasmic Free Calcium Required for Activation of Pathogen Defense in Parsley. *The Plant Cell*, 12, 1425–1440.
- BOGDANOW, B., ZAUBER, H. & SELBACH, M. 2016. Systematic Errors in Peptide and Protein Identification and Quantification by Modified Peptides. *Mol Cell Proteomics*, 15, 2791-801.
- BOHM, H., ALBERT, I., OOME, S., RAAJMAKERS, T. M., VAN DEN ACKERVEKEN, G. & NURNBERGER, T. 2014. A conserved peptide pattern from a widespread microbial virulence factor triggers pattern-induced immunity in Arabidopsis. *PLoS Pathog*, 10, e1004491.

- BOLLER, T. & FELIX, G. 2009. A renaissance of elicitors: perception of microbe-associated molecular patterns and danger signals by pattern-recognition receptors. *Annu Rev Plant Biol*, 60, 379-406.
- BONARDI, V., TANG, S., STALLMANN, A., ROBERTS, M., CHERKIS, K. & DANGL, J. L. 2011. Expanded functions for a family of plant intracellular immune receptors beyond specific recognition of pathogen effectors. *Proc Natl Acad Sci U S A*, 108, 16463-8.
- BOS, J. I., PRINCE, D., PITINO, M., MAFFEI, M. E., WIN, J. & HOGENHOUT, S. A. 2010. A functional genomics approach identifies candidate effectors from the aphid species *Myzus persicae* (green peach aphid). *PLoS Genet*, 6, e1001216.
- BOSE, J., RODRIGO-MORENO, A. & SHABALA, S. 2014. ROS homeostasis in halophytes in the context of salinity stress tolerance. *J Exp Bot*, 65, 1241-57.
- BOTTCHER, C., WESTPHAL, L., SCHMOTZ, C., PRADE, E., SCHEEL, D. & GLAWISCHNIG, E. 2009. The multifunctional enzyme CYP71B15 (PHYTOALEXIN DEFICIENT3) converts cysteine-indole-3-acetonitrile to camalexin in the indole-3-acetonitrile metabolic network of *Arabidopsis thaliana*. *Plant Cell*, 21, 1830-45.
- BOUDSOCQ, M., WILLMANN, M. R., MCCORMACK, M., LEE, H., SHAN, L., HE, P., BUSH, J., CHENG, S. H. & SHEEN, J. 2010. Differential innate immune signalling via Ca²⁺ sensor protein kinases. *Nature*, 464, 418-22.
- BOULAIN, H., LEGEAI, F., GUY, E., MORLIERE, S., DOUGLAS, N. E., OH, J., MURUGAN, M., SMITH, M., JAQUIERY, J., PECCOUD, J., WHITE, F. F., CAROLAN, J. C., SIMON, J. C. & SUGIO, A. 2018. Fast Evolution and Lineage-Specific Gene Family Expansions of Aphid Salivary Effectors Driven by Interactions with Host-Plants. *Genome Biol Evol*, 10, 1554-1572.
- BOUTROT, F., SEGONZAC, C., CHANG, K. N., QIAO, H., ECKER, J. R., ZIPFEL, C. & RATHJEN, J. P. 2010. Direct transcriptional control of the *Arabidopsis* immune receptor FLS2 by the ethylene-dependent transcription factors EIN3 and EIL1. *Proc Natl Acad Sci U S A*, 107, 14502-7.
- BRAUN, S. G., MEYER, A., HOLST, O., PUHLER, A. & NIEHAUS, K. 2005. Characterization of the *Xanthomonas campestris* pv. *campestris* lipopolysaccharide substructures essential for elicitation of an oxidative burst in tobacco cells. *Mol Plant Microbe Interact*, 18, 674-81.
- BREIDEN, M. & SIMON, R. 2016. Q&A: How does peptide signaling direct plant development? *BMC Biol*, 14, 58.
- BRICCHI, I., BERTEA, C. M., OCCHIPINTI, A., PAPONOV, I. A. & MAFFEI, M. E. 2012. Dynamics of membrane potential variation and gene expression induced by *Spodoptera littoralis*, *Myzus persicae*, and *Pseudomonas syringae* in *Arabidopsis*. *PLoS One*, 7, e46673.
- BRUESSOW, F., GOUHIER-DARIMONT, C., BUCHALA, A., METRAUX, J. P. & REYMOND, P. 2010. Insect eggs suppress plant defence against chewing herbivores. *Plant J*, 62, 876-85.
- BRUTUS, A., SICILIA, F., MACONE, A., CERVONE, F. & DE LORENZO, G. 2010. A domain swap approach reveals a role of the plant wall-associated kinase 1 (WAK1) as a receptor of oligogalacturonides. *Proc Natl Acad Sci U S A*, 107, 9452-7.
- BUSCAILL, P., CHANDRASEKAR, B., SANGUANKIATTICHAJ, N., KOURELIS, J., KASCHANI, F., THOMAS, E. L., MORIMOTO, K., KAISER, M., PRESTON, G. M., ICHINOSE, Y. & VAN DER HOORN, R. A. L. 2019. Glycosidase and glycan polymorphism control hydrolytic release of immunogenic flagellin peptides. *Science*, 364.
- CABRAL, C. M., CHERQUI, A., PEREIRA, A. & SIMOES, N. 2004. Purification and characterization of two distinct metalloproteases secreted by the entomopathogenic bacterium *Photorhabdus* sp. strain Az29. *Appl Environ Microbiol*, 70, 3831-8.
- CAI, R., LEWIS, J., YAN, S., LIU, H., CLARKE, C. R., CAMPANILE, F., ALMEIDA, N. F., STUDHOLME, D. J., LINDEBERG, M., SCHNEIDER, D., ZACCARDELLI, M., SETUBAL, J. C., MORALES-LIZCANO, N. P., BERNAL, A., COAKER, G., BAKER, C., BENDER, C. L., LEMAN, S. & VINATZER, B. A. 2011. The plant pathogen *Pseudomonas syringae* pv. *tomato* is

- genetically monomorphic and under strong selection to evade tomato immunity. *PLoS Pathog*, 7, e1002130.
- CAO, Y., LIANG, Y., TANAKA, K., NGUYEN, C. T., JEDRZEJCZAK, R. P., JOACHIMIAK, A. & STACEY, G. 2014. The kinase LYK5 is a major chitin receptor in Arabidopsis and forms a chitin-induced complex with related kinase CERK1. *Elife*, 3.
- CAROLAN, J. C., CARAGEA, D., REARDON, K. T., MUTTI, N. S., DITTMER, N., PAPPAN, K., CUI, F., CASTANETO, M., POULAIN, J., DOSSAT, C., TAGU, D., REESE, J. C., REECK, G. R., WILKINSON, T. L. & EDWARDS, O. R. 2011. Predicted effector molecules in the salivary secretome of the pea aphid (*Acyrtosiphon pisum*): a dual transcriptomic/proteomic approach. *J Proteome Res*, 10, 1505-18.
- CAROLAN, J. C., FITZROY, C. I., ASHTON, P. D., DOUGLAS, A. E. & WILKINSON, T. L. 2009. The secreted salivary proteome of the pea aphid *Acyrtosiphon pisum* characterised by mass spectrometry. *Proteomics*, 9, 2457-67.
- CASTEL, B., NGOU, P. M., CEVIK, V., REDKAR, A., KIM, D. S., YANG, Y., DING, P. & JONES, J. D. G. 2019. Diverse NLR immune receptors activate defence via the RPW8-NLR NRG1. *New Phytol*, 222, 966-980.
- CASTELLO, M. J., MEDINA-PUCHE, L., LAMILLA, J. & TORNERO, P. 2018. NPR1 paralogs of Arabidopsis and their role in salicylic acid perception. *PLoS One*, 13, e0209835.
- CATANZARITI, A. M., LIM, G. T. T. & JONES, D. A. 2015. The tomato I-3 gene: a novel gene for resistance to Fusarium wilt disease. *New Phytol*, 207, 106-118.
- CHASSOT, C., BUCHALA, A., SCHOONBEEK, H. J., METRAUX, J. P. & LAMOTTE, O. 2008. Wounding of Arabidopsis leaves causes a powerful but transient protection against Botrytis infection. *Plant J*, 55, 555-67.
- CHAUDHARY, R., ATAMIAN, H. S., SHEN, Z., BRIGGS, S. P. & KALOSHIAN, I. 2014. GroEL from the endosymbiont *Buchnera aphidicola* betrays the aphid by triggering plant defense. *Proc Natl Acad Sci U S A*, 111, 8919-24.
- CHEN, D., CAO, Y., LI, H., KIM, D., AHSAN, N., THELEN, J. & STACEY, G. 2017. Extracellular ATP elicits DORN1-mediated RBOHD phosphorylation to regulate stomatal aperture. *Nat Commun*, 8, 2265.
- CHEN, X., CHERN, M., CANLAS, P. E., JIANG, C., RUAN, D., CAO, P. & RONALD, P. C. 2010. A conserved threonine residue in the juxtamembrane domain of the XA21 pattern recognition receptor is critical for kinase autophosphorylation and XA21-mediated immunity. *J Biol Chem*, 285, 10454-63.
- CHEN, Y., SINGH, A., KAITHAKOTTIL, G. G., MATHERS, T. C., GRAVINO, M., MUGFORD, S. T., VAN OOSTERHOUT, C., SWARBRECK, D. & HOGENHOUT, S. A. 2020. An aphid RNA transcript migrates systemically within plants and is a virulence factor. *Proc Natl Acad Sci U S A*, 117, 12763-12771.
- CHIN, K., DEFALCO, T. A., MOEDER, W. & YOSHIOKA, K. 2013. The Arabidopsis cyclic nucleotide-gated ion channels AtCNGC2 and AtCNGC4 work in the same signaling pathway to regulate pathogen defense and floral transition. *Plant Physiol*, 163, 611-24.
- CHINCHILLA, D., BAUER, Z., REGENASS, M., BOLLER, T. & FELIX, G. 2006. The Arabidopsis receptor kinase FLS2 binds flg22 and determines the specificity of flagellin perception. *Plant Cell*, 18, 465-76.
- CHINCHILLA, D., ZIPFEL, C., ROBATZEK, S., KEMMERLING, B., NURNBERGER, T., JONES, J. D., FELIX, G. & BOLLER, T. 2007. A flagellin-induced complex of the receptor FLS2 and BAK1 initiates plant defence. *Nature*, 448, 497-500.
- CHINI, A., FONSECA, S., FERNANDEZ, G., ADIE, B., CHICO, J. M., LORENZO, O., GARCIA-CASADO, G., LOPEZ-VIDRIERO, I., LOZANO, F. M., PONCE, M. R., MICOL, J. L. & SOLANO, R. 2007. The JAZ family of repressors is the missing link in jasmonate signalling. *Nature*, 448, 666-71.
- CHINI, A., MONTE, I., ZAMARRENO, A. M., HAMBERG, M., LASSUEUR, S., REYMOND, P., WEISS, S., STINTZI, A., SCHALLER, A., PORZEL, A., GARCIA-MINA, J. M. & SOLANO, R. 2018. An

- OPR3-independent pathway uses 4,5-didehydrojasmonate for jasmonate synthesis. *Nat Chem Biol*, 14, 171-178.
- CHOI, H. W., MANOHAR, M., MANOSALVA, P., TIAN, M., MOREAU, M. & KLESSIG, D. F. 2016. Activation of Plant Innate Immunity by Extracellular High Mobility Group Box 3 and Its Inhibition by Salicylic Acid. *PLoS Pathog*, 12, e1005518.
- CHOI, J., TANAKA, K., LIANG, Y., CAO, Y., LEE, S. Y. & STACEY, G. 2014. Extracellular ATP, a danger signal, is recognized by DORN1 in Arabidopsis. *Biochem J*, 463, 429-37.
- CLAY, N. K., ADIO, A. M., DENOUX, C., JANDER, G. & AUSUBEL, F. M. 2009. Glucosinolate metabolites required for an Arabidopsis innate immune response. *Science*, 323, 95-101.
- CLOUGH, S. J., FENGLER, K. A., YU, I. C., LIPPOK, B., SMITH, R. K. J. & BENT, A. F. 2000. The Arabidopsis *dnd1* "defense, no death" gene encodes a mutated cyclic nucleotide-gated ion channel. *Proc Natl Acad Sci U S A*, 97, 9323-9328.
- COLCOMBET, J. & HIRT, H. 2008. Arabidopsis MAPKs: a complex signalling network involved in multiple biological processes. *Biochem J*, 413, 217-26.
- COLEMAN, A. D., WOUTERS, R. H., MUGFORD, S. T. & HOGENHOUT, S. A. 2015. Persistence and transgenerational effect of plant-mediated RNAi in aphids. *J Exp Bot*, 66, 541-8.
- CONRATH, U., BECKERS, G. J., LANGENBACH, C. J. & JASKIEWICZ, M. R. 2015. Priming for enhanced defense. *Annu Rev Phytopathol*, 53, 97-119.
- CONSONNI, C., BEDNAREK, P., HUMPHRY, M., FRANCOCCI, F., FERRARI, S., HARZEN, A., VER LOREN VAN THEMAAT, E. & PANSTRUGA, R. 2010. Tryptophan-derived metabolites are required for antifungal defense in the Arabidopsis *mlo2* mutant. *Plant Physiol*, 152, 1544-61.
- COOPER, W. R., DILLWITH, J. W. & PUTERKA, G. J. 2010. Salivary proteins of Russian wheat aphid (Hemiptera: Aphididae). *Environ Entomol*, 39, 223-31.
- CORRY, B., ALLEN, T. W., KUYUCAK, S. & CHUNG, S. H. 2001. Mechanisms of permeation and selectivity in calcium channels. *Biophys J*, 80, 195-214.
- CORWIN, J. A. & KLIEBENSTEIN, D. J. 2017. Quantitative Resistance: More Than Just Perception of a Pathogen. *Plant Cell*, 29, 655-665.
- COULDRIDGE, C., NEWBURY, H. J., FORD-LLOYD, B., BALE, J. & PRITCHARD, J. 2007. Exploring plant responses to aphid feeding using a full Arabidopsis microarray reveals a small number of genes with significantly altered expression. *Bull Entomol Res*, 97, 523-32.
- COUTO, D., NIEBERGALL, R., LIANG, X., BUCHERL, C. A., SKLENAR, J., MACHO, A. P., NTOUKAKIS, V., DERBYSHIRE, P., ALTENBACH, D., MACLEAN, D., ROBATZEK, S., UHRIG, J., MENKE, F., ZHOU, J. M. & ZIPFEL, C. 2016. The Arabidopsis Protein Phosphatase PP2C38 Negatively Regulates the Central Immune Kinase BIK1. *PLoS Pathog*, 12, e1005811.
- COUTO, D. & ZIPFEL, C. 2016. Regulation of pattern recognition receptor signalling in plants. *Nat Rev Immunol*, 16, 537-52.
- CRISTESCU, S. M., DE MARTINIS, D., TE LINTEL HEKKERT, S., PARKER, D. H. & HARREN, F. J. 2002. Ethylene production by *Botrytis cinerea* in vitro and in tomatoes. *Appl Environ Microbiol*, 68, 5342-50.
- CUI, H., TSUDA, K. & PARKER, J. E. 2015. Effector-triggered immunity: from pathogen perception to robust defense. *Annu Rev Plant Biol*, 66, 487-511.
- CUI, N., LU, H., WANG, T., ZHANG, W., KANG, L. & CUI, F. 2019. Armet, an aphid effector protein, induces pathogen resistance in plants by promoting the accumulation of salicylic acid. *Philos Trans R Soc Lond B Biol Sci*, 374, 20180314.
- CUKKEMANE, A., SEIFERT, R. & KAUPP, U. B. 2011. Cooperative and uncooperative cyclic-nucleotide-gated ion channels. *Trends Biochem Sci*, 36, 55-64.
- CZECHOWSKI, T., STITT, M., ALTMANN, T., UDVARDI, M. K. & SCHEIBLE, W. R. 2005. Genome-wide identification and testing of superior reference genes for transcript normalization in Arabidopsis. *Plant Physiol*, 139, 5-17.

- DADACZ-NARLOCH, B., BEYHL, D., LARISCH, C., LOPEZ-SANJURJO, E. J., RESKI, R., KUCHITSU, K., MULLER, T. D., BECKER, D., SCHONKNECHT, G. & HEDRICH, R. 2011. A novel calcium binding site in the slow vacuolar cation channel TPC1 senses luminal calcium levels. *Plant Cell*, 23, 2696-707.
- DANON, A., ROTARI, V. I., GORDON, A., MAILHAC, N. & GALLOIS, P. 2004. Ultraviolet-C overexposure induces programmed cell death in Arabidopsis, which is mediated by caspase-like activities and which can be suppressed by caspase inhibitors, p35 and Defender against Apoptotic Death. *J Biol Chem*, 279, 779-87.
- DAVIS, G. K. 2012. Cyclical parthenogenesis and viviparity in aphids as evolutionary novelties. *J Exp Zool B Mol Dev Evol*, 318, 448-59.
- DE LORENZO, G., FERRARI, S., GIOVANNONI, M., MATTEI, B. & CERVONE, F. 2019. Cell wall traits that influence plant development, immunity, and bioconversion. *Plant J*, 97, 134-147.
- DE VOS, M. & JANDER, G. 2009. Myzus persicae (green peach aphid) salivary components induce defence responses in Arabidopsis thaliana. *Plant Cell Environ*, 32, 1548-60.
- DE VOS, M., VAN OOSTEN, V. R., VAN POECKE, R. M., VAN PELT, J. A., POZO, M. J., MUELLER, M. J., BUCHALA, A., MÉTRAUX, J. P., VAN LOON, L. C., DICKE, M. & PIETERSE, C. M. 2005a. Signal signature and transcriptome changes of Arabidopsis during pathogen and insect attack. *Mol. Plant Microbe Interact*, 18, 923-937.
- DE VOS, M., VAN OOSTEN, V. R., VAN POECKE, R. M. P., VAN PELT, J. A., POZO, M. J., MUELLER, M. J., BUCHALA, A. J., MÉTRAUX, J.-P., VAN LOON, L. C., DICKE, M. & PIETERSE, C. M. J. 2005b. Signal Signature and Transcriptome Changes of Arabidopsis During Pathogen and Insect Attack. *MPMI*, 18, 923-937.
- DEDRYVER, C. A., LE RALEC, A. & FABRE, F. 2010. The conflicting relationships between aphids and men: a review of aphid damage and control strategies. *C R Biol*, 333, 539-53.
- DEFALCO, T. A. & ZIPFEL, C. 2021. Molecular mechanisms of early plant pattern-triggered immune signaling. *Mol Cell*, 81, 4346.
- DEMIDCHIK, V., NICHOLS, C., OLIYNYK, M., DARK, A., GLOVER, B. J. & DAVIES, J. M. 2003. Is ATP a signaling agent in plants? *Plant Physiol*, 133, 456-461.
- DEMIDCHIK, V., SHABALA, S., ISAYENKOV, S., CUIN, T. A. & POTTOSIN, I. 2018. Calcium transport across plant membranes: mechanisms and functions. *New Phytol*, 220, 49-69.
- DENOUX, C., GALLETI, R., MAMMARELLA, N., GOPALAN, S., WERCK, D., DE LORENZO, G., FERRARI, S., AUSUBEL, F. M. & DEWDNEY, J. 2008. Activation of defense response pathways by OGs and Flg22 elicitors in Arabidopsis seedlings. *Mol Plant*, 1, 423-45.
- DION, E., ZELE, F., SIMON, J. C. & OUTREMAN, Y. 2011. Rapid evolution of parasitoids when faced with the symbiont-mediated resistance of their hosts. *J Evol Biol*, 24, 741-50.
- DIXON, A. F. G. 1998. *Aphid ecology : an optimization approach*, London, New York, Chapman & Hall.
- DIXON, M. S., JONES, D. A., KEDDLE, J. S., THOMAS, C. M. & JONES, J. D. G. 1996. The Tomato Cf-2 Disease Resistance Locus Comprises Two Functional Genes Encoding Leucine-Rich Repeat Proteins. *Cell*, 84, 451-459.
- DOMAZAKIS, E., WOUTERS, D., VISSER, R. G. F., KAMOUN, S., JOOSTEN, M. & VLEESHOUWERS, V. 2018. The ELR-SOBIR1 Complex Functions as a Two-Component Receptor-Like Kinase to Mount Defense Against Phytophthora infestans. *Mol Plant Microbe Interact*, 31, 795-802.
- DONG, Y., JING, M., SHEN, D., WANG, C., ZHANG, M., LIANG, D., NYAWIRA, K. T., XIA, Q., ZUO, K., WU, S., WU, Y., DOU, D. & XIA, A. 2020. The mirid bug Apolygus lucorum deploys a glutathione peroxidase as a candidate effector to enhance plant susceptibility. *J Exp Bot*, 71, 2701-2712.
- DONGUS, J. A., BHANDARI, D. D., PATEL, M., ARCHER, L., DIJKGRAAF, L., DESLANDES, L., SHAH, J. & PARKER, J. E. 2020. The Arabidopsis PAD4 Lipase-Like Domain Is Sufficient for Resistance to Green Peach Aphid. *Mol Plant Microbe Interact*, 33, 328-335.

- DRUREY, C. 2015. *The dynamics of molecular components that regulate aphid-plant interactions*. Doctoral thesis, University of East Anglia.
- DU, H., XU, H. X., WANG, F., QIAN, L. X., LIU, S. S. & WANG, X. W. 2022. Armet from whitefly saliva acts as an effector to suppress plant defenses by targeting tobacco cystatin. *New Phytol.*
- DU, J., VERZAUX, E., CHAPARRO-GARCIA, A., BIJSTERBOSCH, G., KEIZER, L. C., ZHOU, J., LIEBRAND, T. W., XIE, C., GOVERS, F., ROBATZEK, S., VAN DER VOSSSEN, E. A., JACOBSEN, E., VISSER, R. G., KAMOUN, S. & VLEESHOUWERS, V. G. 2015. Elicitin recognition confers enhanced resistance to *Phytophthora infestans* in potato. *Nat Plants*, 1, 15034.
- DUBIELLA, U., SEYBOLDA, H., DURIANA, G., KOMANDERA, E., LASSIGA, R., WITTEA, C.-P., SCHULZEB, W. X. & ROMEISA, T. 2013. Calcium-dependent protein kinase/NADPH oxidase activation circuit is required for rapid defense signal propagation. *PNAS*, 110.
- DUBOIS, M., VAN DEN BROECK, L. & INZE, D. 2018. The Pivotal Role of Ethylene in Plant Growth. *Trends Plant Sci*, 23, 311-323.
- DUONG, H. N., CHO, S. H., WANG, L., PHAM, A. Q., DAVIES, J. M. & STACEY, G. 2021. Cyclic nucleotide-gated ion channel 6 is involved in extracellular ATP signaling and plant immunity. *Plant J.*
- DUPREE, E. J., JAYATHIRTHA, M., YORKEY, H., MIHASAN, M., PETRE, B. A. & DARIE, C. C. 2020. A Critical Review of Bottom-Up Proteomics: The Good, the Bad, and the Future of this Field. *Proteomes*, 8.
- ELLIS, C., KARAFYLLIDIS, I. & TURNER, J. G. 2002. Constitutive activation of jasmonate signaling in an *Arabidopsis* mutant correlates with enhanced resistance to *Erysiphe cichoracearum*, *Pseudomonas syringae*, and *Myzus persicae*. *Mol Plant Microbe Interact*, 15, 1025-30.
- ELZINGA, D. A., DE VOS, M. & JANDER, G. 2014. Suppression of plant defenses by a *Myzus persicae* (green peach aphid) salivary effector protein. *Mol Plant Microbe Interact*, 27, 747-56.
- ERB, M. & KLIEBENSTEIN, D. J. 2020. Plant Secondary Metabolites as Defenses, Regulators, and Primary Metabolites: The Blurred Functional Trichotomy. *Plant Physiol*, 184, 39-52.
- ERB, M., MELDAU, S. & HOWE, G. A. 2012. Role of phytohormones in insect-specific plant reactions. *Trends Plant Sci*, 17, 250-9.
- ESCUDERO-MARTINEZ, C., RODRIGUEZ, P. A., LIU, S., SANTOS, P. A., STEPHENS, J. & BOS, J. I. B. 2020. An aphid effector promotes barley susceptibility through suppression of defence gene expression. *J Exp Bot*, 71, 2796-2807.
- EULGEM, T. & SOMSSICH, I. E. 2007. Networks of WRKY transcription factors in defense signaling. *Curr Opin Plant Biol*, 10, 366-71.
- EVANS, M. J., CHOI, W. G., GILROY, S. & MORRIS, R. J. 2016. A ROS-Assisted Calcium Wave Dependent on the AtRBOHD NADPH Oxidase and TPC1 Cation Channel Propagates the Systemic Response to Salt Stress. *Plant Physiol*, 171, 1771-84.
- FAN, L., FRÖHLICH, K., MELZER, E., ALBERT, I., PRUITT, R. N., ZHANG, L., ALBERT, M., KIM, S.-T., CHAE, E., WEIGEL, D., GUST, A. A. & NÜRNBERGER, T. 2021. Genotyping-by-sequencing-based identification of *Arabidopsis* pattern recognition receptor RLP32 recognizing proteobacterial translation initiation factor IF1. *bioRxiv preprint*.
- FAN, L., FRÖHLICH, K., MELZER, E., PRUITT, R. N., ALBERT, I., ZHANG, L., JOE, A., HUA, C., SONG, Y., ALBERT, M., KIM, S. T., WEIGEL, D., ZIPFEL, C., CHAE, E., GUST, A. A. & NURNBERGER, T. 2022. Genotyping-by-sequencing-based identification of *Arabidopsis* pattern recognition receptor RLP32 recognizing proteobacterial translation initiation factor IF1. *Nat Commun*, 13, 1294.
- FAULKNER, C., PETUTSCHNIG, E., BENITEZ-ALFONSO, Y., BECK, M., ROBATZEK, S., LIPKA, V. & MAULE, A. J. 2013. LYM2-dependent chitin perception limits molecular flux via plasmodesmata. *Proc Natl Acad Sci U S A*, 110, 9166-70.

- FELIX, G. & BOLLER, T. 2003. Molecular sensing of bacteria in plants. The highly conserved RNA-binding motif RNP-1 of bacterial cold shock proteins is recognized as an elicitor signal in tobacco. *J Biol Chem*, 278, 6201-8.
- FENG, B., LIU, C., DE OLIVEIRA, M. V., INTORNE, A. C., LI, B., BABILONIA, K., DE SOUZA FILHO, G. A., SHAN, L. & HE, P. 2015. Protein poly(ADP-ribosyl)ation regulates arabidopsis immune gene expression and defense responses. *PLoS Genet*, 11, e1004936.
- FEYS, B. J., MOISAN, L. J., NEWMAN, M. A. & PARKER, J. E. 2001. Direct interaction between the Arabidopsis disease resistance signaling proteins, EDS1 and PAD4. *EMBO J*, 20, 5400-11.
- FEYS, B. J., WIERMER, M., BHAT, R. A., MOISAN, L. J., MEDINA-ESCOBAR, N., NEU, C., CABRAL, A. & PARKER, J. E. 2005. Arabidopsis SENESCENCE-ASSOCIATED GENE101 stabilizes and signals within an ENHANCED DISEASE SUSCEPTIBILITY1 complex in plant innate immunity. *Plant Cell*, 17, 2601-13.
- FOKKEMA, N. J., RIPHAGEN, I., POOT, R. J. & DE JONG, C. 1983. Aphid honeydew, a potential stimulant of *Cochliobolus sativus* and *Septoria nodorum* and the competitive role of saprophytic mycoflora. *Trans. British Mycol. Soc.*, 81, 355-363.
- FOYER, C. H., VERRALL, S. R. & HANCOCK, R. D. 2015. Systematic analysis of phloem-feeding insect-induced transcriptional reprogramming in Arabidopsis highlights common features and reveals distinct responses to specialist and generalist insects. *J Exp Bot*, 66, 495-512.
- FRADIN, E. F., ZHANG, Z., JUAREZ AYALA, J. C., CASTROVERDE, C. D., NAZAR, R. N., ROBB, J., LIU, C. M. & THOMMA, B. P. 2009. Genetic dissection of Verticillium wilt resistance mediated by tomato Ve1. *Plant Physiol*, 150, 320-32.
- FREI DIT FREY, N., MBENGUE, M., KWAAITAAL, M., NITSCH, L., ALTENBACH, D., HAWEKER, H., LOZANO-DURAN, R., NJO, M. F., BEECKMAN, T., HUETTEL, B., BORST, J. W., PANSTRUGA, R. & ROBATZEK, S. 2012. Plasma membrane calcium ATPases are important components of receptor-mediated signaling in plant immune responses and development. *Plant Physiol*, 159, 798-809.
- FRERIGMANN, H., PISLEWSKA-BEDNAREK, M., SANCHEZ-VALLET, A., MOLINA, A., GLAWISCHNIG, E., GIGOLASHVILI, T. & BEDNAREK, P. 2016. Regulation of Pathogen-Triggered Tryptophan Metabolism in Arabidopsis thaliana by MYB Transcription Factors and Indole Glucosinolate Conversion Products. *Mol Plant*, 9, 682-695.
- FRITZ-LAYLIN, L. K., KRISHNAMURTHY, N., TOR, M., SJOLANDER, K. V. & JONES, J. D. 2005. Phylogenomic analysis of the receptor-like proteins of rice and Arabidopsis. *Plant Physiol*, 138, 611-23.
- FU, J., SHI, Y., WANG, L., ZHANG, H., LI, J., FANG, J. & JI, R. 2020. Planthopper-Secreted Salivary Disulfide Isomerase Activates Immune Responses in Plants. *Front Plant Sci*, 11, 622513.
- FU, Z. Q. & DONG, X. 2013. Systemic acquired resistance: turning local infection into global defense. *Annu Rev Plant Biol*, 64, 839-63.
- FU, Z. Q., YAN, S., SALEH, A., WANG, W., RUBLE, J., OKA, N., MOHAN, R., SPOEL, S. H., TADA, Y., ZHENG, N. & DONG, X. 2012. NPR3 and NPR4 are receptors for the immune signal salicylic acid in plants. *Nature*, 486, 228-32.
- FUKATSU, T. 2010. Evolution. A fungal past to insect color. *Science*, 328, 574-5.
- FURCH, A. C., VAN BEL, A. J. & WILL, T. 2015. Aphid salivary proteases are capable of degrading sieve-tube proteins. *J Exp Bot*, 66, 533-9.
- FURUKAWA, T., INAGAKI, H., TAKAI, R., HIRAI, H. & CHE, F. S. 2014. Two distinct EF-Tu epitopes induce immune responses in rice and Arabidopsis. *Mol Plant Microbe Interact*, 27, 113-24.
- GALLETTI, R., FERRARI, S. & DE LORENZO, G. 2011. Arabidopsis MPK3 and MPK6 play different roles in basal and oligogalacturonide- or flagellin-induced resistance against Botrytis cinerea. *Plant Physiol*, 157, 804-14.

- GAO, M., WANG, X., WANG, D., XU, F., DING, X., ZHANG, Z., BI, D., CHENG, Y. T., CHEN, S., LI, X. & ZHANG, Y. 2009. Regulation of cell death and innate immunity by two receptor-like kinases in Arabidopsis. *Cell Host Microbe*, 6, 34-44.
- GAO, Q. M., ZHU, S., KACHROO, P. & KACHROO, A. 2015. Signal regulators of systemic acquired resistance. *Front Plant Sci*, 6, 228.
- GAO, X., CHEN, X., LIN, W., CHEN, S., LU, D., NIU, Y., LI, L., CHENG, C., MCCORMACK, M., SHEEN, J., SHAN, L. & HE, P. 2013. Bifurcation of Arabidopsis NLR immune signaling via Ca(2)(+)-dependent protein kinases. *PLoS Pathog*, 9, e1003127.
- GARCIA-CALVO, M., PETERSON, E. P., LEITING, B., RUEL, R., NICHOLSON, D. W. & THORNBERRY, N. A. 1998. Inhibition of human caspases by peptide-based and macromolecular inhibitors. *J Biol Chem*, 273, 32608-13.
- GARCION, C., LOHMANN, A., LAMODIÈRE, E., CATINOT, J., BUCHALA, A., DOERMANN, P. & METRAUX, J.-P. 2008. Characterization and biological function of the ISOCHORISMATE SYNTHASE2 gene of Arabidopsis. *Plant Physiol.*, 147, 1279–1287.
- GE, Y., CAI, Y. M., BONNEAU, L., ROTARI, V., DANON, A., MCKENZIE, E. A., MCLELLAN, H., MACH, L. & GALLOIS, P. 2016. Inhibition of cathepsin B by caspase-3 inhibitors blocks programmed cell death in Arabidopsis. *Cell Death Differ*, 23, 1493-501.
- GEISLER, M., FRANGNE, N., GOMES, E., MARTINOIA, E. & PALMGREN, M. G. 2000. The ACA4 gene of Arabidopsis encodes a vacuolar membrane calcium pump that improves salt tolerance in yeast. *Plant Physiol*, 124, 1814-27.
- GEU-FLORES, F., MOLDRUP, M. E., BOTTCHER, C., OLSEN, C. E., SCHEEL, D. & HALKIER, B. A. 2011. Cytosolic gamma-glutamyl peptidases process glutathione conjugates in the biosynthesis of glucosinolates and camalexin in Arabidopsis. *Plant Cell*, 23, 2456-69.
- GIL, R., SABATER-MUNOZ, B., LATORRE, A., SILVA, F. J. & MOYA, A. 2002. Extreme genome reduction in Buchnera spp.: Toward the minimal genome needed for symbiotic life. *PNAS*, 99, 4454–4458
- GILROY, S., BIALASEK, M., SUZUKI, N., GORECKA, M., DEVIREDDY, A. R., KARPINSKI, S. & MITTLER, R. 2016. ROS, Calcium, and Electric Signals: Key Mediators of Rapid Systemic Signaling in Plants. *Plant Physiol*, 171, 1606-15.
- GILROY, S., SUZUKI, N., MILLER, G., CHOI, W. G., TOYOTA, M., DEVIREDDY, A. R. & MITTLER, R. 2014. A tidal wave of signals: calcium and ROS at the forefront of rapid systemic signaling. *Trends Plant Sci*, 19, 623-30.
- GIMENEZ-IBANEZ, S., BOTER, M., ORTIGOSA, A., GARCIA-CASADO, G., CHINI, A., LEWSEY, M. G., ECKER, J. R., NTOUKAKIS, V. & SOLANO, R. 2017. JAZ2 controls stomata dynamics during bacterial invasion. *New Phytol*, 213, 1378-1392.
- GIMENEZ-IBANEZ, S., HANN, D. R., NTOUKAKIS, V., PETUTSCHNIG, E., LIPKA, V. & RATHJEN, J. P. 2009. AvrPtoB targets the LysM receptor kinase CERK1 to promote bacterial virulence on plants. *Curr Biol*, 19, 423-9.
- GIOLAI, M. 2019. *Spatially resolved transcriptomics reveals plant host responses to the aphid pest Myzus persicae*. Doctoral thesis, University of East Anglia.
- GLAWISCHNIG, E., HANSEN, B. G., OLSEN, C. E. & HALKIER, B. A. 2004. Camalexin is synthesized from indole-3-acetaldoxime, a key branching point between primary and secondary metabolism in Arabidopsis. *PNAS*, 101, 8245–8250.
- GLAZEBROOK, J. 2005. Contrasting mechanisms of defense against biotrophic and necrotrophic pathogens. *Annu. Rev. Phytopathol.*, 43, 205–27.
- GOHRE, V., SPALLEK, T., HAWEKER, H., MERSMANN, S., MENTZEL, T., BOLLER, T., DE TORRES, M., MANSFIELD, J. W. & ROBATZEK, S. 2008. Plant pattern-recognition receptor FLS2 is directed for degradation by the bacterial ubiquitin ligase AvrPtoB. *Curr Biol*, 18, 1824-32.
- GOMEZ-GOMEZ, L. & BOLLER, T. 2000. FLS2: an LRR receptor-like kinase involved in the perception of the bacterial elicitor flagellin in Arabidopsis. *Mol Cell*, 5, 1003-11.

- GÓMEZ-GÓMEZ, L., FELIX, G. & BOLLER, T. 1999. A single locus determines sensitivity to bacterial flagellin in *Arabidopsis thaliana*. *The Plant Journal*, 18, 277–284.
- GONG, B. Q., GUO, J., ZHANG, N., YAO, X., WANG, H. B. & LI, J. F. 2019. Cross-Microbial Protection via Priming a Conserved Immune Co-Receptor through Juxtamembrane Phosphorylation in Plants. *Cell Host Microbe*, 26, 810-822 e7.
- GOUHIER-DARIMONT, C., SCHMIESING, A., BONNET, C., LASSUEUR, S. & REYMOND, P. 2013. Signalling of *Arabidopsis thaliana* response to *Pieris brassicae* eggs shares similarities with PAMP-triggered immunity. *J Exp Bot*, 64, 665-74.
- GOUHIER-DARIMONT, C., STAHL, E., GLAUSER, G. & REYMOND, P. 2019. The *Arabidopsis* Lectin Receptor Kinase LecRK-I.8 Is Involved in Insect Egg Perception. *Front Plant Sci*, 10, 623.
- GRAVINO, M., SAVATIN, D. V., MACONE, A. & DE LORENZO, G. 2015. Ethylene production in *Botrytis cinerea*- and oligogalacturonide-induced immunity requires calcium-dependent protein kinases. *Plant J*, 84, 1073-86.
- GRONNIER, J., FRANCK, C. M., STEGMANN, M., DEFALCO, T. A., ABARCA, A., VON ARX, M., DUNSER, K., LIN, W., YANG, Z., KLEINE-VEHN, J., RINGLI, C. & ZIPFEL, C. 2022. Regulation of immune receptor kinase plasma membrane nanoscale organization by a plant peptide hormone and its receptors. *Elife*, 11.
- GROUX, R., STAHL, E., GOUHIER-DARIMONT, C., KERDAFFREC, E., JIMENEZ-SANDOVAL, P., SANTIAGO, J. & REYMOND, P. 2021. *Arabidopsis* natural variation in insect egg-induced cell death reveals a role for LECTIN RECEPTOR KINASE-I.1. *Plant Physiol*, 185, 240-255.
- GUAN, R., SU, J., MENG, X., LI, S., LIU, Y., XU, J. & ZHANG, S. 2015. Multilayered Regulation of Ethylene Induction Plays a Positive Role in *Arabidopsis* Resistance against *Pseudomonas syringae*. *Plant Physiol*, 169, 299-312.
- GUO, H., ZHANG, Y., TONG, J., GE, P., WANG, Q., ZHAO, Z., ZHU-SALZMAN, K., HOGENHOUT, S. A., GE, F. & SUN, Y. 2020. An Aphid-Secreted Salivary Protease Activates Plant Defense in Phloem. *Curr Biol*, 30, 4826-4836 e7.
- GUST, A. A. & FELIX, G. 2014. Receptor like proteins associate with SOBIR1-type of adaptors to form bimolecular receptor kinases. *Curr Opin Plant Biol*, 21, 104-111.
- GUST, A. A., WILLMANN, R., DESAKI, Y., GRABHERR, H. M. & NURNBERGER, T. 2012. Plant LysM proteins: modules mediating symbiosis and immunity. *Trends Plant Sci*, 17, 495-502.
- HALKIER, B. A. & GERSHENZON, J. 2006. Biology and biochemistry of glucosinolates. *Annu Rev Plant Biol*, 57, 303-33.
- HALTER, T., IMKAMPE, J., MAZZOTTA, S., WIERZBA, M., POSTEL, S., BUCHERL, C., KIEFER, C., STAHL, M., CHINCHILLA, D., WANG, X., NURNBERGER, T., ZIPFEL, C., CLOUSE, S., BORST, J. W., BOEREN, S., DE VRIES, S. C., TAX, F. & KEMMERLING, B. 2014. The leucine-rich repeat receptor kinase BIR2 is a negative regulator of BAK1 in plant immunity. *Curr Biol*, 24, 134-143.
- HANADA, K., TAMAI, M., YAMAGISHI, M., OHMURA, S., SADAWA, J. & TANAKA, I. 1978. Isolation and Characterization of E-64, a New Thiol Protease inhibitor. *Agric. Biol. Chem.*, 42, 523 - 528.
- HANDER, T., FERNANDEZ-FERNANDEZ, A. D., KUMPF, R. P., WILLEMS, P., SCHATOWITZ, H., ROMBAUT, D., STAES, A., NOLF, J., POTTIE, R., YAO, P., GONCALVES, A., PAVIE, B., BOLLER, T., GEVAERT, K., VAN BREUSEGEM, F., BARTELS, S. & STAEL, S. 2019. Damage on plants activates Ca(2+)-dependent metacaspases for release of immunomodulatory peptides. *Science*, 363.
- HARMEL, N., LÉTOCART, E., CHERQUI, A., GIORDANENGO, P., MAZZUCHELLI, G., GUILLONNEAU, F., DE PAUW, E., HAUBRUGE, E. & FRANCIS, F. 2008. Identification of aphid salivary proteins: a proteomic investigation of *Myzus persicae*. *Insect Molecular Biology* 17 165–174.
- HARUTA, M., SABAT, G., STECKER, K., MINKOFF, B. B. & SUSSMAN, M. R. 2014. A peptide hormone and its receptor protein kinase regulate plant cell expansion. *Science*, 343, 408-11.

- HAYAFUNE, M., BERISIO, R., MARCHETTI, R., SILIPO, A., KAYAMA, M., DESAKI, Y., ARIMA, S., SQUEGLIA, F., RUGGIERO, A., TOKUYASU, K., MOLINARO, A., KAKU, H. & SHIBUYA, N. 2014. Chitin-induced activation of immune signaling by the rice receptor CEBiP relies on a unique sandwich-type dimerization. *Proc Natl Acad Sci U S A*, 111, E404-13.
- HE, P., SHAN, L., LIN, N. C., MARTIN, G. B., KEMMERLING, B., NURNBERGER, T. & SHEEN, J. 2006. Specific bacterial suppressors of MAMP signaling upstream of MAPKKK in Arabidopsis innate immunity. *Cell*, 125, 563-75.
- HEESE, A., HANN, D. R., GIMENEZ-IBANEZ, S., JONES, A. M., HE, K., LI, J., SCHROEDER, J. I., PECK, S. C. & RATHJEN, J. P. 2007. The receptor-like kinase SERK3/BAK1 is a central regulator of innate immunity in plants. *Proc Natl Acad Sci U S A*, 104, 12217-22.
- HEGENAUER, V., FÜRST, U., KAISER, B., SMOKER, M., ZIPFEL, C., FELIX, G., STAHL, M. & ALBERT, M. 2016. Detection of the plant parasite *Cuscuta reflexa* by a tomato cell surface receptor. *Science*, 353
- HETTENHAUSEN, C., SCHUMAN, M. C. & WU, J. 2015. MAPK signaling: a key element in plant defense response to insects. *Insect Sci*, 22, 157-64.
- HEWER, A., WILL, T. & VAN BEL, A. J. 2010. Plant cues for aphid navigation in vascular tissues. *J Exp Biol*, 213, 4030-42.
- HILFIKER, O., GROUX, R., BRUESSOW, F., KIEFER, K., ZEIER, J. & REYMOND, P. 2014. Insect eggs induce a systemic acquired resistance in Arabidopsis. *Plant J*, 80, 1085-94.
- HILLEARY, R., PAEZ-VALENCIA, J., VENS, C., TOYOTA, M., PALMGREN, M. & GILROY, S. 2020. Tonoplast-localized Ca(2+) pumps regulate Ca(2+) signals during pattern-triggered immunity in Arabidopsis thaliana. *Proc Natl Acad Sci U S A*, 117, 18849-18857.
- HIND, S. R., STRICKLER, S. R., BOYLE, P. C., DUNHAM, D. M., BAO, Z., O'DOHERTY, I. M., BACCILE, J. A., HOKI, J. S., VIOX, E. G., CLARKE, C. R., VINATZER, B. A., SCHROEDER, F. C. & MARTIN, G. B. 2016. Tomato receptor FLAGELLIN-SENSING 3 binds flgII-28 and activates the plant immune system. *Nat Plants*, 2, 16128.
- HIRAMATSU, A. & OUCHI, T. 1963. On the Proteolytic Enzymes from the Commercial Protease Preparation of *Streptomyces Griseus* (Pronase P). *J Biochem*, 54, 462-4.
- HIRUMA, K., FUKUNAGA, S., BEDNAREK, P., PISLEWSKA-BEDNAREK, M., WATANABE, S., NARUSAKA, Y., SHIRASU, K. & TAKANO, Y. 2013. Glutathione and tryptophan metabolism are required for Arabidopsis immunity during the hypersensitive response to hemibiotrophs. *Proc Natl Acad Sci U S A*, 110, 9589-94.
- HO, C. S., LAM, C. W., CHAN, M. H., CHEUNG, R. C., LAW, L. K., LIT, L. C., NG, K. F., SUEN, M. W. & TAI, H. L. 2003. Electrospray ionisation mass spectrometry: principles and clinical applications. *Clin Biochem Rev*, 24, 3-12.
- HOGENHOUT, S. A., AMMAR EL, D., WHITFIELD, A. E. & REDINBAUGH, M. G. 2008. Insect vector interactions with persistently transmitted viruses. *Annu Rev Phytopathol*, 46, 327-59.
- HOHENSTEIN, J. D., STUDHAM, M. E., KLEIN, A., KOVINICH, N., BARRY, K., LEE, Y. J. & MACINTOSH, G. C. 2019. Transcriptional and Chemical Changes in Soybean Leaves in Response to Long-Term Aphid Colonization. *Front Plant Sci*, 10, 310.
- HOLMAN, J. 2008. BOOK REVIEW: Blackman R.L. & Eastop V.F.: Aphids on the World's Herbaceous Plants and Shrubs. *European Journal of Entomology*, 105, 164-164.
- HOOK, V. Y. & LOH, Y. P. 1984. Carboxypeptidase B-like converting enzyme activity in secretory granules of rat pituitary. *Proc Natl Acad Sci U S A*, 81, 2776-80.
- HORSEFIELD, S., BURDETT, H., ZHANG, X., MANIK, M. K., SHI, Y., CHEN, J., QI, T., GILLEY, J.-S., LAI, J., RANK, M. X., CASEY, L. W., GU, W., ERICSSON, D. J., FOLEY, G., HUGHES, R. O., BOSANAC, T., VON ITZSTEIN, M., P., R., NANSON, J. D., BODEN, M., DRY, I. B., WILLIAMS, S. J., STASKAWICZ, B. J., COLEMAN, M. P., VE, T., DODDS, P. N. & KOBE, B. 2019. NAD+ cleavage activity by animal and plant TIR domains in cell death pathways. *Science*, 365, 793-799.
- HOU, S., LIU, Z., SHEN, H. & WU, D. 2019. Damage-Associated Molecular Pattern-Triggered Immunity in Plants. *Front Plant Sci*, 10, 646.

- HOU, S., WANG, X., CHEN, D., YANG, X., WANG, M., TURRA, D., DI PIETRO, A. & ZHANG, W. 2014. The secreted peptide PIP1 amplifies immunity through receptor-like kinase 7. *PLoS Pathog*, 10, e1004331.
- HOWE, G. A. & JANDER, G. 2008. Plant immunity to insect herbivores. *Annu Rev Plant Biol*, 59, 41-66.
- HUANG, C., YAN, Y., ZHAO, H., YE, Y. & CAO, Y. 2020. Arabidopsis CPK5 Phosphorylates the Chitin Receptor LYK5 to Regulate Plant Innate Immunity. *Front Plant Sci*, 11, 702.
- HUANG, H. J., CUI, J. R., XIA, X., CHEN, J., YE, Y. X., ZHANG, C. X. & HONG, X. Y. 2019. Salivary DNase II from *Laodelphax striatellus* acts as an effector that suppresses plant defence. *New Phytol*, 224, 860-874.
- HUANG, H. J., LU, J. B., LI, Q., BAO, Y. Y. & ZHANG, C. X. 2018. Combined transcriptomic/proteomic analysis of salivary gland and secreted saliva in three planthopper species. *J Proteomics*, 172, 25-35.
- HUFFAKER, A., PEARCE, G. & RYAN, C. A. 2006. Endogenous peptide defense signals in Arabidopsis differentially amplify signaling for the innate immune response. *Proc Natl Acad Sci USA*, 103, 10098-10103
- HUFFAKER, A., PEARCE, G., VEYRAT, N., ERB, M., TURLINGS, T. C., SARTOR, R., SHEN, Z., BRIGGS, S. P., VAUGHAN, M. M., ALBORN, H. T., TEAL, P. E. & SCHMELZ, E. A. 2013. Plant elicitor peptides are conserved signals regulating direct and indirect antiherbivore defense. *Proc Natl Acad Sci U S A*, 110, 5707-12.
- HUOT, B., YAO, J., MONTGOMERY, B. L. & HE, S. Y. 2014. Growth-defense tradeoffs in plants: a balancing act to optimize fitness. *Mol Plant*, 7, 1267-1287.
- IIDA, J., DESAKI, Y., HATA, K., UEMURA, T., YASUNO, A., ISLAM, M., MAFFEI, M. E., OZAWA, R., NAKAJIMA, T., GALIS, I. & ARIMURA, G. I. 2019. Tetrans: new putative spider mite elicitors of host plant defense. *New Phytol*, 224, 875-885.
- IMKAMPE, J., HALTER, T., HUANG, S., SCHULZE, S., MAZZOTTA, S., SCHMIDT, N., MANSTRETTA, R., POSTEL, S., WIERZBA, M., YANG, Y., VAN DONGEN, W., STAHL, M., ZIPFEL, C., GOSHE, M. B., CLOUSE, S., DE VRIES, S. C., TAX, F., WANG, X. & KEMMERLING, B. 2017. The Arabidopsis Leucine-Rich Repeat Receptor Kinase BIR3 Negatively Regulates BAK1 Receptor Complex Formation and Stabilizes BAK1. *Plant Cell*, 29, 2285-2303.
- ISHIHAMA, N. & YOSHIOKA, H. 2012. Post-translational regulation of WRKY transcription factors in plant immunity. *Curr Opin Plant Biol*, 15, 431-7.
- JAMIESON, P. A., SHAN, L. & HE, P. 2018. Plant cell surface molecular cypher: Receptor-like proteins and their roles in immunity and development. *Plant Sci*, 274, 242-251.
- JAOUANNET, M., MORRIS, J. A., HEDLEY, P. E. & BOS, J. I. 2015. Characterization of Arabidopsis Transcriptional Responses to Different Aphid Species Reveals Genes that Contribute to Host Susceptibility and Non-host Resistance. *PLoS Pathog*, 11, e1004918.
- JAOUANNET, M., RODRIGUEZ, P. A., THORPE, P., LENOIR, C. J., MACLEOD, R., ESCUDERO-MARTINEZ, C. & BOS, J. I. 2014. Plant immunity in plant-aphid interactions. *Front Plant Sci*, 5, 663.
- JEHLE, A. K., LIPSCHIS, M., ALBERT, M., FALLAHZADEH-MAMAGHANI, V., FURST, U., MUELLER, K. & FELIX, G. 2013. The receptor-like protein ReMAX of Arabidopsis detects the microbe-associated molecular pattern eMax from *Xanthomonas*. *Plant Cell*, 25, 2330-40.
- JI, R., FU, J., SHI, Y., LI, J., JING, M., WANG, L., YANG, S., TIAN, T., WANG, L., JU, J., GUO, H., LIU, B., DOU, D., HOFFMANN, A. A., ZHU-SALZMAN, K. & FANG, J. 2021. Vitellogenin from planthopper oral secretion acts as a novel effector to impair plant defenses. *New Phytol*, 232, 802-817.
- JIANG, Y., HAN, B., ZHANG, H., MARIAPPAN, K. G., BIGEARD, J., COLCOMBET, J. & HIRT, H. 2019. MAP4K4 associates with BIK1 to regulate plant innate immunity. *EMBO Rep*, 20, e47965.

- JOHANSSON, O. N., FANTOZZI, E., FAHLBERG, P., NILSSON, A. K., BUHOT, N., TOR, M. & ANDERSSON, M. X. 2014. Role of the penetration-resistance genes PEN1, PEN2 and PEN3 in the hypersensitive response and race-specific resistance in *Arabidopsis thaliana*. *Plant J*, 79, 466-76.
- JOHNSON, S. N., ROWE, R. C. & HALL, C. R. 2020. Aphid Feeding Induces Phytohormonal Cross-Talk without Affecting Silicon Defense against Subsequent Chewing Herbivores. *Plants (Basel)*, 9.
- JONES, D. A., THOMAS, C. M., HAMMOND-KOSACK, K. E., BALINT-KURTI, P. J. & JONES, J. D. 1994. Isolation of the tomato Cf-9 gene for resistance to *Cladosporium fulvum* by transposon tagging. *Science*, 266, 789-93.
- JONES, J. D. & DANGL, J. L. 2006. The plant immune system. *Nature*, 444, 323-9.
- JURKOWSKI, G. I., SMITH, J. R. K., YU, I.-C., HAM, J. H., SHARMA, S. B., KLESSIG, D. F., FENGLER, K. A. & BENT, A. F. 2004. *Arabidopsis* DND2, a Second Cyclic Nucleotide-Gated Ion Channel Gene for Which Mutation Causes the "Defense, No Death" Phenotype. *MPMI*, 17, 511-520.
- KADOTA, Y., SKLENAR, J., DERBYSHIRE, P., STRANSFELD, L., ASAI, S., NTOUKAKIS, V., JONES, J. D., SHIRASU, K., MENKE, F., JONES, A. & ZIPFEL, C. 2014. Direct regulation of the NADPH oxidase RBOHD by the PRR-associated kinase BIK1 during plant immunity. *Mol Cell*, 54, 43-55.
- KAISER, B., VOGG, G., FURST, U. B. & ALBERT, M. 2015. Parasitic plants of the genus *Cuscuta* and their interaction with susceptible and resistant host plants. *Front Plant Sci*, 6, 45.
- KAKU, H., NISHIZAWA, Y., ISHII-MINAMI, N., AKIMOTO-TOMIYAMA, C., DOHMAE, N., TAKIO, K., MINAMI, E. & SHIBUYA, N. 2006. Plant cells recognize chitin fragments for defense signaling through a plasma membrane receptor. *PNAS*, 103.
- KATO, H., ONAI, K., ABE, A., SHIMIZU, M., TAKAGI, H., TATEDA, C., UTSUSHI, H., SINGKARABANIT-OGAWA, S., KITAKURA, S., ONO, E., ZIPFEL, C., TAKANO, Y., ISHIURA, M. & TERAUCHI, R. 2020. Lumi-Map, a Real-Time Luciferase Bioluminescence Screen of Mutants Combined with MutMap, Reveals *Arabidopsis* Genes Involved in PAMP-Triggered Immunity. *Mol Plant Microbe Interact*, 33, 1366-1380.
- KATSIR, L., SCHILMILLER, A. L., STASWICK, P. E., HE, S. Y. & HOWE, G. A. 2008. COI1 is a critical component of a receptor for jasmonate and the bacterial virulence factor coronatine. *Proc Natl Acad Sci U S A*, 105, 7100-5.
- KAWAHARADA, Y., KELLY, S., NIELSEN, M. W., HJULER, C. T., GYSEL, K., MUSZYNSKI, A., CARLSON, R. W., THYGESEN, M. B., SANDAL, N., ASMUSSEN, M. H., VINTHER, M., ANDERSEN, S. U., KRUSELL, L., THIRUP, S., JENSEN, K. J., RONSON, C. W., BLAISE, M., RADUTOIU, S. & STOUGAARD, J. 2015. Receptor-mediated exopolysaccharide perception controls bacterial infection. *Nature*, 523, 308-12.
- KEIL, B. 1987. Proteolysis Data Bank: specificity of alpha-chymotrypsin from computation of protein cleavages. *Protein Seq Data Anal*, 1, 13-20.
- KERCHEV, P. I., KARPINSKA, B., MORRIS, J. A., HUSSAIN, A., VERRALL, S. R., HEDLEY, P. E., FENTON, B., FOYER, C. H. & HANCOCK, R. D. 2013. Vitamin C and the abscisic acid-insensitive 4 transcription factor are important determinants of aphid resistance in *Arabidopsis*. *Antioxid Redox Signal*, 18, 2091-105.
- KESARWANI, M., YOO, J. & DONG, X. 2007. Genetic interactions of TGA transcription factors in the regulation of pathogenesis-related genes and disease resistance in *Arabidopsis*. *Plant Physiol*, 144, 336-46.
- KETTLES, G. J. 2011. *Analysis of Arabidopsis thaliana small RNA-mediated defence responses to infestation by the green peach aphid Myzus persicae*. PhD, University of East Anglia.
- KETTLES, G. J., DRUREY, C., SCHOONBEEK, H. J., MAULE, A. J. & HOGENHOUT, S. A. 2013. Resistance of *Arabidopsis thaliana* to the green peach aphid, *Myzus persicae*, involves camalexin and is regulated by microRNAs. *New Phytol*, 198, 1178-90.

- KETTLES, G. J. & KALOSHIAN, I. 2016. The Potato Aphid Salivary Effector Me47 Is a Glutathione-S-Transferase Involved in Modifying Plant Responses to Aphid Infestation. *Front. Plant Sci.*, 7.
- KIEP, V., VADASSERY, J., LATTKE, J., MAASS, J. P., BOLAND, W., PEITER, E. & MITHOFER, A. 2015. Systemic cytosolic Ca(2+) elevation is activated upon wounding and herbivory in Arabidopsis. *New Phytol*, 207, 996-1004.
- KIM, J. H. & JANDER, G. 2007. Myzus persicae (green peach aphid) feeding on Arabidopsis induces the formation of a deterrent indole glucosinolate. *Plant J*, 49, 1008-19.
- KIMURA, S., KAWARAZAKI, T., NIBORI, H., MICHIKAWA, M., IMAI, A., KAYA, H. & KUCHITSU, K. 2013. The CBL-interacting protein kinase CIPK26 is a novel interactor of Arabidopsis NADPH oxidase AtRbohF that negatively modulates its ROS-producing activity in a heterologous expression system. *J Biochem*, 153, 191-5.
- KING, R., BONFIGLIO, R., FERNANDEZ-METZLER, C., MILLER-STEIN, C. & OLAH, T. 2000. Mechanistic investigation of ionization suppression in electrospray ionization. *J Am Soc Mass Spectrom*, 11, 942-50.
- KLOTH, K. J., WIEGERS, G. L., BUSSCHER-LANGE, J., VAN HAARST, J. C., KRUIJER, W., BOUWMEESTER, H. J., DICKE, M. & JONGSMA, M. A. 2016. AtWRKY22 promotes susceptibility to aphids and modulates salicylic acid and jasmonic acid signalling. *J Exp Bot*, 67, 3383-96.
- KOBE, B. & DEISENHOFER, J. 1994. The leucine-rich repeat: a versatile binding motif. *Trends Biochem Sci*, 19, 415-21.
- KOENIG, T., MENZE, B. H., KIRCHNER, M., MONIGATTI, F., PARKER, K. C., PATTERSON, T., STEEN, J. J., HAMPRECHT, F. A. & STEEN, H. 2008. Robust prediction of the MASCOT score for an improved quality assessment in mass spectrometric proteomics. *J Proteome Res*, 7, 3708-17.
- KONG, A. T., LEPREVOST, F. V., AVTONOMOV, D. M., MELLACHERUVU, D. & NESVIZHSHKII, A. I. 2017. MSFragger: ultrafast and comprehensive peptide identification in mass spectrometry-based proteomics. *Nat Methods*, 14, 513-520.
- KONG, L., RODRIGUES, B., KIM, J. H., HE, P. & SHAN, L. 2021. More than an on-and-off switch: Post-translational modifications of plant pattern recognition receptor complexes. *Curr Opin Plant Biol*, 63, 102051.
- KOSETSU, K., MATSUNAGA, S., NAKAGAMI, H., COLCOMBET, J., SASABE, M., SOYANO, T., TAKAHASHI, Y., HIRT, H. & MACHIDA, Y. 2010. The MAP kinase MPK4 is required for cytokinesis in Arabidopsis thaliana. *Plant Cell*, 22, 3778-90.
- KUBICEK, C. P., STARR, T. L. & GLASS, N. L. 2014. Plant cell wall-degrading enzymes and their secretion in plant-pathogenic fungi. *Annu Rev Phytopathol*, 52, 427-51.
- KUNZE, G., ZIPFEL, C., ROBATZEK, S., NIEHAUS, K., BOLLER, T. & FELIX, G. 2004. The N terminus of bacterial elongation factor Tu elicits innate immunity in Arabidopsis plants. *Plant Cell*, 16, 3496-507.
- KUSHNIROV, V. V., DERGALEV, A. A. & ALEXANDROV, A. I. 2020. Proteinase K resistant cores of prions and amyloids. *Prion*, 14, 11-19.
- KUSNIERCZYK, A., WINGE, P., JORSTAD, T. S., TROCZYNSKA, J., ROSSITER, J. T. & BONES, A. M. 2008. Towards global understanding of plant defence against aphids--timing and dynamics of early Arabidopsis defence responses to cabbage aphid (*Brevicoryne brassicae*) attack. *Plant Cell Environ*, 31, 1097-115.
- KWAAITAAL, M., HUISMAN, R., MAINTZ, J., REINSTADLER, A. & PANSTRUGA, R. 2011. Ionotropic glutamate receptor (iGluR)-like channels mediate MAMP-induced calcium influx in Arabidopsis thaliana. *Biochem J*, 440, 355-65.
- LAFLAMME, B., DILLON, M. M., MARTEL, A., ALMEIDA, R. N. D., DESVEAUX, D. & GUTTMAN, D. S. 2020. The pan-genome effector-triggered immunity landscape of a host-pathogen interaction. *Science*, 367, 763-768.

- LARKAN, N. J., LYDIATE, D. J., PARKIN, I. A. P., NELSON, M. N., EPP, D. J., COWLING, W. A., RIMMER, S. R. & BORHAN, M. H. 2013. The Brassica napus blackleg resistance gene LepR3 encodes a receptor-like protein triggered by the *Leptosphaeria maculans* effector AVR_{LM1}. *New Phytol*, 197, 595-605.
- LARKAN, N. J., MA, L. & BORHAN, M. H. 2015. The Brassica napus receptor-like protein RLM2 is encoded by a second allele of the LepR3/Rlm2 blackleg resistance locus. *Plant Biotechnol J*, 13, 983-92.
- LEATHER, S. R. 1989. Do Alate Aphids Produce Fitter Offspring? The Influence of Maternal Rearing History and Morph on Life-History Parameters of *Rhopalosiphum padi* (L.). *Functional Ecology*, 3, 237-244.
- LEBRUN-GARCIA, A., OUAKED, F., CHILTZ, A. & PUGI, A. 1998. Activation of MAPK homologues by elicitors in tobacco cells *The Plant Journal*, 15, 773-781.
- LECOURIEUX, D., MAZARS, C., PAULY, N., RANJEVA, R. & PUGIN, A. 2002. Analysis and effects of cytosolic free calcium increases in response to elicitors in *Nicotiana plumbaginifolia* cells. *Plant Cell*, 14, 2627-41.
- LEE, D. H., LEE, H. S. & BELKHADIR, Y. 2021. Coding of plant immune signals by surface receptors. *Curr Opin Plant Biol*, 62, 102044.
- LEGER, R. J. S., JOSHI, L. & ROBERTS, D. W. 1997. Adaptation of proteases and carbohydrates of saprophytic, phytopathogenic and entomopathogenic fungi to the requirements of their ecological niches. *Microbiology (Reading)*, 143 (Pt 6), 1983-1992.
- LEI, J., S, A. F., SALZMAN, R. A., SHAN, L. & ZHU-SALZMAN, K. 2014. BOTRYTIS-INDUCED KINASE1 Modulates Arabidopsis Resistance to Green Peach Aphids via PHYTOALEXIN DEFICIENT4. *Plant Physiol*, 165, 1657-1670.
- LEI, J. & ZHU-SALZMAN, K. 2015. Enhanced aphid detoxification when confronted by a host with elevated ROS production. *Plant Signal Behav*, 10, e1010936.
- LEITNER, M., BOLAND, W. & MITHOFER, A. 2005. Direct and indirect defences induced by piercing-sucking and chewing herbivores in *Medicago truncatula*. *New Phytol*, 167, 597-606.
- LENG, Q., MERCIER, R. W., YAO, W. Z. & BERKOWITZ, G. A. 1999. Cloning and first functional characterization of a plant cyclic nucleotide-gated cation channel. *Plant Physiology*, 121, 753-761.
- LEON-REYES, A., DU, Y., KOORNNEEF, A., PROIETTI, S., KORBES, A. P., MEMELINK, J., PIETERSE, C. M. & RITSEMA, T. 2010. Ethylene signaling renders the jasmonate response of Arabidopsis insensitive to future suppression by salicylic Acid. *Mol Plant Microbe Interact*, 23, 187-97.
- LI, B., FERREIRA, M. A., HUANG, M., CAMARGOS, L. F., YU, X., TEIXEIRA, R. M., CARPINETTI, P. A., MENDES, G. C., GOUVEIA-MAGESTE, B. C., LIU, C., PONTES, C. S. L., BRUSTOLINI, O. J. B., MARTINS, L. G. C., MELO, B. P., DUARTE, C. E. M., SHAN, L., HE, P. & FONTES, E. P. B. 2019. The receptor-like kinase NIK1 targets FLS2/BAK1 immune complex and inversely modulates antiviral and antibacterial immunity. *Nat Commun*, 10, 4996.
- LI, C., YE, F. L., CHEUNG, A. Y., DUAN, Q., KITA, D., LIU, M. C., MAMAN, J., LUU, E. J., WU, B. W., GATES, L., JALAL, M., KWONG, A., CARPENTER, H. & WU, H. M. 2015a. Glycosylphosphatidylinositol-anchored proteins as chaperones and co-receptors for FERONIA receptor kinase signaling in Arabidopsis. *Elife*, 4.
- LI, F., CHENG, C., CUI, F., DE OLIVEIRA, M. V., YU, X., MENG, X., INTORNE, A. C., BABILONIA, K., LI, M., LI, B., CHEN, S., MA, X., XIAO, S., ZHENG, Y., FEI, Z., METZ, R. P., JOHNSON, C. D., KOIWA, H., SUN, W., LI, Z., DE SOUZA FILHO, G. A., SHAN, L. & HE, P. 2014a. Modulation of RNA polymerase II phosphorylation downstream of pathogen perception orchestrates plant immunity. *Cell Host Microbe*, 16, 748-58.
- LI, G., MENG, X., WANG, R., MAO, G., HAN, L., LIU, Y. & ZHANG, S. 2012. Dual-Level Regulation of ACC Synthase Activity by MPK3/MPK6 Cascade and Its Downstream WRKY

- Transcription Factor during Ethylene Induction in Arabidopsis. *PLOS genetics*, 8, e1002767.
- LI, L., LI, M., YU, L., ZHOU, Z., LIANG, X., LIU, Z., CAI, G., GAO, L., ZHANG, X., WANG, Y., CHEN, S. & ZHOU, J. M. 2014b. The FLS2-associated kinase BIK1 directly phosphorylates the NADPH oxidase RbohD to control plant immunity. *Cell Host Microbe*, 15, 329-38.
- LI, P., SONG, A., GAO, C., JIANG, J., CHEN, S., FANG, W., ZHANG, F. & CHEN, F. 2015b. The over-expression of a chrysanthemum WRKY transcription factor enhances aphid resistance. *Plant Physiol Biochem.*, 95, 26-34.
- LI, Q., XIE, Q.-G., SMITH-BECKER, J., NAVARRE, D. A. & KALOSHIAN, I. 2006. Mi-1-Mediated Aphid Resistance Involves Salicylic Acid and Mitogen-Activated Protein Kinase Signaling Cascades. *MPMI*, 19, 655–664.
- LIANG, X., DING, P., LIAN, K., WANG, J., MA, M., LI, L., LI, L., LI, M., ZHANG, X., CHEN, S., ZHANG, Y. & ZHOU, J. M. 2016. Arabidopsis heterotrimeric G proteins regulate immunity by directly coupling to the FLS2 receptor. *Elife*, 5, e13568.
- LIEBRAND, T. W., VAN DEN BERG, G. C., ZHANG, Z., SMIT, P., CORDEWENER, J. H., AMERICA, A. H., SKLENAR, J., JONES, A. M., TAMELING, W. I., ROBATZEK, S., THOMMA, B. P. & JOOSTEN, M. H. 2013. Receptor-like kinase SOBIR1/EVR interacts with receptor-like proteins in plant immunity against fungal infection. *Proc Natl Acad Sci U S A*, 110, 10010-5.
- LIEBRAND, T. W., VAN DEN BURG, H. A. & JOOSTEN, M. H. 2014. Two for all: receptor-associated kinases SOBIR1 and BAK1. *Trends Plant Sci*, 19, 123-32.
- LIN, G., ZHANG, L., HAN, Z., YANG, X., LIU, W., LI, E., CHANG, J., QI, Y., SHPAK, E. D. & CHAI, J. 2017. A receptor-like protein acts as a specificity switch for the regulation of stomatal development. *Genes Dev*, 31, 927-938.
- LIN, W., LI, B., LU, D., CHEN, S., ZHU, N., HE, P. & SHAN, L. 2014. Tyrosine phosphorylation of protein kinase complex BAK1/BIK1 mediates Arabidopsis innate immunity. *Proc Natl Acad Sci U S A*, 111, 3632-7.
- LIU, B., LI, J. F., AO, Y., QU, J., LI, Z., SU, J., ZHANG, Y., LIU, J., FENG, D., QI, K., HE, Y., WANG, J. & WANG, H. B. 2012. Lysin motif-containing proteins LYP4 and LYP6 play dual roles in peptidoglycan and chitin perception in rice innate immunity. *Plant Cell*, 24, 3406-19.
- LIU, J., LIU, B., CHEN, S., GONG, B. Q., CHEN, L., ZHOU, Q., XIONG, F., WANG, M., FENG, D., LI, J. F., WANG, H. B. & WANG, J. 2018. A Tyrosine Phosphorylation Cycle Regulates Fungal Activation of a Plant Receptor Ser/Thr Kinase. *Cell Host Microbe*, 23, 241-253 e6.
- LIU, S., KRACHER, B., ZIEGLER, J., BIRKENBIHL, R. P. & SOMSSICH, I. E. 2015. Negative regulation of ABA signaling by WRKY33 is critical for Arabidopsis immunity towards Botrytis cinerea 2100. *Elife*, 4, e07295.
- LIU, Y., HUANG, X., LI, M., HE, P. & ZHANG, Y. 2016. Loss-of-function of Arabidopsis receptor-like kinase BIR1 activates cell death and defense responses mediated by BAK1 and SOBIR1. *New Phytol*, 212, 637-645.
- LIU, Y., SUN, T., SUN, Y., ZHANG, Y., RADOJICIC, A., DING, Y., TIAN, H., HUANG, X., LAN, J., CHEN, S., ORDUNA, A. R., ZHANG, K., JETTER, R., LI, X. & ZHANG, Y. 2020. Diverse Roles of the Salicylic Acid Receptors NPR1 and NPR3/NPR4 in Plant Immunity. *Plant Cell*, 32, 4002-4016.
- LIU, Y. & ZHAN, S. 2004. Phosphorylation of 1-Aminocyclopropane-1-Carboxylic Acid Synthase by MPK6, a Stress-Responsive Mitogen-Activated Protein Kinase, Induces Ethylene Biosynthesis in Arabidopsis. *The Plant Cell* 16,, 3386–3399.
- LORENZO, O., PIQUERAS, R., SANCHEZ-SERRANO, J. J. & SOLANO, R. 2003. ETHYLENE RESPONSE FACTOR1 integrates signals from ethylene and jasmonate pathways in plant defense. *Plant Cell*, 15, 165-78.
- LOUIS, J., GOBBATO, E., MONDAL, H. A., FEYS, B. J., PARKER, J. E. & SHAH, J. 2012. Discrimination of Arabidopsis PAD4 activities in defense against green peach aphid and pathogens. *Plant Physiol*, 158, 1860-72.

- LOUIS, J., LEUNG, Q., PEGADARAJU, V., REESE, J. & SHAH, J. 2010. PAD4-Dependent Antibiosis Contributes to the *ssi2* Conferred Hyper-Resistance to the Green Peach Aphid. *MPMI*, 23, 618–627.
- LU, D., LIN, W., GAO, X., WU, S., CHENG, C., AVILA, J., HESE, A., DEVARENNE, T. P., HE, P. & SHAN, L. 2011. Direct ubiquitination of pattern recognition receptor FLS2 attenuates plant innate immunity. *Science*, 332, 1439–42.
- LU, D., WU, S., GAO, X., ZHANG, Y., SHAN, L. & HE, P. 2010. A receptor-like cytoplasmic kinase, BIK1, associates with a flagellin receptor complex to initiate plant innate immunity. *Proc Natl Acad Sci U S A*, 107, 496–501.
- LU, M., ZHANG, Y., TANG, S., PAN, J., YU, Y., HAN, J., LI, Y., DU, X., NAN, Z. & SUN, Q. 2016. AtCNGC2 is involved in jasmonic acid-induced calcium mobilization. *J Exp Bot*, 67, 809–19.
- LUDWIG, A. A., SAITOH, H., FELIX, G., FREYMARK, G., MIERSCH, O., WASTERACK, C., BOLLER, T., JONES, J. D. & ROMEIS, T. 2005. Ethylene-mediated cross-talk between calcium-dependent protein kinase and MAPK signaling controls stress responses in plants. *Proc Natl Acad Sci U S A*, 102, 10736–41.
- MA, C., LIU, Y., BAI, B., HAN, Z., TANG, J., ZHANG, H., YAGHMAIEAN, H., ZHANG, Y. & CHAI, J. 2017. Structural basis for BIR1-mediated negative regulation of plant immunity. *Cell Res*, 27, 1521–1524.
- MA, K. W., NIU, Y., JIA, Y., ORDON, J., COPELAND, C., EMONET, A., GELDNER, N., GUAN, R., STOLZE, S. C., NAKAGAMI, H., GARRIDO-OTER, R. & SCHULZE-LEFERT, P. 2021. Coordination of microbe-host homeostasis by crosstalk with plant innate immunity. *Nat Plants*, 7, 814–825.
- MA, Y., WALKER, R. K., ZHAO, Y. & BERKOWITZ, G. A. 2012. Linking ligand perception by PEPR pattern recognition receptors to cytosolic Ca²⁺ elevation and downstream immune signaling in plants. *Proc Natl Acad Sci U S A*, 109, 19852–7.
- MACHO, A. P., BOUTROT, F., RATHJEN, J. P. & ZIPFEL, C. 2012. Aspartate oxidase plays an important role in Arabidopsis stomatal immunity. *Plant Physiol*, 159, 1845–56.
- MACHO, A. P. & ZIPFEL, C. 2014. Plant PRRs and the activation of innate immune signaling. *Mol Cell*, 54, 263–72.
- MACWILLIAMS, J. R., DINGWALL, S., CHESNAIS, Q., SUGIO, A. & KALOSHIAN, I. 2020. AcDCXR Is a Cowpea Aphid Effector With Putative Roles in Altering Host Immunity and Physiology. *Front Plant Sci*, 11, 605.
- MAEZAWA, K., SHIGENOBU, S., TANIGUCHI, H., KUBO, T., AIZAWA, S. & MORIOKA, M. 2006. Hundreds of flagellar basal bodies cover the cell surface of the endosymbiotic bacterium *Buchnera aphidicola* sp. strain APS. *J Bacteriol*, 188, 6539–43.
- MAIR, A., XU, S. L., BRANON, T. C., TING, A. Y. & BERGMANN, D. C. 2019. Proximity labeling of protein complexes and cell-type-specific organellar proteomes in Arabidopsis enabled by TurboID. *Elife*, 8.
- MALLICK, P., SCHIRLE, M., CHEN, S. S., FLORY, M. R., LEE, H., MARTIN, D., RANISH, J., RAUGHT, B., SCHMITT, R., WERNER, T., KUSTER, B. & AEBERSOLD, R. 2007. Computational prediction of proteotypic peptides for quantitative proteomics. *Nat Biotechnol*, 25, 125–31.
- MANG, H., FENG, B., HU, Z., BOISSON-DERNIER, A., FRANCK, C. M., MENG, X., HUANG, Y., ZHOU, J., XU, G., WANG, T., SHAN, L. & HE, P. 2017. Differential Regulation of Two-Tiered Plant Immunity and Sexual Reproduction by ANXUR Receptor-Like Kinases. *Plant Cell*, 29, 3140–3156.
- MANOHAR, M., TIAN, M., MOREAU, M., PARK, S. W., CHOI, H. W., FEI, Z., FRISO, G., ASIF, M., MANOSALVA, P., VON DAHL, C. C., SHI, K., MA, S., DINESH-KUMAR, S. P., O'DOHERTY, I., SCHROEDER, F. C., VAN WIJK, K. J. & KLESSIG, D. F. 2014. Identification of multiple salicylic acid-binding proteins using two high throughput screens. *Front Plant Sci*, 5, 777.

- MANOSALVA, P., MANOHAR, M., VON REUSS, S. H., CHEN, S., KOCH, A., KAPLAN, F., CHOE, A., MICIKAS, R. J., WANG, X., KOGEL, K. H., STERNBERG, P. W., WILLIAMSON, V. M., SCHROEDER, F. C. & KLESSIG, D. F. 2015. Conserved nematode signalling molecules elicit plant defenses and pathogen resistance. *Nat Commun*, 6, 7795.
- MANTULEF, K. & ZAGOTTA, W. N. 2003. CYCLIC NUCLEOTIDE-GATED ION CHANNELS. *Annu. Rev. Cell Dev. Biol*, 19, 23–44.
- MAO, G., MENG, X., LIU, Y., ZHENG, Z., CHEN, Z. & ZHANGA, S. 2011. Phosphorylation of a WRKY Transcription Factor by Two Pathogen-Responsive MAPKs Drives Phytoalexin Biosynthesis in Arabidopsis. *The Plant Cell*, Vol 23, 1639–1653.
- MARCEC, M. J. & TANAKA, K. 2021. Crosstalk between Calcium and ROS Signaling during Flg22-Triggered Immune Response in Arabidopsis Leaves. *Plants (Basel)*, 11.
- MATHERS, T. C., CHEN, Y., KAITHAKOTTIL, G., LEGEAI, F., MUGFORD, S. T., BAA-PUYOULET, P., BRETAUDEAU, A., CLAVIJO, B., COLELLA, S., COLLIN, O., DALMAY, T., DERRIEN, T., FENG, H., GABALDON, T., JORDAN, A., JULCA, I., KETTLES, G. J., KOWITWANICH, K., LAVENIER, D., LENZI, P., LOPEZ-GOMOLLON, S., LOSKA, D., MAPLESON, D., MAUMUS, F., MOXON, S., PRICE, D. R., SUGIO, A., VAN MUNSTER, M., UZEST, M., WAITE, D., JANDER, G., TAGU, D., WILSON, A. C., VAN OOSTERHOUT, C., SWARBRECK, D. & HOGENHOUT, S. A. 2017. Rapid transcriptional plasticity of duplicated gene clusters enables a clonally reproducing aphid to colonise diverse plant species. *Genome Biol*, 18, 27.
- MATSUMOTO, Y. & HATTORI, M. 2018. The green rice leafhopper, *Nephotettix cincticeps* (Hemiptera: Cicadellidae), salivary protein NcSP75 is a key effector for successful phloem ingestion. *PLoS One*, 13, e0202492.
- MATSUSHIMA, N., MIYASHITA, H., MIKAMI, T. & KUROKI, Y. 2010. A nested leucine rich repeat (LRR) domain: the precursor of LRRs is a ten or eleven residue motif. *BMC Microbiol*, 10, 235.
- MATSUURA, A. & NAKAMURA, M. 2014. Development of neonicotinoid resistance in the cotton aphid *Aphis gossypii* (Hemiptera: Aphididae) in Japan. *Applied Entomology and Zoology*, 49, 535-540.
- MCCONN, M., CREELMAN, R. A., BELL, E., MULLET, J. E. & BROWSE, J. 1997. Jasmonate is essential for insect defense in Arabidopsis. *Proc Natl Acad Sci U S A*, 94, 5473-7.
- MENDY, B., WANG'OMBE, M. W., RADAKOVIC, Z. S., HOLBEIN, J., ILYAS, M., CHOPRA, D., HOLTON, N., ZIPFEL, C., GRUNDLER, F. M. & SIDDIQUE, S. 2017. Arabidopsis leucine-rich repeat receptor-like kinase NILR1 is required for induction of innate immunity to parasitic nematodes. *PLoS Pathog*, 13, e1006284.
- MERSMANN, S., BOURDAIS, G., RIETZ, S. & ROBATZEK, S. 2010. Ethylene signaling regulates accumulation of the FLS2 receptor and is required for the oxidative burst contributing to plant immunity. *Plant Physiol*, 154, 391-400.
- MIAO, Y. T., DENG, Y., JIA, H. K., LIU, Y. D. & HOU, M. L. 2018. Proteomic analysis of watery saliva secreted by white-backed planthopper, *Sogatella furcifera*. *PLoS One*, 13, e0193831.
- MILLER, G., SCHLAUCH, K., TAM, R., CORTES, D., TORRES, M. A., SHULAEV, V., DANGL, J. L. & MITTLER, R. 2009. The Plant NADPH Oxidase RBOHD Mediates Rapid Systemic Signaling in Response to Diverse Stimuli. *Science Signaling*, 2, ra45.
- MIRSKY, A. E. & PAULING, L. 1936. ON THE STRUCTURE OF NATIVE, DENATURED, AND COAGULATED PROTEINS. *PROC. N. A. S.*, 22.
- MITHOFER, A. & BOLAND, W. 2008. Recognition of herbivory-associated molecular patterns. *Plant Physiol*, 146, 825-31.
- MIYA, A., ALBERT, P., SHINYA, T., DESAKI, Y., ICHIMURA, K., SHIRASU, K., NARUSAKA, Y., KAWAKAMI, N., KAKU, H. & SHIBUYA, N. 2007. CERK1, a LysM receptor kinase, is essential for chitin elicitor signaling in Arabidopsis. *Proc Natl Acad Sci U S A*, 104, 19613-8.

- MOLOI, M. J. & VAN DER WESTHUIZEN, A. J. 2006. The reactive oxygen species are involved in resistance responses of wheat to the Russian wheat aphid. *J Plant Physiol*, 163, 1118-25.
- MONAGHAN, J., MATSCHI, S., SHORINOLA, O., ROVENICH, H., MATEI, A., SEGONZAC, C., MALINOVSKY, F. G., RATHJEN, J. P., MACLEAN, D., ROMEIS, T. & ZIPFEL, C. 2014. The Calcium-Dependent Protein Kinase CPK28 Buffers Plant Immunity and Regulates BIK1 Turnover. *Cell host and microbe*, 16, 605-615.
- MORAN, P. J. & THOMPSON, G. A. 2001. Molecular responses to aphid feeding in Arabidopsis in relation to plant defense pathways. *Plant Physiol*, 125, 1074-85.
- MOTT, G. A., THAKUR, S., SMAKOWSKA, E., WANG, P. W., BELKHADIR, Y., DESVEAUX, D. & GUTTMAN, D. S. 2016. Genomic screens identify a new phyto-bacterial microbe-associated molecular pattern and the cognate Arabidopsis receptor-like kinase that mediates its immune elicitation. *Genome Biol*, 17, 98.
- MOU, Z., FAN, W. & DONG, X. 2003. Inducers of Plant Systemic Acquired Resistance Regulate NPR1 Function through Redox Changes. *Cell*, 113, 935-944.
- MOUSAVI, S. A., CHAUVIN, A., PASCAUD, F., KELLENBERGER, S. & FARMER, E. E. 2013. GLUTAMATE RECEPTOR-LIKE genes mediate leaf-to-leaf wound signalling. *Nature*, 500, 422-6.
- MUCHA, S., HEINZLMEIR, S., KRIECHBAUMER, V., STRICKLAND, B., KIRCHHELLE, C., CHOUDHARY, M., KOWALSKI, N., EICHMANN, R., HUCKELHOVEN, R., GRILL, E., KUSTER, B. & GLAWISCHNIG, E. 2019. The Formation of a Camalexin Biosynthetic Metabolon. *Plant Cell*, 31, 2697-2710.
- MUGFORD, S. T., BARCLAY, E., DRUREY, C., FINDLAY, K. C. & HOGENHOUT, S. A. 2016. An Immuno-Suppressive Aphid Saliva Protein Is Delivered into the Cytosol of Plant Mesophyll Cells During Feeding. *Mol Plant Microbe Interact*, 29, 854-861.
- MULLER, T. M., BOTTCHE, C., MORBITZER, R., GOTZ, C. C., LEHMANN, J., LAHAYE, T. & GLAWISCHNIG, E. 2015. TRANSCRIPTION ACTIVATOR-LIKE EFFECTOR NUCLEASE-Mediated Generation and Metabolic Analysis of Camalexin-Deficient *cyp71a12 cyp71a13* Double Knockout Lines. *Plant Physiol*, 168, 849-58.
- MUNDADE, R., OZER, H. G., WEI, H., PRABHU, L. & LU, T. 2014. Role of ChIP-seq in the discovery of transcription factor binding sites, differential gene regulation mechanism, epigenetic marks and beyond. *Cell Cycle*, 13, 2847-52.
- MUNSON, M. A., BAUMANN, P. & KINSEY, M. G. 1991. Buchnera gen. nov. and Buchnera aphidicola sp. nov., a Taxon Consisting of the Mycetocyte-Associated, Primary Endosymbionts of Aphids. *International Journal of Systematic Bacteriology*, 41, 566-568.
- MUTTI, N. S., LOUIS, J., PAPPAN, L. K., PAPPAN, K., BEGUM, K., CHEN, M.-S., PARK, Y., DITTMER, N., MARSHALL, J., REESE, J. C. & REECK, G. R. 2006. A protein from the salivary glands of the pea aphid, *Acyrtosiphon pisum*, is essential in feeding on a host plant. *MPMI*, 105.
- MUTTI, N. S., PARK, Y., REESE, J. C. & REECK, G. R. 2008. RNAi knockdown of a salivary transcript leading to lethality in the pea aphid, *Acyrtosiphon pisum*. *Journal of Insect Science*, 6.
- MYLES, S., PEIFFER, J., BROWN, P. J., ERSOZ, E. S., ZHANG, Z., COSTICH, D. E. & BUCKLER, E. S. 2009. Association mapping: critical considerations shift from genotyping to experimental design. *Plant Cell*, 21, 2194-202.
- NAESSENS, E., DUBREUIL, G., GIORDANENGO, P., BARON, O. L., MINET-KEBDANI, N., KELLER, H. & COUSTAU, C. 2015. A Secreted MIF Cytokine Enables Aphid Feeding and Represses Plant Immune Responses. *Curr Biol*, 25, 1898-903.
- NAFISI, M., GOREGAOKER, S., BOTANGA, C. J., GLAWISCHNIG, E., OLSEN, C. E., HALKIER, B. A. & GLAZEBROOK, J. 2007. Arabidopsis cytochrome P450 monooxygenase 71A13 catalyzes the conversion of indole-3-acetaldoxime in camalexin synthesis. *Plant Cell*, 19, 2039-52.

- NAITO, K., TAGUCHI, F., SUZUKI, T., INAGAKI, Y., TOYODA, K., SHIRAISHI, T. & ICHINOSE, Y. 2008. Amino acid sequence of bacterial microbe-associated molecular pattern flg22 is required for virulence. *Mol Plant Microbe Interact*, 21, 1165-74.
- NAKABO, Y. & PABST, M. J. 1996. Lysis of leukemic cells by human macrophages: inhibition by 4-(2-aminoethyl)-benzenesulfonyl fluoride (AEBSF), a serine protease inhibitor. *Journal of leukocyte biology*, 60, 328-336.
- NARAHASHI, Y. & YANAGITA, M. 1967. Studies on proteolytic enzymes (pronase) of *Streptomyces griseus* K-1. I. Nature and properties of the proteolytic enzyme system. *J Biochem*, 62, 633-41.
- NAVARRO, L., ZIPFEL, C., ROWLAND, O., KELLER, I., ROBATZEK, S., BOLLER, T. & JONES, J. D. 2004. The transcriptional innate immune response to flg22. Interplay and overlap with Avr gene-dependent defense responses and bacterial pathogenesis. *Plant Physiol*, 135, 1113-28.
- NAWRATH, C., HECK, S., PARINTHAWONG, N. & METRAUX, J. P. 2002. EDS5, an essential component of salicylic acid-dependent signaling for disease resistance in Arabidopsis, is a member of the MATE transporter family. *Plant Cell*, 14, 275-86.
- NEWMAN, M. A., SUNDELIN, T., NIELSEN, J. T. & ERBS, G. 2013. MAMP (microbe-associated molecular pattern) triggered immunity in plants. *Front Plant Sci*, 4, 139.
- NG, J. C. & PERRY, K. L. 2004. Transmission of plant viruses by aphid vectors. *Mol Plant Pathol*, 5, 505-11.
- NGOU, B. P. M., AHN, H. K., DING, P. & JONES, J. D. G. 2021. Mutual potentiation of plant immunity by cell-surface and intracellular receptors. *Nature*, 592, 110-115.
- NGOU, B. P. M., DING, P. & JONES, J. D. 2022. Thirty years of resistance: Zig-zag through the plant immune system. *Plant Cell*.
- NGUYEN, C. T., KURENDA, A., STOLZ, S., CHETELAT, A. & FARMER, E. E. 2018. Identification of cell populations necessary for leaf-to-leaf electrical signaling in a wounded plant. *Proc Natl Acad Sci U S A*, 115, 10178-10183.
- NIDERMAN, T., GENETET, L., BRUYÈRE, T., GEES, R., STINTZI, A., LEGRAND, M., FRITIG, B. & MOSINGER, E. 1995. Pathogenesis-Related PR-1 Proteins Are Antifungal. *Plant Physiol*, 108, 17-27.
- NIE, P., LI, X., WANG, S., GUO, J., ZHAO, H. & NIU, D. 2017. Induced Systemic Resistance against *Botrytis cinerea* by *Bacillus cereus* AR156 through a JA/ET- and NPR1-Dependent Signaling Pathway and Activates PAMP-Triggered Immunity in Arabidopsis. *Front Plant Sci*, 8, 238.
- NORDSTROM, K. J., ALBANI, M. C., JAMES, G. V., GUTJAHR, C., HARTWIG, B., TURCK, F., PASZKOWSKI, U., COUPLAND, G. & SCHNEEBERGER, K. 2013. Mutation identification by direct comparison of whole-genome sequencing data from mutant and wild-type individuals using k-mers. *Nat Biotechnol*, 31, 325-30.
- NTOUKAKIS, V., SCHWESSINGER, B., SEGONZAC, C. & ZIPFEL, C. 2011. Cautionary notes on the use of C-terminal BAK1 fusion proteins for functional studies. *Plant Cell*, 23, 3871-8.
- NÜRNBERGER, T., NENNSTIEL, D., JABS, T., SACKS, W. R., HAHLBROCK, K. & SCHEEL, D. 1994. High affinity binding of a fungal oligopeptide elicitor to parsley plasma membranes triggers multiple defense responses. *Cell*, 78, 449-460.
- O'MALLEY, R. C., HUANG, S.-S. C., SONG, L., LEWSEY, M. G., BARTLETTA, NERY, J. R., GALLI, M., GALLAVOTTI, A. & ECKER, J. R. 2016. Cistrome and Epicistrome Features Shape the Regulatory DNA Landscape. *Cell*, 165, 1280-1292.
- OLIVER, K. M., MORAN, N. A. & HUNTER, M. S. 2005. Variation in resistance to parasitism in aphids is due to symbionts not host genotype. *PNAS*, 102, 12795-12800.
- OOME, S., RAAJMAKERS, T. M., CABRAL, A., SAMWEL, S., BOHM, H., ALBERT, I., NURNBERGER, T. & VAN DEN ACKERVEKEN, G. 2014. Nep1-like proteins from three kingdoms of life act as a microbe-associated molecular pattern in Arabidopsis. *Proc Natl Acad Sci U S A*, 111, 16955-60.

- PAN, L., LV, S., YANG, N., LV, Y., LIU, Z., WU, J. & WANG, G. 2016. The Multifunction of CLAVATA2 in Plant Development and Immunity. *Front Plant Sci*, 7, 1573.
- PANT, S. & HUANG, Y. 2021. Elevated production of reactive oxygen species is related to host plant resistance to sugarcane aphid in sorghum. *Plant Signal Behav*, 16, 1849523.
- PARK, C. J., PENG, Y., CHEN, X., DARDICK, C., RUAN, D., BART, R., CANLAS, P. E. & RONALD, P. C. 2008. Rice XB15, a protein phosphatase 2C, negatively regulates cell death and XA21-mediated innate immunity. *PLoS Biol*, 6, e231.
- PEARCE, G. & RYAN, C. A. 2003. Systemic signaling in tomato plants for defense against herbivores. Isolation and characterization of three novel defense-signaling glycopeptide hormones coded in a single precursor gene. *J Biol Chem*, 278, 30044-50.
- PEARCE, G., STRYDOM, D., JOHNSON, S. & RYAN, C. A. 1991. A polypeptide from tomato leaves induces wound-inducible proteinase inhibitor proteins. *Science*, 253, 895-7.
- PECCOUD, J., OLLIVIERA, A., PLANTEGENEST, M. & SIMONA, J.-C. 2009. A continuum of genetic divergence from sympatric host races to species in the pea aphid complex. *PNAS*, 106, 7495–7500.
- PEGADARAJU, V., KNEPPER, C., REESE, J. & SHAH, J. 2005. Premature leaf senescence modulated by the Arabidopsis PHYTOALEXIN DEFICIENT4 gene is associated with defense against the phloem-feeding green peach aphid. *Plant Physiol*, 139, 1927-34.
- PEGADARAJU, V., LOUIS, J., SINGH, V., REESE, J. C., BAUTOR, J., FEYS, B. J., COOK, G., PARKER, J. E. & SHAH, J. 2007. Phloem-based resistance to green peach aphid is controlled by Arabidopsis PHYTOALEXIN DEFICIENT4 without its signaling partner ENHANCED DISEASE SUSCEPTIBILITY1. *Plant J*, 52, 332-41.
- PEITER, E. 2011. The plant vacuole: emitter and receiver of calcium signals. *Cell Calcium*, 50, 120-8.
- PETERSEN, M., BRODERSEN, P., NAESTED, H., ANDREASSON, E., LINDHART, U., JOHANSEN, B., NIELSEN, H. B., LACY, M., AUSTIN, M. J., PARKER, J. E., SHARMA, S. B., KLESSIG, D. F., MARTIENSSON, R., MATTSSON, O., JENSEN, A. B. & MUNDY, J. 2000. Arabidopsis map kinase 4 negatively regulates systemic acquired resistance. *Cell*, 103, 1111-20.
- PFALZ, M., VOGEL, H. & KROYMANN, J. 2009. The gene controlling the indole glucosinolate modifier1 quantitative trait locus alters indole glucosinolate structures and aphid resistance in Arabidopsis. *Plant Cell*, 21, 985-99.
- PFUND, C., TANS-KERSTEN, J., DUNNING, F. M., ALONSO, J. M., ECKER, J. R., ALLEN, C. & BENT, A. F. 2004. Flagellin is not a major defense elicitor in *Ralstonia solanacearum* cells or extracts applied to Arabidopsis thaliana. *Mol Plant Microbe Interact*, 17, 696-706.
- PIASECK, A., JEDRZEJCZAK-REY, N. & BEDNAREK, P. 2015. Secondary metabolites in plant innate immunity: conserved function of divergent chemicals. *New Phytologist* 206, 948–964.
- PIETERSE, C. M., VAN DER DOES, D., ZAMIOUDIS, C., LEON-REYES, A. & VAN WEES, S. C. 2012. Hormonal modulation of plant immunity. *Annu Rev Cell Dev Biol*, 28, 489-521.
- PITINO, M., HOGENHOUT, S. A. & . 2013. Aphid protein effectors promote aphid colonization in a plant species-specific manne. *Mol. Plant Microbe Interact*, 26, 130–139.
- POOSAPATI, S., PORETSKY, E., DRESSANO, K., RUIZ, M., VAZQUEZ, A., SANDOVAL, E., ESTRADA-CARDENAS, A., DUGGAL, S., LIM, J. H., MORRIS, G., SZCZEPANIEC, A., WALSE, S. S., NI, X., SCHMELZ, E. A. & HUFFAKER, A. 2022. A sorghum genome-wide association study (GWAS) identifies a WRKY transcription factor as a candidate gene underlying sugarcane aphid (*Melanaphis sacchari*) resistance. *Planta*, 255, 37.
- POOVAIAH, B. W. & REDDY, A. S. N. 1993. Calcium and signal transduction in plants. *CRC Crit. Rev. Plant Sci*, 12, 185–211.
- POSTMA, J., LIEBRAND, T. W., BI, G., EVRARD, A., BYE, R. R., MBENGUE, M., KUHN, H., JOOSTEN, M. H. & ROBATZEK, S. 2016. Avr4 promotes Cf-4 receptor-like protein association with the BAK1/SERK3 receptor-like kinase to initiate receptor endocytosis and plant immunity. *New Phytol*, 210, 627-42.

- POWELL, G., TOSH, C. R. & HARDIE, J. 2006. Host plant selection by aphids: behavioral, evolutionary, and applied perspectives. *Annu Rev Entomol*, 51, 309-30.
- PRICE, A. H., TAYLOR, A., RIPLEY, S. J., GRIFFITHS, A., TREWAVAS, A. J. & KNIGHT, M. R. 1994. Oxidative Signals in Tobacco Increase Cytosolic Calcium. *Plant Cell*, 6, 1301-1310.
- PRINCE, D. C., DRUREY, C., ZIPFEL, C. & HOGENHOUT, S. A. 2014. The leucine-rich repeat receptor-like kinase BRASSINOSTEROID INSENSITIVE1-ASSOCIATED KINASE1 and the cytochrome P450 PHYTOALEXIN DEFICIENT3 contribute to innate immunity to aphids in Arabidopsis. *Plant Physiol*, 164, 2207-19.
- PRUITT, R. N., LOCCI, F., WANKE, F., ZHANG, L., SAILE, S. C., JOE, A., KARELINA, D., HUA, C., FROHLICH, K., WAN, W. L., HU, M., RAO, S., STOLZE, S. C., HARZEN, A., GUST, A. A., HARTER, K., JOOSTEN, M., THOMMA, B., ZHOU, J. M., DANGL, J. L., WEIGEL, D., NAKAGAMI, H., OECKING, C., KASMI, F. E., PARKER, J. E. & NURNBERGER, T. 2021. The EDS1-PAD4-ADR1 node mediates Arabidopsis pattern-triggered immunity. *Nature*, 598, 495-499.
- PRUITT, R. N., SCHWESSINGER, B., JOE, A., THOMAS, N., LIU, F., ALBERT, M., ROBINSON, M. R., CHAN, L. J. G., LUU, D. D., CHEN, H., BAHAR, O., DAUDI, A., DE VLEESSCHAUWER, D., CADDELL, D., ZHANG, W., ZHAO, X., LI, X., HEAZLEWOOD, J. L., RUAN, D., MAJUMDER, D., CHERN, M., KALBACHER, H., MIDHA, S., PATIL, P. B., SONTI, R. V., PETZOLD, C. J., LIU, C. C., BRODBELT, J. S., FELIX, G. & RONALD, P. C. 2015. The rice immune receptor XA21 recognizes a tyrosine-sulfated protein from a Gram negative bacterium. *Sci. Adv.*, 1, e1500245.
- PUINEAN, A. M., FOSTER, S. P., OLIPHANT, L., DENHOLM, I., FIELD, L. M., MILLAR, N. S., WILLIAMSON, M. S. & BASS, C. 2010. Amplification of a cytochrome P450 gene is associated with resistance to neonicotinoid insecticides in the aphid *Myzus persicae*. *PLoS Genet*, 6, e1000999.
- QI, T., SEONG, K., THOMAZELLA, D. P. T., KIM, J. R., PHAM, J., SEO, E., CHO, M. J., SCHULTINK, A. & STASKAWICZ, B. J. 2018. NRG1 functions downstream of EDS1 to regulate TIR-NLR-mediated plant immunity in *Nicotiana benthamiana*. *Proc Natl Acad Sci U S A*, 115, E10979-E10987.
- QI, Z., VERMA, R., GEHRING, C., YAMAGUCHI, Y., ZHAO, Y., RYAN, C. A. & BERKOWITZ, G. A. 2010. Ca²⁺ signaling by plant *Arabidopsis thaliana* Pep peptides depends on AtPepR1, a receptor with guanylyl cyclase activity, and cGMP-activated Ca²⁺ channels. *Proc Natl Acad Sci U S A*, 107, 21193-8.
- QIU, J. L., FIIL, B. K., PETERSEN, K., NIELSEN, H. B., BOTANGA, C. J., THORGRIMSEN, S., PALMA, K., SUAREZ-RODRIGUEZ, M. C., SANDBECH-CLAUSEN, S., LICHOTA, J., BRODERSEN, P., GRASSER, K. D., MATTSSON, O., GLAZEBROOK, J., MUNDY, J. & PETERSEN, M. 2008. Arabidopsis MAP kinase 4 regulates gene expression through transcription factor release in the nucleus. *EMBO J*, 27, 2214-21.
- RAMSEY, J. S., WILSON, A. C., DE VOS, M., SUN, Q., TAMBORINDEGUY, C., WINFIELD, A., MALLOCH, G., SMITH, D. M., FENTON, B., GRAY, S. M. & JANDER, G. 2007. Genomic resources for *Myzus persicae*: EST sequencing, SNP identification, and microarray design. *BMC Genomics*, 8, 423.
- RANF, S., ESCHEN-LIPPOLD, L., FROHLICH, K., WESTPHAL, L., SCHEEL, D. & LEE, J. 2014. Microbe-associated molecular pattern-induced calcium signaling requires the receptor-like cytoplasmic kinases, PBL1 and BIK1. *BMC Plant Biol*, 14, 374.
- RANF, S., ESCHEN-LIPPOLD, L., PECHER, P., LEE, J. & SCHEEL, D. 2011. Interplay between calcium signalling and early signalling elements during defence responses to microbe- or damage-associated molecular patterns. *Plant J*, 68, 100-13.
- RANF, S., GISCH, N., SCHAFFER, M., ILLIG, T., WESTPHAL, L., KNIREL, Y. A., SANCHEZ-CARBALLO, P. M., ZHRINGER, U., HUCKELHOVEN, R., LEE, J. & SCHEEL, D. 2015. A lectin S-domain receptor kinase mediates lipopolysaccharide sensing in *Arabidopsis thaliana*. *Nat Immunol*, 16, 426-33.

- RANF, S., WUNNENBERG, P., LEE, J., BECKER, D., DUNKEL, M., HEDRICH, R., SCHEEL, D. & DIETRICH, P. 2008. Loss of the vacuolar cation channel, AtTPC1, does not impair Ca²⁺ signals induced by abiotic and biotic stresses. *Plant J*, 53, 287-99.
- RAO, S., ZHOU, Z., MIAO, P., BI, G., HU, M., WU, Y., FENG, F., ZHANG, X. & ZHOU, J. M. 2018. Roles of Receptor-Like Cytoplasmic Kinase VII Members in Pattern-Triggered Immune Signaling. *Plant Physiol*, 177, 1679-1690.
- RAO, S. A., CAROLAN, J. C. & WILKINSON, T. L. 2013. Proteomic profiling of cereal aphid saliva reveals both ubiquitous and adaptive secreted proteins. *PLoS One*, 8, e57413.
- RAO, W., ZHENG, X., LIU, B., GUO, Q., GUO, J., WU, Y., SHANGGUAN, X., WANG, H., WU, D., WANG, Z., HU, L., XU, C., JIANG, W., HUANG, J., SHI, S. & HE, G. 2019. Secretome Analysis and In Planta Expression of Salivary Proteins Identify Candidate Effectors from the Brown Planthopper Nilaparvata lugens. *Mol Plant Microbe Interact*, 32, 227-239.
- RASOOL, B., KARPINSKA, B., PASCUAL, J., KANGASJARVI, S. & FOYER, C. H. 2020. Catalase, glutathione, and protein phosphatase 2A-dependent organellar redox signalling regulate aphid fecundity under moderate and high irradiance. *Plant Cell Environ*, 43, 209-222.
- REDDY, G. V. & MEYEROWITZ, E. M. 2005. Stem-cell homeostasis and growth dynamics can be uncoupled in the Arabidopsis shoot apex. *Science*, 310, 663-7.
- REN, G., WANG, X., CHEN, D., WANG, X. & LIU, X. 2014. Effects of aphids Myzus persicae on the changes of Ca²⁺ and H₂O₂ flux and enzyme activities in tobacco. *Journal of Plant Interactions*, 9, 883-888.
- REUSCHE, M., KLASKOVA, J., THOLE, K., TRUSKINA, J., NOVAK, O., JANZ, D., STRNAD, M., SPICHAL, L., LIPKA, V. & TEICHMANN, T. 2013. Stabilization of cytokinin levels enhances Arabidopsis resistance against Verticillium longisporum. *Mol Plant Microbe Interact*, 26, 850-60.
- REYMOND, P. 2021. Receptor kinases in plant responses to herbivory. *Curr Opin Biotechnol*, 70, 143-150.
- REYMOND, P., BODENHAUSEN, N., VAN POECKE, R. M., KRISHNAMURTHY, V., DICKE, M. & FARMER, E. E. 2004. A conserved transcriptional pattern in response to a specialist and a generalist herbivore. *Plant Cell*, 16, 3132-3147.
- ROBATZEK, S., CHINCHILLA, D. & BOLLER, T. 2006. Ligand-induced endocytosis of the pattern recognition receptor FLS2 in Arabidopsis. *GENES & DEVELOPMENT*, 20, 537-542
- RODRIGUEZ, M. C., PETERSEN, M. & MUNDY, J. 2010. Mitogen-activated protein kinase signaling in plants. *Annu. Rev. Plant Biol.*, 61, 621-649.
- RODRIGUEZ, P. A., STAM, R., WARBROEK, T. & BOS, J. I. 2014. Mp10 and Mp42 from the aphid species Myzus persicae trigger plant defenses in Nicotiana benthamiana through different activities. *Mol Plant Microbe Interact*, 27, 30-9.
- ROMEIS, T., LUDWIG, A. A., MARTIN, R. & JONES, J. D. 2001. Calcium-dependent protein kinases play an essential role in a plant defence response. *EMBO J*, 20, 5556-67.
- RON, M. & AVNI, A. 2004. The receptor for the fungal elicitor ethylene-inducing xylanase is a member of a resistance-like gene family in tomato. *Plant Cell*, 16, 1604-15.
- ROUX, M., SCHWESSINGER, B., ALBRECHT, C., CHINCHILLA, D., JONES, A., HOLTON, N., MALINOVSKY, F. G., TOR, M., DE VRIES, S. & ZIPFEL, C. 2011. The Arabidopsis leucine-rich repeat receptor-like kinases BAK1/SERK3 and BKK1/SERK4 are required for innate immunity to hemibiotrophic and biotrophic pathogens. *Plant Cell*, 23, 2440-55.
- SABRI, A., VANDERMOTEN, S., LEROY, P. D., HAUBRUGE, E., HANCE, T., THONART, P., DE PAUW, E. & FRANCIS, F. 2013. Proteomic investigation of aphid honeydew reveals an unexpected diversity of proteins. *PLoS One*, 8, e74656.
- SACKS, W., NURNBERGER, T., HAHLBROCK, K. & SCHEEL, D. 1995. Molecular characterization of nucleotide sequences encoding the extracellular glycoprotein elicitor from Phytophthora megasperma. *Mol Gen Genet*, 246, 45-55.

- SAMATEY, F. A., IMADA, K., NAGASHIMA, S., VONDERVISZT, F., KUMASAKA, T., YAMAMOTO, M. & NAMBA, K. 2001. Structure of the bacterial flagellar protofilament and implications for a switch for supercoiling. *Nature*, 410, 331-7.
- SANDERS, W. S., BRIDGES, S. M., MCCARTHY, F. M., NANDURI, B. & BURGESS, S. C. 2007. Prediction of peptides observable by mass spectrometry applied at the experimental set level. *BMC Bioinformatics*, 8 Suppl 7, S23.
- SANDSTRÖM, J. & MORAN, N. 1999. How nutritionally imbalanced is phloem sap for aphids? *Entomologia Experimentalis et Applicata*, 91, 203–210.
- SAUR, I. M., KADOTA, Y., SKLENAR, J., HOLTON, N. J., SMAKOWSKA, E., BELKHADIR, Y., ZIPFEL, C. & RATHJEN, J. P. 2016. NbCSPR underlies age-dependent immune responses to bacterial cold shock protein in *Nicotiana benthamiana*. *Proc Natl Acad Sci U S A*, 113, 3389-94.
- SCHEER, J. M. & RYAN, C. A. 2002. The systemin receptor SR160 from *Lycopersicon peruvianum* is a member of the LRR receptor kinase family. *PNAS*, 99, 9585–9590.
- SCHEPERS, M. J., YELLAND, J. N., MORAN, N. A. & TAYLOR, D. W. 2021. Isolation of the *Buchnera aphidicola* flagellum basal body complexes from the *Buchnera* membrane. *PLoS One*, 16, e0245710.
- SCHLAEPPI, K., ABOU-MANSOUR, E., BUCHALA, A. & MAUCH, F. 2010. Disease resistance of *Arabidopsis* to *Phytophthora brassicae* is established by the sequential action of indole glucosinolates and camalexin. *Plant Journal*, 62, 840–851.
- SCHMELZ, E. A., CARROLL, M. J., LECLERE, S., PHIPPS, S. M., MEREDITH, J., CHOUREY, P. S., ALBORN, H. T. & TEAL, P. E. A. 2006. Fragments of ATP synthase mediate plant perception of insect attack. *PNAS*, 103, 8894–8899.
- SCHMELZ, E. A., LECLERE, S., CARROLL, M. J., ALBORN, H. T. & TEAL, P. E. 2007. Cowpea chloroplastic ATP synthase is the source of multiple plant defense elicitors during insect herbivory. *Plant Physiol*, 144, 793-805.
- SCHNATBAUM, K., ZERWECK, J., NEHMER, J., WENSCHUH, H., SCHUTKOWSKI, M. & REIMER, U. 2011. SpikeTides™ - Proteotypic Peptides for Large-Scale MS-Based Proteomics.
- SCHOTT, J., FUCHS, B., BOTTCHER, C. & HILKER, M. 2021. Responses to larval herbivory in the phenylpropanoid pathway of *Ulmus minor* are boosted by prior insect egg deposition. *Planta*, 255, 16.
- SCHUHEGGER, R., NAFISI, M., MANSOUROVA, M., PETERSEN, B. L., OLSEN, C. E., SVATOS, A., HALKIER, B. A. & GLAWISCHNIG, E. 2006. CYP71B15 (PAD3) catalyzes the final step in camalexin biosynthesis. *Plant Physiol*, 141, 1248-54.
- SCHULZE, B., MENTZEL, T., JEHLE, A. K., MUELLER, K., BEELER, S., BOLLER, T., FELIX, G. & CHINCHILLA, D. 2010. Rapid heteromerization and phosphorylation of ligand-activated plant transmembrane receptors and their associated kinase BAK1. *J Biol Chem*, 285, 9444-51.
- SCHWARTZBERG, E. G., TUMLINSON, J. H. & JONES, H. 2014. Aphid honeydew alters plant defence responses. *Functional Ecology*, 28, 386-394.
- SCHWEIGHOFER, A., HIRT, H. & MESKIENE, I. 2004. Plant PP2C phosphatases: emerging functions in stress signaling. *Trends Plant Sci*, 9, 236-43.
- SCHWESSINGER, B., ROUX, M., KADOTA, Y., NTOUKAKIS, V., SKLENAR, J., JONES, A. & ZIPFEL, C. 2011. Phosphorylation-dependent differential regulation of plant growth, cell death, and innate immunity by the regulatory receptor-like kinase BAK1. *PLoS Genet*, 7, e1002046.
- SEGONZAC, C., MACHO, A. P., SANMARTIN, M., NTOUKAKIS, V., SANCHEZ-SERRANO, J. J. & ZIPFEL, C. 2014. Negative control of BAK1 by protein phosphatase 2A during plant innate immunity. *EMBO J*, 33, 2069-79.
- SEIFBARGHI, S., BORHAN, M. H., WEI, Y., MA, L., COUTU, C., BEKKAOUI, D. & HEGEDUS, D. D. 2020. Receptor-Like Kinases BAK1 and SOBIR1 Are Required for Necrotizing Activity of

- a Novel Group of Sclerotinia sclerotiorum Necrosis-Inducing Effectors. *Front Plant Sci*, 11, 1021.
- SERRANO, M., WANG, B., ARYAL, B., GARCION, C., ABOU-MANSOUR, E., HECK, S., GEISLER, M., MAUCH, F., NAWRATH, C. & METRAUX, J. P. 2013. Export of salicylic acid from the chloroplast requires the multidrug and toxin extrusion-like transporter EDS5. *Plant Physiol*, 162, 1815-21.
- SETO, D., KOULENA, N., LO, T., MENNA, A., GUTTMAN, D. S. & DESVEAUX, D. 2017. Expanded type III effector recognition by the ZAR1 NLR protein using ZED1-related kinases. *Nat Plants*, 3.
- SHAN, L., HE, P., LI, J., HEESE, A., PECK, S. C., NURNBERGER, T., MARTIN, G. B. & SHEEN, J. 2008. Bacterial effectors target the common signaling partner BAK1 to disrupt multiple MAMP receptor-signaling complexes and impede plant immunity. *Cell Host Microbe*, 4, 17-27.
- SHANGGUAN, X., ZHANG, J., LIU, B., ZHAO, Y., WANG, H., WANG, Z., GUO, J., RAO, W., JING, S., GUAN, W., MA, Y., WU, Y., HU, L., CHEN, R., DU, B., ZHU, L., YU, D. & HE, G. 2018. A Mucin-Like Protein of Planthopper Is Required for Feeding and Induces Immunity Response in Plants. *Plant Physiol*, 176, 552-565.
- SHAO, Y., GUO, M., HE, X., FAN, Q., WANG, Z., JIA, J. & GUO, J. 2019. Constitutive H₂O₂ is involved in sorghum defense against aphids. *Brazilian Journal of Botany*, 42, 271-281.
- SHARMA, A., KHAN, A. N., SUBRAHMANYAM, S., RAMAN, A., TAYLOR, G. S. & FLETCHER, M. J. 2014. Salivary proteins of plant-feeding hemipteroids - implication in phytophagy. *Bull Entomol Res*, 104, 117-36.
- SHEN, Q., BOURDAIS, G., PAN, H., ROBATZEK, S. & TANG, D. 2017. Arabidopsis glycosylphosphatidylinositol-anchored protein LLG1 associates with and modulates FLS2 to regulate innate immunity. *Proc Natl Acad Sci U S A*, 114, 5749-5754.
- SHEN, W., LIU, J. & LI, J. F. 2019. Type-II Metacaspases Mediate the Processing of Plant Elicitor Peptides in Arabidopsis. *Mol Plant*, 12, 1524-1533.
- SHIMIZU, T., NAKANO, T., TAKAMIZAWA, D., DESAKI, Y., ISHII-MINAMI, N., NISHIZAWA, Y., MINAMI, E., OKADA, K., YAMANE, H., KAKU, H. & SHIBUYA, N. 2010. Two LysM receptor molecules, CEBiP and OsCERK1, cooperatively regulate chitin elicitor signaling in rice. *Plant J*, 64, 204-14.
- SHOALA, T., EDWARDS, M. G., KNIGHT, M. R. & GATEHOUSE, A. M. R. 2018. OXI1 kinase plays a key role in resistance of Arabidopsis towards aphids (*Myzus persicae*). *Transgenic Res*, 27, 355-366.
- SIMON, J.-C., RISPE, C. & SUNNUCKS, P. 2002. Ecology and evolution of sex in aphids. *TRENDS in Ecology & Evolution*, 17, 35-39.
- SMAKOWSKA-LUZAN, E., MOTT, G. A., PARYS, K., STEGMANN, M., HOWTON, T. C., LAYEGHIFARD, M., NEUHOLD, J., LEHNER, A., KONG, J., GRUNWALD, K., WEINBERGER, N., SATBHAI, S. B., MAYER, D., BUSCH, W., MADALINSKI, M., STOLT-BERGNER, P., PROVART, N. J., MUKHTAR, M. S., ZIPFEL, C., DESVEAUX, D., GUTTMAN, D. S. & BELKHADIR, Y. 2018. An extracellular network of Arabidopsis leucine-rich repeat receptor kinases. *Nature*, 553, 342-346.
- SMITH, J. M., SALAMANGO, D. J., LESLIE, M. E., COLLINS, C. A. & HEESE, A. 2014. Sensitivity to Flg22 is modulated by ligand-induced degradation and de novo synthesis of the endogenous flagellin-receptor FLAGELLIN-SENSING2. *Plant Physiol*, 164, 440-54.
- SMITH, M. A. H. & MACKAY, P. A. 1989. Seasonal variation in the photoperiodic responses of a pea aphid population: evidence for long-distance movements between populations. *Oecologia*, 81, 160-165
- SNOECK, S., GUAYAZAN-PALACIOS, N. & STEINBRENNER, A. D. 2022. Molecular Tug-of-War: Plant Immune Recognition of Herbivory. *Plant Cell*.
- SONDERBY, I. E., GEU-FLORES, F. & HALKIER, B. A. 2010. Biosynthesis of glucosinolates – gene discovery and beyond. *Trends in Plant Science*, 15, 283-290.

- SONG, C. J., STEINEBRUNNER, I., WANG, X. Z., STOUT, S. C. & ROUX, S. J. 2006. Extracellular ATP induces the accumulation of superoxide via NADPH oxidases in Arabidopsis. *Plant Physiol*, 140, 1222–1232.
- SONG, W.-Y., WANG, G.-L., CHEN, L.-L., KIM, H.-S., PI, L.-Y., HOLSTEN, T., GARDNER, J., WANG, B., ZHAI, W.-X., ZHU, L.-H., FAUQUET, C. & RONALD, P. 1995. A Receptor Kinase-Like Protein Encoded by the Rice Disease Resistance Gene, Xa21. *Science*, 270.
- SOZEN, C., SCHENK, S. T., BOUDSOCQ, M., CHARDIN, C., ALMEIDA-TRAPP, M., KRAPP, A., HIRT, H., MITHOFER, A. & COLCOMBET, J. 2020. Wounding and Insect Feeding Trigger Two Independent MAPK Pathways with Distinct Regulation and Kinetics. *Plant Cell*, 32, 1988-2003.
- SPALDING, E. P. & HARPER, J. F. 2011. The ins and outs of cellular Ca²⁺ transport. *Curr Opin Plant Biol*, 14, 715–720.
- SPOEL, S. H. & DONG, X. 2008. Making sense of hormone crosstalk during plant immune responses. *Cell Host Microbe*, 3, 348-51.
- STAELE, S., WURZINGER, B., MAIR, A., MEHLMER, N., VOTHKNECHT, U. C. & TEIGE, M. 2012. Plant organellar calcium signalling: an emerging field. *J Exp Bot*, 63, 1525-42.
- STAHL, E., BRILLATZ, T., FERREIRA QUEIROZ, E., MARCOURT, L., SCHMIESING, A., HILFIKER, O., RIEZMAN, I., RIEZMAN, H., WOLFENDER, J. L. & REYMOND, P. 2020. Phosphatidylcholines from *Pieris brassicae* eggs activate an immune response in Arabidopsis. *Elife*, 9.
- STEGMANN, M., MONAGHAN, J., SMAKOWSKA-LUZAN, E., ROVENICH, H., LEHNER, A., HOLTON, N., BELKHADIR, Y. & ZIPFEL, C. 2017. The receptor kinase FER is a RALF-regulated scaffold controlling plant immune signaling.
- STEIN, M., DITTGEN, J., SANCHEZ-RODRIGUEZ, C., HOU, B. H., MOLINA, A., SCHULZE-LEFERT, P., LIPKA, V. & SOMERVILLE, S. 2006. Arabidopsis PEN3/PDR8, an ATP binding cassette transporter, contributes to nonhost resistance to inappropriate pathogens that enter by direct penetration. *Plant Cell*, 18, 731-46.
- STEINBRENNER, A. D., MUNOZ-AMATRIAIN, M., CHAPARRO, A. F., AGUILAR-VENEGAS, J. M., LO, S., OKUDA, S., GLAUSER, G., DONGIOVANNI, J., SHI, D., HALL, M., CRUBAUGH, D., HOLTON, N., ZIPFEL, C., ABAGYAN, R., TURLINGS, T. C. J., CLOSE, T. J., HUFFAKER, A. & SCHMELZ, E. A. 2020. A receptor-like protein mediates plant immune responses to herbivore-associated molecular patterns. *Proc Natl Acad Sci U S A*, 117, 31510-31518.
- STOTZ, H. U., SAWADA, Y., SHIMADA, Y., HIRAI, M. Y., SASAKI, E., KRISCHKE, M., BROWN, P. D., SAITO, K. & KAMIYA, Y. 2011. Role of camalexin, indole glucosinolates, and side chain modification of glucosinolate-derived isothiocyanates in defense of Arabidopsis against *Sclerotinia sclerotiorum*. *Plant J*, 67, 81-93.
- SU, Q., PENG, Z., TONG, H., XIE, W., WANG, S., WU, Q., ZHANG, J., LI, C. & ZHANG, Y. 2019. A salivary ferritin in the whitefly suppresses plant defenses and facilitates host exploitation. *J Exp Bot*, 70, 3343-3355.
- SUN, M., VOORRIPS, R. E., VAN KAAUWEN, M., VISSER, R. G. F. & VOSMAN, B. 2020. The ability to manipulate ROS metabolism in pepper may affect aphid virulence. *Hortic Res*, 7, 6.
- SUN, Y., GUO, H., YUAN, E. & GE, F. 2018. Elevated CO₂ increases R gene-dependent resistance of *Medicago truncatula* against the pea aphid by up-regulating a heat shock gene. *New Phytol*, 217, 1696-1711.
- SYTYKIEWICZ, H. 2016. Deciphering the role of NADPH oxidase in complex interactions between maize (*Zea mays* L.) genotypes and cereal aphids. *Biochem Biophys Res Commun*, 476, 90-5.
- SYTYKIEWICZ, H., CHRZANOWSKI, G., CZERNIEWICZ, P., SPRAWKA, I., LUKASIK, I., GOLAWSKA, S. & SEMPRUCH, C. 2014. Expression profiling of selected glutathione transferase genes in *Zea mays* (L.) seedlings infested with cereal aphids. *PLoS One*, 9, e111863.
- TALKE, I. N., BLAUDEZ, D., MAATHUIS, F. J. M. & SANDERS, D. 2003. CNGCs: prime targets of plant cyclic nucleotide signalling? *Trends in Plant Science*, 8, 286–293.

- TAN, A. K. & EATON, D. L. 1995. Activation and characterization of procarboxypeptidase B from human plasma. *Biochemistry*, 34, 5811-6.
- TANAKA, K., CHOI, J. M., CAO, Y. R. & STACEY, G. 2014. Extracellular ATP acts as a damage-associated molecular pattern (DAMP) signal in plants. *Front. Plant Sci.*, 5.
- TANAKA, K., SWANSON, S. J., GILROY, S. & STACEY, G. 2010. Extracellular nucleotides elicit cytosolic free calcium oscillations in Arabidopsis. *Plant Physiol.*, 154, 705–719.
- TANG, D., WANG, G. & ZHOU, J. M. 2017. Receptor Kinases in Plant-Pathogen Interactions: More Than Pattern Recognition. *Plant Cell*, 29, 618-637.
- TATCHELL, G. M. 1989. An estimate of the potential economic losses to some crops due to aphids in Britain. *Crop Protection*, 8, 25-29.
- THALER, J. S., HUMPHREY, P. T. & WHITEMAN, N. K. 2012. Evolution of jasmonate and salicylate signal crosstalk. *Trends Plant Sci*, 17, 260-70.
- THINES, B., KATSIR, L., MELOTTO, M., NIU, Y., MANDAOKAR, A., LIU, G., NOMURA, K., HE, S. Y., HOWE, G. A. & BROWSE, J. 2007. JAZ repressor proteins are targets of the SCF(CO1) complex during jasmonate signalling. *Nature*, 448, 661-5.
- THOMAS, C. M., JONES, D. A., PARNISKE, M., HARRISON, K., BALINT-KURTI, P. J., HATZIXANTHIS, K. & JONES, J. D. G. 1997. Characterization of the Tomato Cf-4 Gene for Resistance to *Cladosporium fulvum* Identifies Sequences That Determine Recognition Specificity in Cf-4 and Cf-9. *The Plant Cell*, 9, 2209-2224.
- THOMMA, B. P., NELISSEN, I., EGGERMONT, K. & BROEKAERT, W. F. 1999. Deficiency in phytoalexin production causes enhanced susceptibility of Arabidopsis thaliana to the fungus *Alternaria brassicicola*. *Plant J*, 19, 163-71.
- THOMMA, B. P., NURNBERGER, T. & JOOSTEN, M. H. 2011. Of PAMPs and effectors: the blurred PTI-ETI dichotomy. *Plant Cell*, 23, 4-15.
- THOR, K., JIANG, S., MICHARD, E., GEORGE, J., SCHERZER, S., HUANG, S., DINDAS, J., DERBYSHIRE, P., LEITAO, N., DEFALCO, T. A., KOSTER, P., HUNTER, K., KIMURA, S., GRONNIER, J., STRANSFELD, L., KADOTA, Y., BUCHERL, C. A., CHARPENTIER, M., WRZACZEK, M., MACLEAN, D., OLDROYD, G. E. D., MENKE, F. L. H., ROELFSEMA, M. R. G., HEDRICH, R., FEIJO, J. & ZIPFEL, C. 2020. The calcium-permeable channel OSCA1.3 regulates plant stomatal immunity. *Nature*, 585, 569-573.
- THOR, K. & PEITER, E. 2014. Cytosolic calcium signals elicited by the pathogen-associated molecular pattern flg22 in stomatal guard cells are of an oscillatory nature. *New Phytol*, 204, 873-81.
- THORPE, P., COCK, P. J. & BOS, J. 2016. Comparative transcriptomics and proteomics of three different aphid species identifies core and diverse effector sets. *BMC Genomics*, 17, 172.
- TIAN, L., HIRES, S. A., MAO, T., HUBER, D., CHIAPPE, M. E., CHALASANI, S. H., PETREANU, L., AKERBOOM, J., MCKINNEY, S. A., SCHREITER, E. R., BARGMANN, C. I., JAYARAMAN, V., SVOBODA, K. & LOOGER, L. L. 2009. Imaging neural activity in worms, flies and mice with improved GCaMP calcium indicators. *Nat Methods*, 6, 875-81.
- TIAN, W., HOU, C., REN, Z., WANG, C., ZHAO, F., DAHLBECK, D., HU, S., ZHANG, L., NIU, Q., LI, L., STASKAWICZ, B. J. & LUAN, S. 2019. A calmodulin-gated calcium channel links pathogen patterns to plant immunity. *Nature*, 572, 131-135.
- TINTOR, N., ROSS, A., KANEHARA, K., YAMADA, K., FAN, L., KEMMERLING, B., NURNBERGER, T., TSUDA, K. & SAIJO, Y. 2013. Layered pattern receptor signaling via ethylene and endogenous elicitor peptides during Arabidopsis immunity to bacterial infection. *Proc Natl Acad Sci U S A*, 110, 6211-6.
- TJALLINGII, W. F. 2006. Salivary secretions by aphids interacting with proteins of phloem wound responses. *J Exp Bot*, 57, 739-45.
- TJALLINGII, W. F. & HOGENESCH, T. 1993. Fine structure of aphid stylet routes in plant tissues in correlation with EPG signals. *Physiological Entomology*, 18 317-328.

- TORRES, M. A., DANGL, J. L. & JONES, J. D. 2002. Arabidopsis gp91phox homologues AtrbohD and AtrbohF are required for accumulation of reactive oxygen intermediates in the plant defense response. *Proc Natl Acad Sci USA*, 523-528.
- TOYOTA, M., SPENCER, D., SAWAI-TOYOTA, S., JIAQI, W., ZHANG, T., KOO, A. J., HOWE, G. A. & GILROY, S. 2018. Glutamate triggers long-distance, calcium-based plant defense signaling. *Science*, 361, 1112–1115.
- TROUVELOT, S., HELOIR, M. C., POINSSOT, B., GAUTHIER, A., PARIS, F., GUILLIER, C., COMBIER, M., TRDA, L., DAIRE, X. & ADRIAN, M. 2014. Carbohydrates in plant immunity and plant protection: roles and potential application as foliar sprays. *Front Plant Sci*, 5, 592.
- TSUCHIDA, T., KOGA, R., HORIKAWA, M., TSUNODA, T., MAOKA, T., MATSUMOTO, S., SIMON, J.-C. & FUKATSU, T. 2010. Symbiotic Bacterium Modifies Aphid Body Color. *Science*, 330, 1102-1104.
- TSUDA, K., MINE, A., BETHKE, G., IGARASHI, D., BOTANGA, C. J., TSUDA, Y., GLAZEBROOK, J., SATO, M. & KATAGIRI, F. 2013. Dual regulation of gene expression mediated by extended MAPK activation and salicylic acid contributes to robust innate immunity in *Arabidopsis thaliana*. *PLoS Genet*, 9, e1004015.
- TSUDA, K. & SOMSSICH, I. E. 2015. Transcriptional networks in plant immunity. *New Phytol*, 206, 932-947.
- TSUJI, J., JACKSON, E. P., GAGE, D. A., HAMMERSCHMIDT, R. & SOMERVILLE, S. C. 1992. Phytoalexin Accumulation in *Arabidopsis thaliana* during the Hypersensitive Reaction to *Pseudomonas syringae* pv *syringae*. *Plant Physiol*, 98, 1304-9.
- ULKER, B. & SOMSSICH, I. E. 2004. WRKY transcription factors: from DNA binding towards biological function. *Curr Opin Plant Biol*, 7, 491-8.
- UMBRASTE, J., SCHWEIGHOFER, A., KAZANAVICIUTE, V., MAGYAR, Z., AYATOLLAHI, Z., UNTERWURZACHER, V., CHOOPAYAK, C., BONIECKA, J., MURRAY, J. A., BOGRE, L. & MESKIENE, I. 2010. MAPK phosphatase AP2C3 induces ectopic proliferation of epidermal cells leading to stomata development in *Arabidopsis*. *PLoS One*, 5, e15357.
- VAN BEL, A. J. & WILL, T. 2016. Functional Evaluation of Proteins in Watery and Gel Saliva of Aphids. *Front Plant Sci*, 7, 1840.
- VAN DER BURGH, A. M., POSTMA, J., ROBATZEK, S. & JOOSTEN, M. 2019. Kinase activity of SOBIR1 and BAK1 is required for immune signalling. *Mol Plant Pathol*, 20, 410-422.
- VAN DER HOORN, R. A. L. & KAMOUN, S. 2008. From guard to decoy: a new model for perception of plant pathogen effectors. *Plant Cell*, 20, 2009-2017.
- VAN ECK, L., SCHULTZ, T., LEACH, J. E., SCOFIELD, S. R., PEAIRS, F. B., BOTHA, A. M. & LAPITAN, N. L. 2010. Virus-induced gene silencing of WRKY53 and an inducible phenylalanine ammonia-lyase in wheat reduces aphid resistance. *Plant Biotechnol J*, 8, 1023-32.
- VAN EMDEN, H. F. & HARRINGTON, R. 2007. *Aphids as crop pests*, Wallingford, CAB International.
- VAN HAM, R. C. H. J., KAMERBEEK, J., PALACIOS, C., RAUSELL, C., ABASCAL, F., BASTOLLA, U., FERNANDEZ, J. M., JIMENEZ, L., POSTIGO, M., SILVA, F. J., TAMAMES, J., VIGUERA, E., LATORRE, A., VALENCIA, A., MORA, F. & MOYA, A. 2003. Reductive genome evolution in *Buchnera aphidicola*. *PNAS*, 100, 581–586.
- VAN LOON, L. C., REP, M. & PIETERSE, C. M. 2006. Significance of inducible defense-related proteins in infected plants. *Annu Rev Phytopathol*, 44, 135-62.
- VANDERMOTEN, S., HARMEL, N., MAZZUCHELLI, G., DE PAUW, E., HAUBRUGE, E. & FRANCIS, F. 2014. Comparative analyses of salivary proteins from three aphid species. *Insect Mol Biol*, 23, 67-77.
- VANHOOF, G., GOOSSENS, F., DE MEESTER, I., HENDRIKS, D. & SCHARPE, S. 1995. Proline motifs in peptides and their biological processing. *FASEB J*, 9, 736-44.
- VERONESE, P., NAKAGAMI, H., BLUHM, B., ABUQAMAR, S., CHEN, X., SALMERON, J., DIETRICH, R. A., HIRT, H. & MENGISTE, T. 2006. The membrane-anchored BOTRYTIS-INDUCED

- KINASE1 plays distinct roles in Arabidopsis resistance to necrotrophic and biotrophic pathogens. *Plant Cell*, 18, 257-73.
- VETTER, M. M., KRONHOLM, I., HE, F., HAWEKER, H., REYMOND, M., BERGELSON, J., ROBATZEK, S. & DE MEAUX, J. 2012. Flagellin perception varies quantitatively in Arabidopsis thaliana and its relatives. *Mol Biol Evol*, 29, 1655-67.
- VILLARROEL, C. A., JONCKHEERE, W., ALBA, J. M., GLAS, J. J., DERMAUW, W., HARING, M. A., VAN LEEUWEN, T., SCHUURINK, R. C. & KANT, M. R. 2016. Salivary proteins of spider mites suppress defenses in Nicotiana benthamiana and promote mite reproduction. *Plant J*, 86, 119-31.
- VINCENT, T. R. 2016. *The role of calcium signalling in plant-aphid interactions*. Doctoral thesis, University of East Anglia.
- VINCENT, T. R., AVRAMOVA, M., CANHAM, J., HIGGINS, P., BILKEY, N., MUGFORD, S. T., PITINO, M., TOYOTA, M., GILROY, S., MILLER, T. J., HOGENHOUT, S. & SANDERS, D. 2017. Interplay of Plasma Membrane and Vacuolar Ion Channels, Together with BAK1, Elicits Rapid Cytosolic Calcium Elevations in Arabidopsis during Aphid Feeding. *The Plant Cell*, tpc.00136.2017.
- VLOT, A. C., DEMPSEY, D. A. & KLESSIG, D. F. 2009. Salicylic Acid, a multifaceted hormone to combat disease. *Annu Rev Phytopathol*, 47, 177-206.
- VOS, P., SIMONS, G., JESSE, T., WIJBRANDI, J., HEINEN, L., HOGERS, R., FRIJTERS, A., GROENENDIJK, J., DIERGAARDE, P., REIJANS, M., FIERENS-ONSTENK, J., DE BOTH, M., PELEMAN, J., LIHARSKA, T., HONTELEZ, J. & ZABEAU, M. 1998. The tomato Mi-1 gene confers resistance to both root-knot nematodes and potato aphids. *Nat Biotechnol*, 16, 1365-9.
- WALKER, N. D., MCEWAN, N. R. & WALLACE, R. J. 2003. Cloning and functional expression of dipeptidyl peptidase IV from the ruminal bacterium Prevotella albensis M384(T). *Microbiology (Reading)*, 149, 2227-2234.
- WALLING, L. L. 2000. The Myriad Plant Responses to Herbivores. *J Plant Growth Regul*, 19, 195-216.
- WAN, J., TANAKA, K., ZHANG, X. C., SON, G. H., BRECHENMACHER, L., NGUYEN, T. H. & STACEY, G. 2012. LYK4, a lysin motif receptor-like kinase, is important for chitin signaling and plant innate immunity in Arabidopsis. *Plant Physiol*, 160, 396-406.
- WAN, W. L., ZHANG, L., PRUITT, R., ZAIDEM, M., BRUGMAN, R., MA, X., KROL, E., PERRAKI, A., KILIAN, J., GROSSMANN, G., STAHL, M., SHAN, L., ZIPFEL, C., VAN KAN, J. A. L., HEDRICH, R., WEIGEL, D., GUST, A. A. & NURNBERGER, T. 2019. Comparing Arabidopsis receptor kinase and receptor protein-mediated immune signaling reveals BIK1-dependent differences. *New Phytol*, 221, 2080-2095.
- WANG, C., ZHOU, M., ZHANG, X., YAO, J., ZHANG, Y. & MOU, Z. 2017. A lectin receptor kinase as a potential sensor for extracellular nicotinamide adenine dinucleotide in Arabidopsis thaliana. *Elife*, 6.
- WANG, G., ELLENDORFF, U., KEMP, B., MANSFIELD, J. W., FORSYTH, A., MITCHELL, K., BASTAS, K., LIU, C. M., WOODS-TOR, A., ZIPFEL, C., DE WIT, P. J., JONES, J. D., TOR, M. & THOMMA, B. P. 2008a. A genome-wide functional investigation into the roles of receptor-like proteins in Arabidopsis. *Plant Physiol*, 147, 503-17.
- WANG, G., LONG, Y., THOMMA, B. P., DE WIT, P. J., ANGENENT, G. C. & FIERS, M. 2010. Functional analyses of the CLAVATA2-like proteins and their domains that contribute to CLAVATA2 specificity. *Plant Physiol*, 152, 320-31.
- WANG, G., ROUX, B., FENG, F., GUY, E., LI, L., LI, N., ZHANG, X., LAUTIER, M., JARDINAUD, M. F., CHABANNES, M., ARLAT, M., CHEN, S., HE, C., NOEL, L. D. & ZHOU, J. M. 2015a. The Decoy Substrate of a Pathogen Effector and a Pseudokinase Specify Pathogen-Induced Modified-Self Recognition and Immunity in Plants. *Cell Host Microbe*, 18, 285-95.

- WANG, H., LIU, Y., BRUFFETT, K., LEE, J., HAUSE, G., WALKER, J. C. & ZHANG, S. 2008b. Haplo-insufficiency of MPK3 in MPK6 mutant background uncovers a novel function of these two MAPKs in Arabidopsis ovule development. *Plant Cell*, 20, 602-13.
- WANG, J., GRUBB, L. E., WANG, J., LIANG, X., LI, L., GAO, C., MA, M., FENG, F., LI, M., LI, L., ZHANG, X., YU, F., XIE, Q., CHEN, S., ZIPFEL, C., MONAGHAN, J. & ZHOU, J. M. 2018. A Regulatory Module Controlling Homeostasis of a Plant Immune Kinase. *Mol Cell*, 69, 493-504 e6.
- WANG, J., HU, M., QI, J., WANG, G., HAN, Z., QI, Y., WANG, H. W., ZHOU, J. M. & CHAI, J. 2019a. Ligand-triggered allosteric ADP release primes a plant NLR complex. *Science*, 364.
- WANG, L., ALBERT, M., EINIG, E., FURST, U., KRUST, D. & FELIX, G. 2016. The pattern-recognition receptor CORE of Solanaceae detects bacterial cold-shock protein. *Nat Plants*, 2, 16185.
- WANG, N., ZHAO, P., MA, Y., YAO, X., SUN, Y., HUANG, X., JIN, J., ZHANG, Y., ZHU, C., FANG, R. & YE, J. 2019b. A whitefly effector Bsp9 targets host immunity regulator WRKY33 to promote performance. *Philos Trans R Soc Lond B Biol Sci*, 374, 20180313.
- WANG, W., DAI, H., ZHANG, Y., CHANDRASEKAR, R., LUO, L., HIROMASA, Y., SHENG, C., PENG, G., CHEN, S., TOMICH, J. M., REESE, J., EDWARDS, O., KANG, L., REECK, G. & CUI, F. 2015b. Armet is an effector protein mediating aphid-plant interactions. *FASEB J*, 29, 2032-45.
- WARD, J. M. & SCHROEDER, J. I. 1994. Calcium-Activated K⁺ Channels and Calcium-Induced Calcium Release by Slow Vacuolar Ion Channels in Guard Cell Vacuoles Implicated in the Control of Stomatal Closure. *Plant Cell*, 6, 669-683.
- WARI, D., ALAMGIR, K. M., MUJIONO, K., HOJO, Y., TANI, A., SHINYA, T., NAKATANI, H. & GALIS, I. 2019. Brown planthopper honeydew-associated symbiotic microbes elicit momilactones in rice. *Plant Signal Behav*, 14, 1655335.
- WASTERNAK, C. & SONG, S. 2017. Jasmonates: biosynthesis, metabolism, and signaling by proteins activating and repressing transcription. *J Exp Bot*, 68, 1303-1321.
- WEIGEL, D. 2012. Natural variation in Arabidopsis: from molecular genetics to ecological genomics. *Plant Physiol*, 158, 2-22.
- WESTERINK, N., BRANDWAGT, B. F., DE WIT, P. J. & JOOSTEN, M. H. 2004. Cladosporium fulvum circumvents the second functional resistance gene homologue at the Cf-4 locus (Hcr9-4E) by secretion of a stable avr4E isoform. *Mol Microbiol*, 54, 533-45.
- WIDJAJA, M., HARVEY, K. L., HAGEMANN, L., BERRY, I. J., JAROCKI, V. M., RAYMOND, B. B. A., TACCHI, J. L., GRUNDEL, A., STEELE, J. R., PADULA, M. P., CHARLES, I. G., DUMKE, R. & DJORDJEVIC, S. P. 2017. Elongation factor Tu is a multifunctional and processed moonlighting protein. *Sci Rep*, 7, 11227.
- WILDERMUTH, M. C., DEWDNEY, J., WU, G. & AUSUBEL, F. M. 2001. Isochorismate synthase is required to synthesize salicylic acid for plant defence. *Nature*, 414, 562-565.
- WILL, T., FURCH, A. C. & ZIMMERMANN, M. R. 2013. How phloem-feeding insects face the challenge of phloem-located defenses. *Front Plant Sci*, 4, 336.
- WILL, T., KORNEMANN, S. R., FURCH, A. C., TJALLINGII, W. F. & VAN BEL, A. J. 2009. Aphid watery saliva counteracts sieve-tube occlusion: a universal phenomenon? *J Exp Biol*, 212, 3305-12.
- WILL, T., STECKBAUER, K., HARDT, M. & VAN BEL, A. J. 2012. Aphid gel saliva: sheath structure, protein composition and secretory dependence on stylet-tip milieu. *PLoS One*, 7, e46903.
- WILL, T., TJALLINGII, W. F., THONNESSEN, A. & VAN BEL, A. J. 2007. Molecular sabotage of plant defense by aphid saliva. *Proc Natl Acad Sci U S A*, 104, 10536-41.
- WILL, T. & VAN BEL, A. J. 2006. Physical and chemical interactions between aphids and plants. *J Exp Bot*, 57, 729-37.

- WILL, T. & VILCINSKAS, A. 2015. The structural sheath protein of aphids is required for phloem feeding. *Insect Biochem Mol Biol*, 57, 34-40.
- WILLIAMS, G. C. 1975. *Sex and Evolution*, USA, Yale University Press.
- WILLMANN, R., LAJUNEN, H. M., ERBS, G., NEWMAN, M. A., KOLB, D., TSUDA, K., KATAGIRI, F., FLIEGMANN, J., BONO, J. J., CULLIMORE, J. V., JEHLE, A. K., GOTZ, F., KULIK, A., MOLINARO, A., LIPKA, V., GUST, A. A. & NURNBERGER, T. 2011. Arabidopsis lysin-motif proteins LYM1 LYM3 CERK1 mediate bacterial peptidoglycan sensing and immunity to bacterial infection. *Proc Natl Acad Sci U S A*, 108, 19824-9.
- WU, J. & BALDWIN, I. T. 2010. New insights into plant responses to the attack from insect herbivores. *Annu Rev Genet*, 44, 1-24.
- WU, J., HETTENHAUSEN, C., MELDAU, S. & BALDWIN, I. T. 2007. Herbivory rapidly activates MAPK signaling in attacked and unattacked leaf regions but not between leaves of *Nicotiana attenuata*. *Plant Cell*, 19, 1096-122.
- WU, L. H., TSAI, C. M. & FRASCH, C. E. 1987. A method for purification of bacterial R-type lipopolysaccharides (lipooligosaccharides). *Anal Biochem*, 160, 281-9.
- WU, Y., GAO, Y., ZHAN, Y., KUI, H., LIU, H., YAN, L., KEMMERLING, B., ZHOU, J. M., HE, K. & LI, J. 2020. Loss of the common immune coreceptor BAK1 leads to NLR-dependent cell death. *Proc Natl Acad Sci U S A*, 117, 27044-27053.
- WU, Y., ZHANG, D., CHU, J. Y., BOYLE, P., WANG, Y., BRINDLE, I. D., DE LUCA, V. & DESPRES, C. 2012. The Arabidopsis NPR1 protein is a receptor for the plant defense hormone salicylic acid. *Cell Rep*, 1, 639-47.
- WUNSCHE, H., BALDWIN, I. T. & WU, J. 2011. S-Nitrosoglutathione reductase (GSNOR) mediates the biosynthesis of jasmonic acid and ethylene induced by feeding of the insect herbivore *Manduca sexta* and is important for jasmonate-elicited responses in *Nicotiana attenuata*. *J Exp Bot*, 62, 4605-16.
- XIANG, T., ZONG, N., ZHANG, J., CHEN, J., CHEN, M. & ZHOU, J. M. 2011. BAK1 is not a target of the *Pseudomonas syringae* effector AvrPto. *Mol Plant Microbe Interact*, 24, 100-7.
- XIE, K., CHEN, J., WANG, Q. & YANG, Y. 2014. Direct phosphorylation and activation of a mitogen-activated protein kinase by a calcium-dependent protein kinase in rice. *Plant Cell*, 26, 3077-89.
- XU, H. X., QIAN, L. X., WANG, X. W., SHAO, R. X., HONG, Y., LIU, S. S. & WANG, X. W. 2019. A salivary effector enables whitefly to feed on host plants by eliciting salicylic acid-signaling pathway. *Proc Natl Acad Sci U S A*, 116, 490-495.
- XU, J., PADILLA, C. S., LI, J., WICKRAMANAYAKE, J., FISCHER, H. D. & GOGGIN, F. L. 2021. Redox responses of Arabidopsis thaliana to the green peach aphid, *Myzus persicae*. *Mol Plant Pathol*, 22, 727-736.
- XU, J. & ZHANG, S. 2014. RNA interference of plant MAPK cascades for functional studies. *Methods Mol Biol*, 1171, 91-103.
- YAMADA, K., YAMASHITA-YAMADA, M., HIRASE, T., FUJIWARA, T., TSUDA, K., HIRUMA, K. & SAIJO, Y. 2016. Danger peptide receptor signaling in plants ensures basal immunity upon pathogen-induced depletion of BAK1. *EMBO J*, 35, 46-61.
- YAMAGUCHI, Y. & HUFFAKER, A. 2011. Endogenous peptide elicitors in higher plants. *Curr Opin Plant Biol*, 14, 351-7.
- YAMAGUCHI, Y., HUFFAKER, A., BRYAN, A. C., TAX, F. E. & RYAN, C. A. 2010. PEPR2 is a second receptor for the Pep1 and Pep2 peptides and contributes to defense responses in Arabidopsis. *Plant Cell*, 22, 508-22.
- YAMAGUCHI, Y., PEARCE, G. & RYAN, C. A. 2006. The cell surface leucine-rich repeat receptor for AtPep1, an endogenous peptide elicitor in Arabidopsis, is functional in transgenic tobacco cells. *PNAS*, 103, 10104-10109.
- YANG, D. H., HETTENHAUSEN, C., BALDWIN, I. T. & WU, J. 2011. BAK1 regulates the accumulation of jasmonic acid and the levels of trypsin proteinase inhibitors in *Nicotiana attenuata*'s responses to herbivory. *J Exp Bot*, 62, 641-52.

- YANG, F., KIMBERLIN, A. N., ELOWSKY, C. G., LIU, Y., GONZALEZ-SOLIS, A., CAHOON, E. B. & ALFANO, J. R. 2019. A Plant Immune Receptor Degraded by Selective Autophagy. *Mol Plant*, 12, 113-123.
- YANG, L., ZHANG, Y., GUAN, R., LI, S., XU, X., ZHANG, S. & XU, J. 2020a. Co-regulation of indole glucosinolates and camalexin biosynthesis by CPK5/CPK6 and MPK3/MPK6 signaling pathways. *J Integr Plant Biol*, 62, 1780-1796.
- YANG, Y., LIU, J., ZHOU, X., LIU, S. & ZHUANG, Y. 2020b. Identification of WRKY gene family and characterization of cold stress-responsive WRKY genes in eggplant. *PeerJ.*, 17, e8777.
- YANG, Z., MA, L., FRANCIS, F., YANG, Y., CHEN, H., WU, H. & CHEN, X. 2018. Proteins Identified from Saliva and Salivary Glands of the Chinese Gall Aphid *Schlechtendalia chinensis*. *Proteomics*, 18, e1700378.
- YE, W., YU, H., JIAN, Y., ZENG, J., JI, R., CHEN, H. & LOU, Y. 2017. A salivary EF-hand calcium-binding protein of the brown planthopper *Nilaparvata lugens* functions as an effector for defense responses in rice. *Sci Rep*, 7, 40498.
- YEH, Y. H., PANZERI, D., KADOTA, Y., HUANG, Y. C., HUANG, P. Y., TAO, C. N., ROUX, M., CHIEN, H. C., CHIN, T. C., CHU, P. W., ZIPFEL, C. & ZIMMERLI, L. 2016. The Arabidopsis Malectin-Like/LRR-RLK IOS1 Is Critical for BAK1-Dependent and BAK1-Independent Pattern-Triggered Immunity. *Plant Cell*, 28, 1701-21.
- YIN, Z., WANG, N., PI, L., LI, L., DUAN, W., WANG, X. & DOU, D. 2021. *Nicotiana benthamiana* LRR-RLP NbEIX2 mediates the perception of an EIX-like protein from *Verticillium dahliae*. *J Integr Plant Biol*, 63, 949-960.
- YONEKURA, K., MAKI-YONEKURA, S. & NAMBA, K. 2003. Complete atomic model of the bacterial flagellar filament by electron cryomicroscopy. *Nature*, 424, 643-50.
- YOO, S. D. & SHEEN, J. 2008. MAPK signaling in plant hormone ethylene signal transduction. *Plant Signal Behav*, 3, 848-9.
- YOUNES, I. & RINAUDO, M. 2015. Chitin and chitosan preparation from marine sources. Structure, properties and applications. *Mar Drugs*, 13, 1133-74.
- YU, T. Y., SUN, M. K. & LIANG, L. K. 2021. Receptors in the Induction of the Plant Innate Immunity. *Mol Plant Microbe Interact*, 34, 587-601.
- YU, X., XU, G., LI, B., DE SOUZA VESPOLI, L., LIU, H., MOEDER, W., CHEN, S., DE OLIVEIRA, M. V. V., ARIADINA DE SOUZA, S., SHAO, W., RODRIGUES, B., MA, Y., CHHAJED, S., XUE, S., BERKOWITZ, G. A., YOSHIOKA, K., HE, P. & SHAN, L. 2019. The Receptor Kinases BAK1/SERK4 Regulate Ca²⁺ Channel-Mediated Cellular Homeostasis for Cell Death Containment. *Curr Biol*, 29, 3778-3790 e8.
- YUAN, F., YANG, H., XUE, Y., KONG, D., YE, R., LI, C., ZHANG, J., THEPRUNGSIRIKUL, L., SHRIFT, T., KRICHILSKY, B., JOHNSON, D. M., SWIFT, G. B., HE, Y., SIEDOW, J. N. & PEI, Z. M. 2014. OSCA1 mediates osmotic-stress-evoked Ca²⁺ increases vital for osmosensing in Arabidopsis. *Nature*, 514, 367-71.
- YUAN, M., NGOU, B. P. M., DING, P. & XIN, X. F. 2021. PTI-ETI crosstalk: an integrative view of plant immunity. *Curr Opin Plant Biol*, 62, 102030.
- ZECHA, J., SATPATHY, S., KANASHOVA, T., AVANESSIAN, S. C., KANE, M. H., CLAUSER, K. R., MERTINS, P., CARR, S. A. & KUSTER, B. 2019. TMT Labeling for the Masses: A Robust and Cost-efficient, In-solution Labeling Approach. *Mol Cell Proteomics*, 18, 1468-1478.
- ZHANG, J., GAO, J., ZHU, Z., SONG, Y., WANG, X., WANG, X. & ZHOU, X. 2020a. MKK4/MKK5-MPK1/MPK2 cascade mediates SA-activated leaf senescence via phosphorylation of NPR1 in Arabidopsis. *Plant Mol Biol*, 102, 463-475.
- ZHANG, J., LI, W., XIANG, T., LIU, Z., LALUK, K., DING, X., ZOU, Y., GAO, M., ZHANG, X., CHEN, S., MENGISTE, T., ZHANG, Y. & ZHOU, J. M. 2010. Receptor-like cytoplasmic kinases integrate signaling from multiple plant immune receptors and are targeted by a *Pseudomonas syringae* effector. *Cell Host Microbe*, 7, 290-301.
- ZHANG, L., KARS, I., ESSENSTAM, B., LIEBRAND, T. W., WAGEMAKERS, L., ELBERSE, J., TAGKALAKI, P., TJOITANG, D., VAN DEN ACKERVEKEN, G. & VAN KAN, J. A. 2014. Fungal

- endopolygalacturonases are recognized as microbe-associated molecular patterns by the arabidopsis receptor-like protein RESPONSIVENESS TO BOTRYTIS POLYGALACTURONASES1. *Plant Physiol*, 164, 352-64.
- ZHANG, M., CHIANG, Y. H., TORUNO, T. Y., LEE, D., MA, M., LIANG, X., LAL, N. K., LEMOS, M., LU, Y. J., MA, S., LIU, J., DAY, B., DINESH-KUMAR, S. P., DEHESH, K., DOU, D., ZHOU, J. M. & COAKER, G. 2018a. The MAP4 Kinase SIK1 Ensures Robust Extracellular ROS Burst and Antibacterial Immunity in Plants. *Cell Host Microbe*, 24, 379-391 e5.
- ZHANG, M., SU, J., ZHANG, Y., XU, J. & ZHANG, S. 2018b. Conveying endogenous and exogenous signals: MAPK cascades in plant growth and defense. *Curr Opin Plant Biol*, 45, 1-10.
- ZHANG, T., LIU, Y., YANG, T., ZHANG, L., XU, S., XUE, L. & AN, L. 2006. Diverse signals converge at MAPK cascades in plant. *Plant Physiol Biochem*, 44, 274-83.
- ZHANG, W., FRAITURE, M., KOLB, D., LOFFELHARDT, B., DESAKI, Y., BOUTROT, F. F., TOR, M., ZIPFEL, C., GUST, A. A. & BRUNNER, F. 2013. Arabidopsis receptor-like protein30 and receptor-like kinase suppressor of BIR1-1/EVERSHED mediate innate immunity to necrotrophic fungi. *Plant Cell*, 25, 4227-41.
- ZHANG, Y., FU, Y., WANG, Q., LIU, X., LI, Q. & CHEN, J. 2020b. Transcriptome analysis reveals rapid defence responses in wheat induced by phytotoxic aphid *Schizaphis graminum* feeding. *BMC Genomics*, 21, 339.
- ZHAO, Y., HULL, A. K., GUPTA, N. R., GOSS, K. A., ALONSO, J., ECKER, J. R., NORMANLY, J., CHORY, J. & CELENZA, J. L. 2002. Trp-dependent auxin biosynthesis in Arabidopsis: involvement of cytochrome P450s CYP79B2 and CYP79B3. *Genes Dev*, 16, 3100-12.
- ZHENG, Z., QAMAR, S. A., CHEN, Z. & MENGISTE, T. 2006. Arabidopsis WRKY33 transcription factor is required for resistance to necrotrophic fungal pathogens. *Plant J*, 48, 592-605.
- ZHOU, J., WU, S., CHEN, X., LIU, C., SHEEN, J., SHAN, L. & HE, P. 2014. The *Pseudomonas syringae* effector HopF2 suppresses Arabidopsis immunity by targeting BAK1. *Plant J*, 77, 235-45.
- ZHOU, N., TOOTLE, T. L. & GLAZEBROOK, J. 1999. Arabidopsis PAD3 , a Gene Required for Camalexin Biosynthesis, Encodes a Putative Cytochrome P450 Monooxygenase. *The Plant Cell*, 11, 2419–2428.
- ZHOU, N., TOOTLE, T. L., TSUI, F., KLESSIG, D. F. & GLAZEBROOK, J. 1998. PAD4 functions upstream from salicylic acid to control defense responses in Arabidopsis. *Plant Cell*, 10, 1021-30.
- ZHU-SALZMAN, K., SALZMAN, R. A., AHN, J. E. & KOIWA, H. 2004. Transcriptional regulation of sorghum defense determinants against a phloem-feeding aphid. *Plant Physiol*, 134, 420-31.
- ZHU, S., JEONG, R. D., VENUGOPAL, S. C., LAPCHYK, L., NAVARRE, D., KACHROO, A. & KACHROO, P. 2011. SAG101 forms a ternary complex with EDS1 and PAD4 and is required for resistance signaling against turnip crinkle virus. *PLoS Pathog*, 7, e1002318.
- ZHU, Z. 2014. Molecular basis for jasmonate and ethylene signal interactions in Arabidopsis. *J Exp Bot*, 65, 5743-8.
- ZIPFEL, C. 2014. Plant pattern-recognition receptors. *Trends Immunol*, 35, 345-51.
- ZIPFEL, C., KUNZE, G., CHINCHILLA, D., CANIARD, A., JONES, J. D., BOLLER, T. & FELIX, G. 2006. Perception of the bacterial PAMP EF-Tu by the receptor EFR restricts *Agrobacterium*-mediated transformation. *Cell*, 125, 749-60.
- ZOLG, D. P., WILHELM, M., SCHMIDT, T., MEDARD, G., ZERWECK, J., KNAUTE, T., WENSCHUH, H., REIMER, U., SCHNATBAUM, K. & KUSTER, B. 2018. ProteomeTools: Systematic Characterization of 21 Post-translational Protein Modifications by Liquid Chromatography Tandem Mass Spectrometry (LC-MS/MS) Using Synthetic Peptides. *Mol Cell Proteomics*, 17, 1850-1863.